REPORT NO. 183008/1

GROUNDWATER AND SURFACE WATER MODELLING REPORT, RUM JUNGLE STAGE 2A

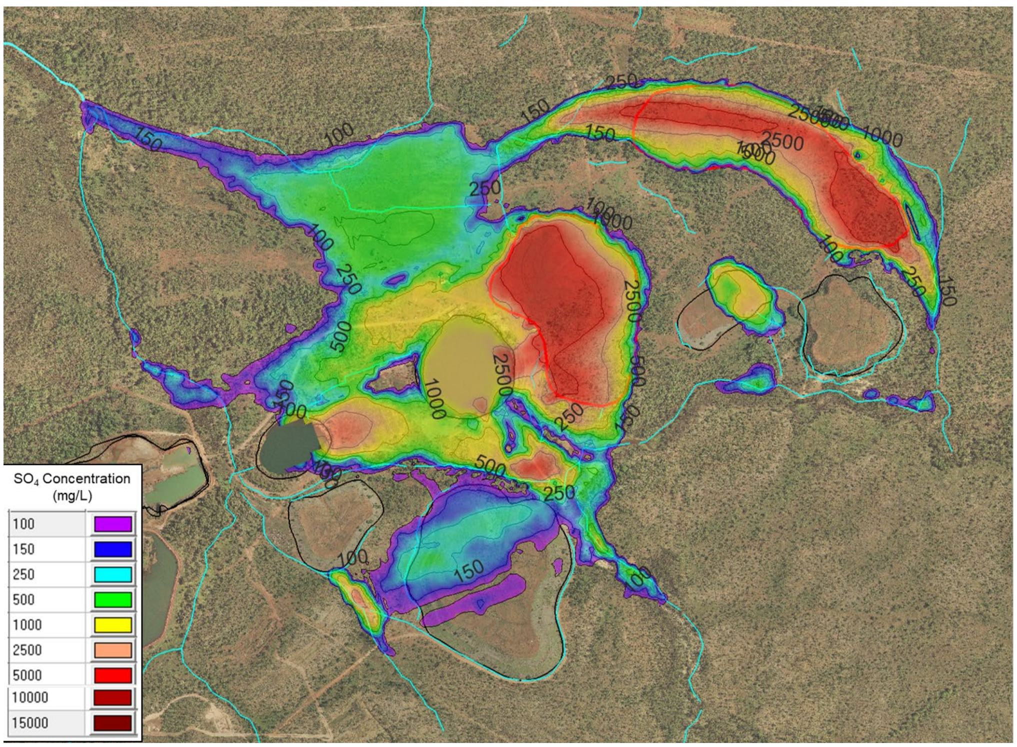

Submitted to:

NORTHERN TERRITORY GOVERNMENT

Prepared by:

Robertson GeoConsultants Inc.
Consulting Engineers and Scientists for the Mining Industry
www.robertsongeoconsultants.com

November 2019

EXECUTIVE SUMMARY

Introduction

This is the Robertson GeoConsultants Inc. (RGC) report on groundwater and surface water modelling for Stage 2A of the Rum Jungle Rehabilitation Project. It was prepared for the Northern Territory (NT) Department of Primary Industry and Resources (DPIR) in support of an Environmental Impact Statement (EIS) for the site. This report is the key deliverable for RGC contract Q-18-0503 with the DPIR and is appended to the EIS.

Background

Water quality at Rum Jungle is degraded by Acid and Metalliferous Drainage (AMD). The primary AMD sources are sulphide-bearing waste rock in the historic Waste Rock Dumps (WRDs) and leached low-grade ore and contaminated soils placed in shallow zones of Dyson's Pit during rehabilitation in 1984/1985 (see Allen and Verhoeven, 1986). AMD reports to groundwater and, in turn, the East Branch of the Finniss River (EBFR), which flows through the mine site. Groundwater quality in some areas of the site is further degraded by historic AMD sources that were eliminated by rehabilitation in the 1980s or by metalliferous liquor lost during an experimental heap leach operation from 1965 to 1971 in the Copper Extraction Pad area.

This report describes a Class 2 groundwater model developed to simulate current conditions on site and predict future conditions during the construction phase of rehabilitation (Stage 3) and conditions once rehabilitation is completed. The groundwater model consists of a transient flow model constructed with the MODFLOW-NWT finite difference code and a transient solute transport model developed using the transport code MT3DMS. Groundwater model development was an iterative process that began in 2011 during Phase I of the Rum Jungle Rehabilitation Project. The latest model was updated in 2019 in support of the Environmental Impact Statement (EIS) for the site.

This report also describes a site-wide Water and Load Balance Model (WLBM) developed in the software GoldSim to simulate streamflow in the EBFR, validate simulated SO_4 and Cu loads from the groundwater model and predict SO_4 and Cu concentrations in the EBFR on a preliminary basis. The WLBM simulates streamflow (discharge) with the Australian Water Balance Model (AWBM) and is used to simulate water management during the construction period of rehabilitation when the Main Pit is backfilled with waste rock and a Seepage Interception System (SIS) is operated to reduce contaminant loads to the EBFR. Several other recovery bores are proposed to improve groundwater quality in the Copper Extraction Pad area and the former ore stockpile area. Flows from each of these bores will report to a Water Treatment Plant (WTP) that will also treat pit water during backfilling.

Study Objectives

Study objectives are to:

- Provide an updated conceptual hydrogeological model for the site that details the hydrogeological and hydrological data that are represented in the numerical groundwater model.
- Detail the structure and calibration of the numerical groundwater model for current conditions and describe how the model was adapted to predict future groundwater conditions.
- Document the groundwater modelling undertaken to predict groundwater flows and SO_4 and Cu loads in groundwater during the construction phase of rehabilitation and post-rehabilitation.
- Detail the structure and validation of the WLBM for the site and simulated SO_4 and Cu concentrations in the EBFR for current conditions.
- Summarize predictive modelling results that constrain the extent and the timing of future water quality improvements after rehabilitation works have been completed.
- Recommend technical studies that may help refine prediction of post-rehabilitation conditions at the site and determine how the future performance of the rehabilitation could be effectively monitored.

Further details on specific modelling objectives are provided in Sections 4 and 5.

Key Findings – Groundwater Modelling

Key findings from the groundwater modelling are summarized below:

- The calibration of the “2016” transient flow model was refined until a satisfactory match of simulated and observed spatial and temporal variations in groundwater levels was achieved (flow calibration). A trial-and-error calibration procedure was adopted, whereby material properties (K, Ss and Sy) as well as recharge and evapotranspiration rates were varied. The zonation of K, recharge and evapotranspiration were also adjusted and additional zones introduced.

- Flow model calibration was achieved in about 46 calibration iterations and the calibrated model is Run No. 46. The normalized root mean square of the errors (NRMS) value for full calibration period is 3.8%. NRMS values for the dry season and the wet season calibration data are 4.7% and 1.3%, respectively. The computed NRMS values are well below the target NRMS of 5% suggesting good calibration to head targets. Calibration statistics and the residual error scatter plots indicate that the head calibration for the numerical model is statistically acceptable for the purpose of this study.

- The transport model was parameterized using the same spatial zonation and calibrated hydraulic properties developed for the flow model. The two additional transport parameters required to solve the transport equation are effective porosity (n_e) and dispersivity (α). N_e was spatially distributed in the model using the same approach as outlined above for hydraulic parameters. The effective porosity values developed in the 2016 model were also adopted for the current model. Dispersivity was assumed to be independent of aquifer type and a uniform distribution was assumed across all model zones/layers using the following dispersivity values: (i) Longitudinal dispersivity (αL) = 10.0 m, (ii) transverse dispersivity (αT) = 0.1 m, and (iii) vertical dispersivity (αV) = 0.01 m.

- Most of the current AMD sources to groundwater were represented in the transport model using constant concentrations applied to the respective foot print area. In this approach, MT3DMS keeps the solute concentration in the respective model nodes fixed at the specified concentration. In the case of surficial contaminant sources (e.g. WRDs) this approach is equivalent to specifying a source concentration in recharge. For selected sources, e.g. Old Tailings Dam area, mill area, a constant concentration was applied to recharge for the current model.

- SO_4 is assumed to be non-reactive ("conservative"), i.e. no geochemical reactions are assumed to influence sulphate transport along the groundwater flow path. Copper transport in groundwater was assumed to be affected by geochemical reactions, including sorption on soils and/or bedrock (e.g. on Fe-oxihydroxides, clays etc.) and the chemical precipitation of copper in bedrock units which have adequate buffering capacity to neutralize AMD (e.g. in Coomalie Dolostone).

- Detailed site-specific information on geochemical controls for copper at Rum Jungle was not available to quantify the relative proportion of these attenuation mechanisms and/or parameterize these reaction models. A range of "attenuation scenarios" for copper were simulated in RGC (2016) to illustrate and bracket the potential influence of these geochemical controls on historic and current copper transport in groundwater and loading to the receiving surface water. These attenuation scenarios included a no attenuation (conservative transport) scenario, moderate attenuation scenario and high attenuation scenario. However, only the "moderate attenuation" scenario could explain estimated loads in the EBFR, thus only this scenario was retained for this report.

- A historic model was developed to simulate groundwater conditions prior to rehabilitation in 1984/1985. The key objective was to provide an initial condition for a model that simulates groundwater conditions since the initial rehabilitation works were completed. This "current conditions" model simulates the period from 1985 to 2018 by applying source terms to current AMD sources, e.g. WRDs, and simulating the residual impacted groundwater that remains due to historic impacts.

- The "current conditions" model simulates the general extent of SO_4 and Cu plumes on site. Cu concentrations in groundwater appear to be over-estimated in some areas, particularly near the WRDs. The model simulates SO_4 and Cu loads in the EBFR reasonably well however, suggesting the model can simulate transport with a reasonable degree of confidence despite the uncertainty in the strength and extent of the Cu plume.

- The groundwater model was modified to simulate groundwater conditions during the construction phase of rehabilitation. This model predicts the SIS that is operated for the duration of the construction period will significantly reduce SO_4 and Cu loads in the EBFR and reduce the extent and strength of SO_4 and Cu plumes near the Main and Intermediate WRDs. The model also predicts the development of new SO_4 plumes from the backfilled Main Pit and the new WSF. The model predicts a minimal Cu plumes migrating from the backfilled Main Pit and the new WSF due to the very low Cu concentrations assumed as source terms and attenuation of Cu in the bedrock aquifer downgradient of the backfilled pit and WSF.
- Post-rehabilitation groundwater conditions were predicted by running the groundwater model for 30 years, assuming saline drainage from the Main Pit backfill and the new WSF is discharged to groundwater and residual impacted groundwater from the old WRD footprints and other sources continues to discharge to the EBFR. The initial conditions used for the post-rehabilitation model runs are predicted groundwater conditions in Year 11, i.e. after 10 years of operating the SIS and recovery bores in the Copper Extraction Pad area and former ore stockpile area.
- The groundwater model predicts high SO_4 concentrations in groundwater near the two WSF footprints. The plume emanating from the WSF footprint nearest the pit is predicted to report to the backfilled Main Pit, mainly from Layers 1 to 4 in the model, i.e. <50 m bgs. Most of the SO_4 load therefore reports to the portion of the pit that is backfilled but it is plausible that the plume reaches the shallow pit lake. The SO_4 plume from the northern WSF footprint migrates along the northern lease boundary to Old Tailings Creek and there is a small plume migrating east to an unnamed drainage.
- The model predicts a less concentrated SO_4 plume is also simulated downgradient of the backfilled Main Pit. This plume is predicted to occur for the 30-year simulation period but backfill materials in the Main Pit are eventually assumed to stop producing impacted seepage and this plume will likely be flushed from groundwater. Post-rehabilitation, the groundwater model predicts 1.3 t/year Cu to the EBFR in Year 15, i.e. 5 years after the SIS ceases to operate. The model predicts the new plume will stabilize in space and loading within a few years after rehabilitation, i.e. well before Year 40. 1.0 t/year Cu (75%) is predicted in the EBFR and 0.3 t/year Cu (25%) reports to the Intermediate Pit in Year 15. These loads come from residual AMD-impacted groundwater near the footprints of the former Main and Intermediate WRDs and are predicted to gradually decrease over time as this groundwater is flushed by rainfall infiltration. The predicted Cu load (0.6 t/year) to the EBFR in Year 40 is about 40%

lower than the predicted load in Year 15 and 75% less than the simulated Cu load for current conditions.

Key Findings – Surface Water Modelling

Key findings from the WLBM are summarized below:

- The WLBM indicates that only the moderate attenuation scenario simulated in RGC (2016) can explain Cu loads in the EBFR for current conditions. The other attenuation scenarios either over-estimated or under-estimated the annual Cu load in the EBFR, hence these scenarios were not retained in the updated groundwater model.

- SO_4 and Cu concentrations were simulated by importing the simulated monthly SO_4 and Cu loads from the groundwater model into the WLBM. For most years, the magnitude and trends in SO_4 and Cu concentrations are simulated reasonably well by the WLBM. These results suggest the magnitude and daily trends in daily SO_4 and Cu concentrations in the EBFR can be simulated with a reasonable degree of confidence, without the need to over-parameterize the groundwater model or the WLBM.

- To predict post-rehabilitation SO_4 and Cu concentrations in the EBFR, the WLBM was not substantially modified. Instead, SO_4 and Cu concentrations were derived by using predicted loads from the groundwater model for Year 40 in the WLBM and eliminating load contributions to the EBFR by interflow from the WRDs. The model was then run assuming the same rainfall pattern observed from 2010 to 2017 and using predicted SO_4 and Cu loads from the groundwater model.

- SO_4 and Cu concentrations in the EBFR are predicted to be much lower than for current conditions due to substantial decrease in SO_4 in groundwater due to operating the SIS recovery bores and the long-term flushing of SO_4 from the former impacted areas that is predicted by the groundwater model. Future Cu concentrations may still exceed the Zone 2 LDWQO at certain times of the year, mainly due to the residual plume of AMD-impacted groundwater from the Intermediate WRD that is predicted downgradient of the remediated footprint.

- Water management during the construction phase of rehabilitation was simulated with the WLBM. The model predicts some spillage to the EBFR during rainfall events such as Tropical Cyclone Carlos in February 2011, which generated the single largest daily discharge ever recorded on the EBFR at gauge GS8150097. During an event of similar magnitude as Tropical Cyclone Carlos, the WLBM simulated the complete filling of the live storage in the system resulting in a small spill of water from the Intermediate Pit, i.e. about 60 L/s for two days.

- Flows of 10 to 100 L/s of treated water to the EBFR during the dry season are predicted while the pit is being backfilled. However, water demands for dust suppression, vehicle washing, nursery supply, and waste rock compaction during WSF construction, amongst other water demands, were not accounted for in the WLBM due to lack of information on the timing and intensity of these demands. Each of these demands could be substantial during the dry season so it is conceivable that there may be much less than 10 to 100 L/s of discharge, if any at all. Flows are then simulated to decrease so further reducing the likelihood of dry season discharge.

Recommendations

Recommended studies and/or additional characterization work to reduce uncertainties in the modelling presented in this report are as follows:

- Complete water quality depth profiles for Main Pit to verify the thickness and volume of the lens of untreated pit water remaining at the bottom of the pit.
- Refine water management strategy to reflect the Stage 3 construction schedule, operating parameters, e.g. Main Pit level, for the conveyor system used for pit backfilling, water demands during the construction period, and water treatment system design.
- Complete a hydrogeological field investigation of the proposed SIS alignments near the Main WRD and Intermediate WRD to support SIS design, including the installation of additional monitoring bores and recovery bores, hydraulic testing, and water quality sampling during long-term pumping tests.
- Complete a hydrogeological field investigation of the Copper Extraction Pad area and former ore stockpile area, including additional monitoring bore and/or recovery bore installation and possible injection/extraction (push-pull) testing to constrain Cu desorption rates and the expected rate and degree of future groundwater quality improvements.
- Complete a hydrogeological field investigation of the proposed WSF footprints and areas upgradient of the footprints and downgradient of the footprints towards the Main Pit and/or Dyson's Area.
- Assess quality of daily streamflow records at GS8150200, GS8150327 and GS8150097, particularly for high flows determined by extrapolation of a rating curve and for low flows during the dry season and address potential implications for predictions.
- Validate the groundwater model to pit water levels and groundwater level data collected during the 2008 Intermediate Pit de-watering trial, when the pit water level was drawn down by 10 m for several weeks, to confirm the predicted extent of groundwater drawdown towards the vine thicket north of the pit.
- Undertake a laboratory geochemical testing program to assess Cu desorption rates from bedrock and/or soils that have been exposed to high Cu concentrations in liquor in the Copper

Extraction Pad area or seepage from the WRDS, including sequential leach testing and/or column tests.

- Conduct waste rock mixing trials to maximize the effectiveness of neutralant addition and ensure that the amount of neutralant added can be confirmed by field testing methods.
- Complete a laboratory geochemical testing program to refine the source term for lime-amended waste rock placed and compacted in the WSF that involves column testing and is supported by numerical modelling of drain-down rates and potential long-term seepage rates to groundwater.
- Estimate the magnitude of contaminant loads (fluxes) from PAF backfill materials in the Main Pit to the overlying pit water column and address potential water quality implications for the EBFR, should it be diverted through the Main Pit.
- Assess risk of flood waters from the EBFR impacting the pit backfilling operation, either by overtopping the EFDC or by reverse flow through the outlet culvert of the Intermediate Pit.
- Update the groundwater model to represent hydrogeological data and information collected during the Stage 3 works and any relevant laboratory testing data collected to refine source terms for the WSF and Main Pit backfill and seepage rates from the WSF.
- Update the WLBM to represent the updated groundwater model and refinements in the water management strategy and predict Cu and other CoC concentrations in the EBFR for a range of future climate conditions.

Report No. 183008/1

GROUNDWATER AND SURFACE WATER MODELLING REPORT, RUM JUNGLE STAGE 2A

Table of Contents

LIST OF TABLES

LIST OF FIGURES

LIST OF ACRONYMS AND ABBREVIATIONS

AHD	Australian Height Datum
Al	Aluminum
AMD	Acid and Metalliferous Drainage
bgs	below ground surface
Co	Cobalt
Cu	Copper
DEM	Digital Elevation Model
DPIR	Department of Primary Industry and Resources
DTW	depth-to-water
EC	Electric Conductivity
EMU	Environmental Monitoring Unit
ET	Evapotranspiration
EBFR	East Branch of the Finniss River
EFDC	East Finniss Diversion Channel
Fe	Iron
HCO_3	Bicarbonate
K_D	Distribution coefficient (linear sorption)
K	Hydraulic conductivity
K_h	Horizontal hydraulic conductivity
K_v	Vertical hydraulic conductivity
LDWQO	Locally-Derived Water Quality Objective
MAP	Mean Annual Precipitation
Mg	Magnesium
Mn	Manganese
MT3DMS	Modular Three-Dimensional Multispecies Transport Model
NAF	Non-acid forming
n	porosity

n_e	effective porosity
Ni	Nickel
NRMS	normalized root mean squared error
NT	Northern Territory
NWT	Newton Formulation for MODFLOW-2005
OKC	O'Kane Consultants Inc.
PAF	Potentially acid forming
Pb	Lead
PVC	polyvinyl chloride
R_f	Retardation factor
RJC	Rum Jungle Complex
RGC	Robertson GeoConsultants Inc.
RN	Registration number (groundwater bores)
SD	Saline Drainage
Se	Selenium
SMD	soil moisture deficit
SO_4	Sulphate
S_S	Specific Storage
S_y	Specific yield
TDS	Total Dissolved Solids
USGS	United States Geological Survey
WRD	Waste Rock Dump
WSF	Waste Storage Facility
Zn	Zinc

REPORT NO. 183008/1

GROUNDWATER AND SURFACE WATER MODELLING REPORT, RUM JUNGLE STAGE 2A

1 INTRODUCTION

1.1 GENERAL

This is the Robertson GeoConsultants Inc. (RGC) report on groundwater and surface water modelling for Stage 2A of the Rum Jungle Rehabilitation Project. It was prepared for the Northern Territory (NT) Department of Primary Industry and Resources (DPIR) in support of an Environmental Impact Statement (EIS) for the site. This report is the key deliverable for RGC contract Q-18-0503 with the DPIR and is appended to the EIS.

1.2 TERMS OF REFERENCE

The former Rum Jungle Mine Site (Rum Jungle) is located 105 km by road south of Darwin in the headwaters of the East Branch of the Finniss River (EBFR). Rum Jungle was one of Australia's first major uranium mines and produced approximately 3,500 tonnes of uranium and 20,000 tonnes of copper concentrate between 1953 and 1971 (Davy, 1975).

Groundwater and surface water quality at Rum Jungle are degraded by Acid and Metalliferous Drainage (AMD). The primary AMD sources are sulphide-bearing waste rock in the historic Waste Rock Dumps (WRDs) and leached low-grade ore and contaminated soils placed in shallow zones of Dyson's Pit during rehabilitation in 1984/1985 (see Allen and Verhoeven, 1986). Groundwater quality in some areas of the site is further degraded by historic AMD sources that were eliminated by rehabilitation in the 1980s or by metalliferous liquor lost during an experimental heap leach operation from 1965 to 1971 in the Copper Extraction Pad area.

AMD impacts to groundwater and to the EBFR have been intensively characterized and monitored by the DPIR since recent rehabilitation planning was initiated in 2010. Routine groundwater and surface water monitoring data collected by the DPIR and information gathered during geotechnical and hydrogeological field investigations in 2014, 2017, and 2018 are the basis for a conceptual hydrogeological model developed by RGC. The model has been developed iteratively since 2011 and was updated in 2019 to include additional information from hydrogeological field investigations in 2017 near the northern site boundary and in 2018 in the Copper Extraction Pad area.

Groundwater conditions are simulated with a numerical groundwater model that consists of a transient flow model and transient solute transport model that simulates sulphate (SO_4) and copper (Cu) transport in groundwater. The groundwater model uses a monthly time step and is calibrated for the period from July 2010 to July 2018. A Water and Load Balance Model (WLBM) was developed in GoldSim in 2019 to validate simulations from the groundwater model and predict SO_4 and Cu concentrations in the EBFR on a preliminary basis. The WLBM simulates streamflow (discharge) with the Australian Water Balance Model (AWBM) and is used to simulate water management during the construction period of rehabilitation.

Detrimental effects of elevated metals due to AMD on aquatic ecosystems in the EBFR and other downstream environmental values are detailed in Hydrobiology Pty Ltd. (2016) and references therein. Aquatic ecosystems are also described in Chapter 12 of this EIS. Hydrobiology Pty Ltd (2016) provides Locally Derived Water Quality Objectives (LDWQOs) for the EBFR. The LDWQOs have been developed since 2013 based on wet season and dry season sampling to assess water quality impacts to downstream environmental values. Cu is one of several metals that exceeds LDWQOs during the wet season when flows in the EBFR (and hence dilution) are highest. Cu is therefore considered a primary Contaminant of Concern (CoC) in the EBFR and decreasing concentrations is a key rehabilitation objective.

1.3 STUDY OBJECTIVES

Study objectives are to:

- Provide an updated conceptual hydrogeological model for the site that details the hydrogeological and hydrological data that are represented in the numerical groundwater model.
- Detail the structure and calibration of the numerical groundwater model for current conditions and describe how the model was adapted to predict future groundwater conditions.
- Document the groundwater modelling undertaken to predict groundwater flows and SO_4 and Cu loads in groundwater during the construction phase of rehabilitation and post-rehabilitation.
- Detail the structure and validation of the WLBM for the site and simulated SO_4 and Cu concentrations in the EBFR for current conditions.

- Summarize predictive modelling results that constrain the extent and the timing of future water quality improvements after rehabilitation works have been completed.
- Recommend technical studies that may help refine prediction of post-rehabilitation conditions at the site and determine how the future performance of the rehabilitation could be effectively monitored.

1.4 REPORT ORGANIZATION

The remainder of this report is subdivided into the following sections:

- **Section 2. Routine Water Monitoring** describes the location and key features of Rum Jungle, and results of routine surface water and groundwater monitoring.
- **Section 3. Conceptual Hydrogeological Model** describes conceptual hydrogeological model for the site, including hydrostratigraphic units, groundwater flow regime, groundwater quality observations, and conceptual groundwater budgets and load balances.
- **Section 4. Numerical Groundwater Model** describes the methods and results of numerical modeling of groundwater flow and transport of SO_4 and Cu in groundwater after rehabilitation.
- **Section 5. Numerical Water and Load Balance Model** describes simulated water and contaminant load balances for the Intermediate Pit and the EBFR for current conditions, the construction period, and post-rehabilitation.
- **Section 6. Key Findings** summarizes key modeling results, and their implications for future rehabilitation planning.
- **Section 7. Recommendations.** provides recommendations for additional studies and post-rehabilitation groundwater and surface water monitoring.

2 ROUTINE WATER MONITORING

2.1 STREAMFLOW GAUGING STATIONS

The EBFR is an intermittent river that flows approximately west and northwest through the former Rum Jungle mine site. Before mining, the EBFR flowed through the area now occupied by the Main Pit and the Intermediate Pit. The EBFR was partially dammed by the Sweetwater Dam and Acid Dam and diverted through the EFDC during mining operations in the 1950s and 1960s. These dams were removed during rehabilitation in 1984 and 1985 and a system of inlets and outlets was installed to convey a portion of flows in the EBFR through the Main Pit and, in turn, the Intermediate Pit. Flows between the pits occur only during high flow periods in the wet season. Flows between the pits occur in a channel near the northern perimeter of the former Copper Extraction Pad area. The EBFR returns to its natural channel near the road bridge near the western lease boundary (towards the Browns site) and flows northwest beyond the mine lease boundary.

Combined flows from the Intermediate Pit and through the EFDC are measured at gauge GS8150200. Gauge GS8150200, and downstream gauges GS8150327 and GS8150097, are shown in Figure 2-1 with catchment areas for each gauge. Each of these gauges is operated by the NT Government as part of regional monitoring. Other gauges have been operated by the DPIR in the past to monitor flows in and out of the pits (GS8150212 and GS8150213) but these gauges are not currently operated. Further details on the streamflow gauges currently operated are summarized below:

- **Gauge GS8150200**. This gauge is in the natural (pre-mining) EBFR channel downstream of the road bridge near the western lease boundary. It was installed in 1981 and records the combined flows of the EBFR through the EFDC and outflows from the Intermediate Pit. This gauge has operated continuously since 1981 and has a catchment area of 53 km^2 that includes most of lease boundary, except for the Old Tailings Dam area and Old Tailings Creek.
- **Gauge GS8150327**. This gauge is about 1.5 km downstream of gauge GS8150200 on private property. It was installed in 2010 at RGC's request to measure streamflow (and water quality) in the EBFR downstream of the entire lease domain, including flows from Old Tailings Creek and groundwater discharge to the EBFR downstream of GS8150200. This gauge has a catchment area of 59 km^2, including a 6 km^2 that is not part of the catchment area of GS8150200.
- **Gauge GS8150097**. Gauge GS8150097 is about 5 km downstream of GS8150327 and has been operated near-continuously since 1965. Several creeks discharge to the EBFR between gauges GS8150327 and GS8150097. This gauge has a catchment area of 65 km^2. This is slightly lower than previous catchment area estimates as RGC understands that the catchment area does not include a right-bank tributary that has been included in previous area estimates (A. Brandis, personal communication).

Gauges GS8150200, GS8150327, and GS8150097 record water level heights (in metres, m) at an irregular time step, with the highest monitoring frequency occurring in flood conditions when the water level is changing rapidly. The measured water levels are converted to equivalent discharge rates using a rating curve defined for each gauge. Discharge is reported in cubic meters per second (m^3/s). Streamflow data for each station seem to be reasonably reliable and no major issues with data quality were identified by RGC while developing the WLBM for the site (see RGC, 2019, for further details).

Streamflow data for each station seem to be reasonably reliable and no major issues with data quality were identified by RGC while developing the WLBM for the site. Peak discharges at gauge GS8150097 do, however, appear to be over-estimated as unit daily discharges can exceed daily rainfall amounts during high flow periods. Also, gauges GS8150200 and GS8150097 sometimes show flows in the dry season when true flows are zero. There are no practical implications to the over-estimation of peak flows in the EBFR as metal concentrations are often lowest during these periods.

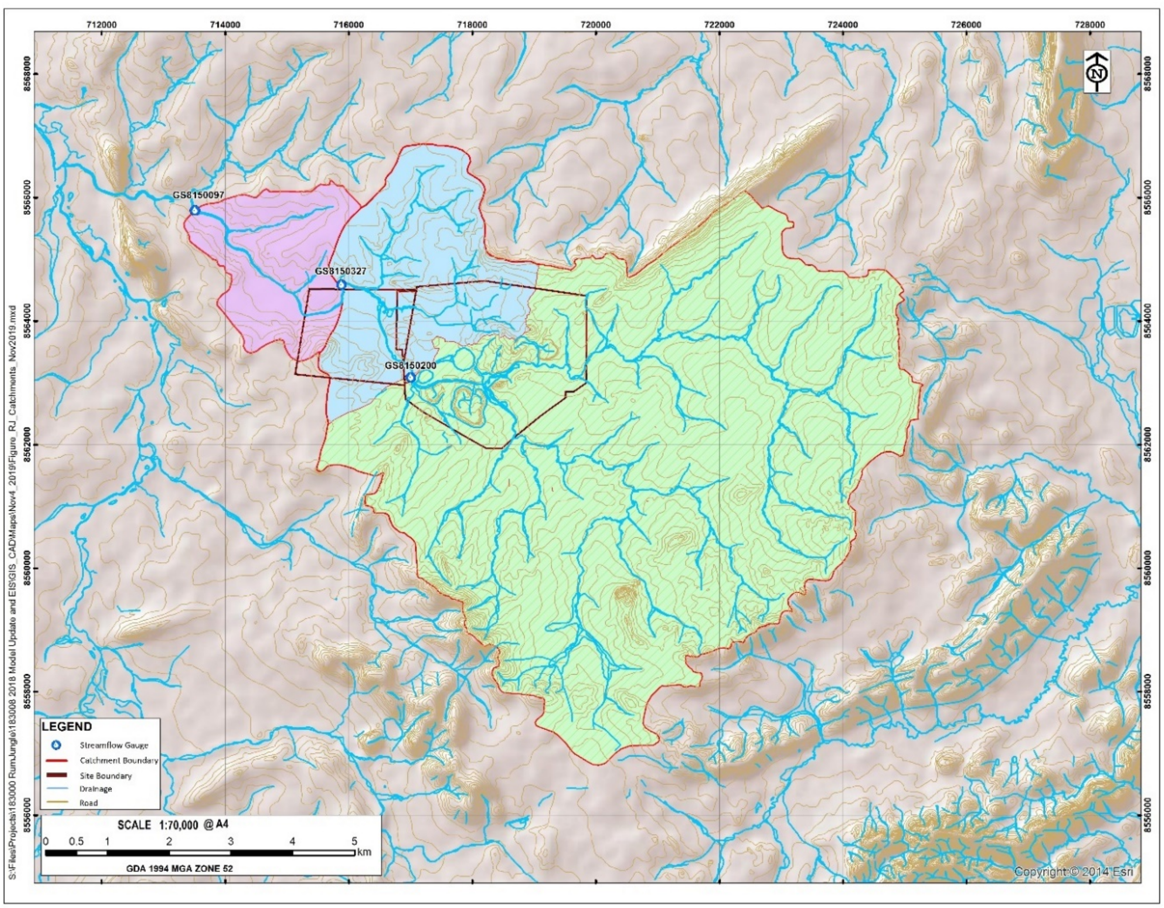

Figure 2-1. Streamflow Gauge Locations and Catchment Areas

2.2 SURFACE WATER QUALITY MONITORING

Water quality in the EBFR is routinely monitored at gauges GS8150200, GS8150327, and GS8150097. Gauge GS8150327 was installed because the EBFR appears to be inadequately mixed at GS8150200 and hence collecting a representative sample for water quality analysis can be problematic (Lawton and Overall, 2002). Gauge GS8150327 was installed in 2010 in part to avoid the mixing issues at GS8150200 and to also provide a record of the total streamflow through the lease boundary, including flows from Old Tailings Creek and groundwater discharge to the EBFR downstream of gauge GS8150200. Grab samples from each gauge have been collected several times per month by the DPIR's Environmental Monitoring Unit (EMU) during the wet season since 2010. Field pH, EC, and water temperature are measured during sampling.

Surface water samples are analyzed for SO_4, Ca, Mg, Na, K, Al-f, Al-t, Fe-f, Fe-t, Cu-f, Cu-t, Co-f, Co-t, Mn-f, Mn-t, Ni-f, Ni-t, U-f, U-t, Zn-f, and Zn-t, where 'f' denotes a filtered (<0.45 µm) sample that is acidified and 't' denotes an acid extractable total concentration, i.e. the concentration in an unfiltered and acidified sample. Total and bicarbonate alkalinity, in mg/L as $CaCO_3$, are determined by titration in the field. EMU also routinely collects duplicate samples and runs routine checks for EC, temperature, and pH measurements in the field and provides a charge (ionic) balance for each sample as part of QA/QC protocols. Hourly measurements of water temperature, EC, pH, and turbidity are made at each gauge.

2.3 GROUNDWATER MONITORING NETWORK

Groundwater monitoring bores are shown in Figure 2-2 with key site features and the mine lease boundary. The groundwater monitoring network consists of a series of historic bores referred to by their Registration Number (RN) and the MB10, MB12, MB14, MB17, and MB18 bore series. The MB prefix stands for "Monitoring Bore" and the integer denotes the year the bore was installed. Most of the bores were installed with 80 mm polyvinyl chloride (PVC) casing and machine-slotted PVC screens. An "S" denotes a shallower bore at a particular location and a "D" denotes the deeper bore, e.g. MB10-08S and MB10-08D. Most of the S and D bores were installed as paired installations, meaning the shallower bore was installed in a second, separate borehole nearby after the deeper bore was completed. Bores MB10-9S and MB10-9D are an exception as these bores were installed as a nested installation with 50 mm PVC casing in a single open borehole (RN022108) that was drilled in the 1983. Several monitoring bores in the Copper Extraction Pad area were also installed in existing exploration holes (see RGC, 2016).

Construction details for the RN and MB bore series are provided in Table 2-1, Table 2-2, and Table 2-3. Most of the RN bores were installed in the 1980s to support previous rehabilitation planning. Many of the RN bores are shallow (< 5 m deep) and therefore dry for part of the year when groundwater levels are below the bottom of the screen. The MB10 bores were installed in areas under-represented by the historic RN bores, either near the WRDs or downgradient to define the extent of groundwater quality impacts north of the central mining area towards the EBFR. The MB12 and MB18 bores were installed in the Copper Extraction Pad area to delineate the spatial extent and depth of groundwater quality impacts in this area. The MB14 (Old Tailings Dam area) and MB17 bores (near northern site boundary) were installed to characterize groundwater conditions near the waste storage facility (WSF) footprints proposed during previous project phases. Each of the MB bores was installed and developed under RGC supervision and further details are provided in RGC (2016) and references therein.

There is a single production bore (PB12-33) on site in the Copper Extraction Pad area. This bore was installed in 2012 to complete a one week pumping test in November 2012 to characterize the hydraulic properties of bedrock in this area and does not have a permanent pump installed. The 2012 pumping test has been interpreted to constrain the hydraulic properties of bedrock between the Main and Intermediate Pits. Additional information on the hydraulic properties near the Main Pit was provided by a geotechnical investigation of the pit rim in 2018 (see SRK, 2018). Monitoring bores were not installed during this investigation but airlift testing and other relevant testing was undertaken and the results were incorporated into RGC's updated conceptual hydrogeological model. Information from a geotechnical drilling program to assess tailings backfill in the Main Pit was also incorporated to confirm the depth to tailings below the pit lake surface.

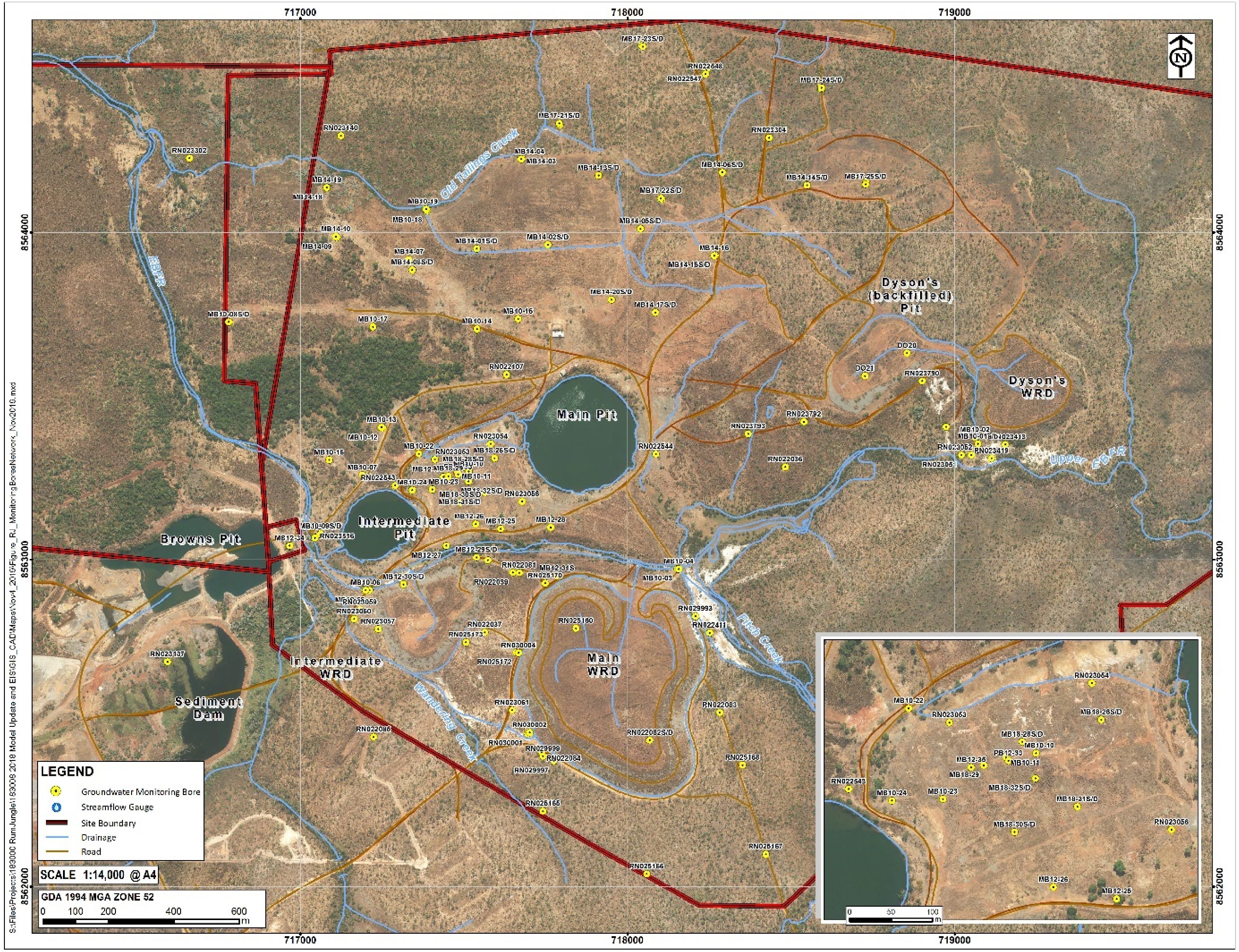

Figure 2-2. Groundwater Monitoring Network at the former Rum Jungle Mine Site

2.4 GROUNDWATER LEVEL MONITORING

The DPIR has routinely monitored groundwater levels in 43 RN bores and 66 additional MB bores installed in 2010, 2012, and 2014. EMU also measured groundwater levels in the MB17 and MB18 bores since they were installed. In 2018, a total of 160 bores were monitored monthly during the dry season and every two weeks during the wet season. This frequency was selected to characterize the substantial intra-annual (seasonal) variations in groundwater levels in some areas of the site and to infer the site-wide groundwater flow field at different times of the year. Depth-to-water measurements are collected manually from each bore with a water level tape. Measurements are collected from the top of the PVC casing and subtracted from professionally-surveyed top-of-casing (TOC) elevations to calculate the geodetic groundwater elevation relative to the Australian Height Datum (AHD), i.e. in m AHD.

Continuous groundwater level monitoring measurements collected by pressure transducers are also available for selected monitoring bores, including bore RN022081 (which has recorded since 1991) and bores MB14-02S/D, MB14-17S/D, and MB14-20S/D. Transducer data for selected MB bores were interpreted to monitor the rapid response of groundwater levels in some area due to rainfall infiltration and to derive recharge rates that were incorporated into the groundwater model.

2.5 GROUNDWATER QUALITY MONITORING

Groundwater quality sampling is routinely undertaken by the DPIR's Environmental Monitoring Unit (EMU). From 2010 to 2018, EMU collected water samples once per year in the dry season and once per year in the wet season from most of the bores on site. Seepage from the toes of the WRDs and Dyson's (backfilled) Pit is also sampled opportunistically by EMU or DPIR staff. In 2018, the scope of routine water quality monitoring was reduced to an annual sampling campaign in the dry season. This change was recommended by RGC because baseline conditions had been well-established from previous monitoring and there have been no changes on site that would necessitate measurements in both the wet season and dry. Dry season sampling is normally planned for August or September. Monthly routine groundwater level and pit water level monitoring continues.

Groundwater is sampled using a pumped "low flow" procedure with field parameters being measured in a flow-through cell in a field laboratory truck to ensure a representative sample is collected. EMU collects manual depth-to-water measurements with a water level tape and records the pH, temperature, and electrical conductivity (EC). Water samples are sent to an accredited laboratory in Darwin for analysis. Groundwater samples are analyzed for SO_4, Ca, Mg, Na, K, Al-f, Fe-f, Cu-f, Co-f, Mn-f, Ni-f, U-f, and Zn-f, where 'f' stands for filtered samples (<0.45 µm) that are acidified. EMU routinely collects duplicate samples and runs routine checks for EC, temperature, and pH measurements in the field and provides a charge (ionic) balance for each sample as part of QA/QC protocols.

Table 2-1. RN Bores in Dyson's Area and Near Main and Intermediate WRDs

Bore ID	Installation Date	Location/description	Borehole Depth	Screened Interval	Stickup[2]	TOC[3]	Screened lithology	Yield
			m bgs[1]	m bgs[1]	m	m AHD		L/s
RN Bores in Dyson's Area								
RN00259	Jul-44	Army bore	0.0	-	-	75.58	-	-
RN022035	May-83	Towards Main Pit	140.6	backfilled	-	68.01	Whites Formation (pyritic)	0.1
RN022036	May-83	Southwest of Dyson's (backfilled) Pit	14.2	7 to 12	0.32	76.06	Geolsec Formation	0.0
RN022544	Jan-84	Near eastern edge of Main Pit	44.5	35.2 to 44.5	0.87	65.78	Whites Formation (pyritic)	9.0
RN023051	Dec-85	Southwest of Dyson's WRD near upper EBFR	3.1	1.7 to 2.4	0.60	64.06	Alluvium	-
RN023052	Dec-85	Southwest of Dyson's WRD near upper EBFR	3.3	1.7 to 2.4	0.67	64.35	Alluviium	-
RN023413	Nov-84	Southwest of Dyson's WRD near upper EBFR	3.2	1.3 to 1.8	1.24	64.72	Laterite	-
RN023414	Nov-84	Southwest of Dyson's WRD near upper EBFR	2.4	1.0 to 1.5	0.86	64.02	Clay	-
RN023415	Nov-84	Southwest of Dyson's WRD near upper EBFR	2.8	1.2 to 1.8	1.33	64.78	Clay	-
RN023416	Nov-84	Southwest of Dyson's WRD near upper EBFR	2.8	1.2 to 1.8	1.11	64.30	Clay	-
RN023417	Nov-84	Southwest of Dyson's WRD near upper EBFR	2.1	0.3 to 0.8	0.69	64.73	Laterite	-
RN023418	Nov-84	Southwest of Dyson's WRD near upper EBFR	2.5	1.0 to 1.3	1.02	64.13	Clay	-
RN023419	Nov-84	Southwest of Dyson's WRD near upper EBFR	3.1	1.2 to 1.7	1.10	64.26	Alluvium	-
RN023420	Nov-84	Southwest of Dyson's WRD near upper EBFR	1.9	1.3 to 1.9	0.00	64.54	Clay	-
RN023790	May-85	Near southwest toe of Dyson's (backfilled) Pit	16.0	10 to 16	0.36	73.95	Geolsec Formation	10.0
RN023791	May-85	Near southern toe of Dyson's (backfilled) Pit	2.8	13 to 19	0.78	80.04	Whites Formation	0.2
RN023792	May-85	West of Dyson's (backfilled) Pit	26.2	20 to 26	0.52	83.80	Geolsec Formation	0.2
RN023793	May-85	West of Dyson's (backfilled) Pit	19.3	13.2 to 19.2	0.49	71.20	Whites Formation	0.2
RN Bores near Main and Intermediate WRDs								
RN022037	May-83	Southeast of the Intermediate WRD	22.8	16 to 22	0.51	67.18	Rum Jungle Complex (wtr)	0.1
RN022039	May-83	Between Main and Intermediate WRDs (near EFDC)	18.0	12 to 18	0.32	67.73	Quartz gravels	5
RN022081	May-83	Between Main and Intermediate WRDs (near EFDC)	43.9	40.7 to 43.9	0.86	68.75	Coomalie Dolostone	7.5
RN022082S	June-83	On top of Main WRD	17.0	11 to 17	0.49	94.24	Rum Jungle Complex (wtr)	0.1
RN022082D	June-83	On top of Main WRD	52.0	37 to 52	0.33	94.38	Rum Jungle Complex	0.1
RN022083	June-83	East of Main WRD near Fitch Creek	17.9	10 to 16	0.35	68.59	Rum Jungle Complex	0.6
RN022084	June-83	Near southwest toe of Main WRD	16.0	10 to 16	0.07	69.15	Rum Jungle Complex (wtr)	<0.1
RN022085	Jun-83	Upgradient of WRDs	32.0	24 to 32	0.92	73.99	Coomalie Dolomite	5
RN022410	Oct-83	East of Main WRD (near drainage channel)	1.9	0.3 to 1.1	0.50	64.45	Rum Jungle Complex (wtr)	0.5
RN022411	Oct-83	East of Main WRD (near drainage channel)	2.3	0.3 to 1.5	0.79	63.90	Alluvium	-
RN022412	Oct-83	East of Main WRD (near drainage channel)	2.7	0.4 to 2.1	0.46	70.43	Rum Jungle Complex (wtr)	0.1
RN022413	Oct-83	East of Main WRD (near drainage channel)	2.8	0.4 to 2.4	0.64	70.14	Sandy clay	0.5
RN022414	Oct-83	East of Main WRD (near drainage channel)	2.9	0.4 to 2.5	0.63	68.90	Rum Jungle Complex (wtr)	0.1
RN022417	Nov-83	Southwest of Main WRD	3.1	0.4 to 2.5	0.89	66.60	Rum Jungle Complex (wtr)	0.1
RN022418	Nov-83	Near southwest toe of Main WRD	2.2	0.4 to 2.0	0.53	64.02	Rum Jungle Complex (wtr)	0.1
RN023057	Oct-83	West of Intermediate WRD	3.4	1.8 to 2.6	0.72	61.77	Whites Formation (wtr)	-
RN023058	Oct-83	West of Intermediate WRD	4.3	2.6 to 3.7	0.65	62.29	Whites Formation (wtr)	-
RN023059	Dec-85	West of Intermediate WRD	5.7	4.2 to 5.2	0.76	60.87	Whites Formation (wtr)	-
RN023060	Dec-85	West of Intermediate WRD	5.1	4.2 to 5.1		60.87	Whites Formation (wtr)	-
RN023061	Dec-85	Near western toe of Main WRD	3.2	1.8 to 2.5	0.74	68.69	Rum Jungle Complex (wtr)	0.1
RN023062	Dec-85	Southwest of Main WRD (near Wandering Creek)	2.8	1.5 to 2.2	0.71	66.28	Rum Jungle Complex (wtr)	0.1
RN023063	Dec-85	Southwest of Main WRD (near Wandering Creek)	2.1	0.9 to 1.3	0.79	65.18	Rum Jungle Complex (wtr)	0.1
RN023064	Dec-85	Southwest of Main WRD (near Wandering Creek)	2.6	1.2 to 1.8	0.82	64.22	Alluvium	-
RN023510	Nov-84	East of Main WRD (near drainage channel)	3.1	1.5 to 2.1	1.05	64.27	Laterite	-
RN023511	Nov-84	East of Main WRD (near drainage channel)	2.6	1.1 to 1.6	1.12	64.20	Laterite	-
RN023512	Nov-84	East of Main WRD (near drainage channel)	2.5	1.1 to 1.5	1.01	64.81	Laterite	-
RN023513	Nov-84	East of Main WRD (near drainage channel)	3.2	1.5 to 2.2	0.97	65.63	Laterite	-
RN023514	Nov-84	Southwest of Main WRD	2.8	1.4 to 1.9	0.98	70.07	Laterite	-
RN025160	Jun-87	On top of Main WRD	16.9	13.9 to 16.9	0.09	87.02	Waste rock	0
RN025161	Jun-87	On top of Main WRD	18.7	15.7 to 18.7	0.03	88.95	Waste rock	-
RN025162	Jun-87	On top of Main WRD	20.8	17.8 to 20.8	0.12	84.63	Waste rock	0
RN025163	Jun-87	Southeast of Main WRD	6.0	backfilled	0.31	73.91	Rum Jungle Complex (wtr)	-
RN025165	Jun-87	Southwest of Main WRD	8.2	5.2 to 8.2	0.56	69.92	Rum Jungle Complex (wtr)	-
RN025166	Jun-87	Southwest of Main WRD	6.2	3.2 to 6.2	0.41	77.19	Rum Jungle Complex (wtr)	-
RN025167	Jun-87	Southeast of Main WRD	6.2	3.2 to 6.2	0.36	70.43	Rum Jungle Complex (wtr)	0.1
RN025168	Jun-87	Southeast of Main WRD	9.5	6.5 to 9.5	0.37	69.89	Rum Jungle Complex (wtr)	0.1
RN025169	Jun-87	North of Main WRD (near EFDC)	5.8	2.8 to 5.8	0.46	74.57	Laterite	-
RN025170	Jun-87	Northwest of Main WRD (near EFDC)	8.9	5.9 to 8.9	0.43	73.31	Rum Jungle Complex (wtr)	0.1
RN025171	Jun-87	Northwest of Main WRD (near EFDC)	6.2	2.8 to 5.8	0.52	65.97	Laterite	-
RN025172	Jun-87	Near western toe of White's Overburden Heap	4.7	1.7 to 4.7	0.35	70.28	Rum Jungle Complex (wtr)	-
RN025173	Jun-87	Near southeastern toe of the Intermediate WRD	7.8	5.1 to 8.1	0.37	64.72	Rum Jungle Complex (wtr)	-
RN029990	May-95	Northeast of Main WRD (near drainage channel)	5.8	1.5 to 5.2	0.30	63.57	Rum Jungle Complex	0.1
RN029991	May-95	Northeast of Main WRD (near drainage channel)	2.8	1.0 to 2.6	0.32	63.81	Rum Jungle Complex	0.1
RN029992	May-95	Northeast of Main WRD (near drainage channel)	5.6	1.5 to 5.2	0.31	63.32	Rum Jungle Complex (wtr)	0.4
RN029993	May-95	Northeast of Main WRD (near drainage channel)	7.5	1.0 to 7.2	0.72	63.88	Clay	-
RN029994	May-95	Northeast of Main WRD (near drainage channel)	2.2	1.0 to 2.5	0.50	64.21	Rum Jungle Complex (wtr)	-
RN029995	May-95	Northeast of Main WRD (near drainage channel)	3.5	1.0 to 3.0	0.56	64.39	Rum Jungle Complex	-
RN029997	May-95	Southwest of Main WRD	3.3	1.0 to 3.3	0.36	70.27	Quartz gravels	-
RN029998	May-95	Southwest of Main WRD	5.6	1.0 to 5.6	0.50	70.41	Quartz gravels	-
RN029999	May-95	Southwest of Main WRD	8.5	1.0 to 7.8	0.63	69.87	Quartz gravels	-
RN030000	May-95	Southwest of Main WRD	0.3	1.0 to 7.4	0.62	69.91	Quartz gravels	-
RN030001	May-95	Southwest of Main WRD	6.8	1.0 to 6.6	0.37	68.53	Quartz gravels	-
RN030002	May-95	Southwest of Main WRD	8.9	1.0 to 8.4	0.57	68.91	Quartz gravels	-
RN030003	May-95	Southwest of Main WRD	4.4	0.9 to 3.7	0.59	68.43	Sandstone	-
RN030004	May-95	Near western toe of Main WRD	3.4	1.5 to 2.9	0.52	70.80	Sandstone	-

1. bgs = below ground surface
3. TOC = Top of casing
Note: wtr = weathered

Table 2-2. RN Bores Near Pits and MB10 and MB12 Bores

Bore ID	Installation Date	Location/description	Borehole Depth	Screened Interval	Stickup[2]	TOC[3]	Screened lithology	Yield
			m bgs[1]	m bgs[1]	m	m AHD		L/s
RN Bores near the Main Pit and Intermediate Pit								
RN022108	May-83	'Open hole' bore near road bridge (now PMB9S/D)	30.0	'open hole'	0.50	59.84	Coomalie Dolostone	30
RN022543	Jan-84	Near Intermediate Open Cut	33.0	23 to 33	1.08	61.25	Coomalie Dolostone	6.00
RN022546	Jan-84	Near White's Open Cut	5.4	backfilled	0.00	64.81	-	-
RN023053	Dec-85	In former copper heap leach area	3.9	2.1 to 3	0.90	61.95	Whites Formation (wtr)	-
RN023054	Dec-85	In former copper heap leach area	3.2	1.2 to 2.6	0.58	61.62	Whites Formation (wtr)	-
RN023055	Dec-85	In former copper heap leach area	4.3	2.5 to 3.6	0.70	62.78	Whites Formation (wtr)	-
RN023056	Dec-85	In former copper heap leach area	5.4	3.9 to 4.7	0.70	64.86	Whites Formation (wtr)	-
RN023516	Nov-84	Near EFDC (west of Intermediate Open Cut)	4.9	3.1 tp 3.9	0.92	60.40	Alluvium	-
RN023517	Nov-84	Near EFDC (west of Intermediate Open Cut)	3.1	1.7 to 2.4	0.80	60.25	Alluvium	-
RN023518	Nov-84	Near EFDC (west of Intermediate Open Cut)	3.0	1.3 to 1.9	0.99	59.34	Alluvium	-
RN023519	Nov-84	Near EFDC (west of Intermediate Open Cut)	4.7	3.0 to 3.8	0.95	59.35	Alluvium	-
RN022085	Jun-83	Upgradient of mine site	32.0	24 to 32	0.92	73.99	Coomalie Dolostone	5
RN Bores in Old Tailings Dam Area								
RN023304	Oct-84	Near northern boundary of mine site	26.4	20.9 to 26.4	0.58	75.97	Coomalie Dolostone	4.0
RN022547	Jan-84	Near northern boundary of mine site	23.0	17 to 23	0.68	75.32	Whites Formation (pyritic)	1.5
RN022548	Jan-84	Near northern boundary of mine site	30.5	27.9 to 30.5	0.06	74.82	Coomalie Dolostone	13.5
RN022107	Jun-83	NW of White's Open Cut	14.8	12.8 to 14.8	0.57	62.88	Coomalie Dolostone	25.0
RN023140	Oct-84	North of Old Tailings Creek	18.0	11 to 16	0.60	62.32	Coomalie Dolostone	4.2
RN023139	Sep-84	West of East Finniss River (d/s of mine site)	30.0		0.68	57.37	Geolsec Formation	0.1
RN023302	Oct-84	North of Old Tailings Creek	12.5	9.5 to 12.5	0.35	57.27	Coomalie Dolostone	1.3
MB10 Bores								
MB10-01a	Nov-10	In drainage channel from Dyson's (backfilled) Open C	3.4	1.4 to 3.4	0.74	69.88	Saprolite	n.d.
MB10-01b	Nov-10	Adjacent to braided channel south of Dyson's (backfil	3.7	2.2 to 3.7	1.22	70.73	Alluvium	n.d.
MB10-02	Nov-10	Bedrock beneath Dyson's area	18.7	12.7 to 18.7	0.68	70.73	Rum Jungle Complex	0.1
MB10-03	Nov-10	Saprolite (and some alluvium) near the head of EFDC	3.5	1.97 to 3.47	0.66	68.56	Saprolite/alluvium	n.d.
MB10-04	Nov-10	Bedrock beneath the EFDC (near White's Overburden	15.3	9.34 to 15.34	0.73	68.76	Rum Jungle Complex	0.1
MB10-05	Nov-10	Near Intermediate Overburden Heap	5.0	2.0 to 5.0	0.77	65.44	Overburden	n.d.
MB10-06	Nov-10	Bedrock near Intermediate Overburden Heap (next to	25.5	13.5 to 25.5	0.73	66.29	Whites Formation	2
MB10-07	Dec-10	Downgradient of Intermediate Open Cut near East Fin	18.0	9 to 18	0.55	65.70	Coomalie Dolostone	1.5
MB10-08S	Nov-10	West of the East Finniss River	14.6	5.56 to 14.56	0.62	65.78	Laterite	n.d.
MB10-08D	Nov-10	West of the East Finniss River	23.0	20 to 23	0.71	65.95	Geolsec Formation	0.1
MB10-09S	Dec-10	Near East Finniss River (formerly RN022108)	29.2	23.4 to 29.4	1.00	65.44	Coomalie Dolostone	n.d.
MB10-09D	Dec-10	Near East Finniss River (formerly RN022108)	61.3	46.26 to 62.26	0.92	65.51	Coomalie Dolostone	n.d.
MB10-10	Dec-10	In former copper heap leach area	32.0	16 to 32	0.55	67.66	Whites Formation	n.d.
MB10-11	Dec-10	In former copper heap leach area	34.5	31.5 to 34.5	0.55	67.61	Alluvium	8
MB10-12	Dec-10	North of former heap leach area	24.6	12.62 to 24.62	0.44	66.73	Coomalie Dolostone	2
MB10-13	Dec-10	North of former heap leach area	60.8	48.77 to 60.77	0.58	66.85	Coomalie Dolostone	2
MB10-14	Dec-10	North of White's Open Cut	16.2	14.23 to 16.23	0.70	69.96	Coomalie Dolostone	50
MB10-15	Dec-10	North of White's Open Cut	24.4	12.41 to 24.41	0.43	68.48	Coomalie Dolostone	1
MB10-16	Dec-10	North of former heap leach area	22.6	13.5 to 22.5	0.26	66.22	Coomalie Dolostone	1
MB10-17	Dec-10	North of former heap leach area	26.0	20 to 26	0.60	68.59	Coomalie Dolostone	10
MB10-18	Nov-10	Near Old Tailings Creek	8.0	1.97 to 7.97	0.48	66.40	Saprolite/alluvium	n.d.
MB10-19	Nov-10	Near Old Tailings Creek	24.5	12.53 to 24.53	0.57	66.35	Coomalie Dolomite	1
MB10-20	Nov-10	Downstream of site	6.9	2.87 to 6.87	1.27	60.48	Alluvium	n.d.
MB10-21	Nov-10	Downstream of site	32.1	12.14 to 32.14	0.67	60.47	Rum Jungle Complex	0.1
MB10-22	Dec-10	Near former heap leach area	24.6	12.58 to 24.58	0.70	67.01	Coomalie Dolostone	n.d.
MB10-23	Dec-10	Near former heap leach area	25.0	13 to 25	0.50	67.25	Coomalie Dolostone	n.d.
MB10-24	Dec-10	Near former heap leach area	16.0	4 to 16	0.61	65.98	Coomalie Dolostone	n.d.

1. bgs = below ground surface
3. TOC = Top of casing
Note: wtr = weathered

Table 2-3. RN Bores in the Old Tailings Dam Area and MB14 Bores

Bore ID	Installation Date	Location/description	Borehole Depth	Screened Interval	Stickup[2]	TOC[3]	Screened lithology	Yield
			m bgs[1]	m bgs[1]	m	m AHD		L/s
MB17 Bores								
MB17-21S	Dec-17	Near northern site boundary	8.0	2.0 to 8.0	0.78	66.06	Coomalie Dolostone (wtr)	n.d.
MB17-21D	Dec-17	Near northern site boundary	24.0	18.0 to 24.0	0.83	65.98	Coomalie Dolostone	n.d.
MB17-22S	Dec-17	Upgradient of Old Tailings Dam area	8.0	2.0 to 8.0	0.86	70.25	Laterite	n.d.
MB17-22D	Dec-17	Upgradient of Old Tailings Dam area	24.0	18.0 to 24.0	0.94	70.32	Geolsec Formation	n.d.
MB17-23S	Dec-17	Near northern site boundary	8.0	2.0 to 8.0	0.87	77.30	Coomalie Dolostone (wtr)	n.d.
MB17-23D	Dec-17	Near northern site boundary	24.0	17.8 to 23.8	0.99	77.42	Coomalie Dolostone	n.d.
MB17-24S	Dec-17	Near northern site boundary	8.0	2.0 to 8.0	0.93	78.59	Laterite	n.d.
MB17-24D	Dec-17	Near northern site boundary	42.0	18.0 to 24.0	0.88	78.50	Coomalie Dolostone (wtr)	n.d.
MB17-25S	Dec-17	Upgradient of Old Tailings Dam area	8.0	2.0 to 8.0	0.85	80.54	Laterite	n.d.
MB17-25D	Dec-17	Upgradient of Old Tailings Dam area	42.0	18.0 to 24.0	0.91	80.62	Whites Formation (wtr)	n.d.
MB18 Bores								
MB18-26S	Dec-18	Beneath former storage ponds	60.0	12.0 to 18.0	0.71	62.29	Whites Formation (wtr)	n.d.
MB18-26D	Dec-18	Beneath former storage ponds	60.0	42.0 to 60.0	0.69	62.27	Whites Formation	n.d.
MB18-28S	Dec-18	Near fault zone (beneath former collection ditch)	60.0	12.0 to 24.0	0.93	62.61	Whites Formation (wtr)	n.d.
MB18-28D	Dec-18	Near fault zone (beneath former collection ditch)	60.0	42.0 to 60.0	0.15	61.83	Whites Formation (fractured)	n.d.
MB18-29	Dec-18	Near fault zone (beneath former collection ditch)	78.0	60.0 to 78.0	0.76	62.65	Whites Formation (fractured)	n.d.
MB18-30S	Dec-18	South of fault zone (towards EFDC)	60.0	13.7 to 19.7	0.86	64.27	Whites Formation	n.d.
MB18-30D	Dec-18	South of fault zone (towards EFDC)	60.0	42.0 to 60.0	0.84	64.25	Whites Formation	n.d.
MB18-31S	Dec-18	South of fault zone (towards EFDC)	60.0	18.0 to 24.0	0.84	63.94	Whites Formation	n.d.
MB18-31D	Dec-18	South of fault zone (towards EFDC)	60.0	42.0 to 60.0	0.85	63.95	Whites Formation	n.d.
MB18-32S	Dec-18	South of fault zone (towards EFDC)	60.0	12.0 to 24.0	0.60	63.04	Whites Formation (wtr)	n.d.
MB18-32D	Dec-18	South of fault zone (towards EFDC)	60.0	42.0 to 60.0	0.60	63.04	Whites Formation	n.d.

1. bgs = below ground surface
3. TOC = Top of casing
Note: wtr = weathered

2.6 PIT WATER MONITORING

Pit water quality profiling was undertaken periodically since rehabilitation in the 1980s to characterize the degree of stratification and mixing in the Main Pit and Intermediate Pit due to inflows from the EBFR (see Lawton and Overall, 2002a,b). Additional profiling was done in 2008 (see Tropical Water Solutions, 2008) and by EMU in 2014. Samples of pit water at surface and flowing from the Intermediate Pit have also been routinely collected by the DPIR and/or EMU. Monitoring was suspended in 2018 and has not been undertaken since. Samples from the pits are also collected as part of routine monitoring undertaken by the operators of the adjacent Browns site for their Waste Discharge License (WDL). Pit water levels in the Main Pit and Intermediate Pit are monitored monthly or every two weeks by the DPIR as part of routine groundwater monitoring. Pit water levels in the Browns Pits are not routinely monitored but some data from 2008 to 2011 are available (see RGC, 2012a).

3 CONCEPTUAL HYDROGEOLOGICAL MODEL

3.1 OVERVIEW

This section describes RGC's conceptual hydrogeological model for the former Rum Jungle Mine Site. Most of the information in this section was first provided in RGC (2016) and that report provides some additional supporting data and text that is not repeated here. Key updates to the conceptual hydrogeological model were made in 2019 to reflect additional information from hydrogeological field investigations in 2017 and 2018 and additional monitoring data collected since RGC (2016) was prepared. The 2018 hydrogeological investigation is particularly important because it shows the copper plume in the Copper Extraction Pad area is much less extensive than assumed in RGC (2016). Information from the 2017 hydrogeological field investigation and subsequent groundwater level monitoring necessitated the refinement of the local groundwater flow field near the northern site boundary and the proposed location of the northern WSF (see Section 2.4.9). Other aspects of the conceptual model (not updated in 2019) are provided here for ease of reference.

3.2 CLIMATE

The site is characterized by a tropical wet-dry season and subjected to monsoon rains due to its location in the Australian summer monsoon belt (Petheram et al., 2018). Monthly rainfall data for the weather station established in 2010 near the Main WRD is summarized in Table 3-1. Rainfall data for the weather station near the Main WRD are used throughout this chapter unless otherwise specified. Any missing data for this station were patched using data from the Batchelor Airport, Station 014727. Mean annual precipitation (MAP) is 1539 mm, all of which occurs as rainfall. More than 90% of MAP occurs during a distinct wet season that lasts from November to April. Mean monthly maximum temperatures at the Batchelor Airport range from 31°C in June to 37°C in October (during the 'build up' to the wet season).

Table 3-1. Historical Average Monthly Rainfall and Extremes for the Study Area

Wet Season	Jul	Aug	Sep	Oct	Nov	Dec	Jan	Feb	Mar	Apr	May	Jun	Annual
Gauge near the Main Waste Rock Dump													
2010/2011	17	0	36	138	84	322	578	697	382	165	0	0	2417
2011/2012	0	0	0	57	112	152	362	230	419	15	30	0	1377
2012/2013	0	0	5	30	138	144	257	237	331	51	185	1	1379
2013/2014	0	5	25	79	193	332	539	373	76	74	33	0	1730
2014/2015	0	0	0	16	72	211	316	255	162	57	0	1	1090
2015/2016	0	0	7	18	48	546	158	161	218	5	124	0	1284
2016/2017	15	0	39	48	141	392	270	275	240	6	1	0	1428
2017/2018	0	0	0	160	207	145	757	110	124	107	0	0	1610
Average	4	1	14	68	124	280	405	292	244	60	47	0	1539
Min	0	0	0	16	48	144	158	110	76	5	0	0	1090
Max	17	5	39	160	207	546	757	697	419	165	185	1	2417
Count	248	248	239	248	235	246	240	220	242	239	247	239	2891

Note: months predominantly patched with data from the Batchelor Airport Weather Station (014272) are in red font

3.3 MODEL DOMAIN

Figure 3-1 shows the conceptual model domain. These boundaries enclose an area of approximately 14.1 km^2 or about 20% of the total catchment area of the EBFR at gauge GS8150097. GS8150097 is approximately 6 km downstream of gauge GS8150327, which was installed in 2010 to define the downstream limit of the model domain. The boundaries of the model domain (shown in red) were defined by local topographic highs and low-lying drainage features so cross-boundary flows into the groundwater system are assumed to be negligible. The area west of the EBFR, including the Browns site, is included in the model domain because future development of the Browns mine could influence the local groundwater flow and contaminant transport within the former Rum Jungle mine site if the pit is expanded and/or de-watered.

Minor groundwater flows could enter the model domain along Fitch Creek and the upper EBFR in Dyson's Area. However, these potential cross-boundary flows are assumed to be negligible relative to the overall water balance due to the absence of significant hydraulic gradients and the shallow thickness of alluvium. Similarly, groundwater outflow ("underflow") leaving the model domain at the downstream boundary along the EBFR (beneath gauge GS8150327) is assumed to be negligible. Instead, it is assumed that all groundwater is forced to discharge into the EBFR at this location due to bedrock outcropping in this area (see RGC, 2016).

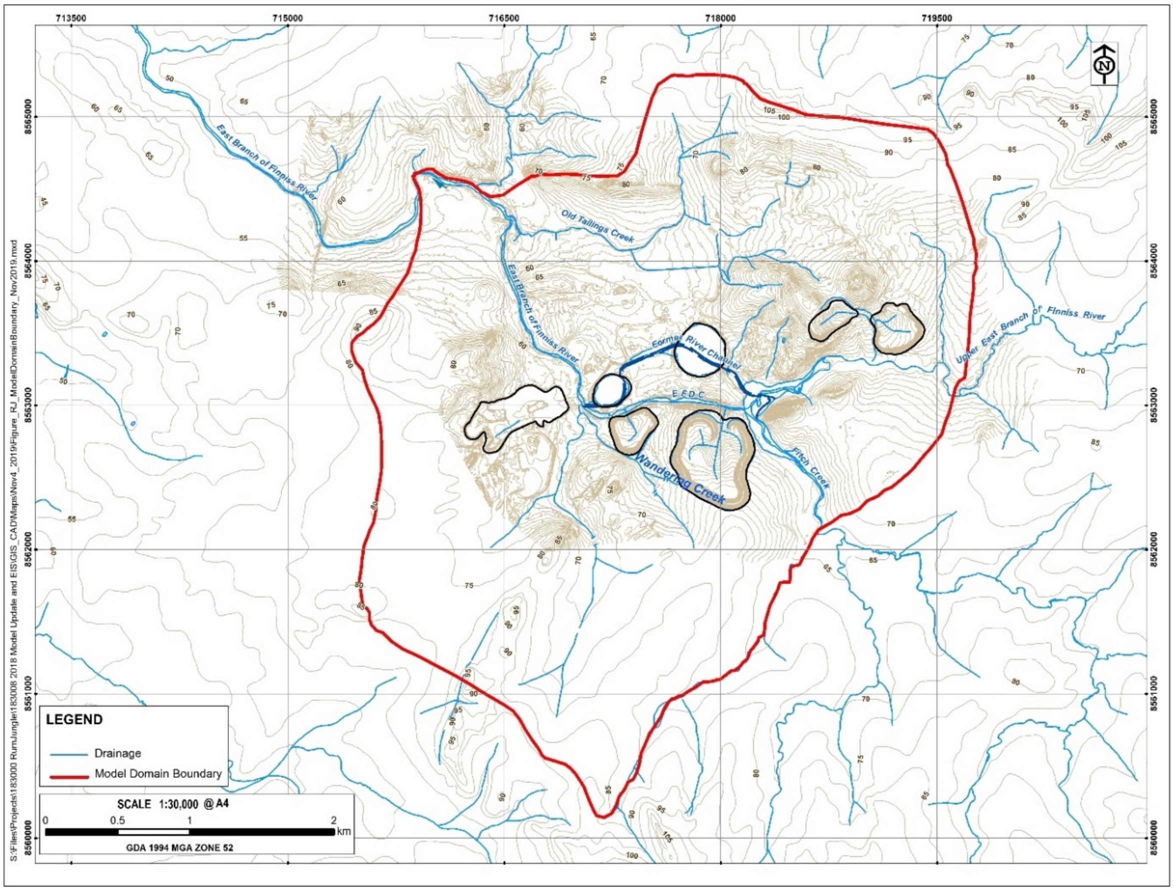

Figure 3-1. Conceptual Model Domain

3.4 LOCAL GEOLOGY

The site is situated in a triangular area of the Rum Jungle mineral field that is bounded by the Giant's Reef Fault to the south and a series of east-trending ridges to the north (Figure 3-2). This triangular area, known as "The Embayment", lies on the shallow-dipping limb of a northeast-trending, south-west plunging asymmetric syncline that has been cut by northerly-dipping faults (McCready et al., 2001). The main lithologic units in The Embayment are the Rum Jungle Complex and meta-sedimentary and subordinate meta-volcanic rocks of the Mount Partridge Group. The Rum Jungle Complex consists mainly of granites and occurs primarily along the south-eastern side of the Giant's Reef Fault. The Mount Partridge Group occurs north of the fault and consists of the following sedimentary units (from younger to older): Geolsec Formation, the Whites Formation, the Coomalie Dolostone, and the Crater Formation.

The Coomalie Dolostone is the predominant lithology to the north of the flooded pits in the Old Tailings Dam area and underlies a portion of the Intermediate WRD and Dyson's WRD. The Rum Jungle

Complex underlies most of the Main WRD and Dyson's WRD. Whites Formation occurs mainly near the pits as it hosted economic mineralization. The Crater Formation only occurs along the northern lease boundary. Sedimentary units are often fractured and karst features are observed in the Coomalie Dolostone. Bedrock is overlain by laterite or saprolite and alluvial sediments occur near Fitch Creek, the upper EBFR, and the natural EBFR channel downstream of gauge GS8150200. There are few sediments in the EFDC, which was cut approximately 5 m into bedrock to accommodate the EBFR during historical mining operations (see Allen and Verhoeven, 1986).

Groundwater flows at the Rum Jungle mine site predominantly occur in shallow residual soils derived from local bedrock and the underlying, moderately-to-slightly weathered and/or fractured bedrock. Rocks of the entire Mount Partridge Group have been folded, faulted and metamorphosed to greenschist facies during the 1880 Ma Barramundi orogeny but the original stratigraphic succession has been preserved (McCready et al., 2004). Brittle failure associated with deformation has produced several faults, some of which follow the northeast-southwest structural trend.

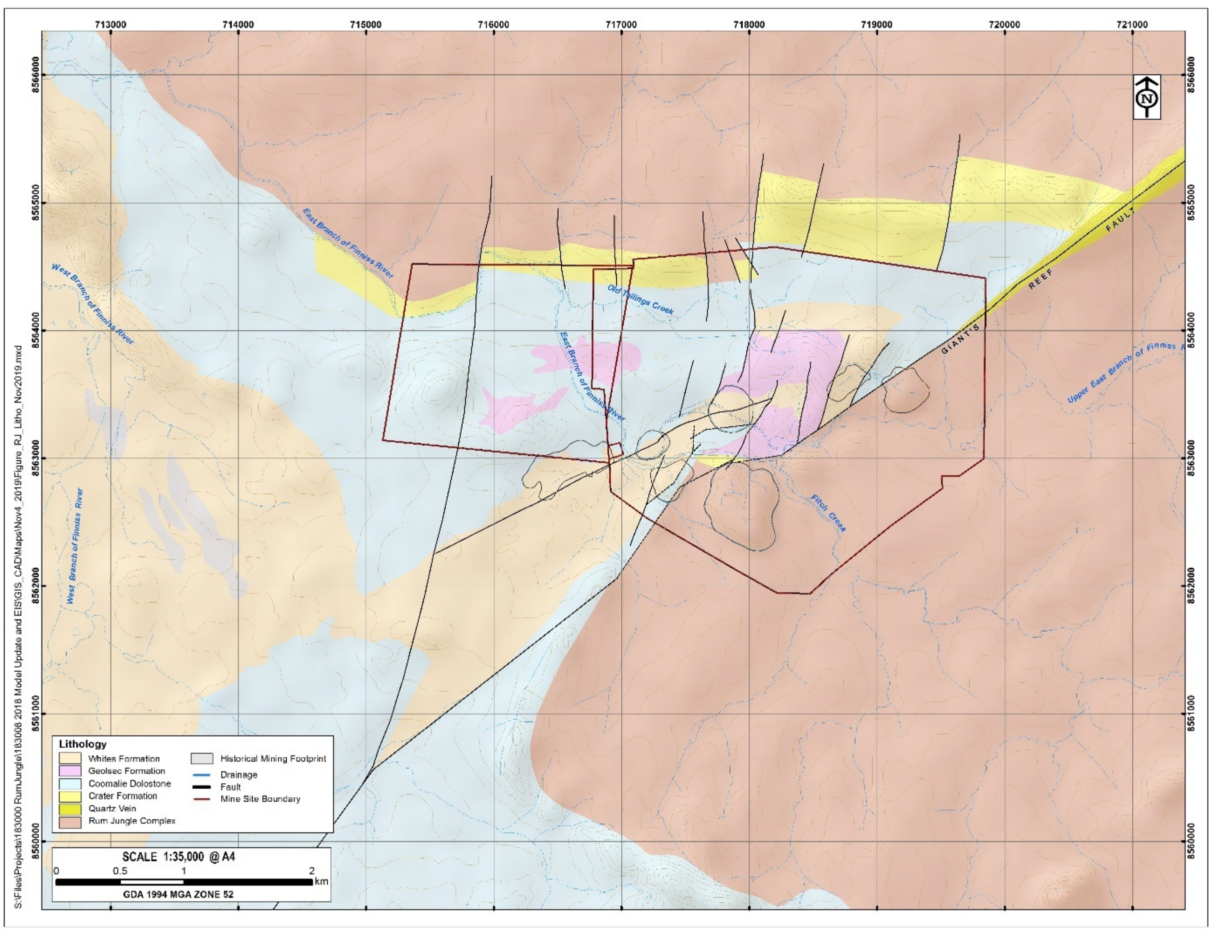

Figure 3-2. Lithologic Units in "The Embayment"

3.5 Hydrostratigraphic Units

The hydrostratigraphic units at the mine site are divided into unconsolidated (overburden) and consolidated (bedrock) units. The units and sub-units are discussed in detail in the subsections below. Figure 3-3 presents a simplified illustration of the hydrostratigraphic units at the mine site as well as the ranges of hydraulic conductivity (K) values estimated for each unit. Table 3-2 summarizes the hydraulic testing results from the 2010, 2012 and 2014 hydrogeological field investigations.

3.5.1 Unconsolidated Materials

Unconsolidated materials consist of laterite, saprolite, and alluvium and mine waste that have been used as fill or placed in the WRDs (see Section 2.4.5.7). Further details on alluvium, laterite, and saprolite are provided below:

- Alluvium is comprised of riverine sands and gravels that occur near the EBFR, including deposits along the EBFR pre-mining channel between the flooded Main Pit and Intermediate Pit. Alluvium deposits up to 9 m thick were observed at monitoring bore MB10-22 along the former course of the EBFR. Alluvial deposits are, however, typically less than 5 m in thickness. Alluvium in the EFDC is assumed to be negligible as the EFDC cuts into bedrock and deposits of transported material along the channel are thin and discontinuous. No hydraulic testing is available for alluvium but it is inferred to be relatively high K, i.e. $5x10^{-5}$ to $5x10^{-4}$ m/s.

- Laterite (and fill materials) that comprises the shallow soil unit extending through the Old Tailings Dam area to the EBFR and some areas of the central mining area, e.g. bores MB12-25 to MB12-29 was encountered at thicknesses of up to 8 m. Slug testing results for monitoring bores screened in laterite and fill indicate K values ranging from 2×10^{-6} m/s to 1×10^{-5} m/s. Infiltration testing conducted during the 2014 geotechnical test pitting program at test pits indicate K values ranging from 8×10^{-5} m/s to 2×10^{-4} m/s. The geometric mean of all available hydraulic testing results for laterite is 2×10^{-5} m/s.

- Saprolite soils that underlie the shallow fill and laterite soils in the Old Tailings Dam area were encountered with thicknesses of up to 8 m but are typically in the range of 2 to 5 m thick. Saprolite was not observed overlying the Geolsec Formation or Whites Formation or the Coomalie Dolostone south of the central mining area (near the Intermediate WRD). Saprolite soils are expected to have K values that are lower than the underlying (moderately to slightly) weathered Coomalie Dolostone. Slug testing at monitoring bores screened in saprolite suggest K values ranging from 7×10^{-7} to 4×10^{-6} m/s with a geometric mean of $2x10^{-6}$ m/s.

Soils testing of laterite and saprolite samples collected from the Old Tailings Dam area during a test pitting program in 2014 indicate grain sizes typical of silts and clays which suggest relatively high porosity and low specific yield (S_y). However, samples collected during a test pitting program in 2015 indicate coarser laterite of sand and gravel at higher elevations to the east of the Old Tailings Dam area suggesting S_y could be higher. S_y values for clays have been estimated by Morris and Johnson (1967) to range from 0% to 6%, with coarser particles increasing S_y to 12%.

Based on the laboratory reported moisture contents of three laterite samples from the Old Tailings Dam area, S_y is estimated to range from 4% to 9% with an average of 7%. The laboratory results for one sample northeast of the Old Tailings Dam area indicated a S_y of 11%. These estimates are also based on assumed dry densities and the assumption that the moisture contents represent specific retention, i.e. gravity drained conditions. If laterite is over-dried due to evaporation, the actual S_y would be lower than estimated. If the soils are not fully drained, the estimates of S_y would also be lower than estimated. Based on the estimated range of S_y from laboratory testing and literature values, a S_y of 5% was assigned to unconsolidated materials with a potential range from 1% to 10%. S_y for unconsolidated materials was further refined during model calibration.

Porosity (n) of fined grained soils like clay can be as high as 50% (Heath 1983). The laboratory analyses for coarse and fine laterites suggest a range of porosity from 37% to 39%. However, the effective porosity (n_e) is typically much lower but higher than the specific yield. n_e for unconsolidated materials was therefore assumed to be twice the highest potential S_y, giving an assumed ne of 20%.

3.5.2 Bedrock

Initially, the bedrock aquifer at the Rum Jungle mine site was subdivided into the following bedrock units to develop a hydrostratigraphic model:

- Rum Jungle Complex (granite).
- Whites Formation (black shale/schist).
- Geolsec Formation (Quartz breccia).
- Coomalie Dolostone (dolostone//tremolite).
- Crater Formation (sandstone).

These bedrock units were further subdivided by the degree of weathering/fracturing, which tends to decrease with depth. Slug testing was conducted in 2010 and 2014 to assess the K of bedrock. Slug testing was also conducted at historical monitoring bores during the 2010 investigation. In 2012, a 7-day pumping test was conducted in the Copper Extraction Pad area and the monitoring data collected from nearby bores were used to assess the K of bedrock (mainly Whites Formation) over a larger area. The following bedrock unit properties were established from this hydraulic testing:

- The Rum Jungle Complex is present along the south-eastern side of the Giant's Reef Fault and therefore underlies the Main WRD and Dyson's WRD. The Rum Jungle Complex also outcrops at the north-west extreme of the model domain in the vicinity of monitoring bores MB10-20 and MB10-21. The slug testing for bores screened in the Rum Jungle Complex indicates that the upper-most 30 m is relatively permeable, suggesting weathering and/or fracturing. K values from slug testing range from 2×10^{-7} to 1×10^{-5} m/s with a geometric mean of 3×10^{-6} m/s. Although hydraulic testing results at greater depths are not available, it is assumed that the K of the Rum Jungle Complex decreases significantly with increasing depth, as bedrock becomes less weathered and more competent.

- The Whites Formation hosts the main mineralization at the mine site and hence occurs in the central mining area, in Dyson's Area, and in the vicinity of the Browns Pit. Slug testing conducted in Whites Formation indicate K ranging from 4×10^{-7} to 4×10^{-5} m/s. K values inferred from the pumping test conducted in 2012 range from 2×10^{-6} to $1\text{x}10^{-5}$ m/s. The geometric mean of all available hydraulic testing results for this unit is 3×10^{-6} m/s.
- The Geolsec Formation extends from immediately north of the Main WRD eastward to Dyson's (backfilled) Pit, wrapping around the CMA and extending northward to the vicinity of monitoring bores MB14-15S/D. Isolated areas of Geolsec Formation are also present underlying the EBFR to the west of the Old Tailings Dam area and north of the central mining area. Slug testing conducted in the Geolsec Formation suggests K values range from 8×10^{-9} to 1×10^{-5} m/s with a geometric mean of 4×10^{-8} m/s. The K of the Geolsec Formation likely decreases with increasing depth
- Coomalie Dolostone underlies most of the EBFR downstream of gauge GS8150200 as well as the entire Old Tailings Dam area extending from the central mining area beyond Old Tailings Creek. Coomalie Dolostone is also present immediately south of the central mining area, extending from the southern perimeter of the Main Pit south-westward beneath the Intermediate WRD and beyond monitoring bore RN022085. Approximately one third to one half of the northern perimeter of the Intermediate Pit cuts into the Coomalie Dolostone while a smaller proportion of the southern perimeter of the Main Pit cuts into it at shallow depth. Slug testing conducted at 13 monitoring bores screened in the Coomalie Dolostone indicate a K ranging from 2×10^{-7} to 2×10^{-3} m/s with a geometric mean of 2×10^{-5} m/s
- Crater Formation has been mapped by Davy (1975) under the north-west corner of Main WRD near the Giant's Reef Fault. It is also mapped along the northern extreme of the Coomalie Dolostone. The Crater Formation was not encountered in any bores and therefore hydraulic testing data is not available. However, it is expected to have a relatively low K compared to the other bedrock formations at the site

No measurements of storage properties were available for the various bedrock units. Instead, representative storage values had to be assigned based on the literature and experience. Based on RGC's previous experience at the nearby Woodcutters site, all bedrock units were assigned a Sy of 0.005 and a specific storage (Ss) of $1\text{x}10^{-6}$. Effective porosity is assumed to be 1%, i.e. twice the assumed specific yield.

3.5.3 Waste Rock and Tailings Properties

Waste rock in the waste rock dumps is assumed to have relatively high permeability and specific yield. As well, the vertical anisotropy is expected to be higher than bedrock at the Mine Site. Based on earlier modelling results (RGC, 2012a) the waste rock in the Main and Intermediate WRDs was assigned a hydraulic conductivity of $6x10^{-5}$ m/s while the waste rock in Dyson's WRD was assigned a conductivity of $6x10^{-6}$ m/s. The vertical anisotropy was assumed to be Kh/Kv=10. These assumed values are in reasonable agreement with the range of K values estimated for waste rock from Rum Jungle ($5x10^{-7}$ m/s to $1x10^{-5}$ m/s) based on more recent laboratory testing (O'Kane Consultants, pers. comm.). This laboratory testing also suggested that the specific yield of waste rock could be in the range of 11% to 16% while total porosity ranged from 26% to 30%, depending on the level of compaction.

No hydraulic testing data is available for the tailings backfill in the Main Pit and Dysons Pit. However, based on experience elsewhere, the tailings can be expected to have a relatively low hydraulic conductivity, in the order of $1x10^{-7}$ to $1x10^{-8}$ m/s, due to the fine grained nature of the tailings. In addition, tailings tend to have some vertical anisotropy (in the order of 5 to 20) due to the placement on a beach. The tailings in Dyson's Pit were discharged from the western pit perimeter, likely resulting in some hydraulic segregation along the beach from west to east. It is therefore likely that the western portion is generally coarser-grained (higher K) then the eastern portion (lower K). Consequently, the tailings in Dyson's (backfilled) Pit were subdivided into a western and eastern portion in the model. The hydraulic properties (K, Sy) of the tailings in each zone were then calibrated using the water table time trends observed in monitoring bores DO20 and DO21. The tailings in the Main Pit are assumed to have a K value on the order $1x10^{-8}$ m/s and a Sy similar to the fine tailings in the eastern half of Dysons backfilled pit. A vertical anisotropy of 10 is assumed for the backfill tailings at both the Main and Dyson's Pits.

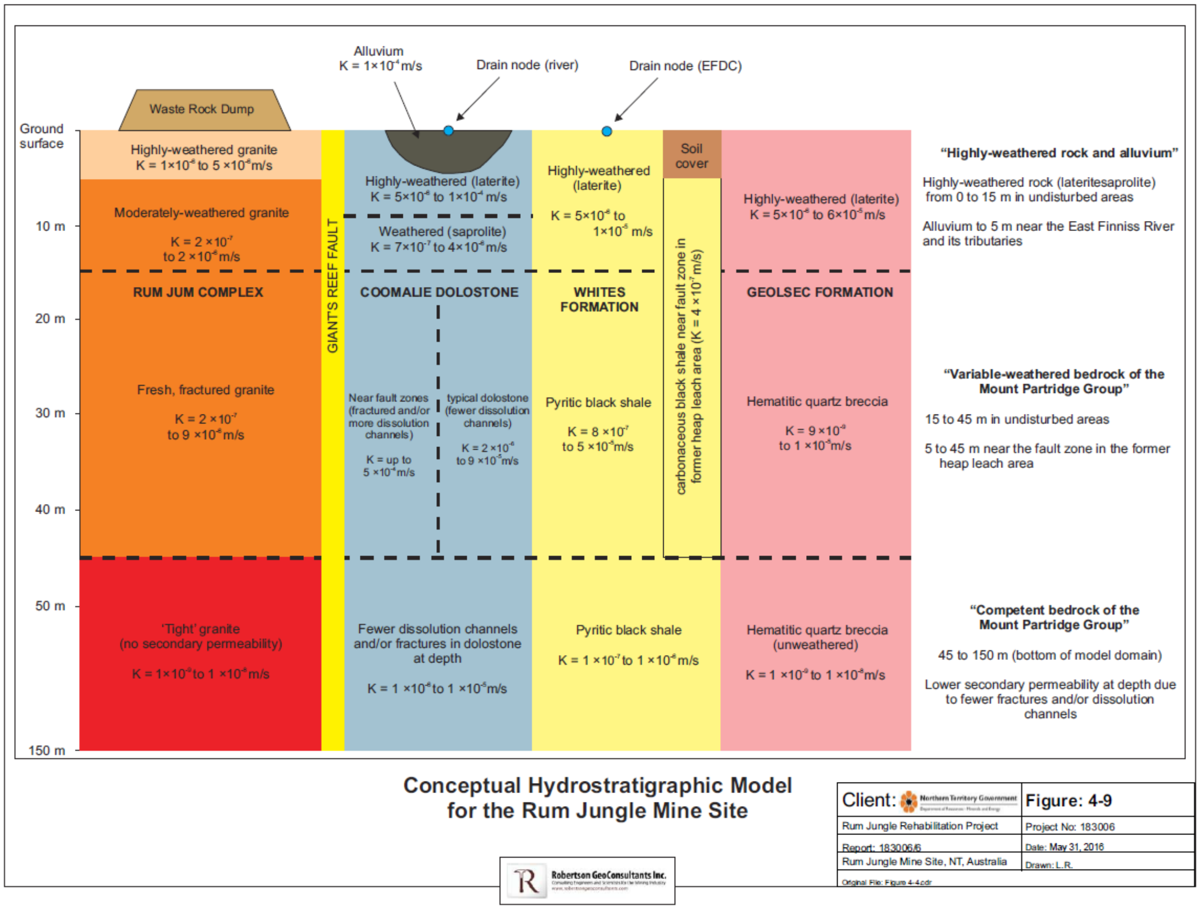

Figure 3-3. Simplified Representation of Conceptual Hydrostratigraphic Model

Table 3-2. Hydraulic Testing Summary

Monitoring Bore ID	Screen Interval (m BGS)	Test Method	Hydraulic Conductivity (m/s)
Laterite		***Geometric Mean =***	***2E-05***
MB10-08S	5 - 14	Slug Test	2E-06
MB14-16	2 - 7	Slug Test	2E-06
MB14-17S	2 - 7	Slug Test	5E-06
MB14-20S	2 - 8	Slug Test	1E-05
2014-TPA-01	4.3	Infiltration Test	2E-04
2014-TPA-02	4.4	Infiltration Test	1E-04
2014-TPA-10	5.5	Infiltration Test	8E-05
Saprolite		***Geometric Mean =***	***2E-06***
MB10-01a	1.4 - 3.4	Slug Test	9E-07
MB10-20	3 - 7	Slug Test	3E-06
MB14-02S	2 - 8	Slug Test	4E-06
MB14-04	2 - 8	Slug Test	7E-07
Whites Formation		***Geometric Mean =***	***3E-06***
MB10-06	13 - 26	Slug Test	4E-05
MB14-14D	24 - 29	Slug Test	8E-07
MB12-35	22 - 34	Pumping Test (DD)	1E-05
		Pumping Test (TR)	3E-06
MB10-10	16 - 32	Slug Test	4E-07
		Pumping Test (DD)	8E-06
		Pumping Test (TR)	6E-06
MB10-11	31 - 34	Pumping Test (DD)	3E-06
		Pumping Test (TR)	2E-06
MB12-33	14 - 32	Pumping Test (TR)	2E-06
Geolsec Formation		***Geometric Mean =***	***2E-07***
MB10-08D	20 - 23	Slug Test	1E-05
MB14-15S	11 - 14	Slug Test	4E-07
MB14-15D	21 - 42	Slug Test	2E-08
MB14-17D	21 - 29	Slug Test	8E-09
Rum Jungle Complex		***Geometric Mean =***	***3E-06***
RN022083	11 - 17	Slug Test	9E-06
RN022084	10 - 16	Slug Test	3E-06
RN023792	20 - 26	Slug Test	1E-05
RN025165	5.2 - 8.2	Slug Test	2E-07
RN025170	5.9 - 8.9	Slug Test	2E-06
RN025173	5.2 - 8.2	Slug Test	4E-06
Coomalie Dolostone		***Geometric Mean =***	***2E-05***
MB10-07	9 - 18	Slug Test	1E-05
MB10-09D	46 - 62	Slug Test	2E-04
MB10-12	13 - 25	Slug Test	3E-06
MB10-13	49 - 61	Slug Test	1E-05
MB10-14	16 - 18	Slug Test	7E-05
MB10-17	20 - 26	Slug Test	5E-04
MB10-22	12 - 24	Slug Test	2E-07
MB14-01D	26 - 32	Slug Test	7E-05
MB14-02D	23 - 29	Slug Test	6E-04
MB14-03	18 - 23	Slug Test	2E-05
MB14-05D	22 - 28	Slug Test	1E-05
MB14-06D	18 - 24	Slug Test	2E-06
MB14-08D	18 - 24	Slug Test	8E-06
MB14-09	10 - 16	Slug Test	2E-03
MB14-13D	13 - 18	Slug Test	5E-05
MB14-18	11 - 17	Slug Test	5E-05
MB14-20D	21 - 27	Slug Test	8E-07

DD = Distance Drawdown
TR = Theis Recovery

3.6 Structural Controls on Groundwater Flow

3.6.1 Faults

There are several faults cutting across the study area with a south-west to north-east to north-south trend. Some of these faults are connected to the Main and Intermediate Pits and may potentially influence the direction of groundwater flow. The low grade metamorphism associated with the fault zones could also potentially influence the hydraulic properties and groundwater flow (potentially acting as a flow barrier or as a preferred flow path). A particularly prominent north-east trending fault runs from the area near bore MB10-14 across the former Copper Extraction Pad area to the Intermediate WRD. Very high airlift yields (~50 L/s) encountered during the drilling of monitoring bore MB10-14 (and at bore RN022107) suggests that secondary permeability in this area is very high due to either the presence of a fracture zone near the fault and/or dissolution channels at shallow depth in the Coomalie Dolostone. Note that this fault eventually coincides with the location of the seepage face that characterizes the north-western toe of the Intermediate WRD. It is therefore conceivable that this seepage face is structurally controlled.

The fault that runs between the Main and the Intermediate Pits is thought to represent a preferential pathway for groundwater and hence, impacted groundwater may flow south-west along the fault towards the Intermediate Pit. Note, however, that the presence of carbonaceous, highly-weathered shale of the Whites Formation may limit preferential movement of (highly-contaminated) groundwater in this area to greater depths (say >15-30 m) where the bedrock is less weathered and more competent. The persistence of high copper concentrations in this area after several decades suggests that groundwater flows are not significantly higher than areas outside of this fault zone.

3.6.2 Cavities and Karst Features

During the drilling investigations conducted at the Rum Jungle Mine Site in 2010, 2012 and 2014, several cavities were encountered in the Coomalie Dolostone. The cavities encountered may be related to faults, however, the potential exists that the cavities represent karst formations. Like faults, karst formations can locally influence groundwater flow, as preferential pathways can exist or form depending on the interconnectivity of karst voids, both horizontally and vertically. Where high interconnectivity of voids exists, relatively high flows to discharge areas (creeks) can occur. Karst voids in the saprolite can also induce flows of nominally perched, shallow groundwater to the deeper, confined aquifer in the underlying Coomalie Dolostone. Preferential pathways due to karst formations can therefore induce rapid migration of tailings impacted groundwater.

During the 2014 hydrogeological investigation, voids generally described as sand filled fractures, were encountered at monitoring bores MB14-02D (screened from 23.1 to 29.1 m bgs) and MB14-09 (screened from 10 to 16 m bgs). K values estimated from hydraulic testing at these monitoring bores were greater than 1x10^{-3} m/s, approximately two orders of magnitude higher than the average of all results. The K values for voids encountered during the 2010 investigation at monitoring bores MB10-09D (screened from 46.3 to 62.3 m bgs) and MB10-17 (screened from 20 to 26 m bgs) were lower than the 2014 void results, but still an order of magnitude higher than the geometric mean. Although the continuity of the voids encountered in the aquifer during the hydrogeological investigations is difficult to assess, the effect on hydraulic conductivity and the potential range of depth where they can occur is well demonstrated at these monitoring bores. Although K values were not shown to be particularly high, voids were encountered at other monitoring bores, including bores MB14-01D, MB14-07, MB14-11&12, MB10-13, MB10-14 and MB10-19, as well bores MB12-27 and MB12-28 to the south of the central mining area. This suggests that karst voids must be expected to be present throughout the Coomalie Dolostone in the study area.

3.6.3 Groundwater Recharge

Cross-boundary groundwater flows into the model domain are considered negligible because the model domain is defined by topographic highs and lows, i.e. no flow boundaries. Therefore, rainfall is the only external source of recharge to the model domain. The only other source of recharge to the groundwater system within the model domain is recharge from the flooded Main and Intermediate Pits during the wet season when the pit water levels rise temporarily above the surrounding groundwater level. Groundwater recharge by rainfall infiltration occurs mainly during the wet season. The amount of precipitation that infiltrates the ground as recharge varies depending on the ground surface type, i.e. bedrock versus unconsolidated soils, the ground slope, and the rate of rainfall and whether it causes local ponding/flood conditions. Further details on recharge are provided in the sub-sections below.

3.6.4 Recharge by Rainfall to Undisturbed Areas

Previous studies have estimated that only 10% of incident rainfall to natural ground surfaces in humid areas of the Northern Territory recharges the groundwater as the remainder of incident rainfall is lost via evapotranspiration and surface runoff (Aquaterrra, 1999, RGC, 2012a). To estimate site-specific recharge, the water table fluctuation method from Healy and Cook (2002) was applied. This method involves interpreting the water table response to individual precipitation events in order to estimate the percentage of incident precipitation that infiltrates and recharges the aquifer. Using an assumed specific yield for laterite and saprolite of 5%, recharge was estimated to range from 19% (MB14-20S) to 30% (MB14-02S) of precipitation with an average of 24% (see RGC, 2016, for further details).

3.6.5 Recharge by Rainfall to the WRDs

Infiltration rates into the waste rock dumps are expected to be higher than infiltration to groundwater via natural ground surfaces, in particular prior to initial rehabilitation in the mid-1980s when the waste rock dumps were uncovered. Daniel et al. (1982) estimated that 50 to 60% of annual rainfall percolated through the Main WRD before rehabilitation. Cover placement as part of rehabilitation works in 1984/1985 reportedly reduced infiltration to 5 to 10% of annual rainfall by the late 1990s. However, the covers are known to have eroded over time reducing their effectiveness. In addition, there is some doubt regarding the reliability of the lysimeter data interpreted in historic reports (Taylor et al., 2003; Phillip and O'Kane, 2006).

Based on previous investigations and preliminary contaminant load estimates from RGC (2011b), a net infiltration rate of 25% of incident rainfall was estimated for the Main and Intermediate WRDs. A net infiltration of 50% of incident rainfall was estimated for Dysons WRD because the cover placed on this dump during rehabilitation works in the mid-1980s was reportedly of lower quality and did not cover the entire dump surface area.

3.6.6 Recharge from the Flooded Pits

Groundwater flow into and out of the Main and Intermediate Pits occurs throughout the year. However, during the dry season when groundwater elevations in the Coomalie Dolostone to the north of the pits decline below the pit lake elevations, both pits become net sources of recharge to the aquifer. The Intermediate Pit cuts into the highly permeable Coomalie Dolostone along its northern perimeter and is therefore expected to be a potentially higher source for groundwater recharge than the Main Pit which is generally surrounded by the less permeable Whites Formation.

3.7 EVAPOTRANSPIRATION AND SOIL MOISTURE DEFICIT

Evapotranspiration will remove water from the shallow groundwater system using two different mechanisms: (i) evaporation from water bodies (e.g. flooded open pits or saturated soils where the groundwater table reaches the ground surface) and (ii) transpiration by vegetation which extracts groundwater from the root zone. Using a regional analysis, mean annual lake evaporation at the Rum Jungle mine site has been estimated is approximately 2,000 mm (5.5 mm/d) and the mean annual actual evapotranspiration is approximately 1,050 mm (2.9 mm/d) (see Section 2.4.2).

Evaporation from the flooded pit lakes has an influence on the groundwater flow system during the dry season when the pit lakes do not receive any recharge (from direct precipitation of the Upper EBFR or the surrounding aquifer) and lake evaporation draws down the pit lake elevation. Based on the lake elevation data for the Main and Intermediate Pits for the dry seasons of 2011 to 2014, an average rate of decline of 5.3 mm/d for the Main Pit and 6.6 mm/d for the Intermediate Pit is calculated. These seasonal declines are in reasonable agreement with the estimated potential lake evaporation rate of

5.5 mm/d for the Mine Site[1]. Evaporation from the pit lakes was not modelled explicitly in the groundwater model. Instead, the observed decline in pit lake elevations was modelled implicitly by assigning seasonally varying pit lake elevations to the constant heads representing the flooded pits.

The rate of actual evapotranspiration from woodlands (primarily eucalyptus trees) which can represent a significant source of groundwater extraction during the dry season. Ecological studies in the study area support the above estimates of actual evapotranspiration. A study conducted by the Department of Lands, Planning and Environment (DLPE, 2000), reported evapotranspiration rates of 7 mm/d for the Berry Creek catchment and 5 mm/d in adjacent catchments. At Howard Springs, approximately 35 km south-east of Darwin, Hutley et al. (2000) determined an average evapotranspiration rate of 2.6 mm/d. At a site near Darwin, O'Grady et al. (1999) concluded that due to groundwater exploitation by tree roots, transpiration rates were higher during the dry season than during the wet season. Evapotranspiration losses are therefore treated differently in the dry season and the wet season. During the wet season, evapotranspiration losses from the shallow groundwater system are offset by recharge of precipitation. The temporal discretization of the model (monthly time steps) does not warrant an explicit simulation of those highly transient near-surface processes. Instead, evapotranspiration losses are implicitly accounted for by reducing the recharge to groundwater from actual precipitation rates observed during model calibration (see above).

During the dry season, evapotranspiration is assumed to be active in areas of dense vegetation of the Rum Jungle mine site, typically located in low-lying flood plains where groundwater levels tend to be near-surface for extended periods into the dry season (for example in the upper EBFR near Dyson's WRD). Evapotranspiration is therefore only considered for densely vegetated areas (based on 2010 aerial photography) during the dry season (during months of no recharge). A potential range of evapotranspiration rates of 1 to 7 mm/d with an average rate of 2 mm/d and an extinction depth of 4 m is conceptualized for the model. These evaporation parameters were later modified as part of model calibration.

During the dry season, evapotranspiration tends to dry the surficial soils below the drainable porosity (or S_y) typically reached by gravity drainage alone resulting in a soil moisture deficit (SMD). Due to this deficit, a portion of the initial precipitation at the beginning of the wet season is required to "wet up" the soil before the aquifer responds, i.e. before the soils re-saturate and the groundwater table rises.

[1] The greater rate of seasonal decline in pit lake elevation in the Intermediate Pit vis-à-vis the Main Pit (delta= 1.3 mm/d) is significant and is inferred to be indicative of higher net seepage losses from the Intermediate Pit to the surrounding bedrock aquifer, in particular the high-K dolostone to the north. The observed incremental decline in pit lake elevation (1.3 mm/d) represents a net seepage flow out of the Intermediate Pit of approximately 0.5 L/s.

The amount of SMD can be expected to vary depending on local soil conditions and preceding dry season conditions. For the nearby Woodcutters mine site, Aquaterra (1999) had estimated that up to 200 mm of precipitation could be required to wet up the surficial soils at the start of the wet season. Based on a review of detailed water level responses observed at monitoring bore RN022081 during the 2010/2011 wet season the SMD for the Rum Jungle Mine Site was estimated to be a minimum of 102 mm.

For the conceptual site model, the SMD to be applied at the start of the wet season was initially assumed to range from 100 to 200 mm depending on preceding climate conditions. These initial estimates of SMD are subject to further model calibration.

3.8 GROUNDWATER FLOW REGIME

3.8.1 Groundwater Level Variations

Groundwater level observations in key areas of the site are provided in Figure 3-4**.** Observations regarding groundwater levels in key areas of the site are summarized below.

- **Dyson's Area**
    - Groundwater levels in bores screened in bedrock to the west of Dysons (backfilled) Pit fluctuate by up to 6 m, i.e. bores RN022036 and RN023792. Fluctuations are similar in magnitude at bore DO21, which is screened in shallow backfill and tailings in Dyson's (backfilled) Pit. At bore DO20 (and bore RN023790), water levels fluctuate to a lesser degree (i.e. 2 to 3 m) than at bores RN022036 and RN023792.
    - Further south, groundwater level fluctuations are more subdued in bores screened in alluvium near the upper EBFR. Groundwater levels in this area often rise in the wet season to near ground surface, indicating groundwater discharge to the river channel from upgradient areas. Conversely, groundwater elevations often drop below the invert elevation of the river.
- **Near Main WRD**
    - Groundwater levels at monitoring bore RN022082D indicate that groundwater mounds beneath the Main WRD throughout the year. This is due to the shallow depth and relatively low K of bedrock underlying the Main WRD and the relatively high recharge rate to groundwater from the WRD compared to the surrounding aquifer.
    - Year-round groundwater mounding under the Main WRD in the granitic bedrock is indicated by groundwater elevations observed at monitoring bores RN022082S and RN022082D. The approximately 0.4 m higher heads observed in bore RN022082D compared to RN022082S indicate an upward gradient. The relatively small change in

groundwater elevation from wet season to dry season (approximately 0.5 m) suggests significant seasonal attenuation of recharge within the Main WRD due to high storage capacity of the waste rock.

- A similar muted seasonal response is observed in monitoring bores RN022411 and RN029993, located along the north-eastern toe of the Main WRD (near Fitch Creek). Here groundwater elevations are near or at surface in the wet season and only decline to slightly more than 1 m below ground surface in the dry season. An aerial photograph from 1952, before the Main WRD existed, suggests the presence of a creek or drainage feature from within the Main WRD footprint to Fitch Creek in this area.
- Along the western toe of the Main WRD, monitoring bores RN025172, RN30001 and RN30002 groundwater elevations are also at or near surface during the wet season and showed limited recession during the dry season, suggesting sustained seepage from the Main WRD.
- Significantly higher seasonal variations (up to 5 m) are observed at monitoring bores MB12-31S and RN25170, located at the north-western toe of the Main WRD. Very similar seasonal trends are observed in other monitoring bores located at greater distance from the Main WRD to the west (e.g. RN25165) and east of the Main WRD (e.g. RN22083 RN25168), suggesting that this area is more influenced by natural recharge than seepage from the Main WRD (possibly due to topographic controls).
- The highest seasonal groundwater level variations in the area are observed in more distant monitoring bores RN025167, RN025166, and RN02165 (6-7 m fluctuation). All of these more distant bores are located well outside the influence of the Main WRD and are representative of natural recharge conditions to the local bedrock aquifer.

- **Near Intermediate WRD**
  - Groundwater levels along the upgradient (south-eastern) toe of the Intermediate Dump (at RN025173 and RN022037) vary seasonally by about 3 m. These seasonal hydrographs are characteristic of groundwater levels in the weathered granite of the Rum Jungle Complex in this reach of the Site and do not suggest significant influence by seepage from the Intermediate WRD.
  - No monitoring bores are located within the footprint of the Intermediate WRD, but groundwater elevations at surrounding monitoring bores do not suggest any mounding beneath this WRD. This may be due to the pre-mining bedrock topography underlying the WRD, as well as the presence of the more permeable Coomalie Dolostone and moderately-permeable Whites Formation beneath the Intermediate WRD.

   - Monitoring bores MB12-30S and MB12-30D are located upgradient along the EFDC showed smaller seasonal variations of up to approximately 2 m in the deep monitoring bore and 2.5 to 3 m in the shallow monitoring bore. The shallow groundwater may fluctuate more due to more direct recharge or surficial runoff.
   - Groundwater levels immediately north of the Intermediate WRD along the EFDC (at monitoring bore MB12-29S screened in laterite) showed a faster response during the onset of the wet season, with up to 4 m water table fluctuation. This well is located in close proximity of an inferred fault (and known seepage area from the Intermediate WRD). Preferential groundwater discharge along a bedrock structure and/or preferential discharge of seepage in this area may explain the rapid groundwater level changes at MB12-29S.
   - Groundwater levels further downgradient to the west (RN023060) and north-west (MB10-05 and MB10-06) of the Intermediate WRD varied approximately 1 to 1.5 m between the wet and dry seasons. Groundwater levels in the deeper bore (MB10-6) screened in weathered schist of the Whites Formation (MB10-6) is consistently higher than in the overlying overburden (MB10-5) indicating an upward gradient and groundwater discharge into the EFDC and/or Intermediate Pit.

- **Near Main and Intermediate Pits**
   - Monitoring bores located in proximity of the Main Pit and screened in Whites Formation (e.g. RN22544) show similar seasonal trends as observed in the Main Pit (about 2 m seasonal fluctuations) suggesting good hydraulic connection. In contrast, groundwater in the Coomalie dolostone to the north of the Main Pit (e.g. RN22107) shows significantly larger seasonal fluctuations (up to 6 m), including higher peaks and lower troughs, implying limited hydraulic connection.
   - Monitoring bores located in the reach between the two pits (primarily screened in Whites Formation) show very similar seasonal trends as observed in the Main and the Intermediate Pit (about 2 to 2.5 m seasonal fluctuations) suggesting that the bedrock aquifer in this area is well connected to the two pits and controlled by pit water levels.
   - Monitoring bores located in immediate proximity of the Intermediate Pit and screened in Coomalie dolostone (e.g. RN022543, MB10-9S/D, and MB10-24) all follow the seasonal water level trends observed in the Intermediate Pit very closely indicating very good hydraulic connection.
   - The hydraulic influence of the Intermediate Pit is still clearly evident in monitoring bores MB10-07 and MB10-16, located further north-west of the Intermediate Pit. However, seasonal groundwater level fluctuations are significantly higher in the Coomalie

dolostone further upgradient (to the north-east) of the Intermediate Pit (e.g. at MB10-12, MB10-13 and MB10-22), illustrating the diminishing hydraulic influence of the Intermediate pit. The higher seasonal variations are primarily a result of higher peaks during the wet season indicating higher recharge in the Coomalie dolostone to the north than in the central mining area.

- **Old Tailings Dam area**
    - Seasonal groundwater levels in the highlands to the east and north east of the Old Tailings Dam area vary up to 8 m between the wet and dry seasons. This area includes monitoring bores RN023304, RN022547, RN022548, MB14-14S/D, MB14-15S/D and MB14-16. At the shallow monitoring bores MB14-06S, MB14-14S groundwater elevations rise close to surface during the wet season.
    - Seasonal groundwater levels in the hill slope immediately east of the Old Tailings Dam area fluctuate with less amplitude than in the highlands. Although the 2014 monitoring bores were only monitored during one wet/dry transition, groundwater levels measured at monitoring bores MB14-17S/D, MB14-05S/D, and MB14-13S/D suggest the seasonal fluctuations are in the range of 6 to 7 m
    - Seasonal groundwater levels observed at monitoring bores installed in the flood plain of the Old Tailings Dam area and to the west of the Old Tailings Dam area vary in the range of 4 to 6 m. The amplitude of the seasonal fluctuations decreases from east to west north of a line roughly defined by monitoring bores MB14-20S/D and MB10-08S/D, and west of monitoring bores MB14-02/D and MB14-13S/D. The reduced seasonal fluctuations are primarily a result of flooding in this low-lying topography during the wet season (limited water table rises) and/or discharge to the nearby Old Tailings Creek.
- **Downstream near EBFR**
    - Seasonal variations in groundwater levels in immediate proximity of the East Branch of the Finniss River (a regional discharge zone for groundwater) are significantly lower than observed further from the river (i.e. only 2 m or so between dry and wet season, compared to 3 to 5 m at bores RN23302 and RN23140).
    - When the groundwater elevations are higher than the river levels, groundwater is discharging to the EBFR. When river levels are higher than groundwater levels, groundwater is being recharged by the EBFR. The available data indicates that the aquifer is recharged by the EBFR during the early part of the wet season while groundwater discharges to the EBFR during the rest of the wet season. For much of the dry season, groundwater is below the EBFR and the river is dry.

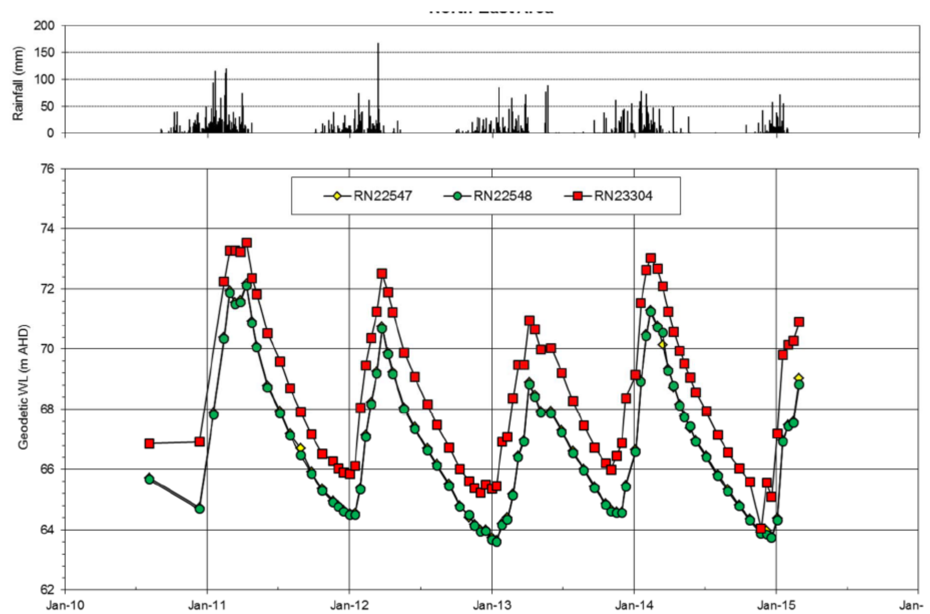

Northeast of Main Pit

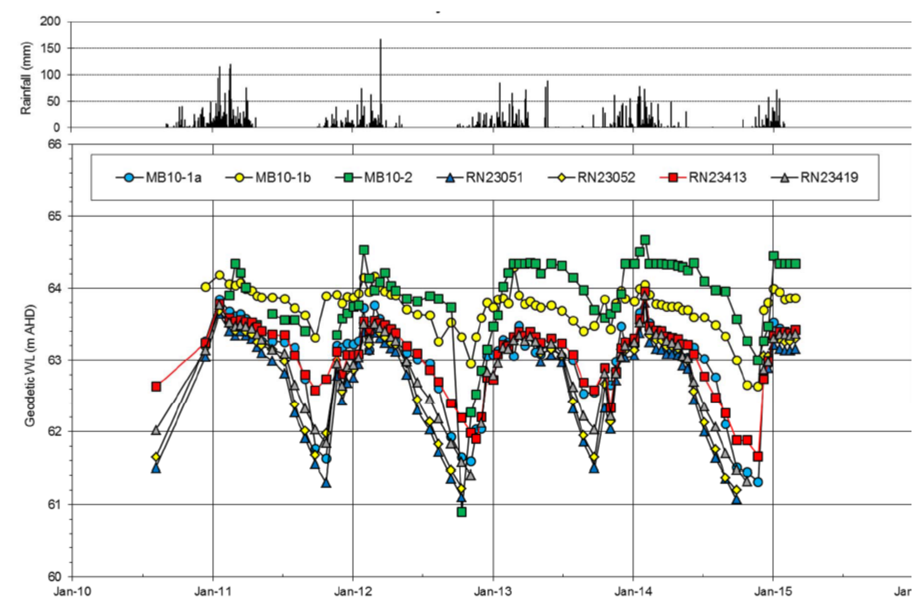

Near Dyson's WRD

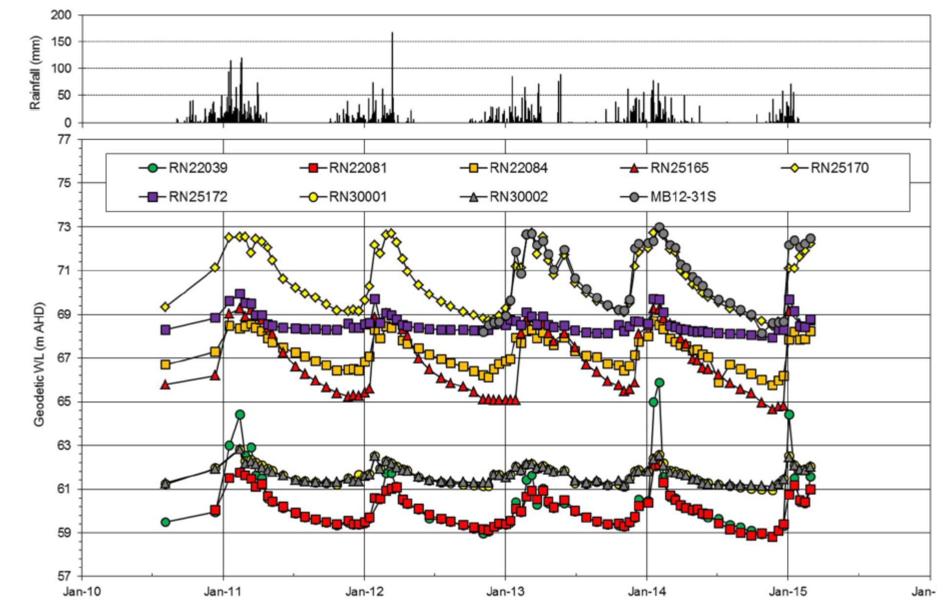

Near Main WRD (west)

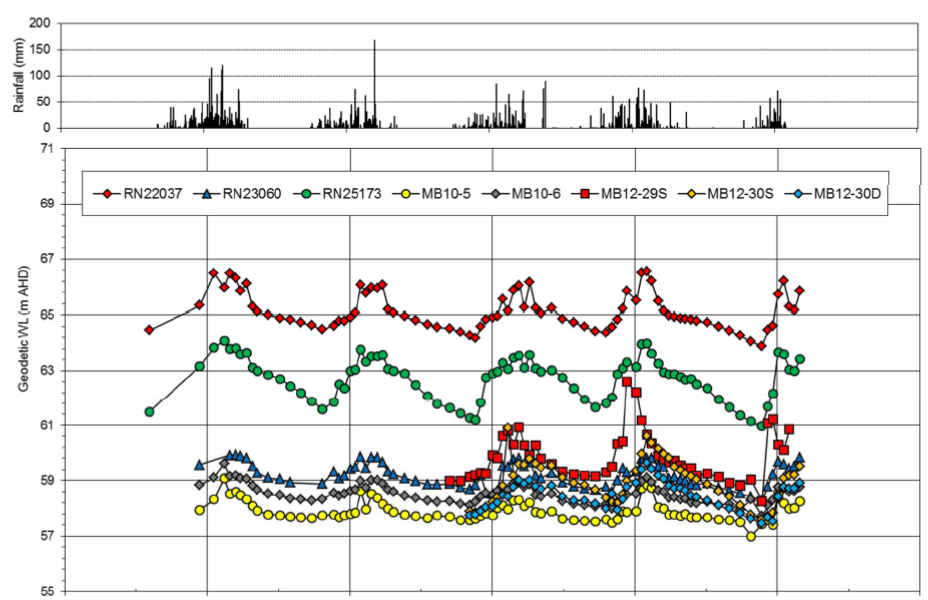

Near Intermediate WRD

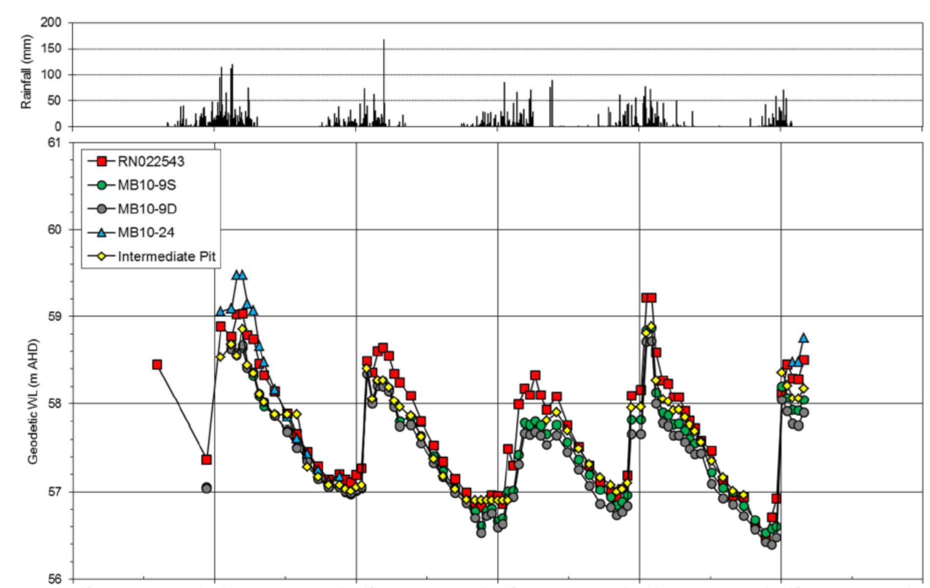

Near Intermediate Pit

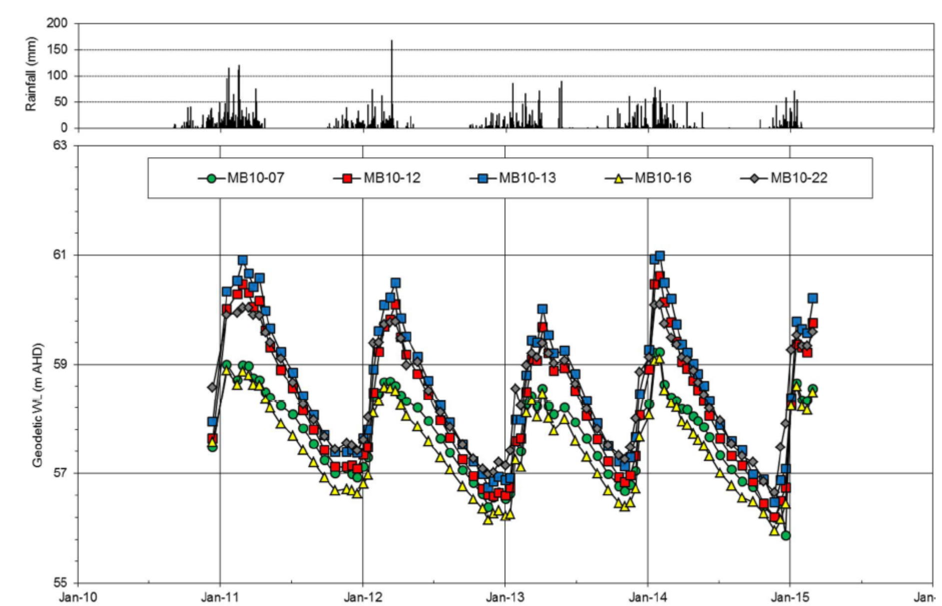

North of central mining area

Figure 3-4. Selected Groundwater Level Time Trends

3.8.2 Inferred Groundwater Flow Field

Figure 3-5 shows the inferred site-wide groundwater flow field during the dry season. This flow field was inferred (manually interpolated) from groundwater levels observed during the dry season. The inferred flow field suggests groundwater follows from higher elevation areas towards the pits in the central mining area and towards the EBFR as it flows through the site. Groundwater discharges to the EBFR within the site and sustains a series of pools year-round, particularly downstream of GS8150200 where the EBFR flows in its natural channel (see RGC, 2016).

Groundwater flows from upland areas to lower elevation areas where the EBFR currently flows and towards its pre-mining course in the central mining area. During the wet season, groundwater discharges to numerous smaller tributary creeks to the EBFR such as Fitch Creek, Wandering Creek and Old Tailings Creek, as well as unnamed creeks and man-made drainage features. During the dry season all drainages dry up as groundwater levels fall below the creek elevation. While groundwater flow may still converge along major drainage lines, e.g. the EBFR downstream of GS8150200, groundwater may also flow beneath smaller (shallower) drainage lines such as the EFDC to other, more downgradient discharge areas including the Intermediate Pit.

Downward hydraulic gradients are generally observed in upland areas during the wet season when high precipitation events recharge the shallow, more permeable laterite soils overlying less permeable saprolite and/or weathered/fractured bedrock. These shallow soils remain saturated throughout the wet season and may act as preferred shallow flow paths towards the nearest drainage line or creek. At the same time, strong downward gradients provide recharge through the less-permeable saprolite into the moderately to highly permeable fractured bedrock. Detailed monitoring of nested monitoring bores near the EBFR and Old Tailings Creek indicate upward gradients from shallow bedrock to surficial soils (alluvium and/or laterite) throughout most of the late wet season and subsequent dry season. These upward gradients represent groundwater discharge to the EBFR and Old Tailings Creek when groundwater elevations reach the inverts of the creeks. Such upward gradients are characteristic of local and regional groundwater discharge zones typically observed in the flood plains of larger creeks and rivers.

Downward gradients have been observed during the onset of the wet season (typically November, December and January) both in the Old Tailings Creek area (e.g. at MB10-18 and MB10-19) and near the EBFR (at MB10-20 and MB10-21 during the 2010/2011 wet season. These downward gradients early in the wet season are inferred to be caused by a faster response in the shallow soils (relative to deeper bedrock) due to (i) direct precipitation, (ii) preferential shallow recharge from the side hills (in more permeable laterite and/or alluvium) and/or (iii) surface runoff from the upstream catchment during precipitation events. Along most of the EFDC reach, upward gradients are observed between the bedrock and the overlying saprolite year-round. The EFDC is cut into bedrock and does not have underlying alluvial soils and therefore groundwater flow from upstream along the channel does not occur. As well, the EFDC does not carry flow from upstream during the early wet season. Hence, downward gradients do not occur along the EFDC.

Groundwater flow within the study area is affected by the Main, Intermediate and Dyson's WRDs. Preferential infiltration through the WRDs and hence above-average recharge to the underlying aquifer can result in local groundwater mounding. Monitoring beneath the Main WRD suggests groundwater is mounding up to 2 m above natural ground surface beneath the Main WRD. Monitoring bores are not present within the footprints of the Intermediate or the Dyson's WRD. However, the presence of toe seepage along the toes of these WRDs suggests that groundwater is mounded (or perched) beneath these WRDs, at least during the wet season. This is evidenced by the well-defined seepage face that discharges highly-impacted seepage (AMD) from the Intermediate WRD directly into the EFDC. Monitoring of groundwater levels at nested monitoring bores MB12-30S and MB12-30D, located in immediate proximity of this seepage face, shows downward gradients year-round (contrary to other reaches along the EFDC). These year-round downward gradients suggest year-round seepage from the foot print of the Intermediate WRD some of which recharges the deeper bedrock aquifer.

Groundwater mounding beneath the footprint of the WRDs can result in radial flow, as observed near the Main WRD. This flow pattern will result in divergent flow of impacted groundwater (radially away from the WRD perimeter) and will enhance the migration of dissolved constituents in groundwater away from the footprint(s) of the WRDs. Radial flow is not evident near the Intermediate WRD, possibly due to the higher permeability of the underlying Whites Formation and Coomalie Dolostone. Near the WRDs, the amplitude of seasonal groundwater fluctuations observed at nearby monitoring bores are less than at distant monitoring bores in undisturbed areas of the Mine Site. The groundwater levels recorded at monitoring bores RN022082S and RN022082D, screened directly beneath the Main WRD, show the least seasonal fluctuation observed anywhere at the Mine Site. An increase in the amplitude of seasonal fluctuations with distance from the Main and Intermediate WRDs is observable. This suggests that WRDs have relatively high storage, which will dampen the high recharge during the wet season and will continue to release seepage held in storage within the WRD throughout most of the dry season (as evidenced by toe seepage year-round).

In the 2016 conceptual model, no information was available to infer the K of shallow bedrock within the southern part of the copper extraction pad area and around the rim of the Main pit. Therefore, this area was conceptualized to have a uniform K of $2x10^{-6}$ m/s based on results from the pumping test at bore PB12-33. However, results from the recent hydraulic testing completed in bores and drill holes within the Copper Extraction Pad area suggest the presence of a K contrast in shallow bedrock of about one order of magnitude, between the northern and southern parts of this area. Hydraulic tests completed in the northern side suggest an estimated K in the range of $2x10^{-6}$ to $4.1x10^{-6}$ m/s while tests completed in the southern side suggest a range of $2x10^{-7}$ to $7x10^{-7}$ m/s. Testing results from drill hole 18DH03 located at the north-west side of the Main Pit rim inferred a low estimate of hydraulic conductivity (7x10-

^{8} m/s) suggesting limited hydraulic connection between the Main pit and the Coomalie Dolostone. These inferred updates to the conceptual flow model were implemented as part of the calibration refinement of the 2019 model.

Near the northern site boundary, groundwater levels at bores MB17-23S/D, MB17-24S and MB17-25 (installed in 2017) ranged from 70 to 72 m AHD, suggest steeper hydraulic gradients from northern and eastern higher topographic relief areas (mainly within the Whites Formation) towards the low-lying areas within the Coomalie Dolostone. This observation was also reflected in the updated inferred groundwater flow field.

3.8.3 Influence of Main and Intermediate Pits

The Main and Intermediate Pits cut deeply into the bedrock aquifer in the central mining area and therefore have a potential to interact significantly with groundwater in adjacent zones of the bedrock aquifer. During active mining (and de-watering), both pits represented major sinks for groundwater and the bedrock aquifer in the central mining area likely featured a significant cone of depression. However, the Main and Intermediate Pits have been flooded now for 40 to 50 years and groundwater levels have reached post-mining steady-state conditions. Note that a cone of depression may, however, still characterize the area near the Browns Pit as it is actively de-watered.

The Main and Intermediate Pits have a strong influence on the groundwater flow field and can act as sources or sinks for groundwater depending on the pit water level and water levels in the surrounding aquifer. A comparison of the Main and Intermediate Pit water levels to groundwater levels in the surrounding aquifer suggests the Main and Intermediate Pits tend to receive flows of groundwater during the wet season but act primarily as sources of water to the groundwater system during the dry season. Higher flows from the Intermediate Pit than the Main Pit are expected due its strong hydraulic connection to the Coomalie Dolostone and the partial backfilling of the Main Pit with low-K tailings which has likely sealed the deeper pit walls from the surrounding bedrock aquifer.

The flooded pits also have an effect of dampening the seasonal fluctuation of groundwater elevations throughout the central mining area. This is evidence by seasonal fluctuations in levels by 5 m or more in undisturbed areas far from the pits and fluctuations in groundwater levels by 3 m or less in the central mining area.

3.8.4 Influence of Browns Oxide Pit

The Browns Oxide pit is the shallowest of the three open pits (< 30 m deep) but it is expected to interact with the groundwater system at the Rum Jungle Mine Site because it is actively de-watered. The Browns Pit is therefore considered a local sink for groundwater (see Coffey, 2006) and likely induces a more south-westerly flow of groundwater west of the Intermediate Pit near the EBFR. Note that information on the groundwater system in proximity of the Browns Oxide Open Pit is generally more limited with monitoring data for several monitoring bores only available for a brief observation period in 2011 and for only one monitoring bore available on a monthly basis from January 2012 to March 2015.

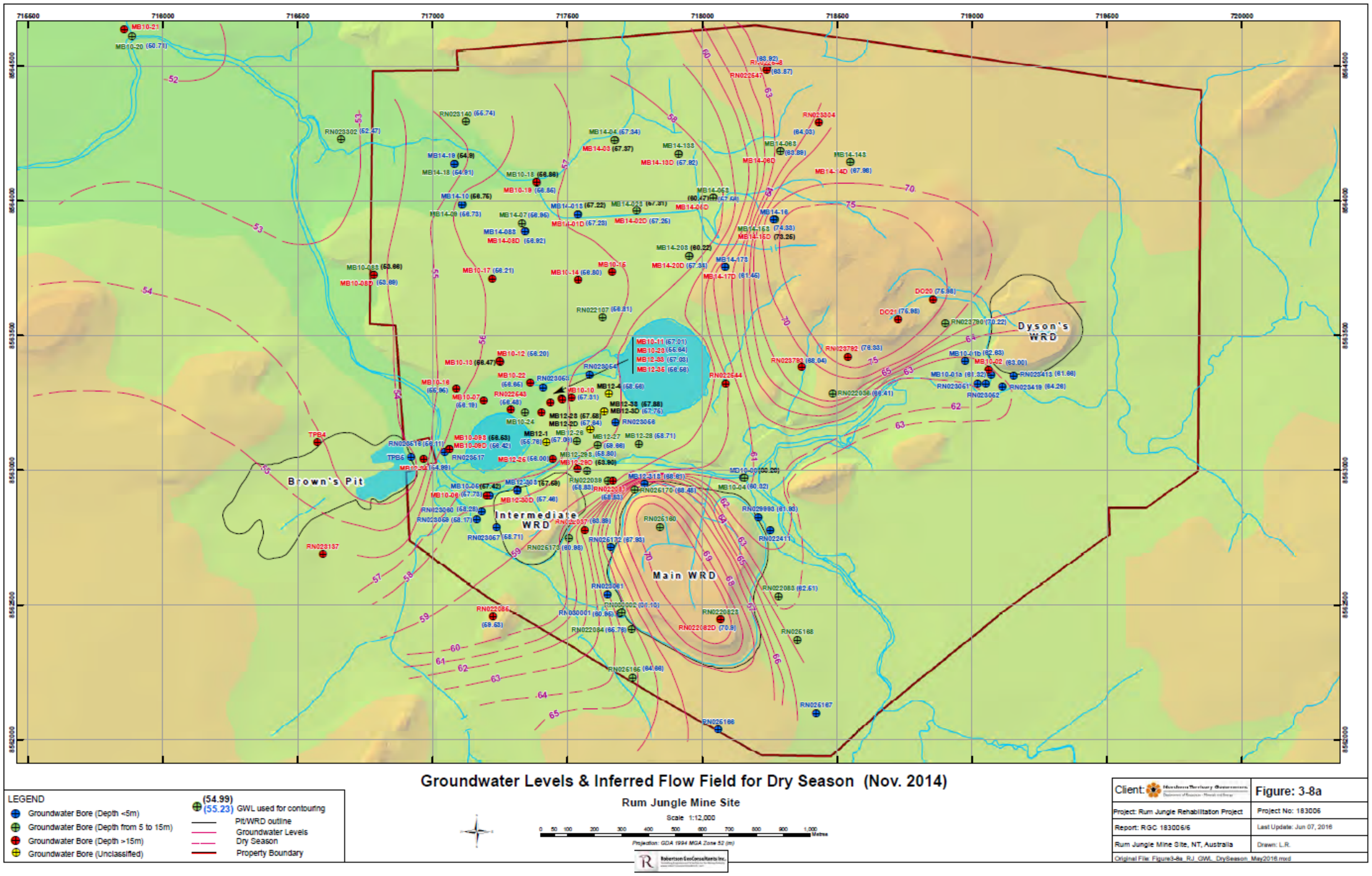

Figure 3-5. Inferred Groundwater Flow Field (Dry Season)

3.9 Groundwater Discharge to the EBFR

The EBFR is the primary discharge point for seepage and groundwater in the model domain. All surface drainages within the domain, whether natural or anthropogenic, ultimately report to the EBFR upstream of GS8150200 or to the EBFR via Old Tailings Creek. Streamflow rates for GS8150200 and GS8150327 suggest 50 to 200 L/s of potential groundwater flows between the gauges. To provide a calibration target for groundwater flows, it was assumed that groundwater flow represents between 12.5% and 25% of average monthly discharge observed in EBFR. Figure 3-6 shows the estimated upper and lower bounds for groundwater flows to the EBFR based on stream gauging data from May 2011 to June 2014.

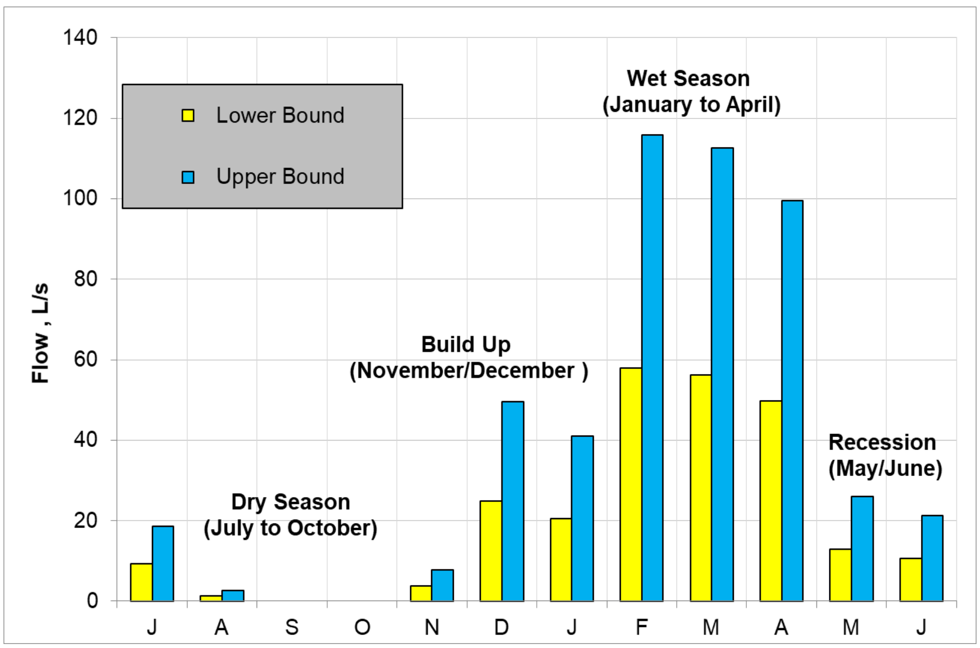

Figure 3-6. Estimated Upper and Lower Bounds for Groundwater Flows to EBFR between Gauging Stations GS8150200 and GS8150327

3.10 Conceptual Groundwater Budget

A conceptual groundwater budget was developed to estimate the magnitude of recharge and major outflows from the model domain. Groundwater flows to and from the pits and the EBFR were estimated using simple Darcy calculations based on weighted K values, typical wet and dry season hydraulic gradients, and assumed aquifer thicknesses. The K values were weighted using typical material thicknesses and the ranges of K values from hydraulic testing and field studies. For calculations near the EBFR, aquifer thickness was assumed to be 45 m and it was assumed that all groundwater in the aquifer from both sides of the EBFR would discharge to the river. For the EFDC, an aquifer thickness of 15 m was assumed and it was assumed that groundwater only discharged from the south (based on the prevailing hydraulic gradient). For recharge on natural terrain, range of 10% to 30% of incident rainfall throughout most of the site was assumed based on available literature and field testing (infiltration tests) on site. Recharge for the Main, Intermediate and Dyson's WRDs likely ranges from 25% to 50% of incident precipitation based on previous estimates, e.g. Davy (1975) and RGC's experience elsewhere.

This simplified analysis (assuming a uniform recharge) for both the upper and lower bounds is shown Table 3-3. Evapotranspiration is accounted for to some extent in the use of net recharge. However, for areas of relatively dense forest, including reaches of the EFDC, the upstream and downstream EBFR, and parts of Fitch Creek and Old Tailings Creek, it is likely that transpiration by the deeply rooted trees is an additional outflow from the site during the dry season and this loss has been included in the analysis assuming a potential range of 1 mm/d to 7 mm/d. The conceptual groundwater budget suggests recharge by rainfall is the dominant inflow, whereas the primary outflow boundary for the model domain is discharge to the EBFR. The actual outflow via evapotranspiration depends on the area of the model domain where it is significant. The inflow and outflow estimates for the Main Pit suggest a net inflow (out of the model domain) while estimates for the Intermediate Pit suggest a net outflow (into the model domain).

Table 3-3. Conceptual Groundwater Budget for the Rum Jungle Mine Site

Component	Flow, Mm^3 Lower Bound	Flow, Mm^3 Upper Bound	Comment
Inflows			
Recharge by rainfall (undisturbed areas)	1.7	5.1	Assuming 1307 mm rainfall and percentage recharge ranging from 10% to 30%
Recharge by rainfall (mine waste units)	0.1	0.3	Assuming 1307 mm rainfall and 25 to 50% recharge to mine waste units
Flows from the Main Pit	0.01	0.1	Assuming dry season gradients, 45 m aquifer thickness, and K = 1E-6 to 1E-5 m/s
From the Intermediate Pit	0.02	0.3	Assuming dry season gradients, 45 m aquifer thickness, and K = 1E-5 to 9E-5 m/s
Total:	**1.9**	**5.9**	
Outflows			
Evapotranspiration	0.2	1.4	Assumed range of 1 mm/d to 7 mm/d, 6 months of the year, all significantly treed areas
To the Main Pit	0.03	0.2	Assuming wet season gradients, 45 m aquifer thickness, and K = 2E-6 to 1E-5 m/s
To the Intermediate Pit	0.01	0.1	Assuming wet season gradients, 45 m aquifer thickness, and K = 2E-6 to 1E-5 m/s
To the Browns Oxide Pit	0.3	0.8	Best judgement from previous model results and preliminary water level surveys
To the upper EBFR	0.2	0.9	Assuming wet season gradients, 45 m thick aquifer, and K = 2E-6 to 1E-5 m/s
To Fitch Creek	0.1	0.4	Assuming wet season gradients, 45 m thick aquifer, and K = 2E-6 to 1E-5 m/s
To the EFDC	0.1	0.4	Assuming wet season gradients, 15 m thick aquifer, and K = 2E-6 to 1E-5 m/s
To the EBFR d/s of gauge GS8150200	0.4	1.8	Assuming wet season gradients, 45 m thick aquifer, and K = 2E-5 to 9E-5 m/s
Total:	**1.3**	**5.8**	

Note 1: Flows to the flooded Pits and tributaries of the East Branch of the Finniss River were estimated via Darcy flow calculations

Note 2: Net rainfall is mean annual rainfall minus soil moisture deficit of 150 mm/yr

3.11 GROUNDWATER QUALITY IMPACTS

Observed SO_4 and Cu concentrations in groundwater (and inferred plumes) are shown in Figure 3-7 and Figure 3-8, respectively. Further details on the derivation of these plumes is provided in RGC (2016). Groundwater quality impacts in key areas of the site are discussed below. Additional water quality observations are provided in RGC (2016).

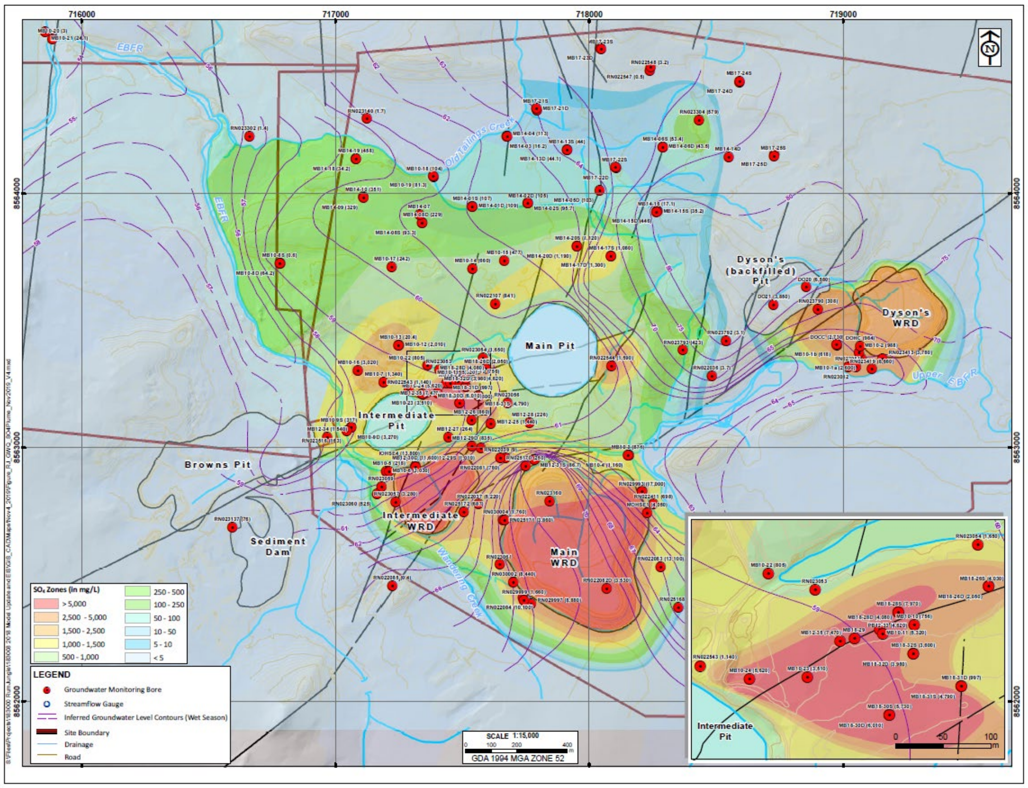

Figure 3-7. Observed Sulphate Concentrations and Inferred Plumes, Current Conditions

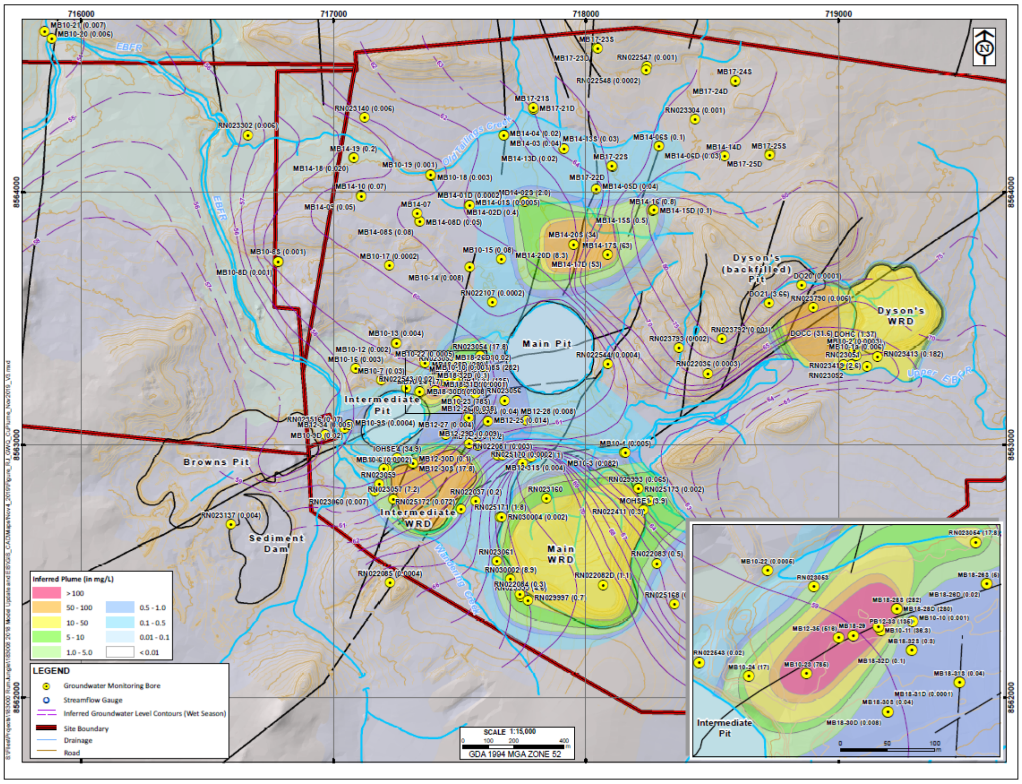

Figure 3-8. Observed Copper Concentrations and Inferred Copper Plumes, Current Conditions

3.11.1 Background Water Quality

Groundwater not impacted by AMD within the former Rum Jungle mine site is typically circum-neutral to slightly alkaline and characterized by alkalinity values up to 200 mg/L as $CaCO_3$, depending on the screened lithology. SO_4 concentrations in unimpacted groundwater typically range from 1 to 5 mg/L SO_4 and Cu-t concentrations are typically 0.001 to 0.006 mg/L. Elevated Mn concentrations are observed in groundwater from the Coomalie Dolostone, e.g. at bore RN022085.

3.11.2 Groundwater Quality in Dyson's Area

Dyson's Area is upstream of the central mining area near the eastern lease boundary. The upper EBFR is unimpacted before it flows through Dyson's Area towards the confluence between the upper EBFR and Fitch Creek about 1 km downstream near the Main WRD. The AMD sources in this area are Dyson's WRD and Dyson's (backfilled) Pit. Representative seepage and groundwater quality observations in Dyson's Area are provided in Table 3-4.

Groundwater quality impacts in Dyson's Area are summarized below:

- **Dyson's WRD**.
  - Dyson's WRD contains PAF-II (15%), PAF-III (40%), and NAF (45%) waste rock removed from Dyson's pit during mining (see RGC and DJEE, 2019). Dyson's WRD is unlined and was constructed on or near the floodplain of the upper EBFR. The base of the dump is therefore often inundated by the creek during the wet season and there are multiple seepage areas where AMD reports directly to the EBFR. The top of Dyson's WRD was covered during initial rehabilitation in the 1980s but the batters (side-slopes) of the dump were not covered (see Allen and Verhoeven, 1986). As a result, there is substantial infiltration of rainfall through the batter slopes.
  - Seepage from Dyson's WRD is acidic (pH < 5) and is characterized by elevated SO_4 and metal concentrations. However, metal concentrations in seepage from Dyson's WRD are much lower than in seepage from Dyson's (backfilled) Pit (and the other WRDs) due to the lower sulphide content of the PAF-III and NAF waste rock in this dump. This lower sulphide content is related to the mineralogy of the Dyson's ore body, which was mined solely for uranium during the initial stages of mining operations.
  - Groundwater from bores RN023413 and RN023415 (screened in the EBFR channel) are impacted primarily by seepage from Dyson's WRD. Groundwater from these bores is characterized by elevated SO_4 and moderate metal concentrations, e.g. up to 2.6 mg/L Cu. Groundwater from other bores in this area, e.g. MB10-2, is typically characterized by elevated SO_4 concentrations but lower metal concentrations, depending in part on the proximity of the bore to Dyson's WRD.
- **Dyson's (backfilled) Pit**
  - Dyson's Pit was mined to 47 m below ground surface (bgs) and partially backfilled with tailings during mining operations. These tailings were placed hydraulically (as a slurry) and have since consolidated. Dyson's Pit was further backfilled with well-consolidated historic tailings removed from the Old Tailings Dam area during initial rehabilitation in the 1980s. Tailings were hauled from the Old Tailings Dam area by truck and placed on the historic tailings. The shallow (above-grade) zone of Dyson's Pit was then backfilled in 1984 with leached, low-grade ore (from Intermediate Pit) and contaminated soils removed from the Copper Extraction Pad area. The backfilled pit was later covered to reduce rainfall infiltration, with a rock-lined drain along the centre-line conveying rainfall runoff to the upper EBFR (see Allen and Verhoeven, 1986).
  - Shallow backfill materials in Dyson's Pit are a mix of PAF-I (70%), PAF-II (20%) and PAF-III (30%) materials (see RGC and DJEE, 2019). These materials are separated from deeper tailings by a drainage layer underlain by a geosynthetic layer. The

drainage layer between the tailings and shallow backfill materials conveys seepage to a toe drain along the southern batter of the backfilled pit. This seepage is predominantly derived from drainage from shallow backfill materials in the pit that are recharged by rainfall infiltration through the cover.

- Seepage from Dyson's Pit reports directly to the upper EBFR via a surface channel that originates from the toe drain and/or to groundwater that ultimately discharges to the EBFR. Seepage is characterized by elevated concentrations of SO_4 and most metals, including Cu, Co, and Mn. Metal concentrations in seepage are comparable to seepage from the Intermediate WRD, as the backfill materials are predominantly low-grade ore removed from the Intermediate ore body for heap leaching (see Davey, 1975). Groundwater from bore MB10-1b is impacted by seepage from Dyson's (backfilled) Pit. This bore is screened in the drainage channel that conveys seepage from shallow backfill materials to the upper EBFR. Groundwater is often acidic and characterized by elevated SO_4 and metals, particularly in the wet season when seepage expresses from the nearby toe drain.
- Tailings in deeper portions of Dyson's Pit are not considered a significant source of AMD because they are submerged year-round and therefore not oxidizing (see RGC, 2016). Most of the AMD generated by PAF materials in Dyson's WRD and Dyson's (backfilled) Pit reports directly to the EBFR or to groundwater that ultimately discharges to the EBFR within Dyson's Area. Impacted groundwater, for instance, does not appear to be transported westward beyond Dyson's Area due to local topography and/or the low permeability of bedrock, e.g. Rum Jungle Complex and Geolsec Formation to the west.

Table 3-4. Representative Groundwater Quality and Seepage Water Quality Observations for Dyson's Area and near the Main WRD

Bore ID	Screened Lithology	Screened Interval, m bgs	Dry Season						Wet Season					
			Sampling Date	Field pH	SO_4, mg/L	Cu, mg/L	Fe, mg/L	Zn, mg/L	Sampling Date	Field pH	SO_4, mg/L	Cu, mg/L	Fe, mg/L	Zn, mg/L
Dyson's WRD														
Toe seepage	n/a	n/a	Dec-11	4.4	332	4.0	0.9	0.1	Apr-12	4.3	984	1.4	0.6	0.2
Dyson's (backfilled) Open Pit														
Toe seepage	n/a	n/a	Dec-11	3.8	2,990	29.0	0.1	0.9	Apr-12	4.0	2,730	31.6	0.1	1.0
Near Dyson's WRD														
MB10-1a	Saprolite	1.4 to 3.4	-	-	-	-	-	-	Feb-12	6.3	2,600	0.006	7.4	0.1
MB10-2	Rum Jungle Complex	12.7 to 18.7	Sep-12	6.9	815	0.0018	1.1	0.004	Feb-12	6.9	988	0.0003	1.4	0.010
RN023413	Laterite	1.3 to 1.8	Oct-11	3.5	2,730	0.7	133.0	0.2	Apr-09	-	3,780	0.2	126.0	0.3
RN023419	Alluvium	1.2 to 1.7	-	-	-	-	-	-	Apr-09	-	8,660	2.6	29.6	0.8
Near or within Dyson's (backfilled) Pit														
DO20	Tailings	16.0 to 19.0	-	-	-	-	-	-	Sep-11	5.2	6,580	0.0001	435.0	0.1
DO21	Shallow backfill and tailings	14.7 to 17.7	-	-	-	-	-	-	Sep-11	4.7	3,850	3.7	145.0	1.6
MB10-1b	Alluvium	2.2 to 3.7	Nov-10	3.5	2,720	31.7	0.400	1.000	Mar-12	4.5	618	1.7	0.048	0.047
RN023790	Geolsec Formation	10.0 to 16.0	Sep-12	7.1	264	0.025	0.0	0.002	Apr-11	7.1	308	0.006	0.2	0.017
West of Dyson's Area (towards the Main Pit)														
RN022036	Geolsec Formation	7.0 to 12.0	Sep-12	6.5	3	0.0094	0.006	0.003	Feb-12	6.4	4	0.0003	0.002	0.002
RN023792	Geolsec Formation	20.0 to 26.0	Sep-12	7.3	3	0.003	0.034	0.000	Feb-12	7.2	3	0.001	0.006	0.002
RN023793	Whites Formation	13.2 to 19.2	Sep-12	5.8	424	0.022	0.6	0.005	Apr-11	5.9	423	0.002	0.2	0.003

Note: Values in red are lower than the indicated reporting limit

3.11.3 Groundwater Quality near Main WRD

The Main WRD is the largest of the historic dumps in terms of footprint area and volume. It is unlined and contains a mixture of PAF-I (15%), PAF-II (35%), PAF-III (25%), and NAF (25%) waste rock removed during mining the Main ore body together with a small volume of PAF waste rock re-located from the Main North WRD during rehabilitation in the 1980s (see RGC and DJEE, 2019). The Main WRD was re-graded and covered at that time to prevent AMD by reducing rainfall infiltration and oxygen ingress. The cover was considered effective, at least initially, although its performance was found to have deteriorated in the 1990s (Taylor et al., 2003). A contemporary assessment of cover performance assessment has not been done.

Representative seepage and groundwater quality observations near the Main WRD are provided in Table 3-5. Key observations are summarized below:

- Seepage from the Main WRD reports to groundwater and to a collection ditch along the western toe of the dump near the main access road to the site. Seepage samples from the ditch are acidic (pH 3 to 4) and characterized by highly-elevated concentrations of SO_4 and most metals. This seepage occurs in the wet season and often persists during the early dry season and is likely comprised of toe seepage and AMD-impacted groundwater that upwells to the ditch. Seepage from this ditch reports to Fitch Creek near the head of the EFDC (near bores MB10-3 and MB10-4).
- Groundwater near the Main WRD can be characterized by 10,000 to 15,000 mg/L SO_4 and up to 20 mg/L Cu. Concentrations in groundwater can exceed concentrations observed in toe seepage (AMD) from the collection ditch near the eastern toe, implying residual impacts due to more concentrated AMD that formed in the past (before 1980s remediation) or the occurrence of AMD that is more concentrated than the AMD that reports to the ditch (see RGC, 2016). Groundwater from most bores is, however, characterized by much lower Cu concentrations than observed at bores RN022083 and RN022084, implying attenuation in the aquifer and that Cu is not transported far beyond the perimeter of the Main WRD.
- Groundwater impacted by AMD from the Main WRD reports to the EBFR via Fitch Creek or the EFDC and may also be transported northward beneath the EFDC via deeper flowpaths in the bedrock aquifer. This suggests a portion of the AMD generated by the Main WRD could report to groundwater downgradient near the Intermediate WRD and possibly the EBFR downstream of GS8150200 should it upwell. However, Cu concentrations in groundwater migrating northeast from the Main WRD, e.g. near bores RN022081 and MB12-31S, are relatively low, suggesting groundwater-borne Cu loads are relatively low in this direction.

Table 3-5. Representative Groundwater Quality and Seepage Water Quality Results, Main WRD Area

Bore ID	Screened Lithology	Screened Interval, m bgs	*Dry Season* Sampling Date	Field pH	SO_4, mg/L	Cu, mg/L	Fe, mg/L	Zn, mg/L	*Wet Season* Sampling Date	Field pH	SO_4, mg/L	Cu, mg/L	Fe, mg/L	Zn, mg/L
Main WRD														
Toe seepage	n/a	n/a	Aug-10	3.7	5,190	4.4	4.8	7.1	May-12	3.3	4,050	3.9	3.5	6.5
Main WRD (East)														
RN022082D	Rum Jungle Complex	37.0 to 52.0*	Oct-12	4.4	6,100	1.8	9.5	6.2	Feb-12	4.3	3,530	1.1	5.9	5.5
RN022083	Rum Jungle Complex	10.0 to 16.0	Oct-14	6.0	9,190	0.0	0.0	0.01	Feb-14	6.1	13,100	0.5	0.0	0.02
RN022411	Alluvium	0.3 to 1.5	-	-	-	-	-	-	Feb-11	4.2	698	0.3	3.6	1.0
RN022417	Rum Jungle Complex (wtr)	0.4 to 2.5	-	-	-	-	-	-	Apr-09	-	3,230	20.1	1.8	6.7
RN025168	Rum Jungle Complex (wtr)	6.5 to 9.5	-	-	-	-	-	-	Apr-09	6.1	2	0.004	0.2	0.01
RN029993	Clay	1.0 to 7.2	Sep-12	6.0	16,300	0.0	2.2	0.14	Feb-12	6.0	17,000	0.1	0.1	0.05
Main WRD (Southwest)														
RN022084	Rum Jungle Complex	10 to 16	Oct-14	5.0	8,680	9.5	2.7	12.9	Feb-14	6.3	10,100	0.3	1.8	0.2
RN025165	Rum Jungle Complex	5.2 to 8.2	Oct-10	6.2	98	0.01	3.8	0.1	-	-	-	-	-	-
RN029997	Quartz gravels	1.0 to 3.3	Oct-10	5.2	8,880	0.7	0.4	1.0	-	-	-	-	-	-
RN029999	Quartz gravels	1.0 to 7.8	Oct-10	3.8	1,660	4.6	-	2.8	-	-	-	-	-	-
RN030002	Rum Jungle Complex	1.0 to 8.4	Oct-10	3.8	8,440	8.9	6.2	15.7	-	-	-	-	-	-
RN030004	Sandstone	1.5 to 2.9	Aug-10	7.2	1,760	0.002	0.2	0.0	-	-	-	-	-	-
Main WRD (Northwest)														
RN025170	Whites Formation	5.9 to 8.9	Oct-10	7.2	326	0.0043	0.40	0.035	Feb-12	6.9	250	0.0002	0.02	0.001
MB12-31S	Laterite	1.7 to 7.7	Oct-14	7.2	122	0.073	0.02	0.007	Apr-15	7.2	87	0.004	0.01	0.005
RN022081	Coomalie Dolostone	40.7 to 43.9	Sep-10	7.0	787	0.000	0.4	0.005	Feb-14	7.3	780	0.003	0.1	0.002
RN022039	Coomalie Dolostone	12.0 to 18.0	Sep-10	5.1	4	0.00	0.2	0.03	Feb-14	5.7	9	0.01	0.1	0.02
Main WRD (West)														
RN022037	Rum Jungle Complex (wtr)	16.0 to 22.0	Aug-10	6.2	5,680	0.2	0.2	0.2	Feb-12	6.1	5,220	0.2	1.2	0.2
RN025172	Rum Jungle Complex	1.7 to 4.7	Sep-12	5.6	3,110	0.0	0.4	0.2	Feb-14	5.6	687	0.1	0.1	0.1
Main WRD (North)														
RN025169	Laterite	2.8 to 5.8	-	-	-	-	-	-	Feb-14	6.4	91	0.1	0.004	0.01
RN025171	Laterite	2.8 to 5.8	-	-	-	-	-	-	Feb-13	5.7	3,860	1.8	1.0	0.6
MB10-3	Saprolite	2.0 to 3.5	Dec-10	3.8	1,160	3.6	0.6	1.4	Mar-15	5.6	874	0.1	9.8	0.8
MB10-4	Rum Jungle Complex	9.3 to 15.3	Dec-10	6.8	1,090	0.002	0.2	0.01	Mar-15	6.5	1,160	0.005	0.4	0.01

* Below the top of the Main WRD

Note: Values in red are lower than the indicated reporting limit

3.11.4 Groundwater Quality near the Intermediate WRD

The Intermediate WRD is much smaller than the Main WRD and contains only PAF-I and PAF-II (the most AMD-generating PAF types) material according to RGC and DJEE (2019). Metal concentrations in seepage from the Intermediate WRD, including Cu, Co, Fe, Mn, Ni, and Zn are typically (much) higher than in seepage from the Main WRD and Dyson's WRD, most likely due to consistently higher sulphide content and the polymetallic nature of waste rock in the Intermediate WRD compared with the other WRDs.

The Intermediate WRD is unlined and most of it was re-graded and covered during initial rehabilitation in 1985 to reduce rainfall infiltration and oxygen ingress. However, the northern toe of the dump was not re-graded or covered due to insufficient funds (see Allen and Verhoeven, 1986). The ungraded toe of the dump terminates at the EFDC and appears to convey a substantial volume of toe seepage directly to the EFDC. This is evidenced by a pool of seepage in the EFDC that is sustained in the dry season by toe seepage and/or groundwater discharge. This seepage is often routinely sampled to characterize water quality. Since the seepage face is submerged during the wet season seepage samples cannot be collected during this period of the year.

Seepage (AMD) from the Intermediate WRD is particularly detrimental to EBFR water quality due to its proximity to the EFDC and the propensity for seepage to occur throughout the dry season and accumulate in the EFDC, thereby contributing to a “first flush” event each year. However, most of the AMD generated by the Intermediate WRD likely reports to groundwater beneath the dump via basal seepage and may migrate towards the Intermediate Pit via deeper flowpaths beneath the EFDC. Representative seepage and groundwater quality observations near the Intermediate WRD are provided in Table 3-6. Most of the groundwater near the Intermediate WRD is characterized by elevated SO_4 but low concentrations of most metals, including Cu. Bores MB12-30S and MB12-30D are exceptions, as these bores are screened at the toe of the Intermediate WRD near the edge of the EFDC. Low concentrations of Cu and other metals suggest attenuation of metals in groundwater or that the most impacted groundwater in this area has not been identified.

Of interest are potentially high concentrations in deeper groundwater beneath the Intermediate WRD that may migrate northward beneath the EFDC towards the Intermediate Pit based on the prevailing hydraulic gradients in this area. Further drilling in this area is needed to determine whether impacted groundwater exists at depth and whether it is being transported northward. This is a critical area of the site as the extent of residual AMD-impacted groundwater near the EFDC is a key factor in determining post-rehabilitation Cu loads in the EBFR. Additional monitoring bores and recovery bores (for pump testing) are warranted.

Table 3-6. Representative Groundwater and Seepage Water Quality Results, Intermediate WRD Area

Bore ID	Screened Lithology	Screened Interval, m bgs	*Dry Season* Sampling Date	Field pH	SO_4, mg/L	Cu, mg/L	Fe, mg/L	Zn, mg/L	*Wet Season* Sampling Date	Field pH	SO_4, mg/L	Cu, mg/L	Fe, mg/L	Zn, mg/L
Unimpacted groundwater														
RN022085	Coomalie Dolostone	1.5 to 7.5	Nov-09	7.1	0.6	0.0010	0.02	0.0025	Jan-09	7.2	0.4	0.0004	0.02	0.0005
Intermediate WRD														
Toe seepage	n/a	-	Aug-10	3.3	13,800	34.9	349	156	Apr-15	4.4	3,840	17.8	145.0	29.1
Intermediate WRD (North)														
MB10-5	Laterite/fill	2.0 to 5.0	Nov-10	6.6	463	0.019	0.200	0.800	Apr-15	6.9	218	0.001	0.004	0.005
MB10-6	Whites Formation	13.5 to 25.5	Nov-10	7.2	931	0.0027	0.200	0.000	Apr-15	7.2	1,030	0.0002	0.012	0.002
MB12-25	Whites Formation	12.9 to 18.9	Oct-14	6.6	1,570	0.057	0.06	0.007	Feb-14	6.5	1,440	0.014	0.01	0.042
MB12-29S	Laterite	7.0 to 10.0	Nov-12	6.7	1,010	0.200	0.10	0.060	-	-	-	-	-	-
MB12-29D	Coomalie Dolostone	14.9 to 17.9	Nov-12	7.3	835	0.009	0.020	0.008	-	-	-	-	-	-
MB12-30D	Whites Formation	12.3 to 18.3	-	-	-	-	-	-	Apr-15	6.2	11,600	0.1	5.6	1.1
MB12-30S	Whites Formation/waste rock	1.5 to 7.5	-	-	-	-	-	-	Apr-15	4.4	3,840	17.8	145.0	29.1
RN023057	Whites Formation (wtr)	1.8 to 2.6	-	-	-	-	-	-	Apr-09	-	3,280	7.2	40.8	4.6
RN023060	Whites Formation (wtr)	4.2 to 5.1	Aug-11	6.5	596	0.008	0.126	0.007	Feb-12	6.5	525	0.007	0.032	0.008
Intermediate WRD (Southeast)														
RN025173	Rum Jungle Complex	5.1 to 8.1	Aug-10	6.1	3,800	0.040	0.200	0.045	Feb-12	6.1	3,790	0.002	0.020	0.005
RN022037	Rum Jungle Complex	16.0 to 22.0	Aug-10	6.2	5,680	0.2	0.2	0.2	Feb-12	6.1	5,220	0.2	1.2	0.2

Note: Values in red are lower than the indicated reporting limit

3.11.5 Groundwater Quality in Copper Extraction Pad area

An experimental heap leaching operation was conducted in the Copper Extraction Pad area from 1965 to 1971. The heap leaching process initially involved piling low-grade (<2% Cu content) sulphide ore from the Intermediate ore body onto a low-permeable pad and then spraying the top of the pile with an acidic (pH 2) mixture of mill process water, barren liquor, and pit water from the Main Pit. Liquor drained from the sulphide pile (nominally pH 1.5) was then pumped onto a pile of oxide ore to leach additional copper before the pregnant liquor was pumped to launders for copper recovery by cementation (see Davy, 1975, for further details).

Substantial losses of metalliferous liquor containing an estimated 1000 mg/L Cu occurred during the operation, primarily from an unlined storage ditch adjacent to the heap leach pad (see Davey, 1975). Overflow from the ditch and excess barren liquors (pH < 2) were also discharged to Copper Creek, which flowed northwest to the EBFR. In 2010, near-undiluted liquor was identified during a hydrogeological field investigation in this area (see RGC, 2011). Cu concentrations of up to 1000 mg/L Cu are observed in several monitoring bores in this area, i.e. MB10-23 and MB12-35 (see

Table **3-7**).

The liquor in the Copper Extraction Pad area appears to be restricted to a narrow zone of the bedrock aquifer that may correspond to a fault that is oriented east-to-west across the area between the Main Pit and Intermediate Pit. Cu concentrations have not been diluted since liquor was lost in the 1960s, implying that impacted water may reside in a system of cavities that may not be interconnected and could be isolated from groundwater in the surrounding bedrock aquifer. This would suggest the liquor does not report to the Intermediate Pit or to the EBFR and is therefore a localized groundwater quality issue. Several recovery bores screened in bedrock near the fault zone are planned to improve groundwater quality in this area (see Section 4.7).

The previously inferred copper plume (from RGC, 2016f) extended to fully cover the former Copper Extraction Pad area. Figure 3-9 shows the refined extent of the copper plume in this area. Recent groundwater quality sampling, within the southern side of the pad area, from bores MB18-30S/D, MB18-31S/D and MB18-32S/D show elevated sulphate concentrations (range from 1000 to 6000 mg/L) but low copper concentrations in the range of 0.0001 to 0.3 mg/L. However, observed copper concentrations in the northern side of the pad area show elevated concentrations for both sulphate and copper (particularly at MB18-28S, MB18-29, MB10-11, MB12-35 and MB12-33) with ranges from 750 to 8500 mg/L and 53 to 560 mg/L, respectively. Therefore, it was conceptualized that the copper plume is limited to the northern side of the pad area with an approximate length of 325m and width of 120m, while the sulphate plume is inferred to cover the full extent of the extraction pad area.

Table 3-7. Representative Groundwater and Seepage Water Quality Results, Central Mining Area

Bore ID	Screened Lithology	Screened Interval, m bgs	*Dry Season*						*Wet Season*					
			Sampling Date	Field pH	SO_4, mg/L	Cu, mg/L	Fe, mg/L	Zn, mg/L	Sampling Date	Field pH	SO_4, mg/L	Cu, mg/L	Fe, mg/L	Zn, mg/L
Bores neart the Main Pit														
RN022544	Whites Formation	35.2 to 44.5	Sep-10	7.5	3,880	0.0008	2.0	0.010	Mar-11	6.5	1,590	0.0004	1.8	0.006
RN022107	Coomalie Dolostone	12.8 to 14.8	Aug-10	6.2	1,300	0.0005	3.800	0.4480	Mar-15	8.5	841	0.0002	0.010	0.0004
Bores near the former Copper Extraction Pad														
MB10-10	Whites Formation	16.0 to 32.0	Dec-10	6.7	71	0.001	2.0	0.013	Feb-14	6.7	756	0.001	1.8	0.015
MB10-11	Whites F. (sand-filled cavity)	31.5 to 34.5	Dec-10	5.0	5,600	137.0	36.3	9.2	Feb-14	5.5	5,320	36.3	3.4	5.4
MB10-22	Coomalie Dolostone	12.6 to 24.6	Dec-10	7.7	944	0.0014	0.4	0.005	Apr-15	7.8	805	0.0005	0.2	0.002
MB10-23	Coomalie Dolostone	13.0 to 25.0	Dec-10	3.5	5,190	506	13.0	10.5	Apr-15	4.0	3,510	785	36.5	12.0
MB10-24	Coomalie Dolostone	4.0 to 16.0	Oct-14	3.5	1,050	52.6	0.6	1.4	Apr-15	3.6	5,620	17.3	0.3	0.4
MB12-35	Coomalie Dolostone	22.1 to 34.1	Oct-14	4.4	8,500	511	79.1	11.6	Feb-14	4.2	7,470	516	92.2	11.1
MB18-26D	Whites Formation	42.0 to 60.0	-	-	-	-	-	-	Jan-19	6.3	2,050	0.019	12.2	0.2
MB18-26S	Whites Formation	12.0 to 18.0	-	-	-	-	-	-	Jan-19	5.1	4,030	5.4	72.1	3.0
MB18-28D	Whites Formation	42.0 to 60.0	-	-	-	-	-	-	Jan-19	4.2	4,080	280	0.3	8.8
MB18-28S	Whites Formation	12.0 to 24.0	-	-	-	-	-	-	Jan-19	4.9	7,970	282	101	12.7
MB18-30D	Whites Formation	42.0 to 60.0	-	-	-	-	-	-	Jan-19	6.2	6,010	0.008	24.4	0.1
MB18-30S	Whites Formation	13.7 to 19.7	-	-	-	-	-	-	Jan-19	5.9	5,730	0.040	116	0.7
MB18-31D	Whites Formation	42.0 to 60.0	-	-	-	-	-	-	Jan-19	6.5	997	0.0001	8.9	0.007
MB18-31S	Whites Formation	18.0 to 24.0	-	-	-	-	-	-	Jan-19	6.1	4,790	0.044	18.9	0.1
MB18-32D	Whites Formation	42.0 to 60.0	-	-	-	-	-	-	Jan-19	5.9	3,980	0.1	87.2	0.8
MB18-32S	Whites Formation	12.0 to 24.0	-	-	-	-	-	-	Jan-19	5.6	3,600	0.3	60.0	1.1
PB12-33	Whites Formation	14.1 to 32.1	Nov-12	4.7	5,480	225.0	6.9	8.9	Feb-14	5.3	4,620	135.0	2.8	7.7
Bores near the Intermediate Pit (or immediately north)														
MB10-12	Coomalie Dolostone	12.6 to 24.6	Dec-10	7.2	2,520	0.001	0.200	0.001	Mar-15	7.2	2,010	0.002	0.014	0.009
MB10-13	Coomalie Dolostone	48.8 to 60.8	Dec-10	8.1	35	0.000	0.200	0.000	Mar-15	7.8	20	0.004	0.004	0.004
MB10-16	Coomalie Dolostone	13.5 to 22.5	Aug-11	6.9	3,070	0.000	1.1	0.003	Feb-14	7.1	3,020	0.003	2.4	0.017
MB10-7	Coomalie Dolostone	9.0 to 18.0	Aug-11	7.3	1,410	0.000	**0.020**	0.002	Mar-15	7.3	1,340	0.026	**0.010**	0.022
RN022543	Coomalie Dolostone	23.0 to 33.0	Oct-12	7.6	1,380	0.000	0.026	0.0	Feb-14	7.5	1,140	0.018	0.014	0.1
Bores near the EFDC (north side)														
MB12-26	Whites Formation	9.0 to 11.0	Oct-14	6.4	973	0.069	**0.02**	0.006	Feb-14	6.4	860	0.038	**0.01**	0.015
MB12-27	Coomalie Dolostone	8.7 to 11.7	Oct-14	7.3	302	0.015	0.092	0.001	Feb-14	7.3	264	0.004	0.012	0.004
MB12-28	Coomalie Dolostone	9.4 to 15.4	Oct-14	6.9	337	0.023	0.1	0.003	Feb-14	6.7	226	0.008	0.1	0.024
MB10-14	Coomalie Dolostone	14.2 to 16.2	Dec-10	6.1	737	0.018	**0.20**	0.015	Mar-12	6.6	660	0.008	**0.02**	0.013
MB10-15	Coomalie Dolostone	12.4 to 24.4	Dec-10	6.6	554	0.0	**0.2**	0.1	Apr-11	7.4	477	0.1	**0.2**	0.1
MB10-17	Coomalie Dolostone	20 to 26	Dec-10	6.7	288	0.001	**0.2**	0.000	Mar-11	6.9	242	0.000	**0.2**	0.003
Bores west of the Intermediate Pit														
MB10-9D	Coomalie Dolostone	46.3 to 62.3	Dec-10	6.7	2,910	0.056	7.6	0.1	Mar-15	6.5	3,270	0.018	2.1	0.1
MB10-9S	Coomalie Dolostone	23.4 to 29.4	Dec-10	7.5	236	0.012	0.2	0.002	Mar-15	7.3	317	0.000	0.1	0.003
MB12-34	Coomalie Dolostone	48.7 to 60.7	Oct-14	7.2	1,630	0.002	0.7	0.005	Feb-14	7.0	1,540	0.005	0.7	0.005
RN023516	Alluvium	3.1 to 3.9	Sep-12	5.5	197	0.1	0.2	0.2	Feb-13	5.4	163	0.1	0.6	0.2

Note: Values in red are lower than the indicated reporting limit

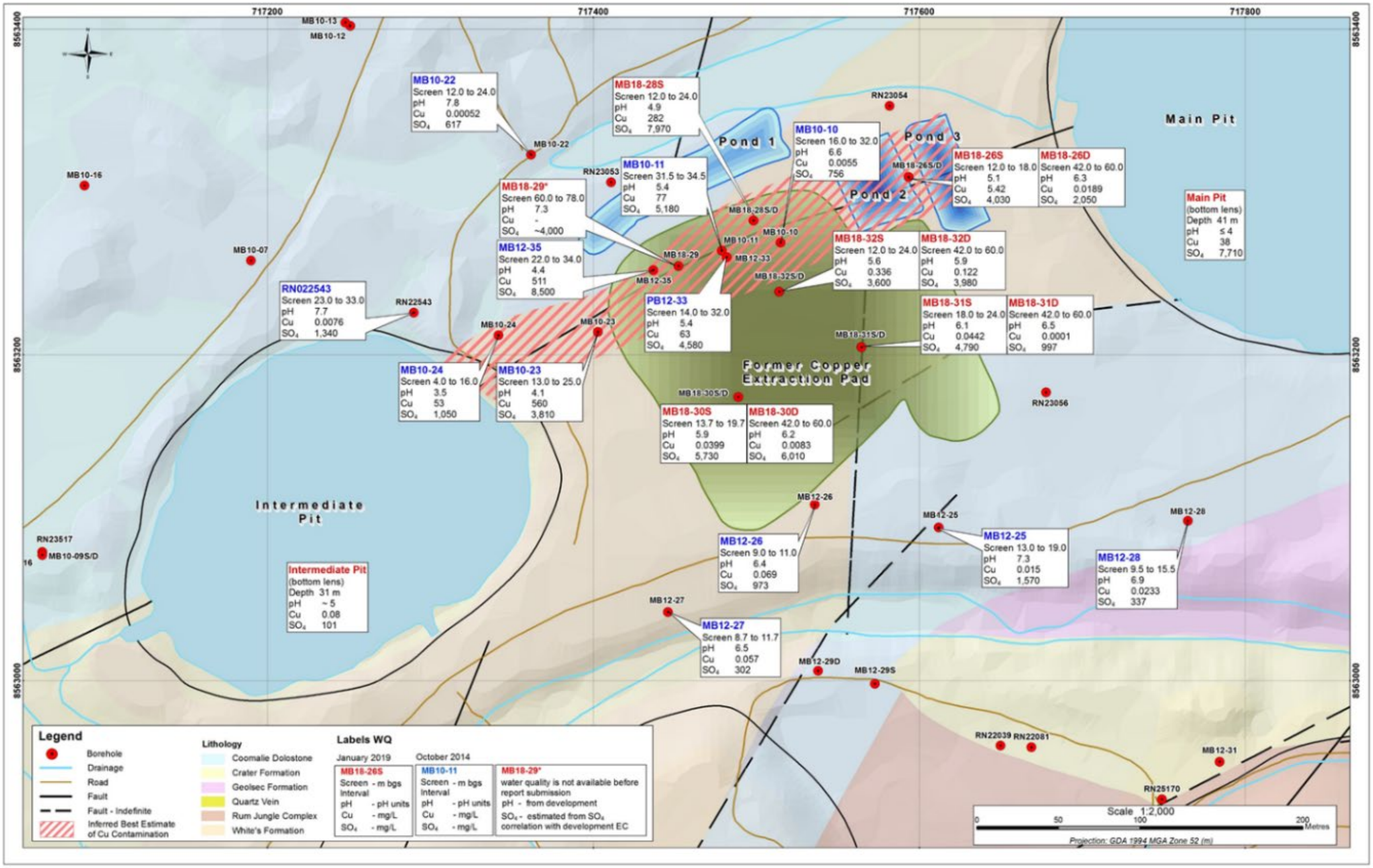

Figure 3-9. Water Quality in the Central Mining Area

3.11.6 Groundwater Quality in Old Tailings Dam area

Tailings were discharged to the Old Tailings Dam area during historic mining operations in the 1950s and 1960s. Tailings accumulated behind a series of small impoundments near Old Tailings Creek and were subsequently eroded during the wet season (see Davey, 1975). Most of the tailings that were in the Old Tailings Dam area were re-located to Dyson's Pit during initial rehabilitation in the 1980s and the area was subsequently covered and re-vegetated. Some small amounts of residual tailings have been identified but they are not considered a significant AMD source to groundwater.

Groundwater in the Old Tailings Dam area is characterized by elevated SO_4 concentrations but metal concentrations tend to be low (see Table 3-8), likely due to attenuation (neutralization) in groundwater in the Coomalie Dolostone. Groundwater in the former ore stockpile area near the Main Pit is an exception, as elevated Cu concentrations are observed in groundwater from bores MB14-20S/D and MB14-17S/D. These concentrations are attributed to seepage from a surface ore stockpile that was removed during initial rehabilitation in the 1980s and are unrelated to historic tailings.

Elevated Cu concentrations in groundwater in this area may also come from AMD generated by local waste rock and/or ore that was covered during initial rehabilitation. Impacted groundwater (at least with respect to metals) appears to be restricted to the former ore stockpile area and is unlikely to account for a substantial load to the Main Pit or the EBFR. A recovery bore is planned as part of the remediation project to improve local groundwater quality in this area (see Section 4.7).

Table 3-8. Representative Groundwater and Seepage Water Quality Results, Old Tailings Dam Area and Downstream near EBFR

			Dry Season						*Wet Season*					
Bore ID	**Screened Lithology**	**Screened Interval, m bgs**	**Sampling Date**	**Field pH**	**SO_4, mg/L**	**Cu, mg/L**	**Fe, mg/L**	**Zn, mg/L**	**Sampling Date**	**Field pH**	**SO_4, mg/L**	**Cu, mg/L**	**Fe, mg/L**	**Zn, mg/L**
Unimpacted groundwater														
RN023302	Coomalie Dolostone	9.5 to 12.5	Aug-10	7.1	1	0.000	0.200	0.014	Feb-12	7.2	1	0.006	0.002	0.002
RN023140	Coomalie Dolostone	11.0 to 16.0	Aug-10	7.1	2	0.000	0.200	0.012	Feb-12	7.2	2	0.006	0.002	0.002
Bores to the northwest of the Main Pit														
MB14-05D	Coomalie Dolostone	21.6 to 27.6	Dec-14	7.3	101	0.005	0.020	0.001	Apr-15	7.5	103	0.036	0.002	0.002
MB14-06D	Coomalie Dolostone	18.0 to 24.0	Dec-14	7.6	44	0.007	0.020	0.002	Apr-15	7.5	44	0.028	0.002	0.003
MB14-15D	Geolsec Formation	21.0 to 42.0	Dec-14	6.9	604	0.0	0.020	0.021	Apr-15	7.1	446	0.1	0.002	0.007
MB14-17S	Fill/Lat./Geolsec Formation	2.1 to 7.1	-	-	-	-	-	-	Apr-15	5.1	1,080	62.6	0.1	8.3
MB14-17D	Geolsec Formation	21.0 to 28.0	-	-	-	-	-	-	Apr-15	5.2	1,300	52.7	0.020	8.5
MB14-20S	Saprolite	2.0 to 8.0	-	-	-	-	-	-	Mar-15	4.8	1,120	33.6	0.1	6.3
MB14-20D	Coomalie Dolostone	21.0 to 27.0	Dec-14	6.2	1,360	3.7	0.04	4.2	Mar-15	6.1	1,190	8.3	0.01	6.1
RN022547	Coomalie Dolostone	17.0 to 23.0	Aug-10	7.1	0	0.000	0.4	0.018	Feb-12	6.8	1	0.001	9.9	0.009
RN022548	Coomalie Dolostone	27.9 to 30.5	Aug-10	7.4	1	0.000	1.8	0.004	Feb-12	7.4	3	0.000	2.1	0.001
RN023304	Coomalie Dolostone	20.9 to 26.4	Aug-10	7.1	667	0.000	0.200	0.014	Mar-12	7.1	579	0.001	0.044	0.001
Bores in the former Old Tailings Dam area														
MB10-8S	Laterite	20.0 to 23.0	Nov-10	7.2	4	0.001	0.2	0.000	Feb-12	7.7	64	0.001	0.2	0.002
MB10-8D	Geolsec Formation	5.6 to 14.6	Dec-10	7.5	29	0.000	0.200	0.000	Feb-12	6.8	1	0.001	0.002	0.003
MB10-18	Saprolite/alluvium	2.0 to 8.0	Dec-10	7.3	109	0.001	0.200	0.000	Feb-12	7.3	104	0.003	0.002	0.017
MB10-19	Coomalie Dolostone	12.5 to 24.5	Dec-10	7.4	80	0.000	0.200	0.000	Feb-12	7.5	81	0.001	0.002	0.006
MB14-01S	Saprolite	2.0 to 6.5	Dec-14	7.2	172	0.003	0.020	0.001	Apr-15	7.4	107	0.001	0.002	0.001
MB14-01D	Coomalie Dolostone	25.8 to 31.8	Apr-15	7.4	109	0.000	0.002	0.001	Apr-15	7.4	109	0.000	0.002	0.001
MB14-02S	Rum Jungle Complex	2.0 to 8.0	-	-	-	-	-	-	Apr-15	6.0	96	2.0	0.002	0.6
MB14-02D	Coomalie Dolostone	23.1 to 29.1	Dec-14	7.5	122	0.0	0.020	0.0	Apr-15	7.2	105	0.4	0.002	0.2
MB14-03	Saprolite	17.8 to 22.8	Dec-14	7.3	21	0.00	0.020	0.004	Apr-15	7.4	16	0.04	0.002	0.001
MB14-04	Saprolite	2.3 to 8.3	Dec-14	7.2	62	0.01	0.020	0.001	Apr-15	7.6	113	0.02	0.002	0.004
MB14-06S	Siltstone	2.0 to 8.0	-	-	-	-	-	-	Apr-15	6.5	53	0.1	0.002	0.1
MB14-06D			Dec-14	7.6	44	0.0	0.020	0.0	Apr-15	7.5	44	0.0	0.002	0.0
MB14-08S	Lat./Sap./Coomalie Dolostone	2.0 to 5.0	-	-	-	-	-	-	Apr-15	7.2	93	0.1	0.002	0.031
MB14-08D	Coomalie Dolostone	17.5 to 23.5	-	-	-	-	-	-	Apr-15	7.2	229	0.05	0.002	0.004
MB14-09	Coomalie Dolostone	10.0 to 16.0	-	-	-	-	-	-	Apr-15	6.7	329	0.05	0.002	0.010
MB14-10	Saprolite	2.2 to 5.2	-	-	-	-	-	-	Apr-15	6.7	351	0.1	0.002	0.009
MB14-13S	Lat./Sap./Coomalie Dolostone	2.0 to 8.0	-	-	-	-	-	-	Apr-15	6.3	44	0.03	0.048	0.009
MB14-13D	Coomalie Dolostone	13.0 to 18.0	-	-	-	-	-	-	Apr-15	6.9	44	0.02	0.002	0.002
MB14-15S	Geolsec Formation	11.0 to 14.0	-	-	-	-	-	-	Apr-15	6.1	35	0.5	0.004	0.2
MB14-16	Laterite/Fill	2.0 to 7.0	-	-	-	-	-	-	Apr-15	5.3	17	0.8	0.012	0.3
MB14-18	Coomalie Dolostone	11.0 to 17.0	-	-	-	-	-	-	Apr-15	7.3	34	0.02	0.02	0.002
MB14-19	Saprolite	2.0 to 6.2	-	-	-	-	-	-	Apr-15	7.0	458	0.2	0.002	0.016
RN023302	Coomalie Dolostone	9.5 to 12.5	Aug-10	7.1	1	0.0003	0.2	0.0	Feb-12	7.2	1	0.01	0.002	0.002
Bores downstream near EBFR (GS8150327)														
MB10-20	Alluvium	2.9 to 6.9	Dec-10	5.7	529	0.00	0.4	0.02	Feb-14	5.4	3	0.01	1.2	0.01
MB10-21	Rum Jungle Complex	12.0 to 32.0	Dec-10	6.9	3	0.00	0.200	0.01	Feb-14	6.9	24	0.01	0.002	0.01

Note: Values in red are lower than the indicated reporting limit

3.11.7 Groundwater Quality Downstream near EBFR

Groundwater quality near the EBFR adjacent to the Old Tailings Dam area (at bores MB10-8S/D) is characterized by relatively low SO_4 and most metals related to AMD. These low concentrations are consistent with only modest AMD impacts to groundwater migrating west towards the EBFR from the Old Tailings Dam area and/or residual impacted groundwater from the central mining area (at least towards GS8150200), most likely due to attenuation in groundwater in the Coomalie Dolostone.

Further downstream (near gauge GS8150327), groundwater from bores MB10-20 and MB10-21 is characterized by low SO_4 and metal concentrations. Gauge GS8150327 was installed in 2010 to record loads in the EBFR from the entire lease boundary, including groundwater flows downstream of gauge GS8150200 and flows from Old Tailings Creek. Bore MB10-21 is screened in low-permeable bedrock that conveys minimal groundwater flows, suggesting minimal cross-boundary flows of groundwater impacted by recharge from the nearby EBFR (see RGC, 2016).

3.12 CONTAMINANT TRANSPORT IN GROUNDWATER

3.12.1 Geochemical Controls on Solute Transport in Groundwater

RGC assumes that SO_4 behaves conservatively in groundwater. This implies that SO_4 is not removed or retarded in groundwater by geochemical reactions or adsorption and is therefore transported at a rate that is nearly equivalent to the linear velocity of groundwater. Locally, this assumption may not be valid due to the precipitation of secondary minerals, such as Fe- and/or Al hydroxide sulphates. However, at the regional scale of the transient flow model, these changes in SO_4 concentrations are likely small, and would not affect the overall conclusions drawn from the solute transport modelling.

Dissolved metals, such as Cu, cannot be assumed to behave conservatively in groundwater because their mobility is often hindered by geochemical reactions along a flow path. Reduced mobility (and hence slower rate of transport) that is caused by metals adsorbing to aquifer materials or precipitating to form secondary minerals. These mechanisms are often pH dependent, and not only retard the movement of metals in groundwater, but also provide a future source of metals to groundwater if the metals are eventually released by desorption or if they begin to dissolve.

For Cu, groundwater and soil chemistry strongly influence the speciation of Cu (and, in turn, how it behaves along a flowpath). For instance, in aerobic, alkaline systems, $CuCO_3$ is the dominant, soluble copper species. The cupric ion (Cu^{2+}), and hydroxide complexes, i.e. $CuOH^+$ and $Cu(OH)_2$, are also common under these conditions. Each of these copper species can form strong complexes with humic acids, and the affinity of Cu for these acids increases as pH increases. Moreover, Cu adsorption to hydrous iron oxides that precipitate from groundwater also increases at higher pH. Together, these factors explain the high retardation factors that are often assigned to Cu under near-neutral-to-alkaline conditions.

According to RGC and DJEE (2019), the concentrations of metals in leachate from waste rock samples from the WRDs at the Rum Jungle Mine Site are likely controlled by the solubilities of hydroxide and carbonate phases in waste rock, and by the adsorption of metal ions to both the primary bulk solid phases (e.g. chlorite, muscovite) and to secondary, precipitated Fe and Al hydroxide phases. These controlling processes (solubility and adsorption) are a function of pH, with the extent of metal precipitation and metal adsorption typically increasing as the pH increases from an acidic initial condition, to near-neutral or alkaline pH conditions (i.e. along a ‘pH adsorption edge’).

Adsorption is likely to be the more important process at lower metal concentrations, i.e. in groundwater, as opposed to seepage, and when the pH of pore water initially increases from a more acidic starting value near AMD sources. The latter typically occurs over a 1 to 2 unit pH range for the types of aluminosilicate phases that dominate the mineralogy of the wastes at the Rum Jungle Mine Site (see RGC, 2019). The exact range of pH values that defines the 'pH adsorption edge', which reflects range of processes that act to remove metals from pore water at a site or in a WRD. Regardless, the key finding is that Cu will be removed from groundwater and would reside on aquifer materials until it desorbs or becomes irreversibly adsorbed by ageing. This is consistent with observed groundwater quality impacts at the Rum Jungle Mine Site, which show that Cu concentrations are very high in groundwater near the WRDs but are much lower (if not absent) from groundwater downgradient (see below).

3.12.2 Transport Parameters

No direct or indirect measurements of the parameters that control solute transport (n_e and dispersivity) are available within the model domain. Therefore, RGC assumed n_e was twice as high as the S_y estimated provided above as a default conceptualization of the system. For dispersivity, RGC acknowledged the scale-dependent nature of dispersion and estimated longitudinal dispersivity (α_L) by using a well-known published empirical plot of longitudinal dispersivity versus the scale of the study (Xu and Eckstein, 1995). From experience at other sites, the transverse (α_T) and vertical (α_V) dispersivity values were estimated using typical ratios of α_L/α_T and α_L/α_V of 100 and 1000, respectively. Accordingly, dispersivity values of 10 m, 0.1 m and 0.01 m were selected for α_L, α_T, and α_V, respectively, for the conceptual transport model. For retardation factors (R_f), RGC assumed that values for lateritic soils from Brazil (from de Matos et al., 2001) were representative of laterite and other soils. De Matos et al. (2001) estimated R_f for Cu, as well as Cd, Pb, and Zn for soils using leaching columns. The average R_f for Cu in the nine soils from that study was 3.5. RGC assumed R_f = 3.5 for laterite (and saprolite) to simulate Cu transport.

3.13 CONCEPTUAL LOAD BALANCES

RGC developed a conceptual load balance model to explain contaminant loads to the EBFR before and after initial rehabilitation in 1984/1985. The contaminant load balance model for pre-rehabilitation conditions was calibrated to average load estimates from 1969 to 1984 whereas the load balance for current conditions was calibrated to estimated loads from 2010 to 2018. Further details are provided below.

3.13.1 Load Balance for Historic Conditions (Pre-1985)

A conceptual load balance for the EBFR prior to rehabilitation is provided in Table 3-9. Water quality results were compiled from historic reports, including Davy (1975), and various monitoring reports issued by DPIR. Of interest are the higher concentrations of SO_4 and dissolved metals in historic seepage from the Main and Intermediate WRDs historically and the high concentrations of SO_4 and dissolved metals in pit water immediately before it was treated in 1985 (see Davy, 1975, for additional details). RGC estimated annual loads as the product of annual recharge (in ML) and the likely SO_4 and

Cu concentration in seepage from each source. For the WRDs (which were un-covered), RGC assumed that 50% of annual rainfall infiltrated to groundwater. Other assumed recharge values, i.e. for the Old Tailings Dam area, are provided in the table.

Surface water loads to the East Branch of the Finniss River were not well-constrained prior to rehabilitation, so loads were estimated as the difference between the observed loads in the river and estimated loads to groundwater. For instance, the SO_4 load from surface water from the Old Tailings Dam area and the flooded pit was estimated to be 2,871 t/year (or about 40% of the annual load in the East Branch of the Finniss River). This same approach was used for Cu, but 30% of Cu was assumed to be lost in the sub-surface by adsorption to aquifer materials and/or the precipitation of Cu hydroxides from groundwater (due to increasing pH conditions along the flowpath). In general, the historic load balance is consistent with load estimates from Davy (1975) for the 1973/1974 wet season, and further refinement was unnecessary because the historic loads were only intended to constrain conditions immediately prior to rehabilitation in 1984/1985, and thereby establish the initial site condition for transport modelling.

Table 3-9. Contaminant Loads to Groundwater and the East Branch of the Finniss River (Before Rehabilitation), 1969 to 1984

Source	Area, m^2	SO_4, mg/L	Cu, mg/L	Recharge, mm	Recharge (or Flow), ML	SO_4 Load, t/yr	Cu Load, t/yr
Estimated Contaminant Loads to Groundwater (before rehabilitation), 1438 mm rainfall							
Seepage from the Main WRD	330,000	10,000	100	650	215	2,145	21
Seepage from the Intermediate WRD	80,000	25,000	225	650	52	1,300	12
Seepage from Dyson's WRD	90,000	5,000	8	650	59	293	0.4
Seepage from Old Tailings Dam	275,000	5,000	30	400	110	550	3
Seepage from former mill area	54,000	5,000	60	144	8	39	0.5
Seepage from Copper Extraction Pad area (shallow)	34,000	2,500	8	264	9	22	0.1
Sub-total:	**863,000**	**n/a**	**n/a**	**n/a**	**452**	**4,349**	**37**
Estimated Losses from Groundwater							
Geochemical reactions (e.g. precipitation), 30% for Cu	n/a	n/a	n/a	n/a	n/a	0	-11
Estimated Contaminant Loads to EBFR from Surface Water							
Surface loads (e.g. from tailings, pit water)	n/a	n/a	n/a	n/a	145	2,871	30
TOTAL:	**n/a**	**n/a**	**n/a**	**n/a**	**597**	**7,220**	**56**
Observed Contaminant Loads in the East Branch of the Finniss River Mean Annual Loads, 1969 to 1984						**7,220**	**56**
Additional loads to groundwater							
Liquor lost from collection ditch near heap leach pad (1965 to 1970)	5,985	8,500	1,000	10,540	63	536	63.1
Liquor lost from collection ditch near heap leach pad (1971 to 1984)	5,985	4,250	500	3,162	19	80	9.5
TOTAL:		n/a	n/a	n/a	82	617	73

3.13.2 Load Balance for Current Conditions (1985 to 2018)

Under current conditions, the only sources of AMD to shallow groundwater and the EBFR are the three (covered) WRDs and Dyson's (backfilled) Pit. Conceptual load balances for current conditions are provided in Table 3-10 and Table 3-11. Loads in Table 3-10 correspond to an annual rainfall of 1757 mm (the average rainfall for 2010 to 2015) whereas loads in Table 3-11 correspond to MAP (1459 mm). For the load estimates, annual recharge to the Main and Intermediate WRDs was assumed to be 25% of annual rainfall. 50% of annual rainfall was assumed to infiltrate through Dyson's WRD (because this WRD was only partially covered) and 10% infiltration was assumed for Dyson's (backfilled) Pit. Percentage recharges for the WRDs are based, in part, on a load balance for the EBFR that is based on the 2012 low-flow seepage survey (see RGC, 2012b), and some professional judgment regarding the likely infiltration rates to waste rock with a thin, degraded cover.

Together, seepage from the three WRDs and Dyson's (backfilled) Pit account for an estimated 1,147 t SO_4/year and 2.2 t Cu/year to the EBFR assuming average annual rainfall. Diffuse sources, such as contaminated soils and severely-impacted groundwater in the Copper Extraction Pad area, account for an additional 694 t SO_4/year and 0.6 t Cu/year. Loads from these sources report mainly to the Intermediate Open Pit via groundwater, and their magnitude corresponds well to loads from the Intermediate Pit at gauge GS8150212 (at the outlet of the Intermediate Pit).

Table 3-10. Estimated Contaminant Loads to Groundwater and the EBFR, 2010 to 2015

Source	Area, m^2	SO_4, mg/L	Cu, mg/L	Recharge, mm	Recharge (or Flow), ML	SO_4 Load, t/yr	Cu Load, t/yr
Estimated Contaminant Loads to Groundwater (2010 to 2015), 1757 mm rainfall							
Seepage from the Main WRD	285,000	5,000	5	397	113	566	0.6
Seepage from the Intermediate WRD	73,000	15,000	35	397	29	435	1.0
Seepage from the Dyson's (backfilled) Pit	61,000	2,500	30	176	11	27	0.3
Seepage from Dyson's WRD	94,000	2,500	3	794	75	187	0.2
Seepage from former mill area	208,000	1,500	-	325	68	101	-
Seepage from Copper Extraction Pad area (shallow)	34,000	5,000	8	264	9	45	0.1
Sub-total:	**755,000**	**n/a**	**n/a**	**n/a**	**304**	**1,360**	**2.2**
Residual groundwater	n/a	n/a	n/a	n/a	n/a	805	1.0
TOTAL:		n/a	n/a	n/a	n/a	2,165	3.2
Observed Contaminant Loads in the East Branch of the Finniss River Mean Annual Loads, 2010 to 2015						**2,165**	**3.2**

Table 3-11. Estimated Contaminant Loads to Groundwater and the EBFR, Current Conditions ('Average Year')

Source	Area, m^2	SO_4, mg/L	Cu, mg/L	Recharge, mm	Recharge (or Flow), ML	SO_4 Load, t/yr	Cu Load, t/yr
Estimated Contaminant Loads to Groundwater (2010 to 2015), 1438 mm rainfall							
Seepage from the Main WRD	285,000	5,000	5	325	93	463	0.5
Seepage from the Intermediate WRD	73,000	15,000	35	325	24	356	0.8
Seepage from the Dyson's (backfilled) Pit	61,000	2,500	30	196	12	30	0.4
Seepage from Dyson's WRD	94,000	2,500	3	650	61	153	0.2
Seepage from former mill area	208,000	1,500	-	144	30	45	-
Seepage from Copper Extraction Pad area (shallow)	34,000	5,000	8	144	5	24	0.0
Sub-total:	**755,000**	**n/a**	**n/a**	**n/a**	**224**	**1,071**	**1.8**
Diffuse sources (e.g. contaminated soils, liquor, etc.)	n/a	n/a	n/a	n/a	n/a	769	0.9
TOTAL:		n/a	n/a	n/a	n/a	1,840	2.7
Observed Contaminant Loads in the East Branch of the Finniss River Mean Annual Loads, Adjusted for 'Average Year'						**1,840**	**2.7**

4 NUMERICAL GROUNDWATER MODEL

4.1 OVERVIEW

4.1.1 Previous Modelling

Groundwater conditions are simulated with a transient groundwater flow model constructed with the MODFLOW-NWT finite difference code and transient solute transport model developed using the transport code MT3DMS. Together, the numerical flow and transport models are referred to as the "groundwater model" throughout the EIS. The groundwater model is a numerical representation of RGC's updated conceptual hydrogeological model for the site (see Section 3).

Groundwater model development was an iterative process that began in 2011 during Phase I of the Rum Jungle Rehabilitation Project when the initial conceptual hydrogeological model for the site was developed. A numerical groundwater flow model was later developed (RGC, 2012). A transport model, based on an average steady-state flow field, was incorporated into the groundwater model in 2016 (see RGC, 2016). A fully transient flow and transport model was developed in 2019 for the EIS (this report).

4.1.2 Model Classification

The current groundwater model is a Class 2 model as defined by the Australian Groundwater Modelling Guidelines (Barrett, 2012), although some components of the model are consistent with a Class 3 model. The model was developed in a manner that is consistent with other available modelling guidelines, including the modelling guidelines for British Columbia that RGC developed in association with SRK Consulting (North America) (see BC Ministry of Environment, 2012). Further details on the groundwater model, its calibration, and predictive modelling for the construction period of rehabilitation and post-rehabilitation are provided below.

4.2 FLOW MODEL SETUP

4.2.1 Modelling Objectives

Modelling objectives are as follows:

- Update the transient flow and transport model to represent the updated conceptual hydrogeological model provided in Section 3.
- Predict groundwater flows and associated contaminant loads (SO_4 and Cu) to the EBFR and the Main Pit and Intermediate Pit during the construction phase of rehabilitation.
- Assess the performance of the SIS bores proposed to reduce loads in the EBFR and the extent of AMD-impacted groundwater during the construction phase.

- Predict post-rehabilitation groundwater flow and associated contaminant loading (SO_4 and Cu) to EBFR once the Main Pit is backfilled and the WSF has been constructed.

4.2.2 Key Assumptions

The conceptual hydrogeological model was represented numerically using the following simplifying assumptions:

- The aquifer system at the Rum Jungle Mine Site can be subdivided into hydrostratigraphic units that represent either mine waste (i.e. waste rock and/or tailings) or the naturally-occurring bedrock aquifer and unconsolidated units.
- Each hydrostratigraphic unit can be represented as a single model layer with representative hydraulic properties (i.e. permeability, anisotropy, storage) and groundwater recharge can be estimated as a proportion of incident rainfall.
- Water movement in the hydrostratigraphic units follows Darcy's law and hence can be modelled using the 'equivalent porous medium' approach, i.e. the use of effective (or 'bulk') hydraulic properties to approximate conditions in the aquifer.
- The flooded Main, Intermediate and Brown's Oxide Pits can be represented by 'specified head boundaries' that are equivalent to observed water levels in the pit lakes during the simulation period (2010 to 2018).
- Shallow creeks and seepage areas within the model domain can be adequately represented by drain nodes that have been set below the ground surface and receive groundwater flows from the surrounding aquifer.
- Sections of the EBFR downstream of Old Tailings Creek can be represented by 'specified head boundaries' that are nearly equivalent to observed groundwater levels in monitoring bores near the river.

These assumptions and other aspects of the numerical representation of the conceptual model are explained in more detail in the sub-sections below.

4.2.3 Code Selection

RGC used the USGS code MODFLOW-NWT to construct the groundwater flow model (see Niswonger et al., 2011 for details on this code). The model was setup in GMS v.10.3.7, a widely-used software package that provides a full suite of options to pre/post-process numerical models (Aquaveo LLC, 2018).

MODFLOW was run transiently and hence recharge was applied on a month-by-month basis over the course of the simulation period. A transient model was used to simulate the pronounced seasonality in groundwater levels (and flows) at the site. This approach provides greater accuracy and confidence in model calibration as well as in prediction of various rehabilitation options.

All drainage features, i.e. groundwater discharge to rivers, drainage lines, seepage faces, etc., were simulated using the drain (DRN) package. Also used were the recharge (RCH), time-variant specified head (CHD), and evapotranspiration (EVT1) packages, which are further described in subsequent sections.

4.2.4 Model Domain and Boundary Conditions

Boundaries of the numerical model domain are shown in Figure 4-1. The model domain was defined by local topographic highs and low-lying drainage features which are conceptualized to represent no-flow boundaries. All external boundaries of the model domain represent no-flow boundaries except for the most downgradient (northern) boundary representing the EBFR which is represented by a constant head. This approach implicitly assumes that cross-boundary flows into or out of the groundwater system are negligible. For this reason, net recharge by rainfall and inflows from the flooded Main and Intermediate Pits are the only sources of water to the groundwater system within the model domain, whereas any outflows are accounted for by groundwater discharge and evapotranspiration.

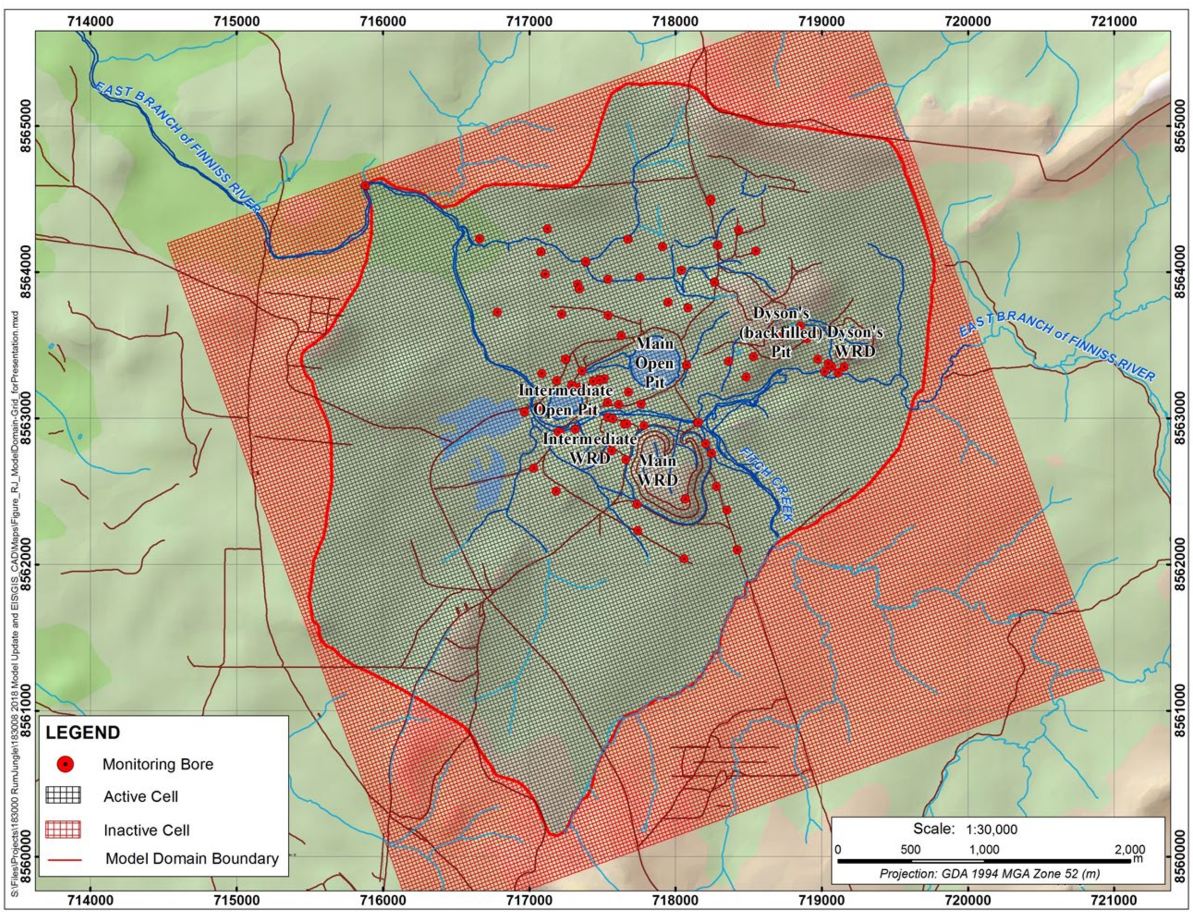

Figure 4-1. Model Domain, Finite Difference Grid, and Boundary Conditions

4.2.5 Grid Design and Spatial Discretization

The numerical model domain was spatially discretized into a uniform grid with cell dimensions of 25 m by 25 m (see Figure 4-2). The thickness of the cells varies depending on the thickness of the hydrostratigraphic unit. The model is composed of 7 layers and extends from a maximum elevation of approximately 100 m AHD to a minimum elevation of -90 m AHD. Surface topography from a Lidar survey completed in 2010 was used to define the top of Layer 1, including the WRDs and Dyson's (backfilled) Pit and an east-west cross-section view showing the vertical discretization of model layers are also shown in Figure 4-2.

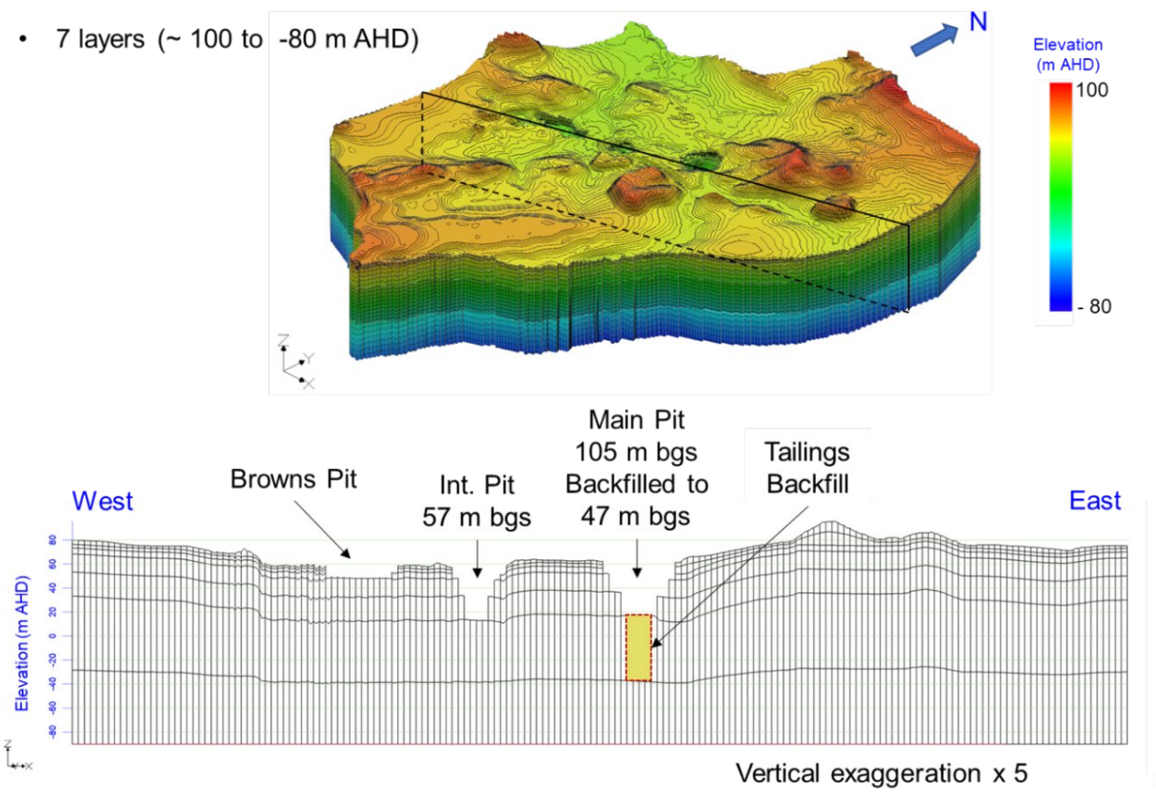

Figure 4-2. Surface Topography and Cross-Section

Layer 1 represents unconsolidated materials, including laterite, fill, and s waste rock in the WRDs and has a minimum thickness of 2 m. Layer 2 represents saprolite (where present). The top of bedrock (i.e. top of Layer 3) was based on an interpolation of top of bedrock elevations observed at historical and new bores. In undisturbed areas of the site the overburden profile was assumed to comprise 40% laterite (Layer 1) and 60% saprolite (Layer 2). In areas with less than approximately 5 m of unconsolidated materials, Layer 2 is assigned bedrock properties and has a minimum thickness of 3

m. Layers 3 through 5 represent shallow, partially weathered and fractured bedrock and have minimum thicknesses of 5 m, 15 m, and 25 m. Layers 6 and 7 represent deeper, fresh and typically low permeability bedrock and have minimum thicknesses of 60 m or greater.

All cells are active within the model domain except for cells in Layers 1 through 5 representing mined-out portions of the Main, Intermediate and Browns Pit. The depths of the pits were approximated as closely as possible in the model. The Main Pit and Intermediate Pit were excavated into fresh bedrock to depths of approximately 105 m and 57 m bgs respectively (in Layer 5 and Layer 6, respectively). However, the Main Pit was subsequently backfilled with tailings to a depth of about 47 m bgs. These tailings are explicitly included in the model (in Layer 6). The Browns Pit was only mined in the upper weathered bedrock and is represented in the model to a depth of approximately 20 m (in Layers 1, 2 and 3).

4.2.6 Temporal Discretization

The flow and transport models were set up in two phases. The first phase ("historic" flow and transport model) was set up to run for a period of 25 years prior to rehabilitation, i.e. nominally the period from January 1960 to December 1984. The historic model was run as a steady state flow, transient transport simulation with 25 annual transport time steps.

The second phase ("current" flow and transport model) was set up to run for a period of 34 years post-rehabilitation, i.e. the period from January 1985 to December 2018. This current phase was run as a transient flow and transport simulation with 408 monthly stress periods. The flow model code (MODFLOW) was setup with a single time step in each stress period, while the transport model code (MT3DMS) was setup to automatically select the appropriate transport step size. Initial heads and initial concentrations for the current model were taken from the output from the last time step of the historic model.

4.2.7 Recharge

The RCH package in MODFLOW was used to simulate the rainfall-induced net recharge to the groundwater system. The recharge model applied here follows the same assumptions used in the 2016 model. i.e. recharge for each monthly time step, for the period from January 1985 to December 2018, is assumed to represent a fixed percentage of the incident precipitation during this month. In addition, recharge to the groundwater system can only occur after initial "wetting up" of the unsaturated soils/saprolite during the early portion of the wet season (see RGC, 2016 for details).

The recharge polygons and their local recharge rate from the 2016 model were subsequently modified during model calibration to better match observed water levels or reduce excessive heads. Previous calculations completed for contaminant loadings from the WRDs indicated recharge rates of 15% for Dyson's (backfilled) Pit, 25% for the Main and Intermediate WRDs and 50% for Dyson's WRD. These earlier estimates of recharge (or “net percolation”) through the existing cover over the mine waste facilities are still considered valid and therefore, were not varied during calibration of the current model.

4.2.8 Evapotranspiration

The evapotranspiration polygons and their rates from the 2016 model were modified as required in each area to better match observed water levels during calibration. Evapotranspiration was applied only during months of no precipitation, as ET is implicitly accounted for in the use of “net” recharge.

4.2.9 Internal Sources and Sinks

A 3D view of the model grid showing boundary conditions and internal sources nodes are shown in Figure 4-3.

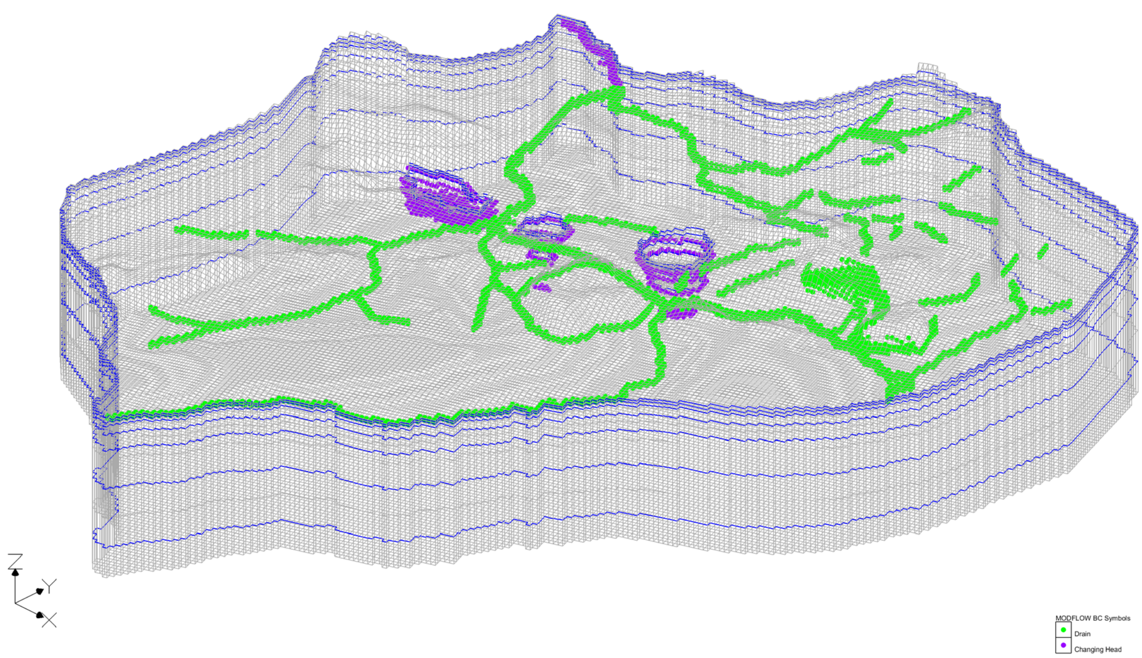

Figure 4-3. Boundary Conditions and Drain Nodes

<u>**Time Variant Constant Head Boundaries**</u>

Model cells immediately surrounding the flooded Main and Intermediate Pits (in Layers 3, 4, and 5) and cells in layer 6 representing bedrock and/or backfilled tailings beneath the pit floor were simulated using the CHD package in MODFLOW. These cells were assigned specified heads equal to the geodetic elevation of the water level in the pit lakes using a time variant constant head boundary. Note that surface flow within the flooded pits themselves is not simulated by the groundwater model so cells representing the flooded portion of the pits were set to be inactive.

Heads in cells along the edge of the Browns Oxide Open Pit were assigned based on water level data collected by HAR Resources (J. Hill, personal communication). Specifically, pit water levels and groundwater levels at monitoring bore TPB5 were used to represent the pit lake via a time variant constant head boundary. Note that the water level in the Browns Oxide pit varies primarily as a result of de-watering (as opposed to seasonal variations in rainfall and river flow) and hence the pattern in water levels differs from that of the Main and Intermediate Pits. The water level in Brown's Oxide Pit remained depressed below model layers 1 and 2 so time variant constant heads were only placed in Layer 3 around the pit. In addition, a time variant constant head polygon was used throughout the entire footprint of the pit in Layer 4.

For the period from January 1985 to November 2010, pit lake levels were assigned a typical seasonal trend, which was calculated as the average of observed pit levels within the calibration period. Some monitoring data for pit levels were missing or reported measurements did not appear to be accurate. In those cases, estimates of pit lake elevations were made based on groundwater elevations at nearby monitoring bores.

Drains

Relatively shallow creeks or drainage lines, engineered drainage features, and areas where seepage is known to express itself at ground surface are represented by drain nodes in Layers 1 and 2 of the model (see Figure 4-3). The East Branch of the Finniss River and the EFDC are relatively deep and are known to incise through surficial soils (Layers 1 and 2) into shallow bedrock. Therefore, the drain nodes for these features are applied to Layer 3 as well as Layers 1 and 2. Drain nodes can only receive groundwater discharge from the simulated groundwater system and are characterized by a geodetic elevation and a conductance that represents the ease with which water can flow to the drain from the surrounding aquifer.

In general, drain elevations across the model domain were set to 0.2 m below ground surface based on the DTM provided by DPIR and drain conductances were set to one or two orders of magnitude higher than K values for the surrounding aquifer. In other words, groundwater discharge was assumed to be solely controlled by the permeability of the surrounding aquifer material. All shallow surface drainages, including Fitch Creek, Wandering Creek, and Old Tailings Creek, were simulated by drains in layers 1 and 2. All larger surface drainages, including the East Branch of the Finniss River and the EFDC were extended into model layer 3.

In addition, drains were placed in Layer 1 and 2 along the edges of the waste rock dumps and Dysons (backfilled) Pit to allow discharge of shallow seepage along the side slopes of the mine waste units (or the rock drain in the case of Dysons backfilled pit). The EBFR is a major discharge zone for groundwater across the study area and was represented by drains starting from Dyson's Area and continuing downstream to the confluence of Old Tailings Creek with the EBFR. From Old Tailings Creek to the downstream terminus of the EBFR in the model domain, time variant constant heads were assigned based on groundwater levels observed at monitoring bore MB10-20. The value of the specified head is slightly lower than the observed groundwater level due to some assumed head losses in the aquifer between the monitoring bore and the river.

4.2.10 Solver and Convergence Criteria

For the simulation of groundwater flow the MODFLOW-NWT package was used. To solve the flow equation, the GMSRES Matrix solver was used with a head convergence criterion (HEADTOL) of 0.0001 m, a flux (FLUXTOL) convergence criterion of 0.005 m^3/s and a maximum number of outer iterations (MAXITEROUT) of 3000. All other settings were kept at their default, including 0.00001 m thickness for adjusting coefficients.

4.3 FLOW MODEL CALIBRATION – CURRENT CONDITIONS

4.3.1 Calibration Approach

The calibration of the "2016" transient groundwater flow model was refined until a satisfactory match of simulated and observed spatial and temporal variations in groundwater levels was achieved (flow calibration). The trial-and-error calibration procedure was adopted. Material properties (K, Ss and Sy), as well as recharge and evapotranspiration rates were varied. The zonation of K, recharge and evapotranspiration were also adjusted, or additional zones introduced. Model calibration was achieved in about 46 calibration iterations and the calibrated model is Run No. 46.

The principle of parsimony was followed during calibration, i.e. an effort was made to maintain the model complexity to a minimum. The effects of incremental changes to the flow calibration were assessed by visually comparing observed and simulated time trends.

4.3.2 Groundwater Level Targets

The calibration targets for observed groundwater elevations were extended to cover the period from December 2010 to December 2018. In total, groundwater level measurements for 117 monitoring bores were available to calibrate the transient flow model. Most of the bores were monitored monthly in the dry season and every two weeks in the wet season until 2018. A single water level survey of the MB17 and MB18 series was completed in mid-December 2018 and was also used for model calibration.

4.3.3 Flow Targets

Measurements of EBFR discharge at gauging stations GS8150200 and GS8150327 were used to determine the total volume of runoff and groundwater flow to the EBFR between the stations. This volume was then apportioned to derive a calibration flow target. For the purpose of this study, the model was considered adequately calibrated if the simulated groundwater flow to the EBFR in the reach between gauging station GS8150200 (at the bridge near the Intermediate Pit) and GS8150327 (model domain boundary) falls within the estimated upper and lower bounds from the conceptual model (see Section 3.9).

4.3.4 Goodness-of-Fit and Calibration Statistics

The goodness-of-fit of the simulated flow field (head solution) to observed groundwater levels was evaluated by:

- Computing calibration statistics for the full calibration period, December 2010 to December 2018, using 6373 observation from 117 monitoring bores.
- Computing calibration statistics for the 2017/2018 wet season and dry season.
- Checking for spatial bias in residuals for a representative wet season and dry season; and
- Inspecting (visually) the simulated versus observed seasonal time trends in groundwater levels.

Figure 4-4 and Figure 4-5 show scatter plots of simulated versus observed heads and relevant calibration statistics. The calibration of a numerical model is typically considered good if the normalized root mean square of the errors (NRMSE) is less than 5%. The calculated NRMSE values for the full calibration period, the dry season and the wet season data sets are 3.8%, 4.7% and 1.3%, respectively. The computed NRMS values are well below the target NRMS of 5% suggesting good calibration to head targets.

The respective residual means are -0.26 m, 0.54 m and 0.32 m, respectively. These statistics and visual inspection of the scatter plots suggest that the residuals do not show any systematic bias across the observed head range and lie largely on average within the acceptable range of +/- 2m.

The calibration statistics and the residual error scatter plots indicate that the head calibration for the numerical model is statistically acceptable for the purpose of this study.

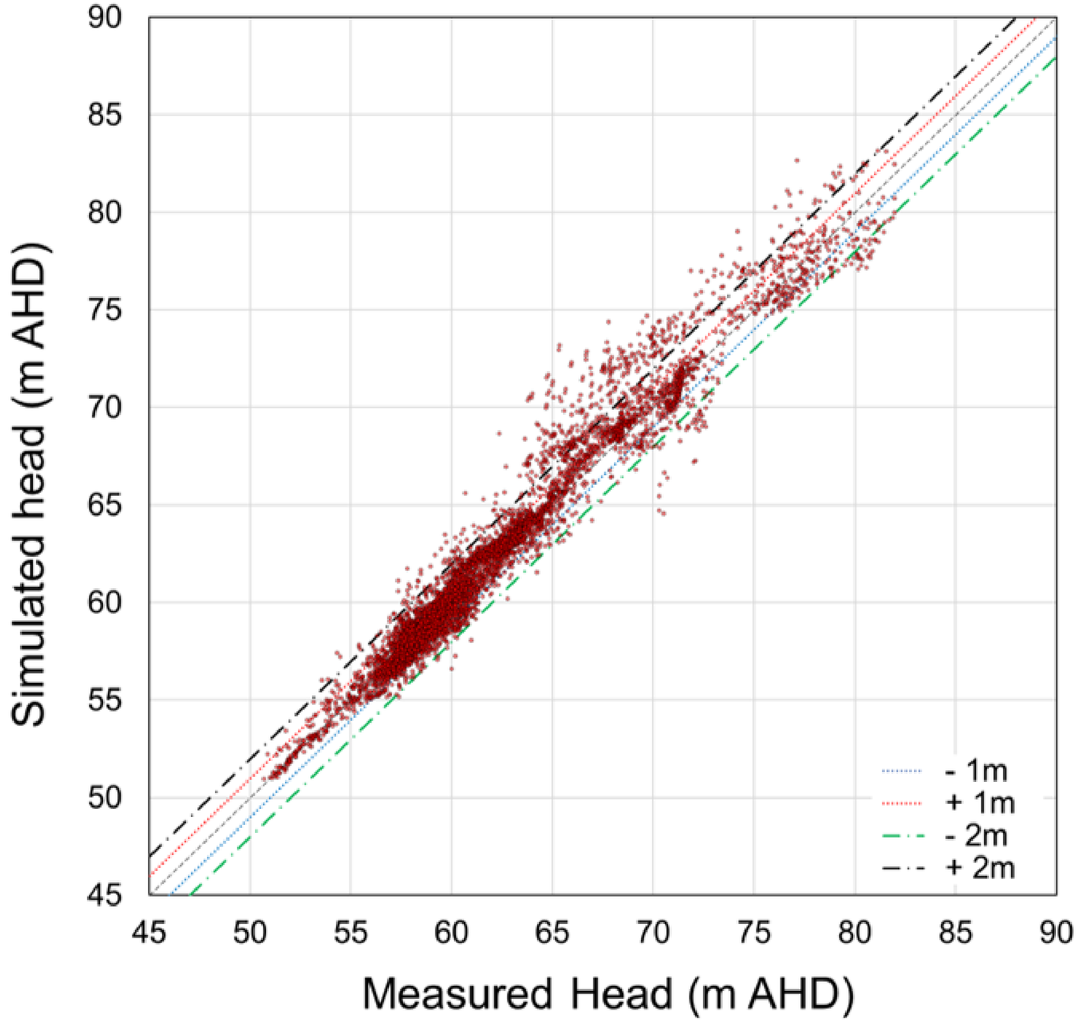

Number	6373
Max Residual (m)	7.77
Min Residual (m)	0.00
Residual Mean (m)	-0.26
Absolute Residual Mean (m)	0.80
Standard Error of Estimate	0.01
Root Mean Square	1.19
Normalized Root Mean Squared	3.81%
Correlation Coefficient	0.98

Figure 4-4. Simulated versus Observed Heads and Relevant Calibration Statistics for the Full Calibration Period (December 2010 to December 2018)

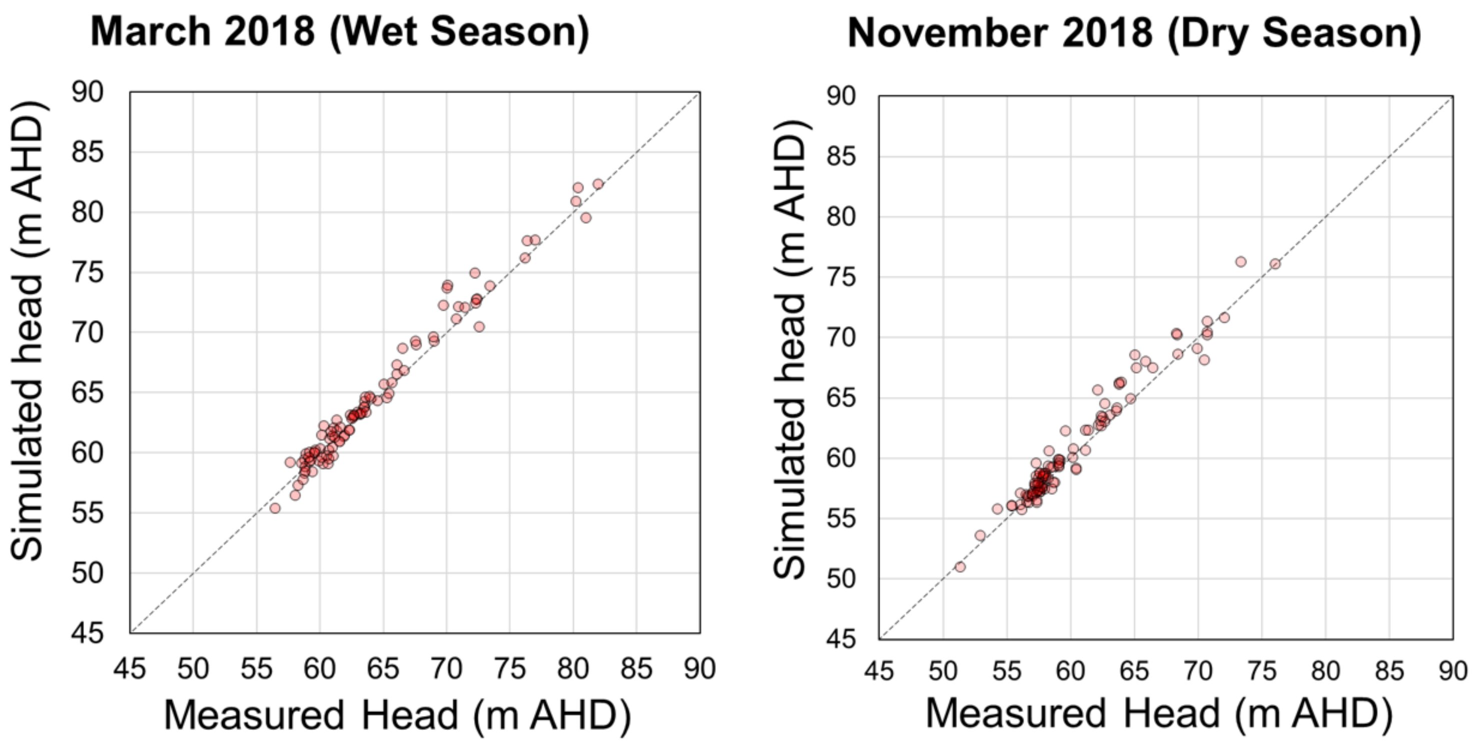

Number	93
Max Residual (m)	3.84
Min Residual (m)	0.00
Residual Mean (m)	0.32
Absolute Residual Mean (m)	0.80
Standard Error of Estimate	0.11
Root mean square	1.08
Normalized Root mean squared	1.3%
Correlation Coefficient	0.99

Number	102
Max Residual (m)	3.55
Min Residual (m)	0.01
Residual Mean (m)	0.54
Absolute Residual Mean (m)	0.84
Standard Error of Estimate	0.10
Root mean square	1.15
Normalized Root mean squared	4.7%
Correlation Coefficient	0.98

Figure 4-5. Simulated versus Observed Heads and Relevant Calibration Statistics for 2018 Wet and Dry Seasons

4.3.5 Comparison of Flow Calibration Targets

Figure 4-6 shows the simulated groundwater discharge into the EBFR between gauging stations GS8150200 and GS8150327. Also shown are the conceptual upper and lower bounds for groundwater discharge representing 25% and 12.5% of total stream flow at GS8150327, respectively (see Section 3.9).

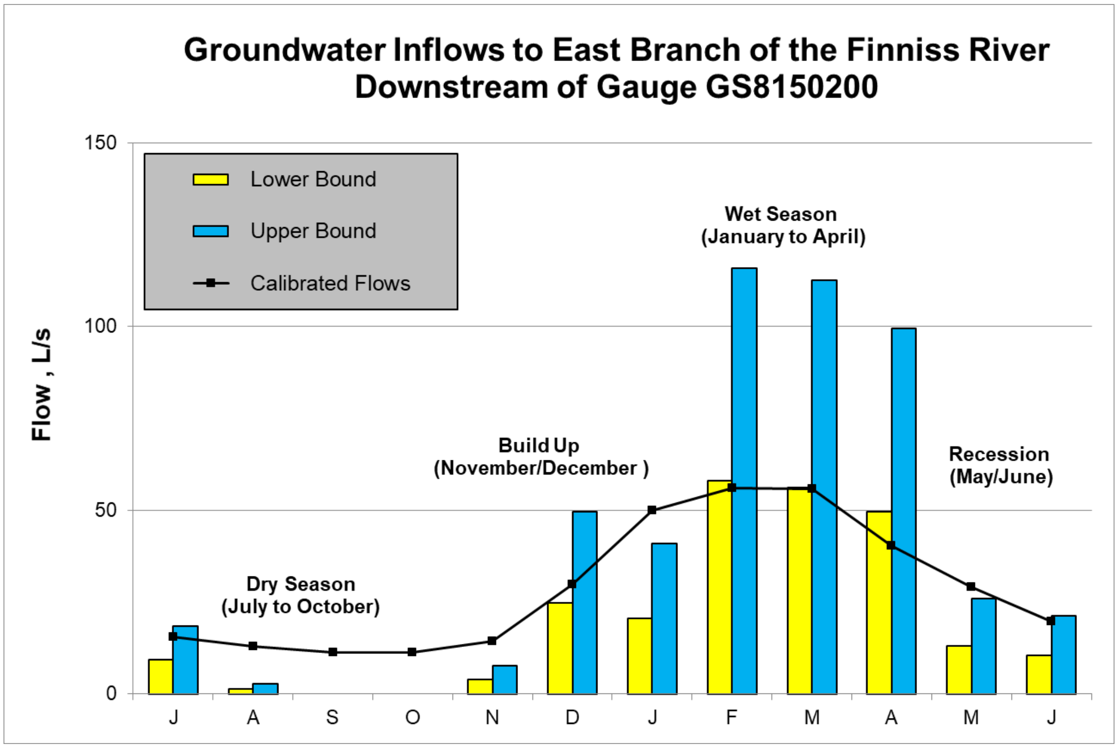

Figure 4-6. Simulated versus Estimated Groundwater Inflows to the EBFR Downstream of Gauge GS8150200

The simulated groundwater flows to the EBFR generally fall within the estimated upper and lower bounds during the wet season from December to June. The calibrated groundwater recharge rates in the numerical model in the catchment of the EBFR downstream of the CMA range from 20% to 30% with an approximate average of 25%. As a result, the simulated stream flows are expected to track closest to the upper bound (25%). This is observed during the early and late wet seasons. However, during the wettest periods when flows are the highest the simulated discharge rates are closer to the lower bound (12.5%). This likely reflects an actual decrease in infiltration rates that occurs during periods of high precipitation when groundwater levels rise to surface and the aquifer is near capacity. The proportion of streamflow due to surface runoff is higher during these periods.

During the dry season, the numerical model “over-predicts” discharge to the EBFR. Note, however, that groundwater discharge during the dry season is predicted to primarily occur downstream of the confluence of Old Tailings Creek with the EBFR where the EBFR is represented in the model by time variant constant heads. In contrast, simulated dry season flows in the EBFR between gauge GS8150200 and Old Tailings Creek where the EBFR is represented by drain nodes typically decline to less than 2 L/s.

During the dry season, the elevations assigned to the constant head nodes along the lower EBFR are lower than the actual invert of the EBFR (as observed in the field). In other words, the simulated discharge to these constant heads represents groundwater flow in the alluvium and shallow bedrock underlying the EBFR rather than discharge to surface.

Additional studies would be required to determine whether the alluvium/bedrock along the EBFR channel is capable of transmitting the predicted dry season groundwater baseflow (~20 L/s).

4.4 Flow Model Results

4.4.1 Simulated Groundwater Level Time Trends

Simulated versus observed seasonal time trends of groundwater levels for selected monitoring bores in different reaches of the Rum Jungle mine site, covering the entire calibration period (December 2010 to December 2018), are illustrated in Figure 4-7, Figure 4-8, and Figure 4-9. In all plots the dashed line indicates the ground surface elevation. In general, the heads simulated by the calibrated flow model match the seasonal variations in observed groundwater levels very well, including the sharp rise in groundwater levels typically observed during the onset of the wet season and the long, gradual recession during the dry season. However, some local discrepancies were observed suggesting local heterogeneity not accounted for in the model.

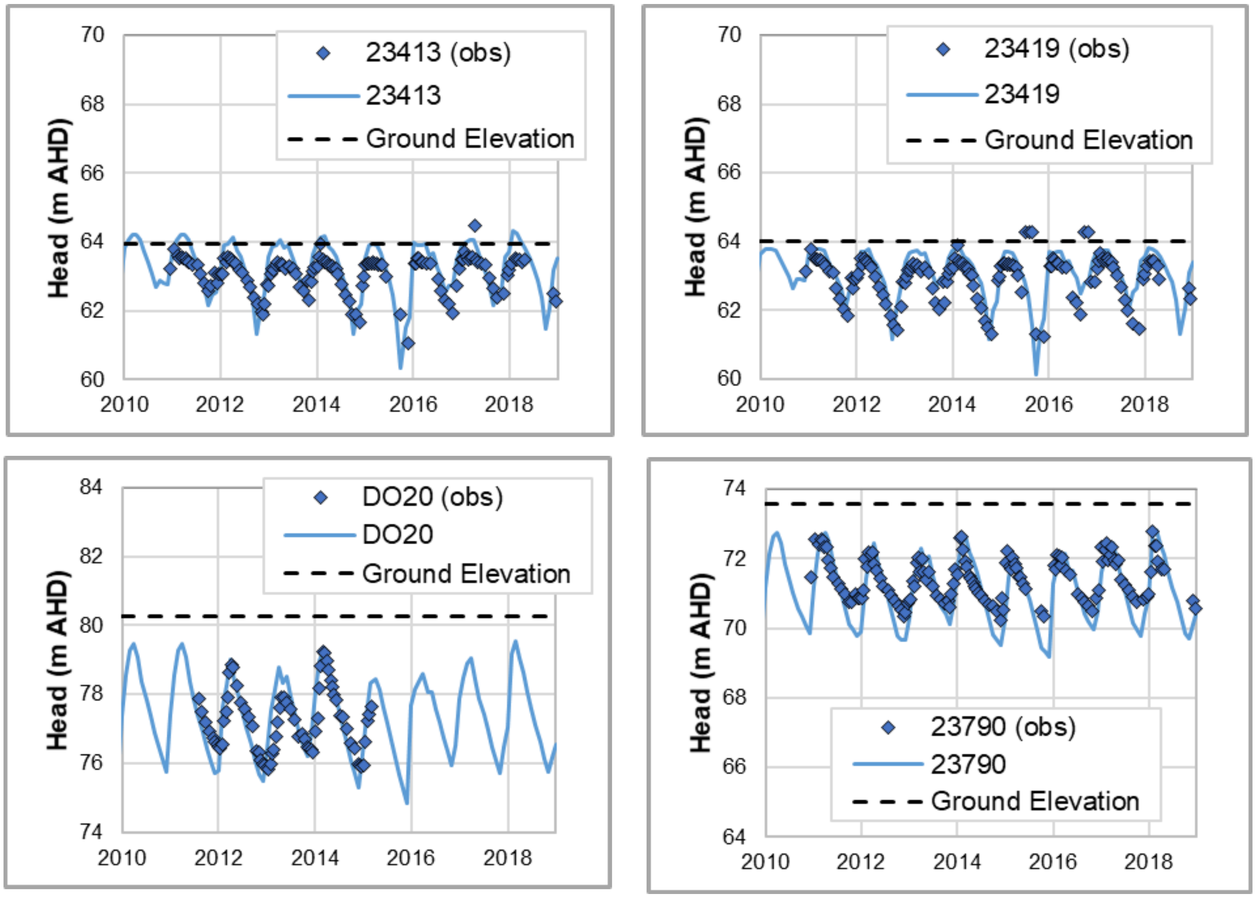

Figure 4-7. Simulated Heads, Dyson's Area

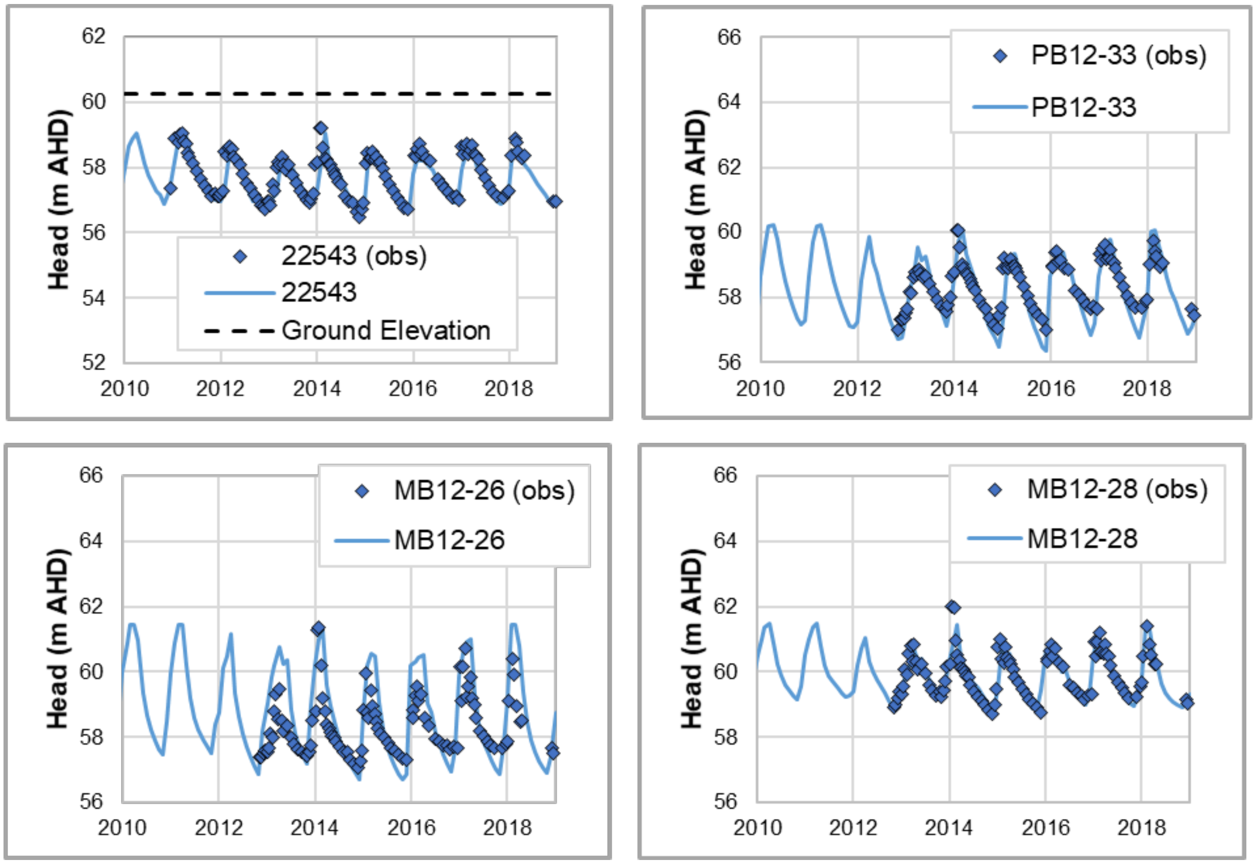

Figure 4-8. Simulated Heads, Central Mining Area

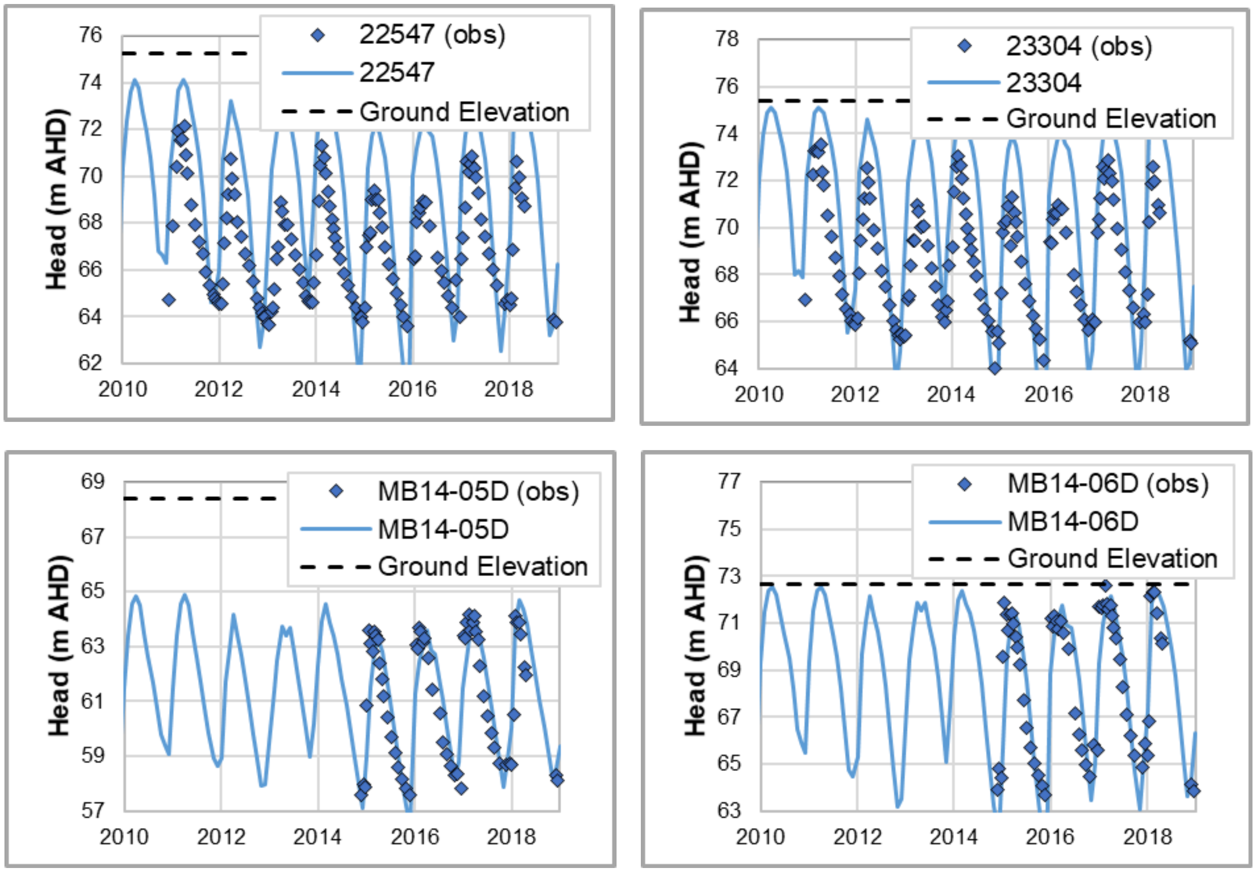

Figure 4-9. Simulated Heads, Upland Area (Northeast)

4.4.2 Simulated Flow Field

The simulated flow fields for the 2018 dry and wet seasons are shown in Figure 4-10. This figure also shows groundwater head equipotential lines and arrows indicating the direction of groundwater flow.

Key observations of the simulated flow field are summarized below:

- In general, the simulated flow fields compare reasonably well with the conceptual flow fields (see Section 3.8).
- Groundwater at the mine site is predicted to follow topography, i.e. flow from upland areas to lower elevation areas.
- The simulated groundwater flow field is affected by the WRDs (Main, Intermediate and Dyson's). Preferential infiltration into these WRDs and hence above-average recharge to the underlying aquifer is simulated to result in local groundwater mounding.

- The model predicts steeper hydraulic gradients during wet season compared to dry season. For example, the simulated hydraulic gradient towards the EBFR downstream of the Intermediate Pit is 0.009 m/m in the wet season compared to 0.004 m/m for the dry season.
- The flooded Main and Intermediate Pits have a strong influence on the groundwater flow field. They act as a source or sink for groundwater depending on the difference between pit water level and groundwater levels in the surrounding aquifer. This interaction imposes seasonal stability on the groundwater flow field, particularly in the central mining area.

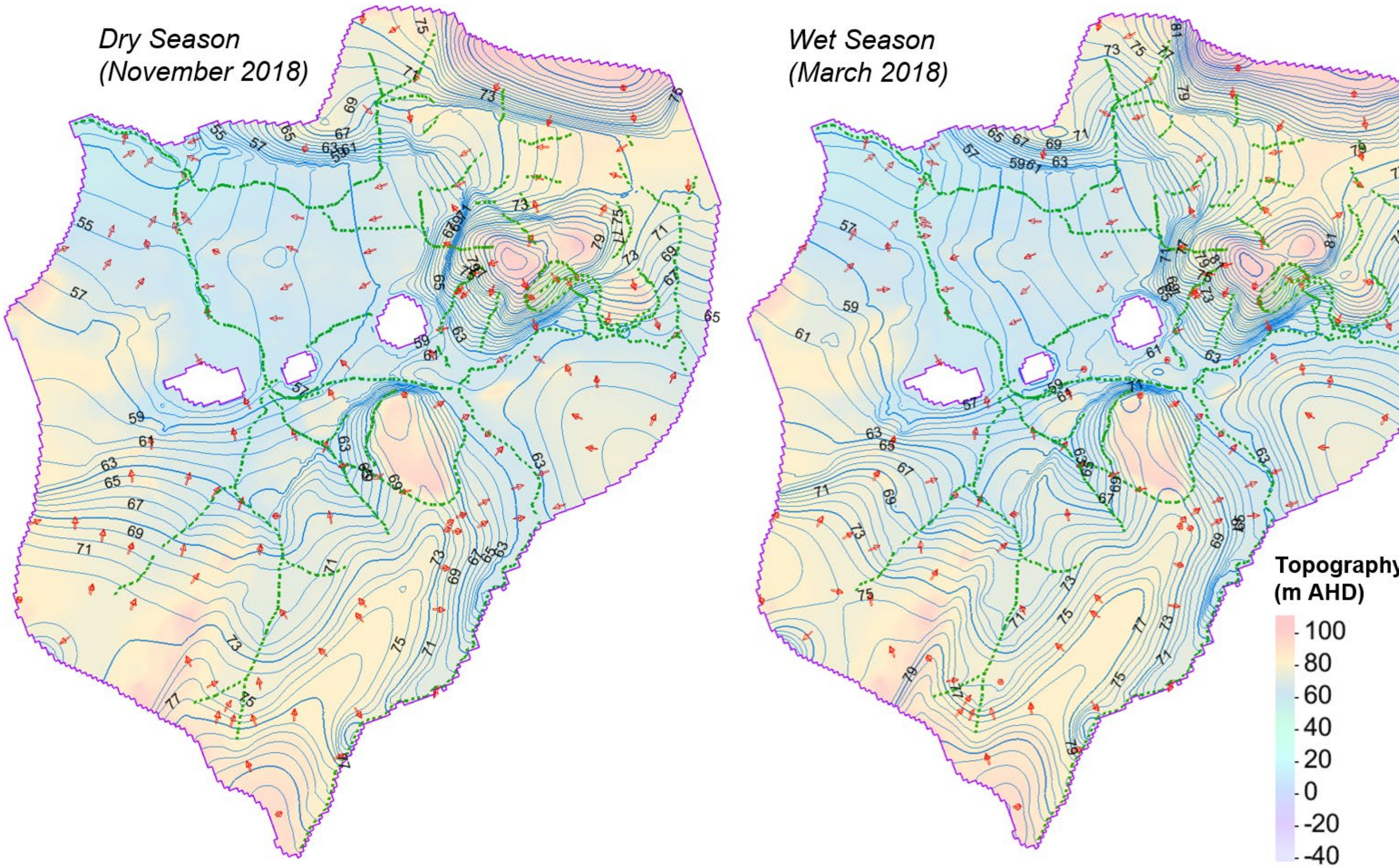

Figure 4-10. Simulated Groundwater Flow Field, Wet and Dry Seasons 2018

4.4.3 Simulated Water Balance

To calculate the water balance for the numerical model, flow output was averaged from January 2011 to December 2018. Table 4-1 and Figure 4-11 present the average water balance for this 8-year simulation period. Inflows represent flows entering the groundwater model and outflows represent flows leaving the groundwater model.

Table 4-1. Average Water Balance (Jan 2011 to Dec 2018)

Component	Flow	
	L/s	Mm^3/yr
Inflows		
Recharge to undisturbed areas	123.5	3.9
Recharge to mine waste units	7.8	0.2
Time Variant Constant Heads (Pits)	5.8	0.2
Time Variant Constant Heads (EFBR D/S	0.1	0.0
Storage	45.0	1.4
Total:	*182.2*	5.7
Outflows		
Evapotranspiration	17.1	0.5
Drains	89.4	2.8
Time Variant Constant Heads (Pits)	20.5	0.6
Time Variant Constant Heads (EFBR D/S	13.0	0.4
Storage	42.3	1.3
Total:	*182.3*	*5.7*

MODEL WIDE INFLOWS

MODEL WIDE OUTFLOWS

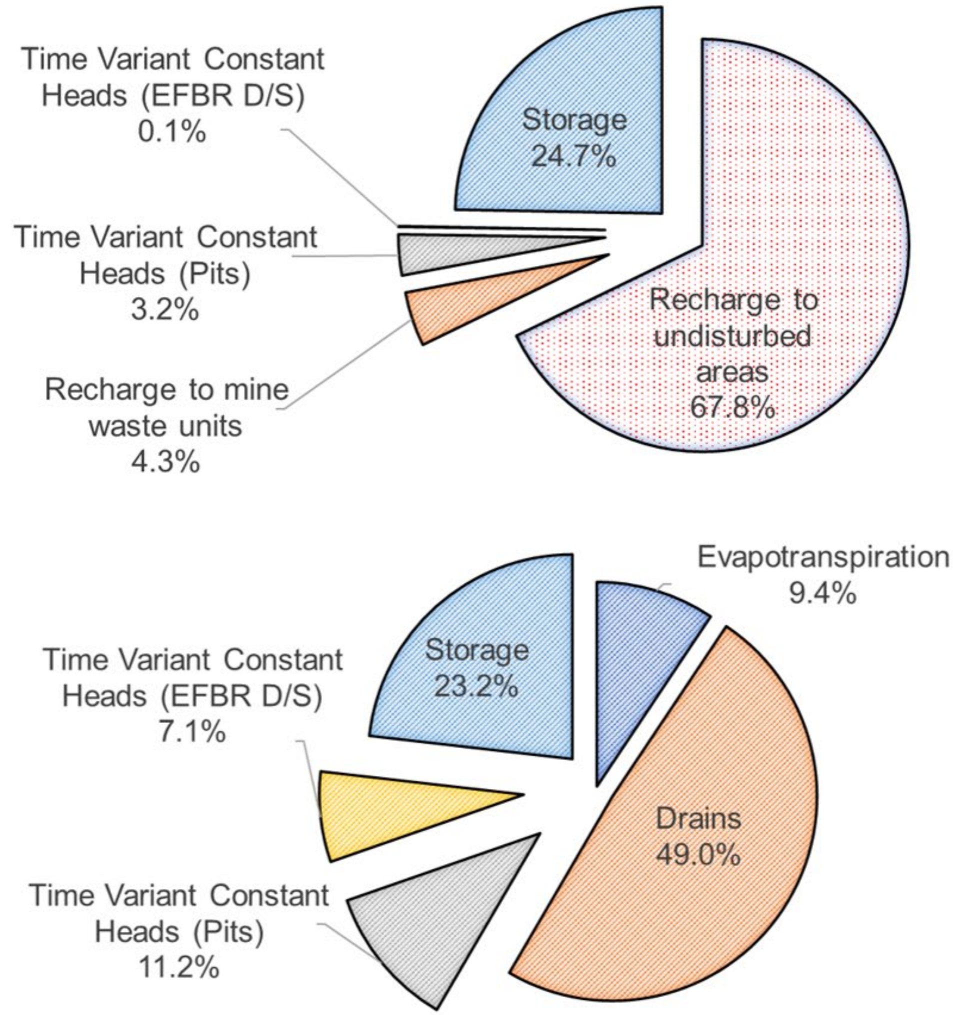

Figure 4-11. Simulated Model Wide Water Balance (Average: 2011 to 2018)

The main sources of inflow to the model include recharge and the time variant constant heads in the Main, Intermediate and Brown's Oxide pits. Outflows include groundwater discharges to drains, the time variant constant heads and evapotranspiration. Flows in and out of storage as groundwater levels rise and fall seasonally represent additional sources of outflow and inflow to the groundwater system, respectively.

The total simulated 8-year average inflow to the model is 182.2 L/s and the total outflow is 182.3 L/s. The water balance error for the calibrated transient model is very small (i.e. 0.07 L/s or 0.04%). Table 4-2 and Figure 4-12 provide a further breakdown of the simulated inflows and outflows by specific areas and site features of interest. Natural recharge across the entire model domain accounts for approximately 96% of the model inflow. The remaining inflows to the model are from the Main, Intermediate and Brown's Oxide pits. The significantly higher inflow to the groundwater system of 5.1 L/s from the Intermediate Pit can be attributed to the presence of high permeability Coomalie Dolostone along much of its northern perimeter. Brown's Oxide Pit is also cut well into the Coomalie Dolostone; however, ongoing pumping of the pit maintains it as a net sink for groundwater. The Main Pit is cut into low K formations including the Crater Formation (east and west) and Geolsec Formation in the north, hence the relatively low average inflow to the groundwater system from the Main pit of 0.1 L/s.

Groundwater discharge to the EBFR and its tributaries represents about 70% of all simulated outflows from the calibrated model. Groundwater discharge to the three open pits represents an additional 16% of the simulated outflow and ET losses represent the remaining 14%. The simulated water balance of the calibrated model is generally consistent with the conceptual water balance, i.e. the simulated average annual inflows and outflows fall within the upper and lower bounds estimated during conceptual modelling. The simulated average recharge in the calibrated model of 123.5 L/s falls approximately halfway between the estimated lower and upper bound of recharge for the conceptual water balance (54 to 163 L/s, respectively). The simulated average groundwater discharge to the EBFR and its tributaries in the calibrated model (89.4 L/s) also falls within the conceptual range of 22.8 to 108 L/s, although it is closer to its upper bound.

Table 4-2. Average Water Balance (Jan 2011 to Dec 2018)

Inflow and Outflow contributions of site features

Component	Flow	
	L/s	Mm^3/yr
Inflows		
Recharge to undisturbed areas	123.5	3.9
Recharge to mine waste units	7.8	0.2
Inflows from the Main Pit	0.1	0.0
Inflows from the Intermediate Pit	5.1	0.2
Inflows from Brown's Oxide Pit	0.6	0.0
Outflows		
Evapotranspiration	17.1	0.5
To the Main Pit	2.8	0.1
To the Intermediate Pit	1.9	0.1
To the Browns Oxide Pit	15.8	0.5
To the upper EBFR	14.3	0.5
To Fitch Creek	5.2	0.2
To the EFDC	2.3	0.1
To Wandering Creek	3.8	0.1
To Old Tailings Creek	9.4	0.3
To the EBFR d/s of gauge GS8150200	42.7	1.3
Other unnamed creeks and tributaries	11.7	0.4

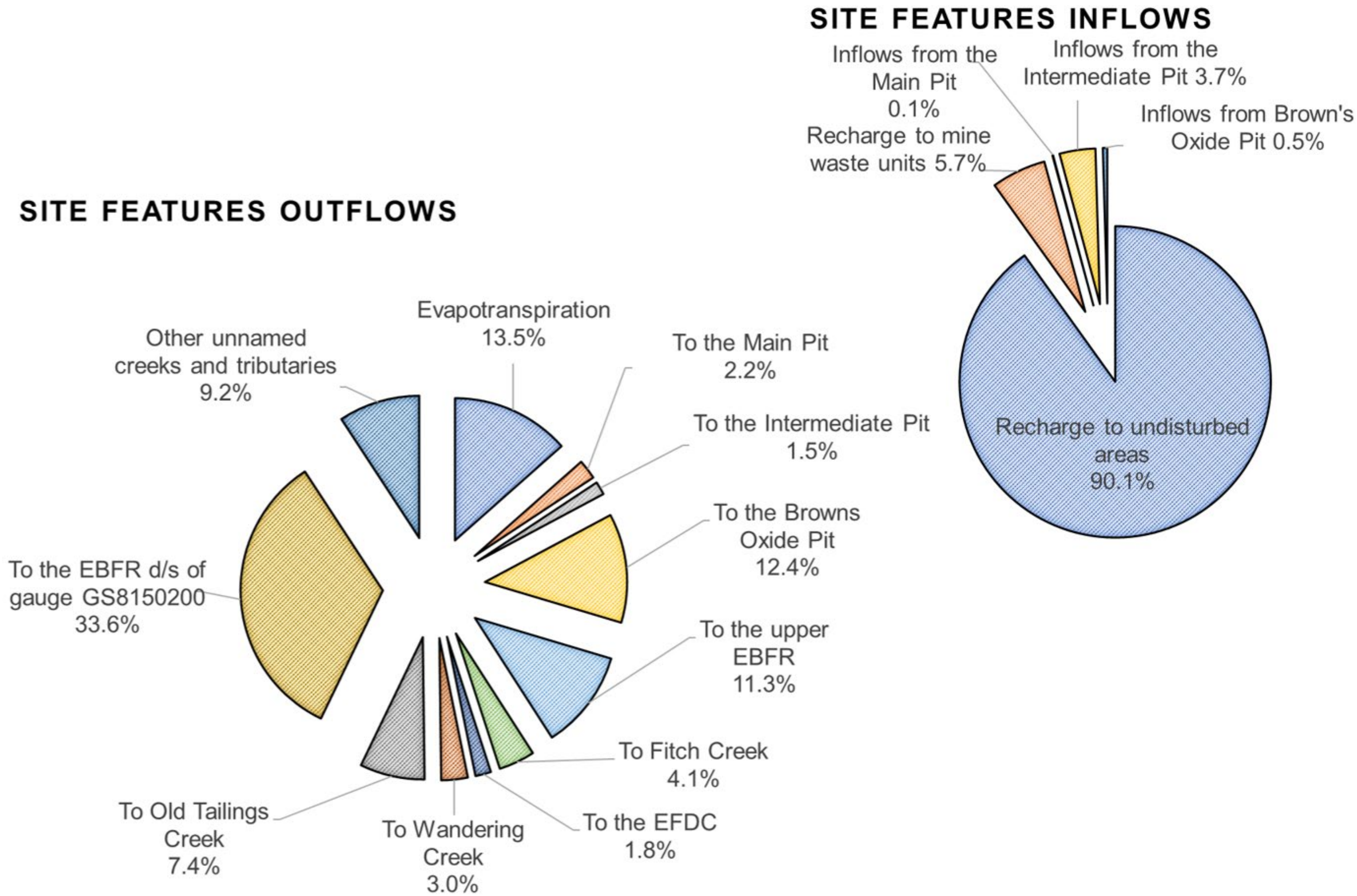

Figure 4-12. Simulated Site Features Inflows and Outflows (Average: 2011 to 2018)

4.4.4 Calibrated Material Properties

Calibrated recharge and evapotranspiration rates are shown in Figure 4-13. Some local modifications were done to the 2016 recharge and evapotranspiration models within the copper extraction pad area, south of the Main Pit and north-eastern model domain areas to improve model calibration.

The calibrated hydraulic properties from the 2016 model were modified to reflect the updated conceptual model (Section 3) within and around the footprint of the stage 2 WSF and within the Copper Extraction Pad area. Figure 4-14 and Figure 4-15 show the zonation of calibrated hydraulic conductivity (K) across the model domain resulting from the parameterization and re-calibration of the model, for all seven model layers.

Represented in the model are laterite, saprolite, Whites Formation, Geolsec Formation, Rum Jungle Complex, Crater Formation, Coomalie Dolostone and mine waste (waste rock and tailings). The calibrated values used for each and a comparison with measured field values are detailed below.

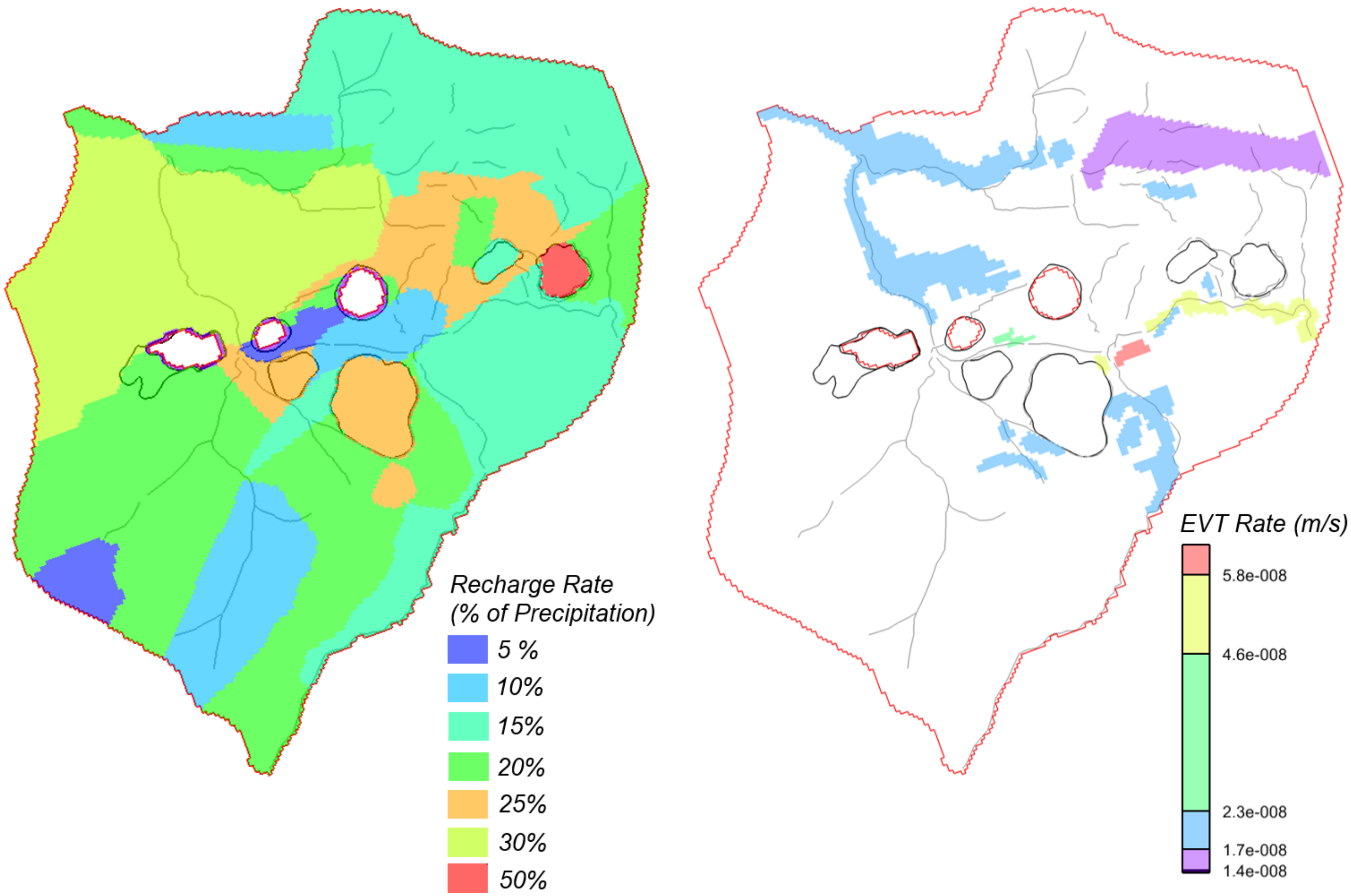

Figure 4-13. Calibrated Recharge and Evapotranspiration Rates

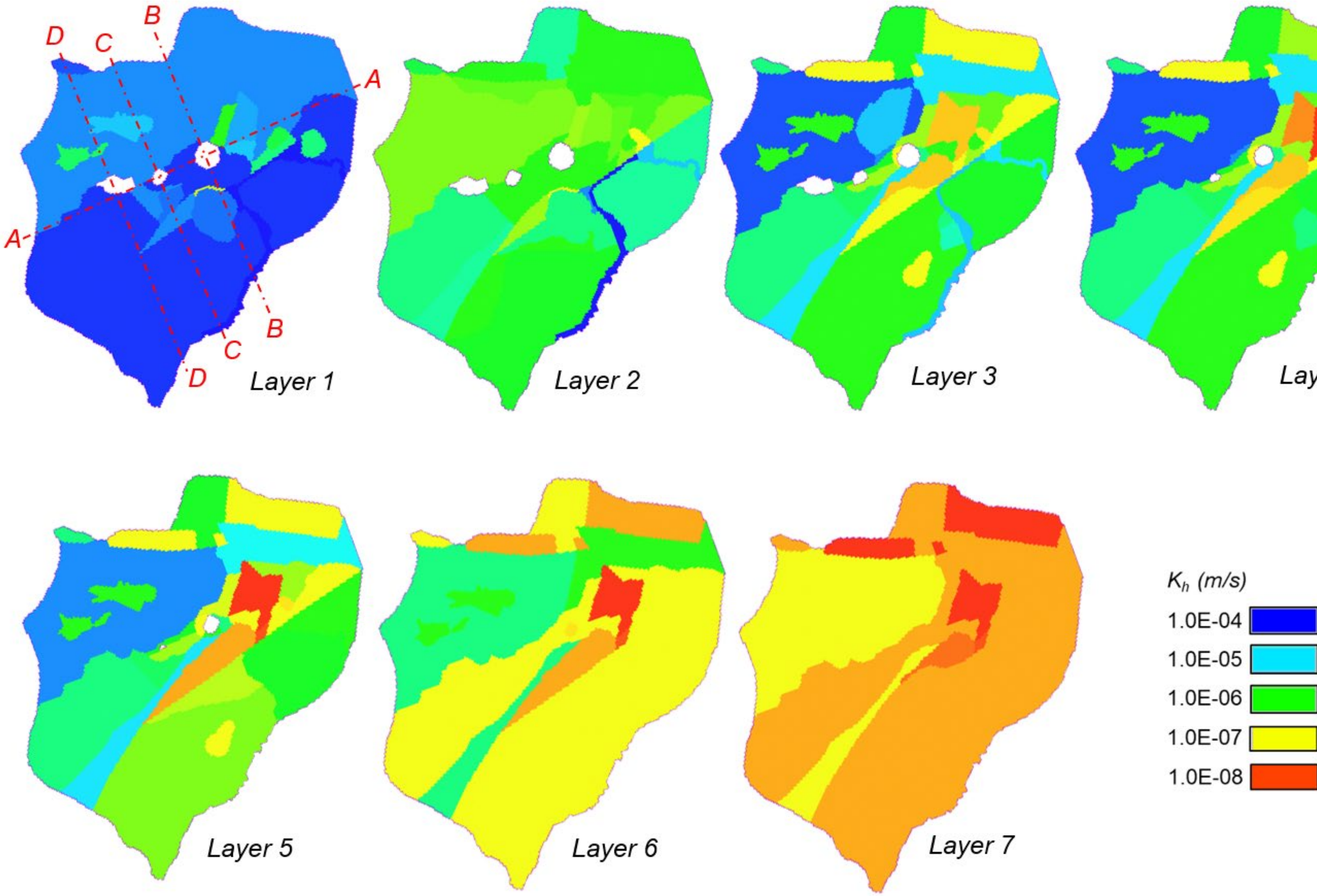

Figure 4-14. Calibrated Zonation for Hydraulic Conductivity - Layers 1 to 7

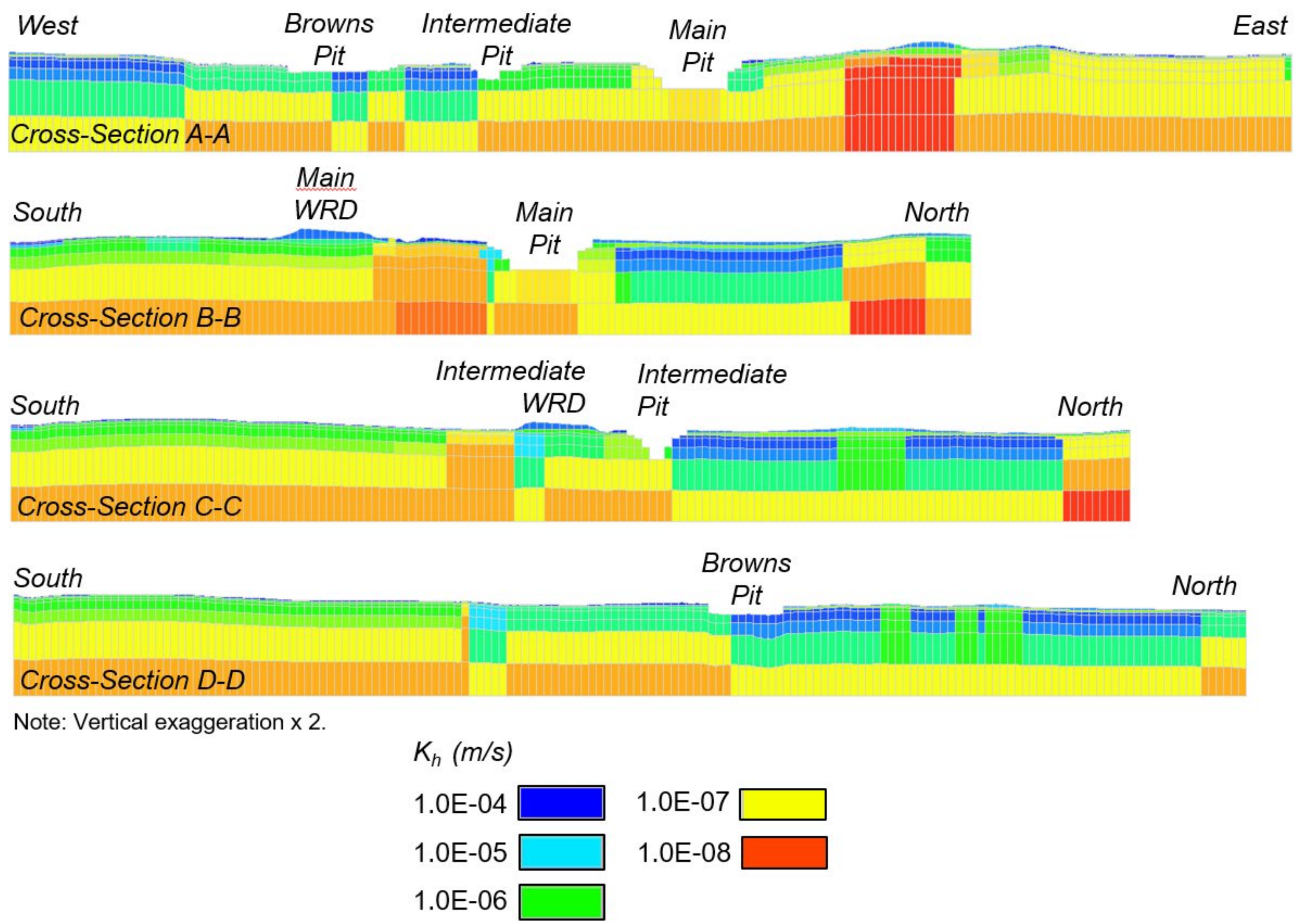

Figure 4-15. Calibration for Zonation for Hydraulic Conductivity - Cross Sections A-A to D-D

4.5 TRANSPORT MODEL SETUP

4.5.1 Transport Modelling Objectives

The overall objective of the solute transport modelling was to better understand the sources, geochemical controls and current extent of water quality impacts in groundwater at the Rum Jungle mine site. Specific transport modelling objectives include:

- Simulate the transport of SO_4 and Cu in groundwater for current hydraulic and geochemical conditions.
- Delineate the spatial extent and associated mass of SO_4 and Cu in the local groundwater system.
- Estimate the current loads of SO_4 and Cu to the open pits and EBFR.
- Characterize model uncertainty and how it could affect simulated SO_4 and Cu concentrations in the EBFR.

In addition, the results of this modelling effort provide a suitable benchmark (and initial conditions) for the prediction of future contaminant transport to assess the environmental effects of the preferred rehabilitation strategy.

4.5.2 Code Selection

Solute transport for sulphate and copper was simulated using the transport code MT3DMS (Zheng and Wang, 1999). The model was set up in GMS v.10.3.7, a widely-used software package that provides a full suite of options to pre/post-process numerical models (Aquaveo, 2018).

4.5.3 Boundary Conditions

All external boundary condition used in the flow model (Section 4.2.4) remained unchanged for the transport model. No-flow boundaries also represent a barrier to solute transport, i.e. no mass flux occurs across a no-flow boundary. Any groundwater exiting along a prescribed head boundary is assigned the simulated sulphate (or copper) concentration in the respective boundary cells, i.e. an equivalent sulphate (or copper) mass is removed from the boundary cell.

4.5.4 Transport Parameters

The transport model was parameterized using the same spatial zonation and calibrated hydraulic properties developed for the flow model (see Section 4.4.4). The two additional transport parameters required to solve the transport equation are effective porosity (n_e) and dispersivity (α).

The effective porosity was spatially distributed in the model using the same approach as outlined above for hydraulic parameters. The same effective porosity values developed in the 2016 model were also adopted for the 2019 model. Dispersivity was assumed to be independent of aquifer type and a uniform distribution was assumed across all model zones/layers using the following dispersivity values:

- Longitudinal dispersivity (α_L): 10.0 m
- Transverse dispersivity (α_T): 0.1 m
- Vertical dispersivity (α_V): 0.01 m.

4.5.5 Source Terms

The key sources of SO_4 and Cu loading to groundwater for historic and current conditions at the Rum Jungle mine site include:

- Dyson's WRD and backfilled Dysons Pit.
- Main and Intermediate WRDs.
- Copper Extraction Pad Area.
- Former Mill and Ore Stockpile Area.
- Old Tailings Dam.

In addition, highly contaminated pit water in the Main Pit and Intermediate Pit represented a potential source of SO_4 and Cu to groundwater prior to rehabilitation in 1984/85 (historic model only).

Based on a review of historic and current seepage water quality and reconciliation of contaminant loads observed in the receiving surface water, source concentrations and associated loads were estimated for historic and current conditions.

Table 4-3 and Table 4-4 summarize the source concentrations and numerical implementation of these sources in the transport model for historic and current conditions, respectively. Figure 4-16, Figure 4-17 and Figure 4-18 show the distribution of source terms implemented in the numerical model for historic and current conditions, respectively. The majority of contaminant sources were represented in the transport model using constant concentrations applied to the respective foot print area. In this approach, MT3DMS keeps the solute concentration in the respective model nodes fixed at the specified concentration. In the case of surficial contaminant sources (e.g. WRDs) this approach is equivalent to specifying a source concentration in recharge[2]. For selected, surficial contaminant sources (e.g. Old Tailings Dam area, mill area), a constant concentration was applied to recharge for the current model.

[2] The use of constant concentrations (as opposed to specified concentrations applied to recharge) was preferred because MT3D can only apply solute loads via recharge to the aquifer in MODFLOW-NWT if the uppermost cell is "wet". However, many contaminant source areas include "dry" cells in layer 1.

Simulated source terms for SO_4 and Cu within the Copper Extraction Pad area were modified to match the updated conceptual model in this area:

- Seepage from the collection ditch located along the northern toe of the heap leach pad area, which was excavated to store sulphide liquor. It is conceptualized that for the period from 1965 to 1971, a seepage rate of about 2.0 L/s was lost from this ditch to groundwater at 1000 mg/L Cu and 8500 mg/L SO_4. These estimated seepage rate and concentrations was reduced for the period from 1972 to 1984 to 0.6 L/s at 500 mg/L for Cu and 4250 mg/L for SO_4. This ditch is not simulated to be a source of contamination for the period from 1985 onwards.
- Seepage from the pad area is assumed as a source for SO_4 only for the period 1965 to 1985 at a concentration of 5000 mg/L.

Table 4-3. Sulphate and Copper Source Terms for Historic Transport Model (Pre-Rehabilitation)

Source	Area (m^2)	Type	Concentration (mg/L)	Layer(s)	Recharge (mm/yr)
Historic SO4 Source Term Properties					
Main WRD	285,000	Constant	10,000	1 - 2	653
Intermediate WRD	73,000	Constant	25,000	1 - 2	653
Dyson'sWRD	94,000	Constant	5,000	1 - 2	653
CEPA Ditch 1965 to 1970	5,985	Recharge Conc	8500	1	10540
CEPA Ditch 1971 to 1984	5,985	Recharge Conc	4250	1	3162
Heap Leach Pile	32,100	Recharge Conc	5000	1	65
Main Pit		Constant	6,050 - 10,000	3 - 6	
Intermediate Pit		Constant	2,500	2 - 5	
Dyson's (backfilled) Pit	61,000	Constant	2,500	1 - 6	196
Old Tailings Dam	271,000	Constant	2,500	1 - 2	391
Mill Area	54,000	Constant	5,000	1 - 2	325
Historic Cu Source Term Properties					
Main WRD	285,000	Constant	100	1 - 2	653
Intermediate WRD	73,000	Constant	225	1 - 2	653
Dyson'sWRD	94,000	Constant	7.5	1 - 2	653
CEPA Ditch 1965 to 1970	5,985	Recharge Conc	1000	1	10540
CEPA Ditch 1971 to 1984	5,985	Recharge Conc	500	1	3162
Heap Leach Pile		-	-	-	-
Main Pit		-	-	-	-
Intermediate Pit		Constant	60	2 - 5	
Dyson's (backfilled) Pit	61,000	Constant	8	1 - 5	196
Old Tailings Dam	241,000	Recharge Conc	30	1	391
Mill Area	54,000	Constant	60	1 - 2	325

Table 4-4. Sulphate and Copper Source Terms for Current Transport Model (1985 - 2018)

Source	Area (m^2)	Type	Concentration (mg/L)	Layer(s)	Recharge (mm/yr)
Current SO4 Source Term Properties					
Main WRD	285,000	Constant	5,000	1 - 2	325
Intermediate WRD	73,000	Constant	15,000	1 - 2	325
Dyson'sWRD	94,000	Constant	2,500	1 - 2	653
CEPA Ditch		-	-	-	-
Heap Leach Pile		-	-	-	-
Main Pit		Constant	2,000	6	
Intermediate Pit		-	-	-	-
Dyson's (backfilled) Pit	61,000	Constant	2,500	1 - 2	196
Old Tailings Dam	241,000	Recharge Conc	500	1	391
Mill Area NW	47,000	Recharge Conc	1,500	1	391
Mill Area SE	158,000	Recharge Conc	1,500	1	325
Mill Area SW	3,000	Recharge Conc	1,500	1	261
Current Cu Source Term Properties					
Main WRD	330,000	Constant	5	1 - 2	325
Intermediate WRD	80,000	Constant	35	1 - 2	325
Dyson'sWRD	90,000	Constant	3	1 - 2	653
CEPA Ditch		-	-	-	-
Heap Leach Pile		-	-	-	-
Main Pit		Constant	30	6	
Intermediate Pit		-	-	-	-
Dyson's (backfilled) Pit	50,000	Constant	30	1 - 2	196
Old Tailings Dam	400,000	-	-	-	-

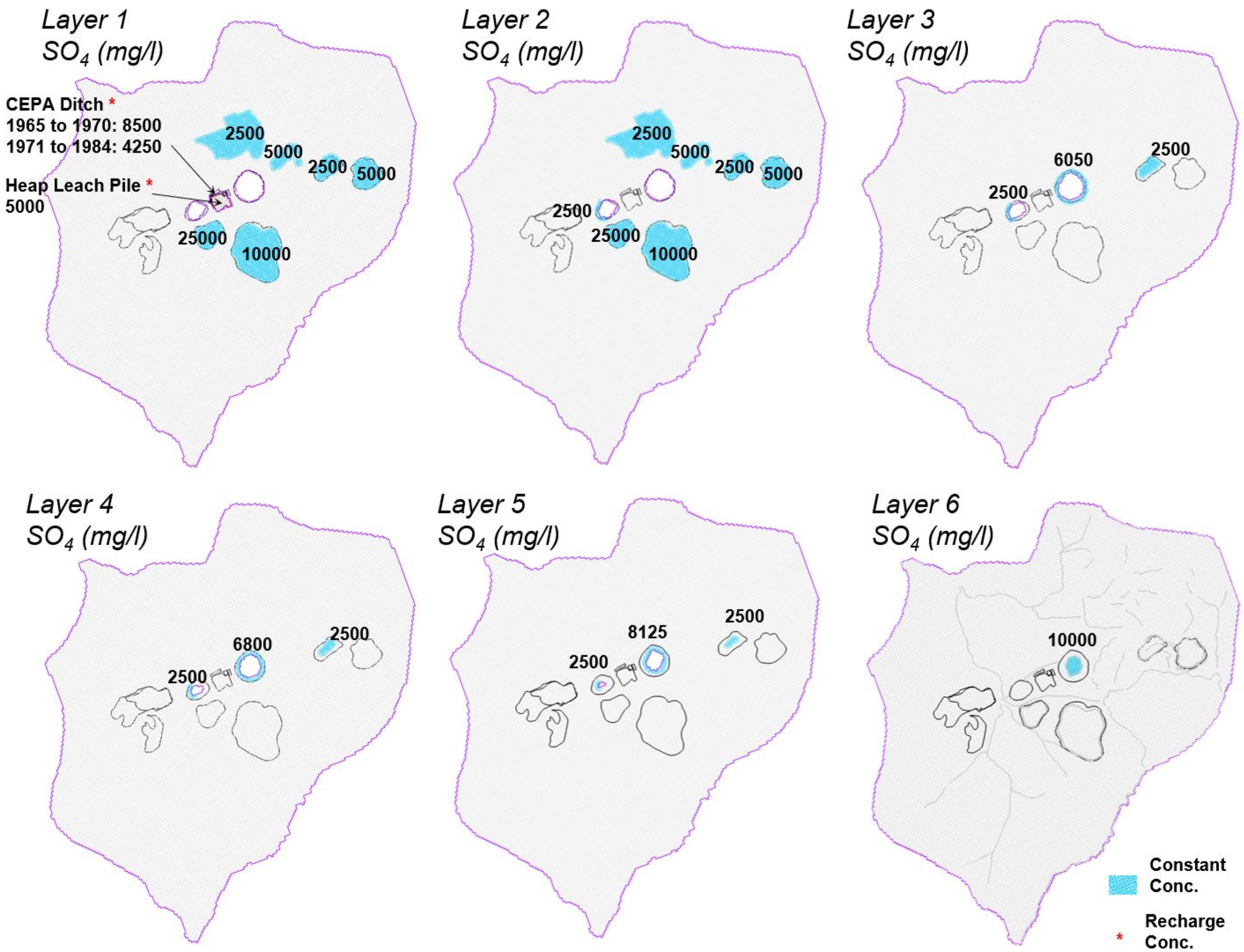

Figure 4-16. Sulphate Source Terms for Historic Transport Model

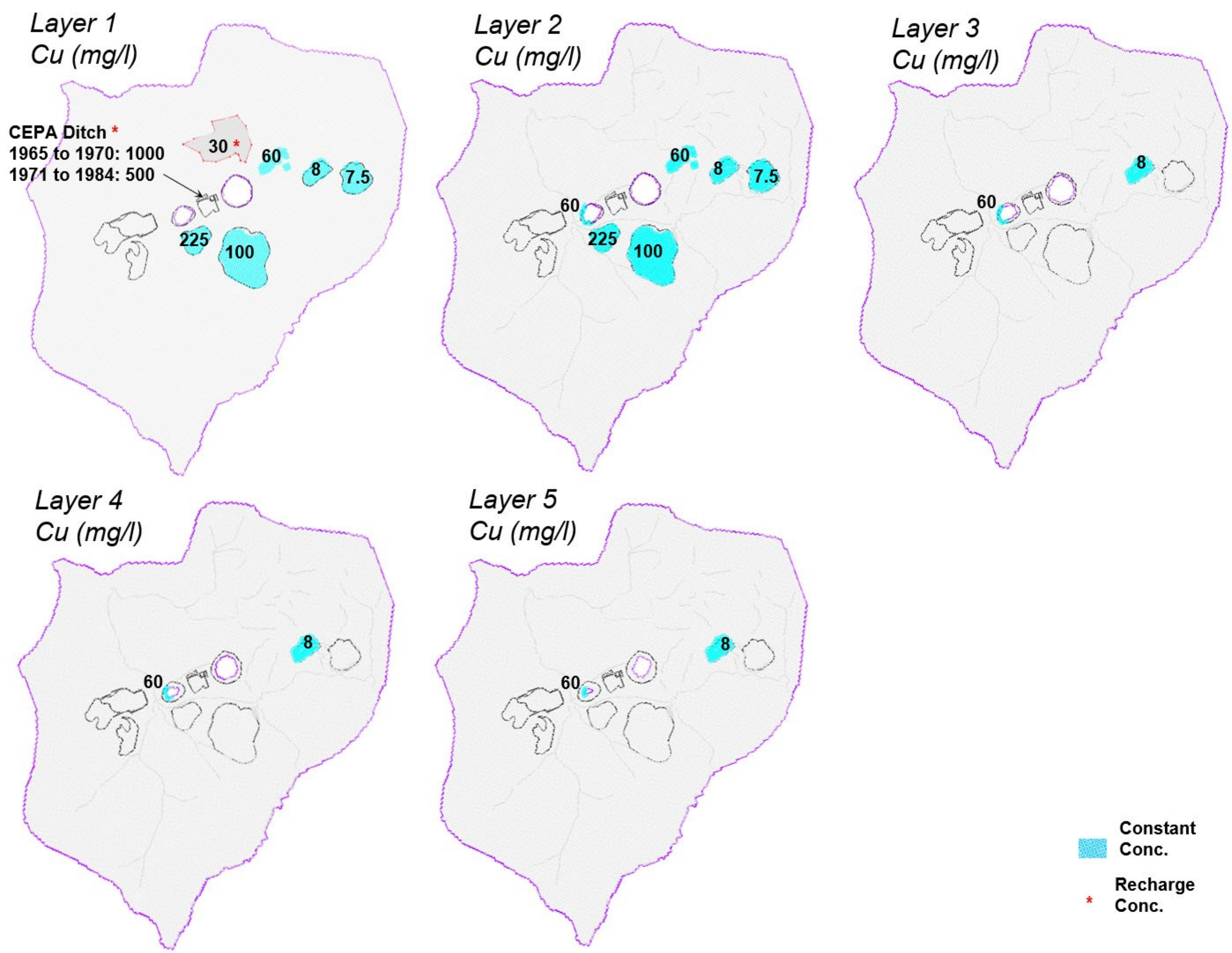

Figure 4-17. Copper Source Terms for Historic Transport Model

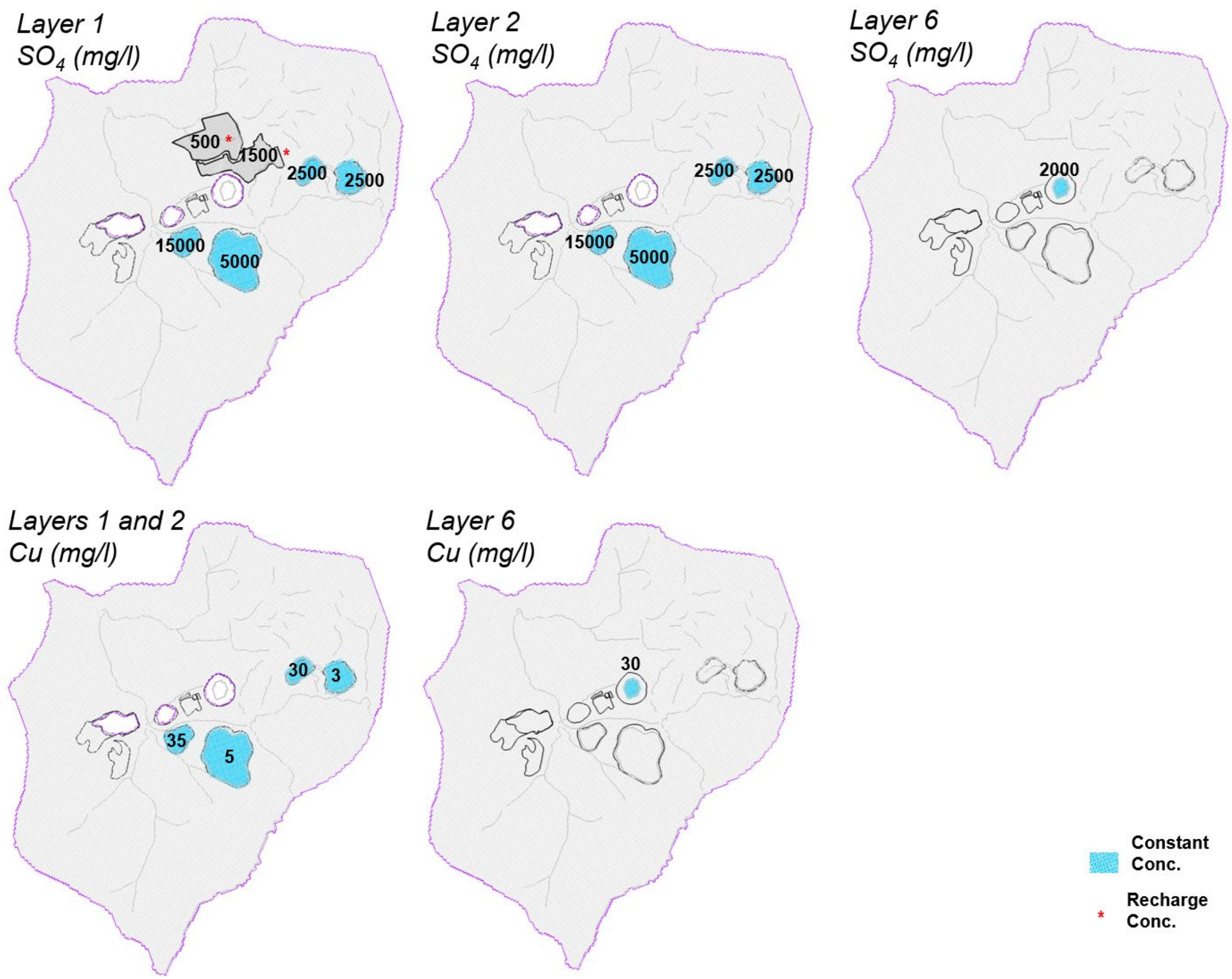

Figure 4-18. Sulphate and Copper Source Terms for Current Transport Model

4.5.6 Geochemical Reactions

SO_4 is assumed to be non-reactive ("conservative"), i.e. no geochemical reactions are assumed to influence sulphate transport along the groundwater flow path. Copper transport in groundwater was assumed to be affected by geochemical reactions, including sorption on soils and/or bedrock (e.g. on Fe-oxihydroxides, clays etc.) and the chemical precipitation of copper as copper hydroxides or Cu hydroxyl carbonates-malachite (pH-controlled) in bedrock units which have adequate buffering capacity to neutralize AMD (e.g. in Coomalie Dolostone). Detailed site-specific information on geochemical controls for copper at Rum Jungle was not available to quantify the relative proportion of these attenuation mechanisms and/or parameterize these reaction models.

Instead, a range of "attenuation scenarios" for copper were simulated in RGC (2016) to illustrate and bracket the potential influence of these geochemical controls on historic and current copper transport in groundwater and loading to the receiving surface water. These attenuation scenarios included a "no attenuation" (conservative transport) scenario, "moderate attenuation" scenario and "high attenuation" scenario. However, only the "moderate attenuation" scenario could explain estimated loads in the EBFR, thus only this scenario was retained for this phase of modeling.

Sorption refers to the mass transfer process between the solute dissolved in groundwater (aqueous phase) and the solute sorbed on the porous medium (solid phase). For the purpose of this study, sorption was assumed to be a linear reversible process which is represented in the transport model by the retardation equation, $R = 1 + \rho_b / n * K_d$, where R is the retardation factor, ρ_b is the bulk density (in kg/L), n is the porosity and K_d is the distribution coefficient (slope of linear isotherm) in L/kg.

In alkaline groundwater conditions, as observed in Coomalie Dolostone, copper is known to precipitate out as copper hydroxide or copper carbonate. This was represented in the transport model by applying a rate constant for chemical precipitation of copper to both dissolved and sorbed concentrations. All model zones representing Coomalie Dolostone were assigned a first-order reaction rate of $ß = 1\ s^{-1}$. This rate constant was sufficiently high that essentially all dissolved copper in solution is removed from the groundwater system.

All laterite or saprolite (in model layers 1 and 2) was assigned a retardation factor of 3.5 to represent weak sorption and all bedrock other than Coomalie Dolostone was assigned a retardation factor of 100 to represent strong sorption. Figure 4-19 and Figure 4-20 show the spatial distribution of respective K_D and ß values assigned to the numerical model for the moderate attenuation scenario[3].

---

[3] Bulk density values assumed in the model to compute retardation factors ranged from 1,600 kg/m^3 for overburden to 2,400-2,800 kg/m^3 for bedrock (depending on lithology).

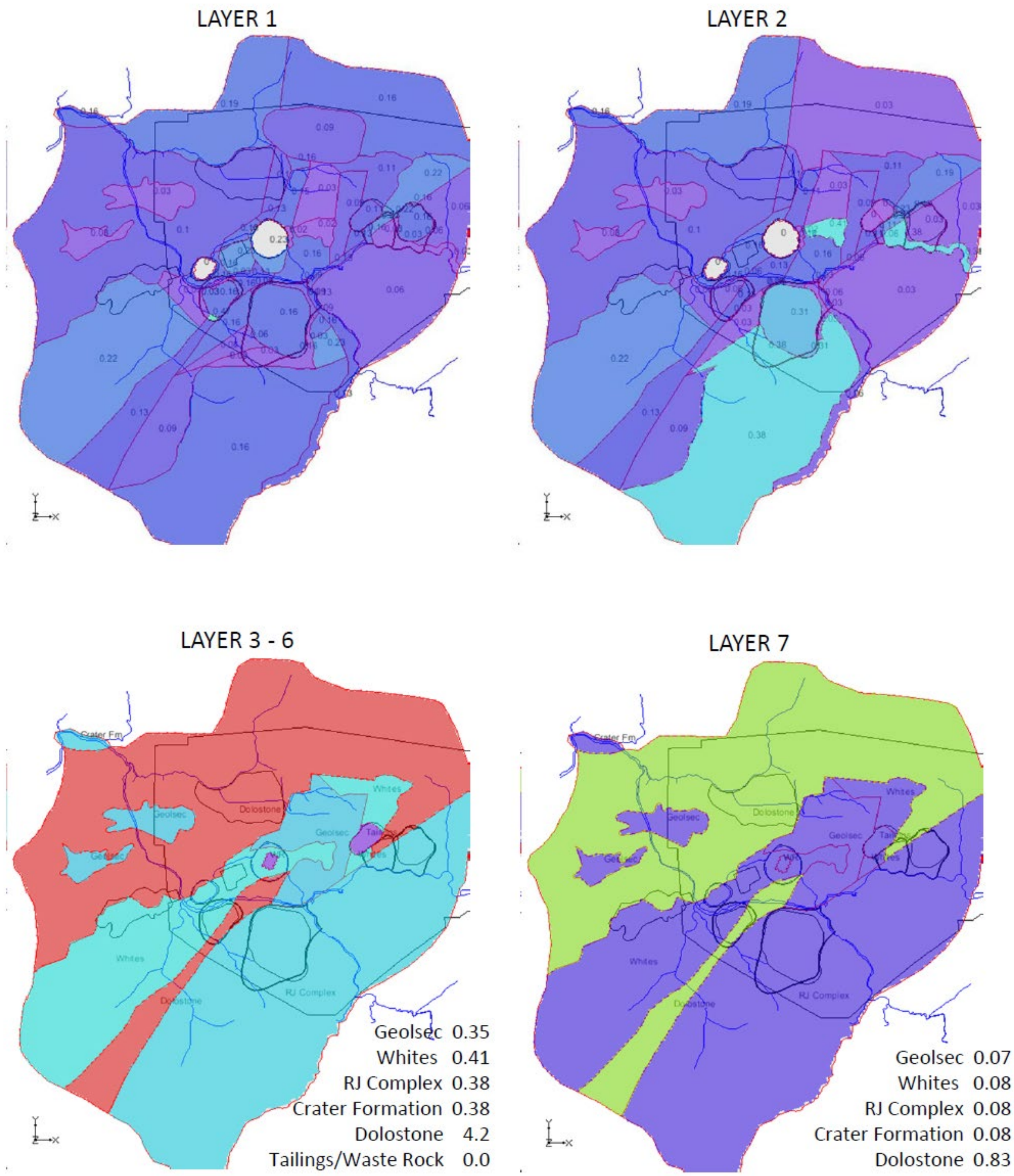

Figure 4-19. Sorption Distribution Coefficients (K_D) for Copper Transport Model (in L/kg)

Layer 3 – 7:

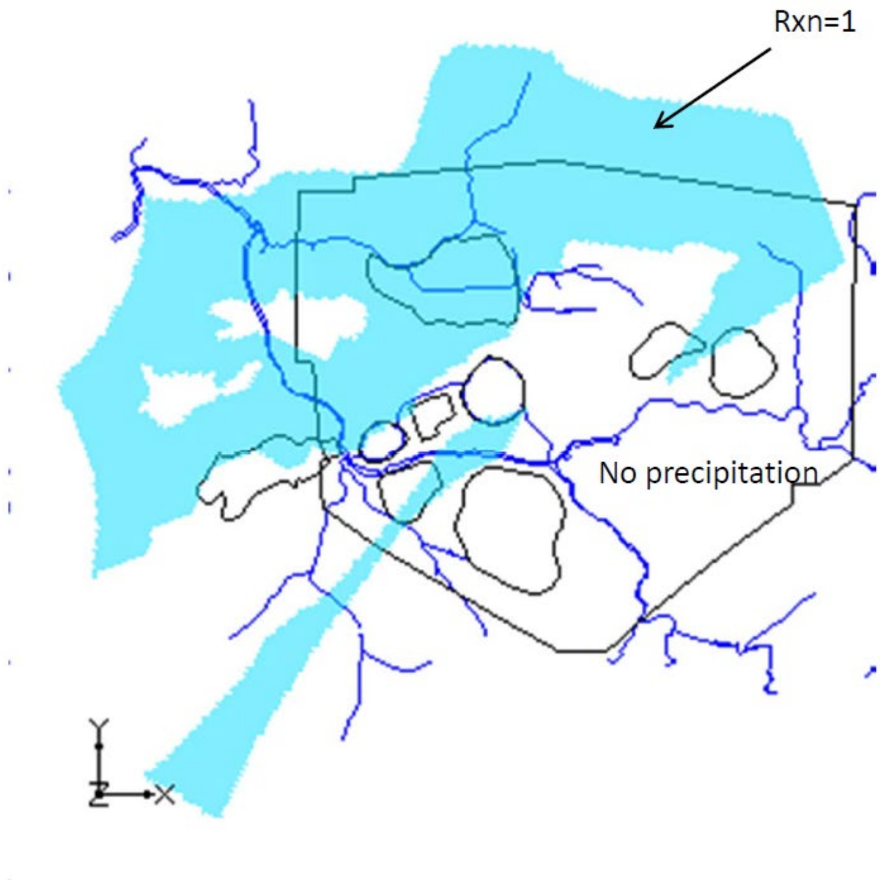

*No precipitation in Layers 1 & 2

Figure 4-20. Bedrock Zones Assigned Chemical Properties (β = 1 s-1)

4.5.7 Initial Concentrations

For the historic model, an initial background concentration of 0 mg/L SO_4 (and 0 mg/L Cu) was applied over the entire domain in every variable-head cell. It is acknowledged that this is a highly simplified assumption. However, this assumption does not significantly influence the final solution of the historic model (of primary interest here) because the sulphate and copper plumes approach steady-state in less than 25 years. For the current model, the simulated sulphate (or copper) concentrations simulated by the historic model for the final time step (end of 1984) were used as initial concentrations.

4.5.8 Solver and Convergence Criteria

The advection component of the advection-dispersion ("ADE") equation was solved using:

- The standard finite difference method with upstream weighting for copper simulations; and,
- The Hybrid MOC/MMOC (HMOC) method with the First order Euler tracking algorithm for sulphate simulations.

The dispersion and sinks/sources components were solved implicitly with the generalized conjugate gradient solver ("GCG"), using the Symmetric Successive Over Relaxation (SSOR) preconditioner and a maximum relative concentration change (CCLOSE) of 10^{-4}.

4.6 TRANSPORT SIMULATIONS

4.6.1 Calibration Approach

The solute transport models for sulphate and copper were qualitatively calibrated by ensuring the models meet the following two general calibration targets:

- The simulated spatial distribution of sulfate and copper concentrations ("plumes") are generally consistent with the inferred sulfate and copper plumes prior to rehabilitation in the 1980s and under current conditions developed as part of conceptual modeling, and
- The simulated total sulfate and copper loads to the EBFR are generally consistent with estimated loads to the EBFR prior to rehabilitation in the 1980s and under current conditions developed as part of conceptual modeling.

A detailed quantitative calibration of the solute transport model using historic time trends of sulphate and copper was beyond the scope of this study. Nevertheless, the qualitative calibration of the solute transport model is considered adequate to provide indicative predictions of the future groundwater quality in response to the proposed rehabilitation works. An extensive sensitivity analysis for current and future conditions has been completed to assess the remaining uncertainty of these solute transport predictions (see Sections 4.7 and 4.10).

4.6.2 Historic Model

Figure 4-21 shows the simulated sulphate and copper concentrations for historic conditions, i.e. prior to rehabilitation in 1984/1985. The simulated spatial distribution of sulphate and copper concentrations for 1984 are generally consistent with the (limited) observations on groundwater quality available for the period immediately prior to rehabilitation in the mid-1980s (see Davy, 1975). The groundwater model simulates SO_4 plumes emanating (migrating) from each of the active AMD sources and residual impacted groundwater in the Old Tailings Dam area, the former ore stockpile area, and in the Copper Extraction Pad area. SO_4 concentrations are highest near the Main and Intermediate WRDs and near Dyson's (backfilled) Pit. Simulated Cu plumes are less spatially extensive than the simulated SO_4 plume, as the model simulates substantial retardation of these plumes due to adsorption and attenuation of Cu in the aquifer.

The model predicts the presence of several distinct historic plumes caused by historic seepage from the different known (or inferred) mine waste units present prior to rehabilitation in the mid 1980's:

- In Dyson's Area, the SO_4 plume reaches peak concentrations of about 5,000 mg/L SO_4; this plume discharges to the Upper EBFR and smaller northern tributaries. In this area, the copper plume reaches peak concentrations of about 8 mg/L Cu; this plume discharges to the Upper EBFR and smaller northern tributaries.
- In proximity of Main and Intermediate WRD, the sulphate plume reaches peak concentrations of 10,000 and 25,000 mg/L SO_4, respectively. The sulphate plume from the Main WRD discharges to Fitch Creek to the east, Wandering Creek to the southwest and the EBFR to the north. To the west, the sulphate plume merges with the (more concentrated) plume from the Intermediate WRD and discharges to the EBFR and to the Intermediate Pit.
- In the copper extraction pad area, simulated sulphate concentrations are assumed to be elevated (5000 mg/L) to significant depth in bedrock (layers 2-6) because of historic leach operations. This plume is limited to the immediate foot print of the CEPA and discharges into the Intermediate Pit. In this area, copper concentrations are highly elevated (up to 500 mg/L Cu) along the collection ditch (located along the northern toe of the heap leach pad area) to significant depth in bedrock (layers 2-5) because of historic leach operations.
- Seepage from the former mill area and associated ore stockpiles (to the northeast of the Main Pit) is predicted to migrate in a southwesterly direction towards the Main Pit. Simulated peak concentrations of sulphate in this mill site plume reach 5,000 mg/L in overburden soils.
- Seepage from the historic tailings placed in the Old Tailings Dam area (with an estimated source concentration of 2,500 mg/L) is predicted to have produced a historic sulphate plume of significant spatial extent, covering the former foot print area of the OTD and significant portions of the Coomalie dolostone aquifer to the west. The majority of the sulphate plume

(primarily in overburden) discharges to Old Tailings Creek while a smaller proportion (in deeper bedrock) discharges directly to the EBFR (between gauging stations GS8150200 and GS8150327).

- Chemical precipitation assumed for dolostone completely removes copper from the aqueous phase, thus effectively eliminating any copper plume in those bedrock unit. This affects primarily the copper plume in the OTD area.

The historic flow and transport model was used to compute the historic mass fluxes ("loads") of sulphate and copper to the receiving surface water. Table 4-5 summarizes these loads (in t/yr) at specified model reaches (Figure 4-22).

Table 4-5. Simulated Historic Sulphate and Copper Loads to EBFR (By Reach) (1984)

Reach	Description	SO_4		Cu	
		t/year	%	t/year	%
A	Dyson's Area	496	13.4%	1.4	8.6%
B	Main WRD (east)	1182	31.8%	8.8	53.7%
C	Main WRD (west) and Int. WRD	326	8.8%	2.3	13.8%
D	Middlebrook Creek	0	0.0%	0.0	0.0%
E	EFDC near Main and Int. WRDs	1248	33.6%	2.9	17.9%
F	Former stockpile area	117	3.2%	1.0	5.9%
G	EBFR downstream of GS8150200	208	5.6%	0.0	0.0%
H	EBFR in Old Tailings Dam area	69	1.9%	0.0	0.0%
I	EBFR near GS8150327	67	1.8%	0.0	0.0%
	Simulated Load to EBFR:	**3713**	100.0%	**16.4**	100.0%
-	To Main Pit	125	23.5%	0.5	25.1%
-	To Int. Pit	409	76.5%	1.6	74.9%
-	To Browns Pit	0	0.0%	0.0	0.0%
-	To Model Flooding Drains	0	0.0%	0.0	0.0%
	Simulated Load to Pits:	**535**	100.0%	**2.1**	100.0%

The simulated historic sulphate loads are summarized as follows:

- The total historic sulphate load discharging to the receiving surface water prior to rehabilitation (in 1984) is predicted to be about 4,248 t/yr (3,713 t/yr to EBFR and 535 t/yr to open pits).
- The highest proportion of this sulphate load is predicted to discharge in EFDC (Reach E, 29%) and East to the Main WRD (Reach B, 28%).
- Historic sulphate load to the Upper EBFR (Dyson's area, Reach A, 12%), west to the Main WRD and Intermediate WRD (Reach C, 8%) and to the EBFR downstream of station GS8150200 (Reach G, 5%) are predicted to be significantly smaller.

- The historic sulphate flux to the Intermediate Pit (about 10% of total) is higher than to the Main Pit (3% of total) because of discharge of highly impacted groundwater from the CEPA and the Intermediate WRD.

The simulated historic load balance for sulphate (Table 4-5) agrees very well with the conceptual load balance for historic conditions discussed in Section 3-13. The simulated historic sulphate load (4,248 t/yr) explains about 98% of the historic sulphate load in groundwater estimated using conceptual modeling (4,349 t/yr). Furthermore, the respective simulated sulphate loads discharging to surface water near major point sources (primarily WRDs) agree reasonably well with historic load estimates for those point sources.

The simulated historic copper loading to surface water are summarized as follows:

- The total historic copper load discharging to the receiving surface water is predicted to be about 19 t/yr.
- The highest proportion of this copper load is predicted to discharge East to the Main WRD (Reach B, 48%), in EFDC (Reach E, 16%) and west to the Main WRD and Intermediate WRD (Reach C, 12%).
- Historic copper load to the Upper EBFR (Dyson's area, Reach A, 8%) and to the former stockpile area (Reach F, 6%) are predicted to be significantly smaller.
- The historic sulphate flux to the Intermediate Pit (about 9% of total) is higher than to the Main Pit (3% of total) because of discharge of highly impacted groundwater from the CEPA and the Intermediate WRD.

The simulated copper load reporting to surface water via groundwater can be expected to be substantially smaller, if compared to the total load entering the groundwater system, due to chemical attenuation of copper along the flow path. In the conceptual load balance for copper an estimated 30% was assumed to be lost due to chemical attenuation. However, this value represents only an initial "educated guess". Copper loads to the EBFR via surface sources (e.g. surface runoff from exposed tailings and WRDs, copper loads from acidic pit lakes) represent significant (but difficult to quantify) additional sources which make it difficult to constrain the "loss term" for copper.

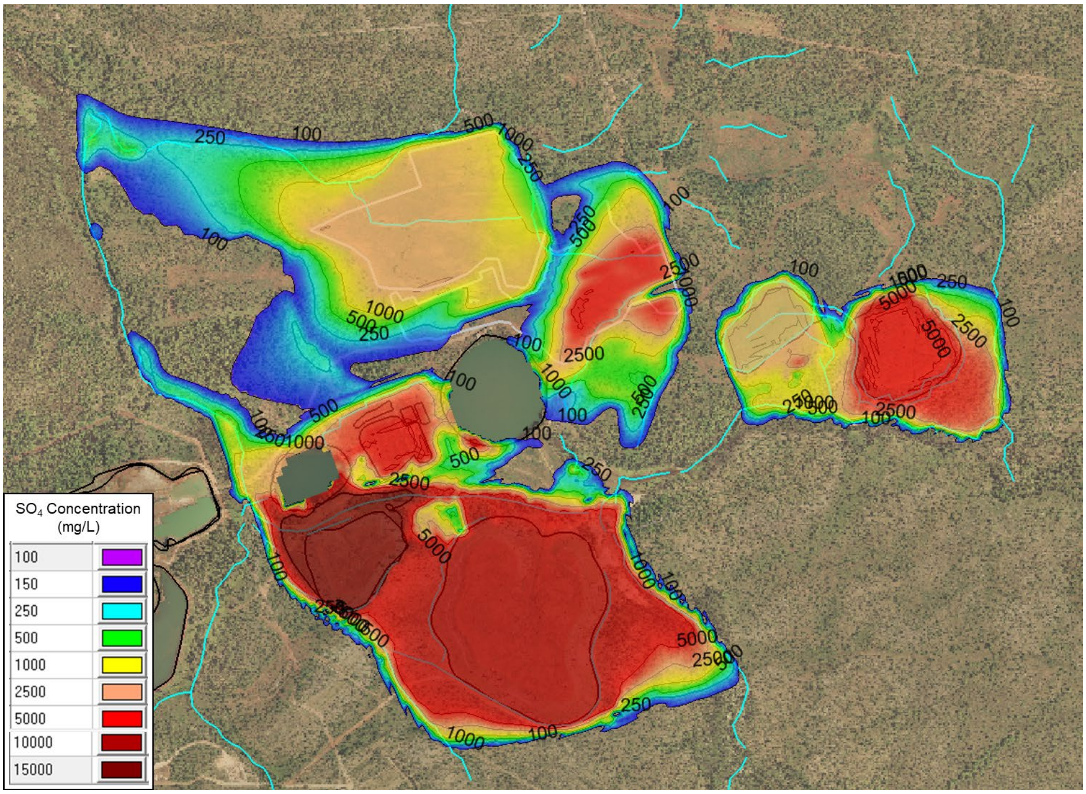

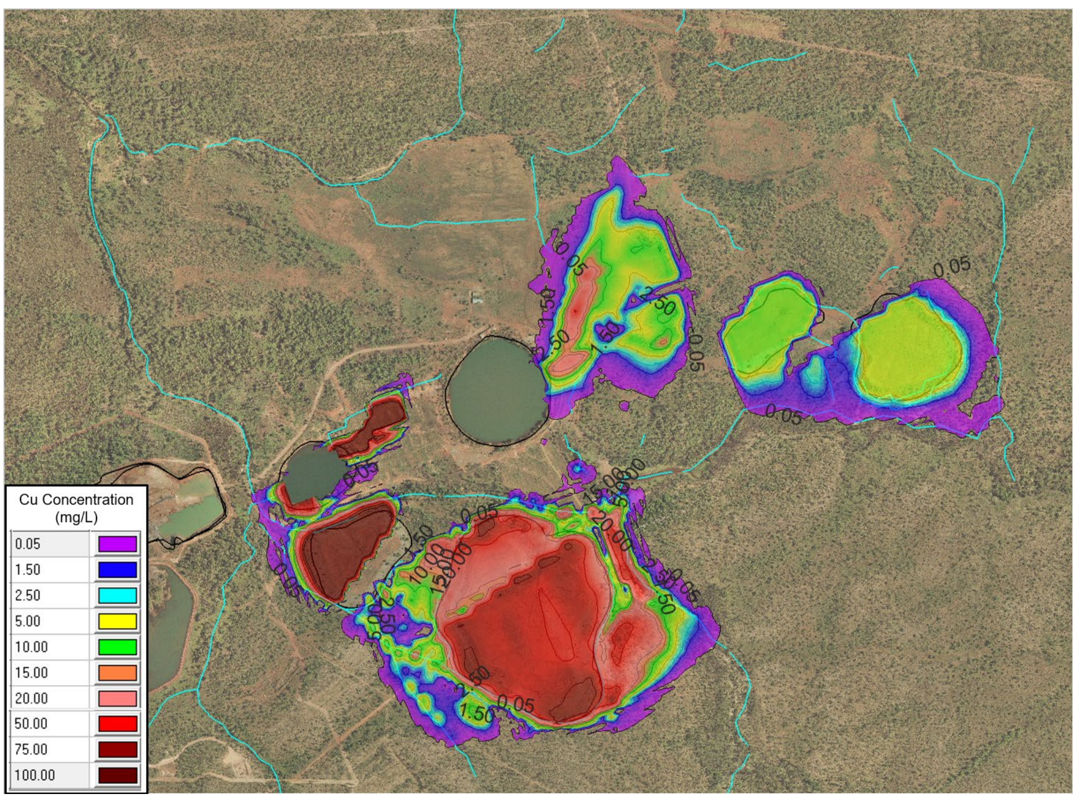

Figure 4-21. Simulated Sulphate Plume (top), Simulated Copper Plume (bottom), 1984

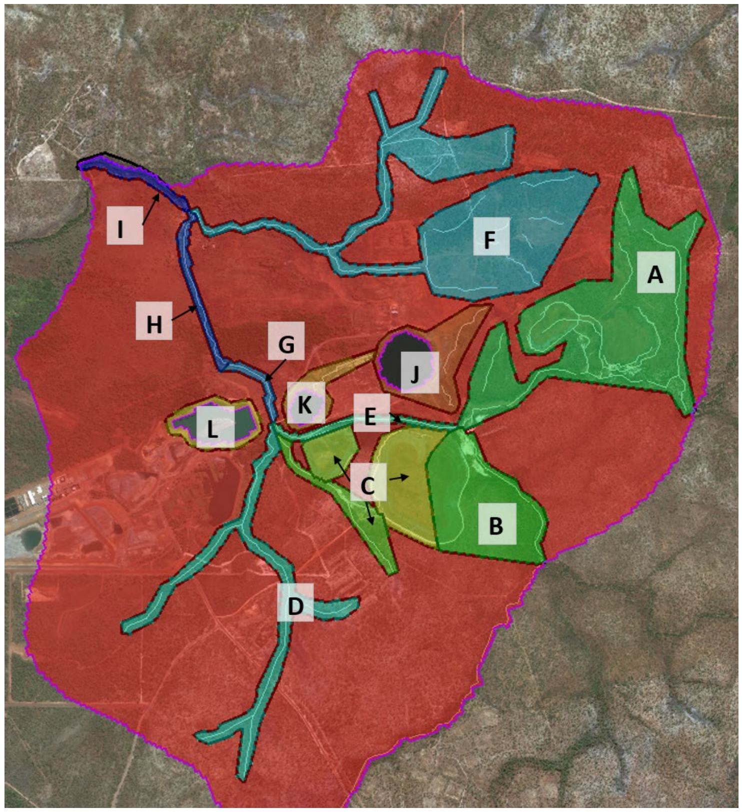

Figure 4-22. EBFR Reaches in Groundwater Model

4.6.3 Current Conditions Model

Simulated SO_4 and Cu plumes for current conditions are provided in Figure 4-23, Figure 4-24 and Figure 4-25. Simulated SO_4 and Cu loads to the EBFR (by reach) are summarized in Table 4-6 and Table 4-7, respectively. The simulated spatial distribution of sulphate and copper concentrations for current conditions are generally consistent with current groundwater quality observations (see Figure 3-7 and 3-8) although simulated Cu concentrations nearest the WRDs are typically higher than observed.

The model predicts the following significant changes to sulphate and copper concentrations in groundwater for current conditions vis-à-vis historic, pre-rehabilitation conditions:

- A reduction in sulphate and copper loading for all WRDs (due to cover placement in 1984/85) does not significantly change the spatial extent of the associated sulphate plumes in groundwater. However, concentrations in laterite/saprolite and bedrock decrease significantly as a result of reduced loading.
- The removal of the ore stockpiles in the former mill site have reduced the sulphate and copper load and hence concentrations in groundwater in that area (northeast of the Main Pit).

However, contaminated soils remaining in this area (and other areas between the Main Pit and the Old Tailings Dam area) represent a secondary source of SO_4 (~1,500 mg/L) and Cu (~10 mg/L)).

- Removal of the historic tailings from the Old Tailings Dam area has resulted in significant clean-up of the historic sulphate plume in this area. However, a residual sulphate plume is predicted to be present in the former OTD foot print area (~500 mg/L SO_4) due to ongoing seepage from residual tailings not removed during rehabilitation works.

The predicted current sulphate loads are summarized as follows (Table 4-6):

- The total current sulphate load in groundwater discharging to the receiving surface water is predicted to be about 1,458 t/yr. This load represents only about 35% of the historic sulphate load in groundwater, i.e. an almost threefold decrease.
- The highest proportion of current sulphate load in groundwater is predicted to discharge into the EFDC (Reach E, 34%), followed by Dyson's area (Reach A, 17%), Main WRD east (Reach B, 15%) and Main WRD west (Reach C, 13%).
- Sulphate loading to the Main Pit (5%) and Intermediate Pit (5%) represents a small component to total sulphate load.

The simulated current load balance for sulphate agrees reasonably well with the conceptual sulphate load balance for current conditions described in Section 3. The simulated current sulphate load (1,458 t/yr) is about 28% higher than the current sulphate load in groundwater estimated using known point sources (1,138 t/yr) but is about 22% lower than observed sulphate loading to the EBFR (1,840 t/yr). The discrepancy between those estimates is attributed to "diffuse" sources such as seepage from residual contamination in the CEPA, the Old TDF and other areas with contaminated soils and/or residual mine waste. Given the uncertainty in the magnitude of these diffuse sources, the simulated conditions for SO_4 are considered a reasonable representation of current conditions, and therefore provide a suitable reference against which to evaluate the effect of future rehabilitation.

The simulated current copper loading to surface water is summarized as follows (Table 4-7):

- The total current copper load discharging to the receiving surface water is predicted to be about 3.1 t/yr. This represents a 6-fold reduction in copper load from groundwater to surface water since rehabilitation in the mid-1980s.
- Seepage to the EFDC represents the highest current copper load (Reach E, 42%), followed by Dyson's area (Reach A, 16%), Main WRD east (Reach B, 13%) and Main WRD west (Reach C, 13%).

- Residual copper loading from the CEPA to the Intermediate Pit is predicted to be a major source of copper loading for current conditions (13.5%).

The simulated current copper load from groundwater to surface water (3.1 t/yr) is in good agreement with observed total copper load in the EBFR (2.7 t/yr), see Section 3.14.2.

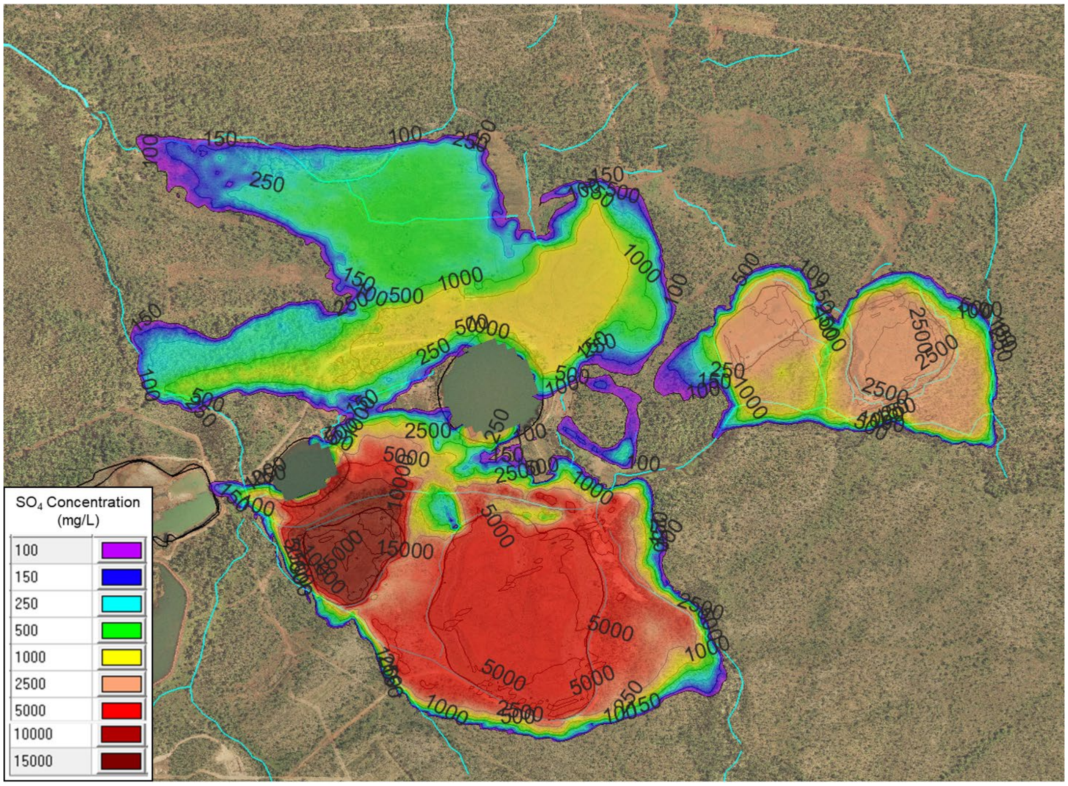

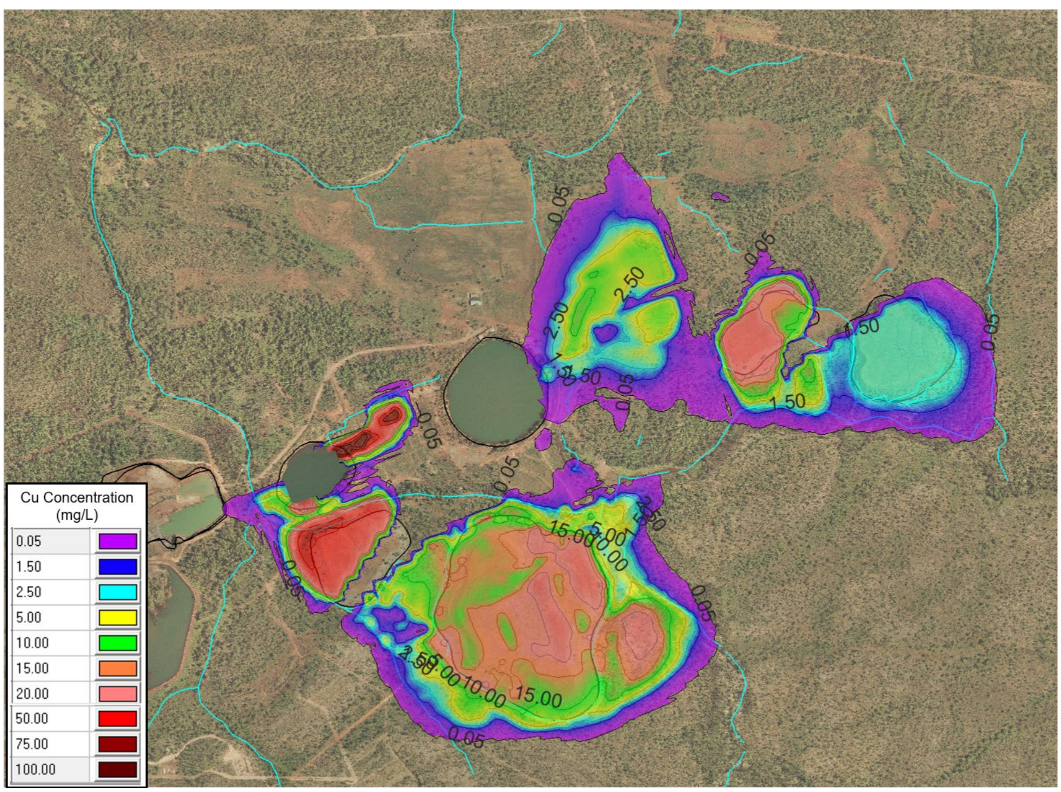

Figure 4-23. Simulated Sulphate Plume (top), Simulated Copper Plume (bottom), Model Layer 3 for Current Conditions

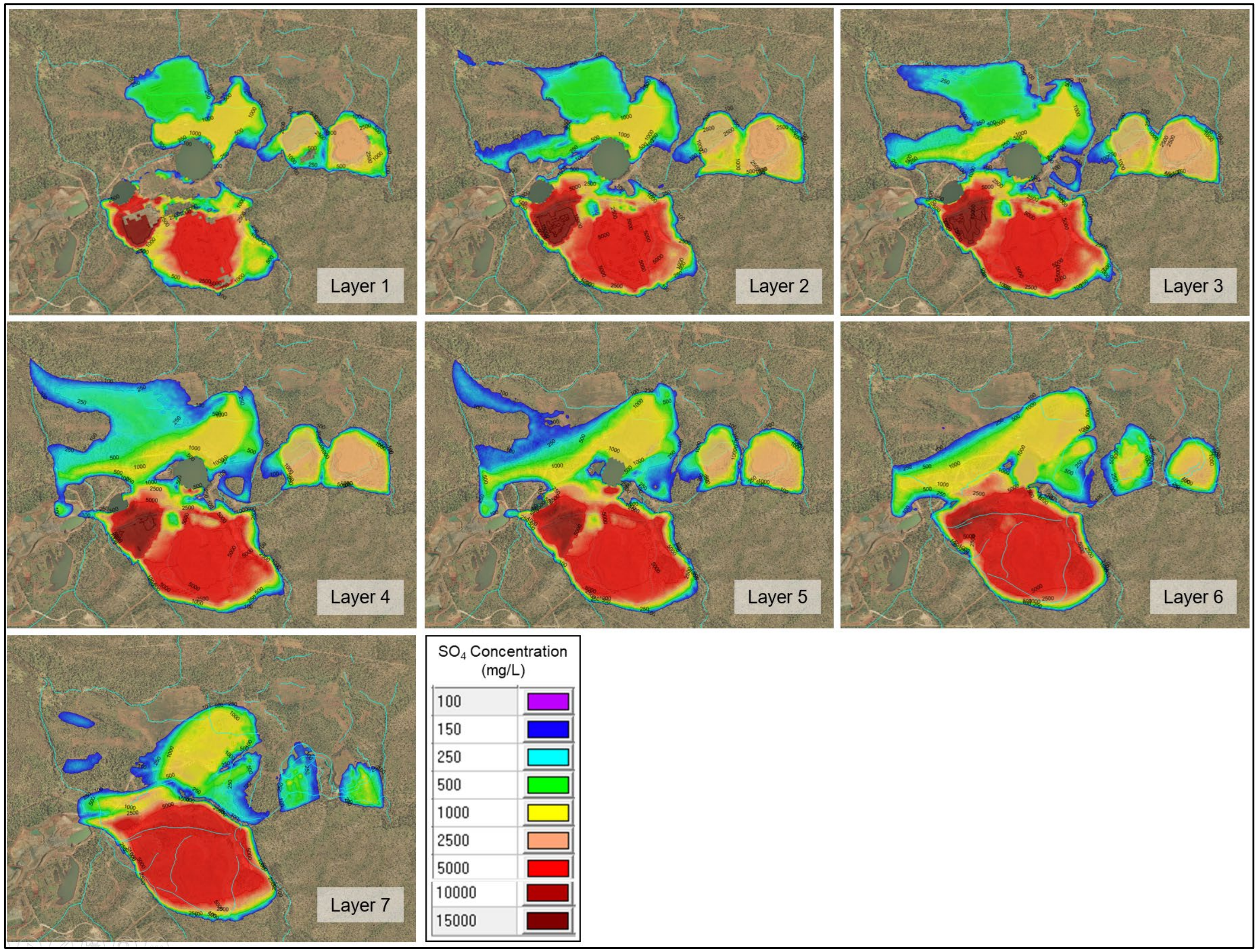

Figure 4-24. Simulated Sulphate Plume for Model Layers 1 to 7, Current Conditions

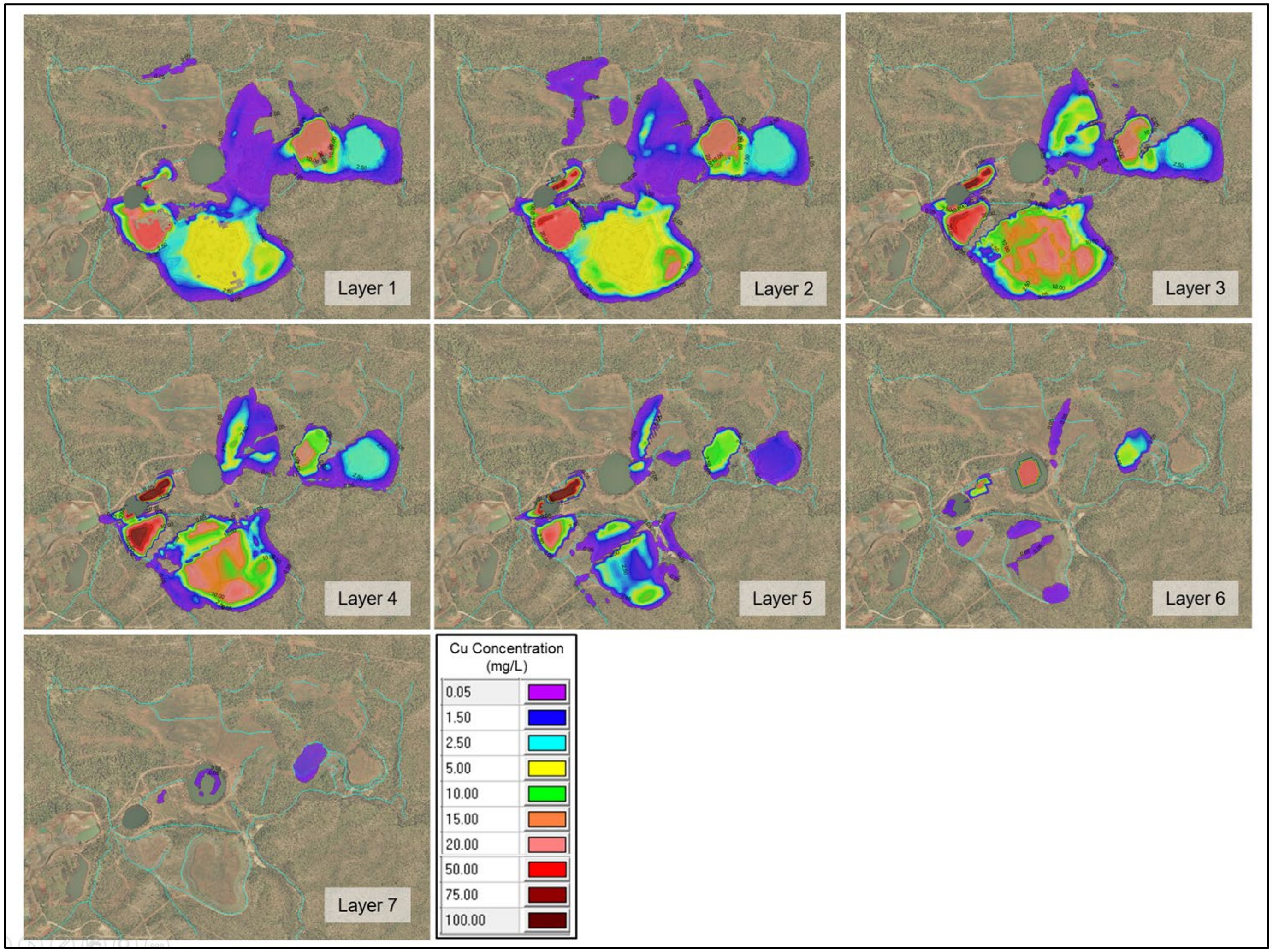

Figure 4-25. Simulated Copper Plume for Model Layers 1 to 7, Current Conditions

Table 4-6. Simulated Sulphate Loads to EBFR (By Reach) and Pits

	Reach Description	2010/2011 Water Year	2011/2012 Water Year	2012/2013 Water Year	2013/2014 Water Year	2014/2015 Water Year	2015/2016 Water Year	2016/2017 Water Year	2017/2018 Water Year	Average (2010 to 2018)	
		t/year	t/year	t/year	t/year	t/year	t/year	t/year	t/year	t/year	%
A	Dyson's Area	294	208	224	252	178	169	223	245	224	19%
B	Main WRD (east)	272	197	192	226	161	152	190	219	201	17%
C	Main WRD (west) and Int. WRD	224	142	136	170	114	108	146	193	154	13%
D	Middlebrook Creek	0	0	0	0	0	0	0	0	0	0%
E	EFDC near Main and Int. WRDs	605	469	447	531	417	418	480	501	484	41%
F	Former stockpile area	39	16	17	31	11	14	27	38	24	2%
G	EBFR downstream of GS8150200	70	64	43	64	52	54	63	57	58	5%
H	EBFR in Old Tailings Dam area	21	18	17	20	23	22	23	21	21	2%
I	EBFR near GS8150327	10	10	14	15	14	15	13	14	13	1%
	Simulated Load to EBFR:	**1537**	**1126**	**1090**	**1308**	**970**	**951**	**1166**	**1288**	**1179**	**100%**
-	To Main Pit	78	53	61	67	46	48	59	71	61	43%
-	To Int. Pit	48	66	88	68	53	59	63	71	64	45%
-	To Browns Pit	8	2	18	13	9	8	9	9	9	7%
-	To Model Flooding Drains	22	3	1	12	0	0	6	19	8	6%
	Simulated Load to Pits:	**157**	**124**	**168**	**160**	**109**	**115**	**136**	**170**	**142**	**100%**
	TOTAL:	**1,694**	**1,250**	**1,258**	**1,468**	**1,078**	**1,067**	**1,302**	**1,458**	**1,322**	**-**

Table 4-7. Simulated Copper Loads to EBFR (By Reach) and Pits

	Reach Description	2010/2011 Water Year	2011/2012 Water Year	2012/2013 Water Year	2013/2014 Water Year	2014/2015 Water Year	2015/2016 Water Year	2016/2017 Water Year	2017/2018 Water Year	Average (2010 to 2018)	
		t/year	t/year	t/year	t/year	t/year	t/year	t/year	t/year	t/year	%
A	Dyson's Area	0.5	0.3	0.4	0.5	0.3	0.3	0.4	0.5	0.4	17%
B	Main WRD (east)	0.5	0.3	0.3	0.4	0.3	0.3	0.3	0.4	0.4	15%
C	Main WRD (west) and Int. WRD	0.5	0.3	0.3	0.3	0.2	0.2	0.3	0.4	0.3	13%
D	Middlebrook Creek	0.0	0.0	0.0	0.0	0.0	0.0	0.0	0.0	0.0	0%
E	EFDC near Main and Int. WRDs	1.6	1.2	1.2	1.4	1.1	1.1	1.3	1.3	1.3	54%
F	Former stockpile area	0.0	0.0	0.0	0.0	0.0	0.0	0.0	0.0	0.0	0%
G	EBFR downstream of GS8150200	0.0	0.0	0.0	0.0	0.0	0.0	0.0	0.0	0.0	0%
H	EBFR in Old Tailings Dam area	0.0	0.0	0.0	0.0	0.0	0.0	0.0	0.0	0.0	0%
I	EBFR near GS8150327	0.0	0.0	0.0	0.0	0.0	0.0	0.0	0.0	0.0	0%
	Simulated Load to EBFR:	**3.1**	**2.1**	**2.2**	**2.6**	**1.9**	**1.9**	**2.3**	**2.6**	**2.3**	**100%**
-	To Main Pit	0.1	0.1	0.1	0.1	0.1	0.1	0.1	0.1	0.1	14%
-	To Int. Pit	0.4	0.4	0.4	0.4	0.3	0.3	0.4	0.4	0.4	85%
-	To Browns Pit	0.0	0.0	0.0	0.0	0.0	0.0	0.0	0.0	0.0	0%
-	To Model Flooding Drains	0.0	0.0	0.0	0.0	0.0	0.0	0.0	0.0	0.0	0%
	Simulated Load to Pits:	**0.5**	**0.4**	**0.5**	**0.5**	**0.3**	**0.4**	**0.5**	**0.5**	**0.5**	**100%**
	TOTAL:	**3.5**	**2.6**	**2.7**	**3.1**	**2.2**	**2.3**	**2.8**	**3.1**	**2.8**	**-**

4.7 SENSITIVITY ANALYSIS FOR CURRENT CONDITIONS MODEL

4.7.1 Approach

Due to the uncertainty in key model input parameters, a sensitivity analysis was completed to evaluate the sensitivity of the calibrated model to variations in parameter values.

This analysis was carried out by systematically adjusting the following flow and transport parameters:

- Hydraulic conductivity
- Natural recharge
- Specific yield
- Specific storage
- Evapotranspiration
- Retardation factor (R_f) for Cu simulations

- Effective Porosity (n_e)
- Dispersivity (α_L)

Each model input parameter was adjusted, one at a time, up or down from the calibrated value and within a plausible range. The model was rerun transiently for the period January 1985 to December 2018 using this adjusted ("perturbed") set of model parameters. In the case of evapotranspiration, rather than adjusting rates, the EVT Package in GMS was completely disabled for a single simulation.

For each sensitivity run, calibration statistics were evaluated for the full calibration period, December 2010 to December 2018, using 6373 observations from 117 monitoring bores. As well, predicted average flows to the EFDC and the EFBR, between gauging stations GS8150200 and GS8150327 (referred to as "EBFR D/S") were compared to calibrated model flow estimates. In addition, simulated total SO_4 and Cu groundwater loads were compared to the simulated base case model.

4.7.2 Sensitivity Runs

Table 4-8 presents a summary of calibration statistics for a total of 9 flow sensitivity runs which were conducted as part of the sensitivity analysis for current conditions. Figure 4-26 shows plot of simulated versus estimated groundwater inflows, for each of these sensitivity runs, to the EBFR D/S, compared to the calibrated model run (base case). Table 4-9 and Table 4-10 present a summary of estimated total (to the entire EBFR, within the model domain including load discharge to the pits) loads for flow and transport sensitivity runs for SO_4 (13 runs) and Cu (17 runs), respectively.

Generally, results of sensitivity analyses show that simulated heads and flows are notably sensitive to perturbations in hydraulic conductivity, recharge, specific yield of overburden and removal of evapotranspiration and are not sensitive to changes in specific storage. Simulated loads (SO_4 and Cu) show significant sensitivity to changes in recharge, hydraulic conductivity, porosity and longitudinal dispersivity, while showing limited sensitivity to changes in specific yield of overburden and specific storage.

Other key findings of the sensitivity analysis can be summarized as follows:

- Increasing the hydraulic conductivity (K) by 25%, provides a slight improvement to calibration statistics, and causes a 12% increase in EBFR D/S flow (Figure 4-26) that is particularly noticeable during the wet season and still falls between upper and lower bound targets.
- Decreasing K by 25%, causes some deterioration to calibration statistics, albeit still within acceptable limits (NRMSE is less than 5%). However, this perturbation also causes the EBFR D/S flow to decrease by 15% and to drop below the lower bound target (Figure 4-26).
- Changing K by 25% up and down causes only minor changes in predicted SO_4 and Cu loads (+/- 2 to 4%).

- Changing recharge by a factor of 1.5 up and down causes significant variations in predicted average flows to EBFR D/S (18% to 20%), as well as SO_4 loads (33% to 46%) and Cu loads (24% to 32%).
- The removal of evapotranspiration in the model causes a deterioration in head calibration statistics (NRMSE ~ 5%), increases simulated flows to EBFR D/S by 18% and increases simulated SO_4 and Cu loads by 12% and 10%, respectively.
- Increasing and decreasing porosity (n_e) and longitudinal dispersivity (α_L) by two-fold result in only small impact on simulated loads for both SO_4 and Cu (~ 1% to 5%).
- Increasing and decreasing the retardation factor by 50%, causes a corresponding 12.5% increase and 17% decrease in simulated Cu loads, respectively.

4.7.3 Implications

The simulated results of increasing K values by 25% are considered credible as it provides similar head statistics, flows, and loads compared to the base case. Note that, as part of the sensitivity analysis conducted by RGC (2016), calibrated K values were increased by half an order of magnitude (i.e. five-fold). This increase resulted in unacceptable deterioration in calibration statistics for both wet and dry seasons. It is therefore inferred that, according to the current combination of model parameters, the calibrated K values are well constrained with limited margin of increase by approximately 25 %.

Results from recharge sensitivity are considered credible to represent interannual variations in recharge rather than long term average conditions. These sensitivity runs will be carried forward to predictions to illustrate the sensitivity of model predictions to such interannual variability in future meteorological conditions.

The simulated SO_4 and Cu loads are not very sensitive to the range of transport parameters used in the sensitivity analysis (n_e, α_L and R_f). This is a result of the fact that source loading has been fairly constant since rehabilitation works in the 1980s and the simulated SO_4 and Cu plumes have approached steady-state conditions. Nevertheless, the selected range of transport parameters (n_e, α_L and R_f) used in this sensitivity analysis is considered plausible and the same range was also carried forward to predictions to examine their impact on the gradual clean-up of the bedrock aquifer due to rehabilitation works and post-rehabilitation activities.

Table 4-8. Calibration Statistics and Predicted Flows for Sensitivity Analyses (Flow Model)

Run ID	Description	Calibration Statistics				Flows	
		ME (m)	MAE (m)	RMSE (m)	NRMSE (%)	EBFR D/S (L/s)	EFDC (L/s)
R46	Calibration Run	*-0.26*	*0.80*	*1.19*	*3.81%*	*28.9*	*2.2*
Sensitivity to Hydraulic Conductivity (K)							
R51	Decrease K in all units by 25%	-0.59	0.92	1.38	4.42%	24.9	2.1
R52	Increase K in all units by 25%	0.01	0.81	1.17	3.73%	32.3	2.3
Sensitivity to Recharge							
R61	Decrease Recharge (/1.5)	0.33	0.85	1.21	3.87%	23.5	1.7
R60	Increase Recharge (x1.5)	-0.69	0.98	1.49	4.78%	34.6	3.0
Sensitivity to Overburden Specific Yield (Sy)							
R57	Decrease Overburden Specific Yield (/1.5)	-0.01	0.89	1.30	4.15%	27.9	2.2
R58	Increase Overburden Specific Yield (x1.5)	-0.44	0.87	1.30	4.17%	29.8	2.3
Sensitivity to Specific Storage (Ss)							
R55	Decrease Specific Storage by an order of magnitude	-0.25	0.80	1.19	3.82%	28.8	2.2
R56	Increase Specific Storage by an order of magnitude	-0.31	0.81	1.20	3.83%	29.1	2.2
Sensitivity to Evapotranspiration							
R62	Remove Evapotranspiration	-0.63	0.99	1.56	4.98%	32.3	2.4

ME - Residual mean error
MAE - Absolute residual mean error
RMSE = Root Mean Square Error
NRMSE = Normalized Root Mean Square Error
EBFR D/S = East Branch of Finniss River between gauge stations GS8150200 and GS8150327
EFDC = East Finniss Diversion Channel

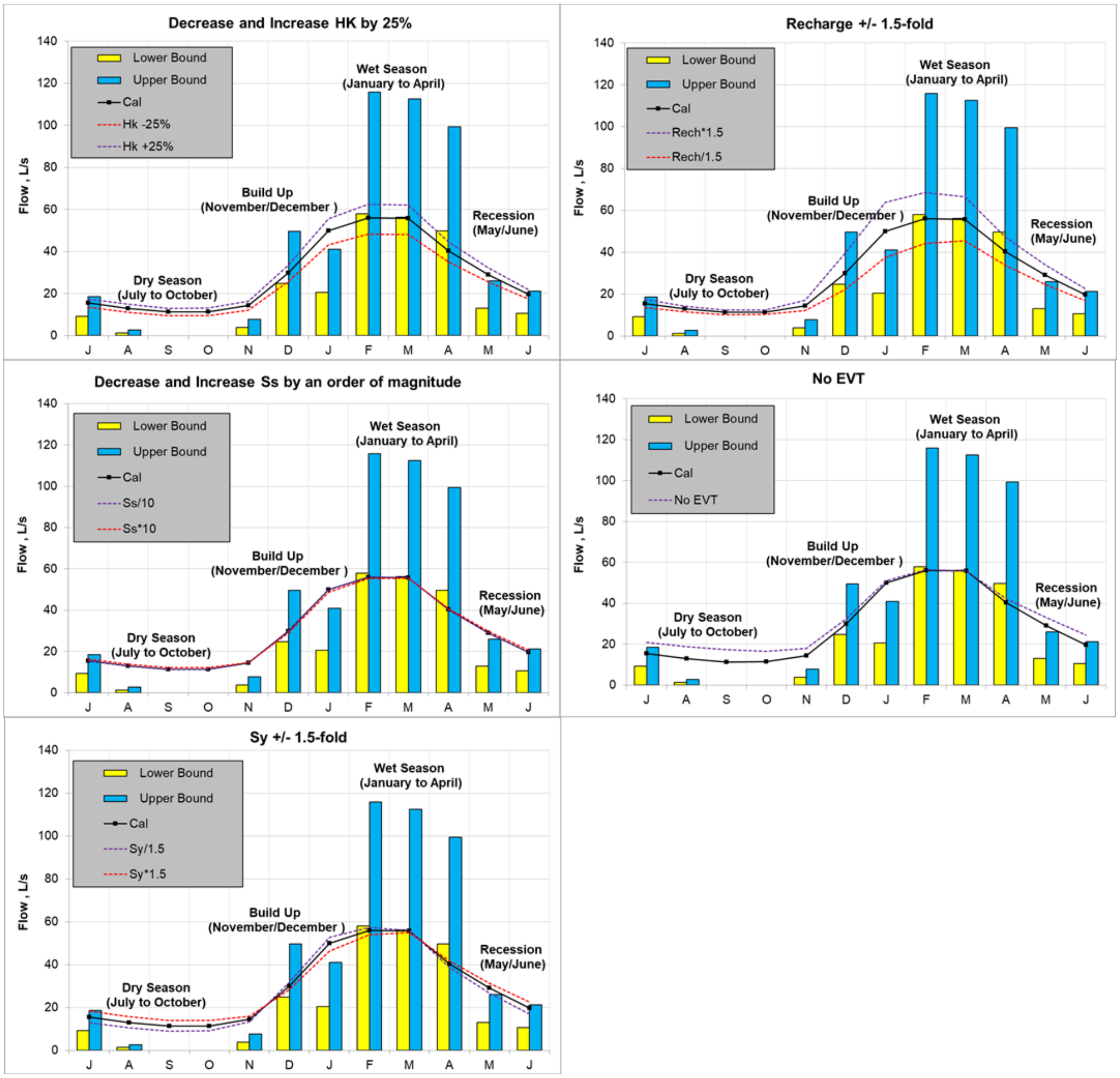

Figure 4-26. Simulated versus Estimated Groundwater Inflows to the EBFR D/S for Sensitivity Runs Compared to Calibrated Model

Table 4-9. Simulated Total Sulphate Load to EBFR (2017/2018) for Sensitivity Analyses

Run ID	Description	SO4 Load	Difference vs Base Case	
		(t/year)	(t/year)	(%)
SO4_R46	*Base Case*	*1458.3*	-	-
Sensitivity to Hydraulic Conductivity (K)				
SO4_R52	Increase K in all units by 25%	1503.6	45.2	3.1%
SO4_R51	Decrease K in all units by 25%	1409.1	-49.3	-3.4%
Sensitivity to Recharge				
SO4_R60	Increase Recharge (x1.5)	2128.6	670.3	46.0%
SO4_R61	Decrease Recharge (/1.5)	979.2	-479.1	-32.9%
Sensitivity to Overburden Specific Yield (Sy)				
SO4_R58	Increase Overburden Specific Yield (x1.5)	1459.2	0.9	0.1%
SO4_R57	Decrease Overburden Specific Yield (/1.5)	1455.4	-2.9	-0.2%
Sensitivity to Specific Storage (Ss)				
SO4_R56	Increase Specific Storage by an order of magnitude	1455.0	-3.3	-0.2%
SO4_R55	Decrease Specific Storage by an order of magnitude	1459.8	1.5	0.1%
Sensitivity to Evapotranspiration				
SO4_R62	Remove Evapotranspiration	1635.3	177.0	12.1%
Sensitivity to Porosity				
SO4_R71	Increase Porosity (x2)	1524.3	66.0	4.5%
SO4_R72	Decrease Porosity (/2)	1441.9	-16.4	-1.1%
Sensitivity to Longitudinal Dispersivity				
SO4_R73	Increase Longitudinal Dispersivity (x2)	1520.0	61.7	4.2%
SO4_R74	Decrease Longitudinal Dispersivity (/2)	1425.8	-32.5	-2.2%

Table 4-10. Simulated Total Copper Load to EBFR (2017/2018) for Sensitivity Analyses

Run ID	Description	Cu Load (t/year)	Difference vs Base Case (t/year)	Difference vs Base Case (%)
Cu_R44	Base Case	3.09	-	-
Sensitivity to Hydraulic Conductivity (K)				
Cu_R52	Increase K in all units by 25%	3.15	0.07	2.2%
Cu_R51	Decrease K in all units by 25%	2.97	-0.12	-3.7%
Sensitivity to Recharge				
Cu_R60	Increase Recharge (x1.5)	4.08	0.99	32.1%
Cu_R61	Decrease Recharge (/1.5)	2.34	-0.75	-24.2%
Sensitivity to Overburden Specific Yield (Sy)				
Cu_R58	Increase Overburden Specific Yield (x1.5)	3.07	-0.02	-0.6%
Cu_R57	Decrease Overburden Specific Yield (/1.5)	3.13	0.05	1.6%
Sensitivity to Specific Storage (Ss)				
Cu_R56	Increase Specific Storage by an order of magnitude	3.07	-0.02	-0.5%
Cu_R55	Decrease Specific Storage by an order of magnitude	3.09	0.00	0.0%
Sensitivity to Evapotranspiration				
Cu_R62	Remove Evapotranspiration	3.39	0.31	9.9%
Sensitivity to Retardation Factor (Rf)				
Cu_R79	Increase Rf of Overburden and Bedrock by 20%	3.26	0.17	5.5%
Cu_R80	Decrease Rf of Overburden and Bedrock by 20%	2.89	-0.20	-6.3%
Cu_R81	Increase Rf of Overburden and Bedrock by 50%	3.47	0.39	12.5%
Cu_R82	Decrease Rf of Overburden and Bedrock by 50%	2.56	-0.52	-17.0%
Sensitivity to Porosity				
Cu_R77	Increase Porosity (x2)	3.20	0.11	3.7%
Cu_R78	Decrease Porosity (/2)	3.03	-0.06	-1.8%
Sensitivity to Longitudinal Dispersivity				
Cu_R75	Increase Longitudinal Dispersivity (x2)	3.06	-0.03	-1.0%
Cu_R76	Decrease Longitudinal Dispersivity (/2)	3.11	0.03	0.8%

4.8 PREDICTIVE MODELLING – CONSTRUCTION PHASE

4.8.1 Overview

The calibrated groundwater flow and transport model was used to predict the groundwater flows and transport of sulphate and copper during the construction phase of the rehabilitation project for the Rum Jungle project. The construction phase is projected to take ten years and include the following main activities that are relevant to groundwater:

- Drawdown of the pit water level in the Intermediate Pit (Year 1 to 5).
- Removal of waste rock from Main Dump, Intermediate Dump and Dyson's backfilled Pit (Year 1 to 5).
- Backfilling of the Main Pit with waste rock (Year 1 to 4).
- Construction of a new waste storage facility (Year 6 to 10).
- Operation of several seepage recovery bores to clean up residual groundwater contamination (Year 1 to 10).

The following sections describe the numerical representation of this construction phase and the predicted groundwater flows and contaminant loads in the aquifer and to the receiving surface water (open pits and EBFR).

4.8.2 Model Setup for Construction Phase

The numerical model for current conditions was modified to represent the future construction phase conditions. Changes to the current model included the following modifications:

- Model Inputs for recharge (the MODFLOW RCH Package) was extended into the future for the simulation of the construction phase and post-rehabilitation conditions. To this end, the same long-term average recharge conditions used in the 2016 model were also adopted in this model.
- The Multi-Node Well (MNW2) Package for MODFLOW was added to simulate pumping from 13 SIS bores located east and west of the Main WRD and north of the Intermediate WRD (see
- Figure 4-27. Location Map for Groundwater Recovery Bores and New WSF Footprint
-). These SIS bores are intended to reduce loads to the EBFR during the construction phase of rehabilitation and reduce the extent of impacted groundwater (plumes) that may discharge to the EBFR post-rehabilitation.
- The Multi-Node Well (MNW2) Package was also used to simulate pumping from four recovery (pumping) bores located in the heap leach area and the former ore stock pile area (see
- Figure 4-27. Location Map for Groundwater Recovery Bores and New WSF Footprint

-). These four pumping bores are intended to improve groundwater quality locally in these areas. The SIS bores and pumping bores combined are referred to as “recovery bores”.
- All recovery bores are assigned a depth of 30 m bgs and a maximum drawdown of 15 m below average head conditions. All bores are assigned to start in the Wet season of Year 1 and stop at the end of Year 10 Wet Season.
- From Year 1 to Year 4 (during backfilling of the Main Pit), the time variant Constant Head boundaries (CHD) assigned to model cells immediately surrounding the flooded Main Pit (in Layers 3 to 6) were assigned a fixed pit water level (59 m AHD) in the Main Pit. The CHD boundaries assigned to model cells immediately surrounding the flooded Intermediate Pit (in Layers 2 to 6) were assigned a fixed pit water level (49 m AHD) approximately 8 m below the invert elevation of the outlet to provide adequate live storage to prevent spillage from the Intermediate Pit during backfilling. Note that surface flow within the flooded pits themselves is not simulated by the groundwater model so cells representing the flooded portion of the pits were set to be inactive.
- The model was numerically split into two models at the end of Year 4 wet season. This is when the backfill of the Main Pit with waste rock and cover material is assumed to be completed. This split was implemented to allow the simulation of an open pit for Years 1 to 4 and to explicitly represent the backfill materials in the model by activating the model cells in layers 1 to 5 within the open Main Pit for Years 5 to 10.
- From Year 5 to Year 10 (backfilled Main Pit), model layer 1 was assigned a top elevation of 57 m AHD, which allowed the simulation of a shallow lake (above the top of layer 1) with a minimum submergence depth of 2 m below the minimum observed pit water level of approximately 59 m AHD. This model layer 1 was assigned a thickness of about 2.5 m and hydraulic conductivity of $1x10^{-5}$ m/s and represents a clean cover of fine sandy material. The backfill waste rock materials are represented in model layers 2 to 5 and are assigned a K value of $1x10^{-6}$ m/s.
- Seepage from these backfill materials is represented with constant concentration boundary conditions which are assigned 2,000 mg/L SO_4 and 0.2 mg/L Cu, based on batch testing results provided in RGC and DJEE (2019). This concentration is intended to approximate the release of stored SO_4 and Cu in lime-amended backfill materials. This concentration was assumed to be constant for the construction phase and the 30-year post-rehabilitation simulation period, as scoping calculations suggest it will take 20 to 30 years for the pore volume of the Main Pit to be flushed. Unlike backfill material in the new WSF, SO_4 and Cu concentrations will eventually decrease as the concentrations are not sustained by future oxidation of (submerged) sulphide materials.

- The zonation of the recharge (RCH) MODFLOW package and the constant concentration boundary conditions for MT3DMS were modified in tandem to accommodate the progressive reduction in the extents of the WRD footprints and the footprint of Dyson's (backfilled) Pit each year as material is hauled to either the WSF or the Main Pit. This was done by assuming any changes in the residual footprint areas at the end of a Dry Season are represented in the subsequent wet Season, based on footprint areas provided by SLR (see Figure 4-28).
- Seepage to groundwater from the new WSF (see Figure 4-27 for footprint locations) is assumed to start in Year 6 at a rate of 21 mm/yr through the horizontal top and 17 mm/yr for the side-slopes, as per infiltration rates for the "Cover #3 Low NP" cover alternative estimated by O'Kane Consultants (2013). Seepage from the new WSF to groundwater is assigned 10,000 mg/L SO_4 and 0.2 mg/L Cu as per RGC and DJEE (2019).
- Simulated heads and concentrations from the current model for the end of 2018 dry season were used as initial conditions for the construction phase models.

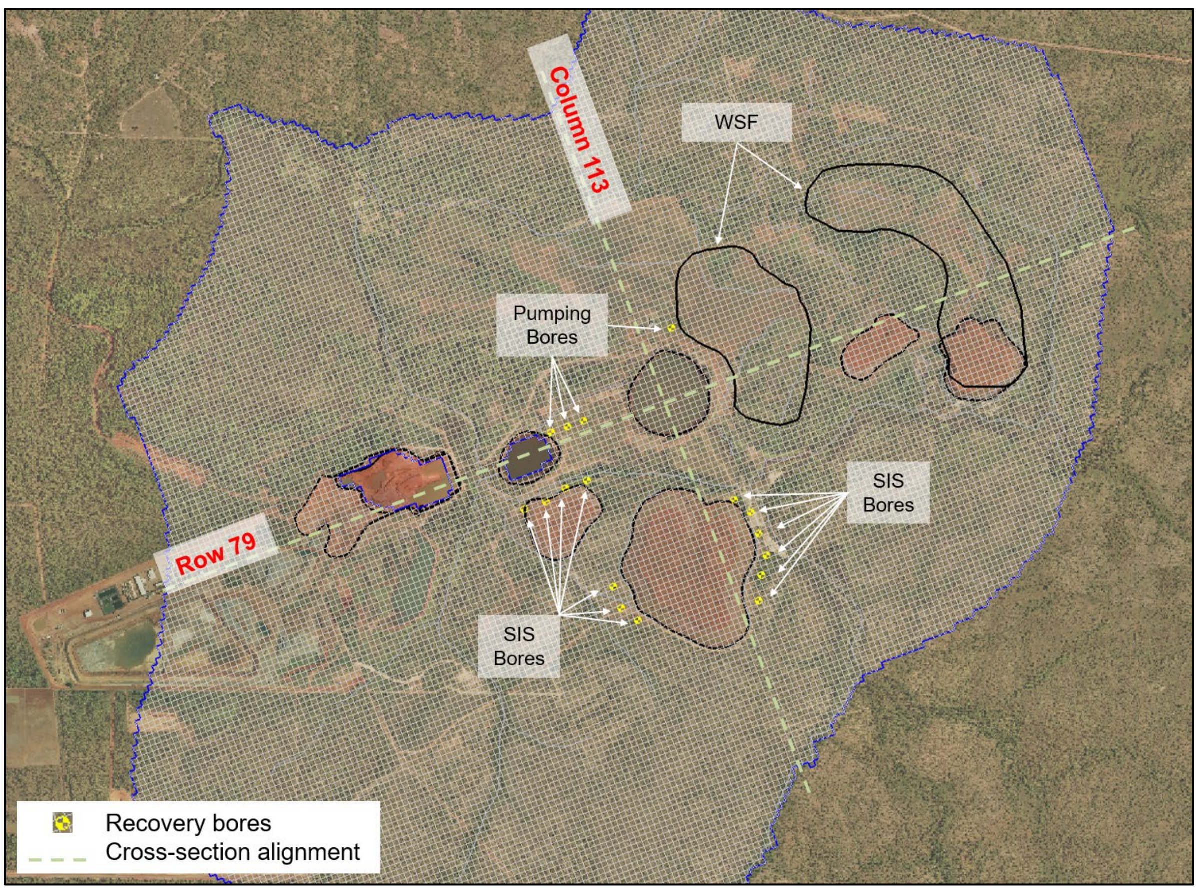

Figure 4-27. Location Map for Groundwater Recovery Bores and New WSF Footprint

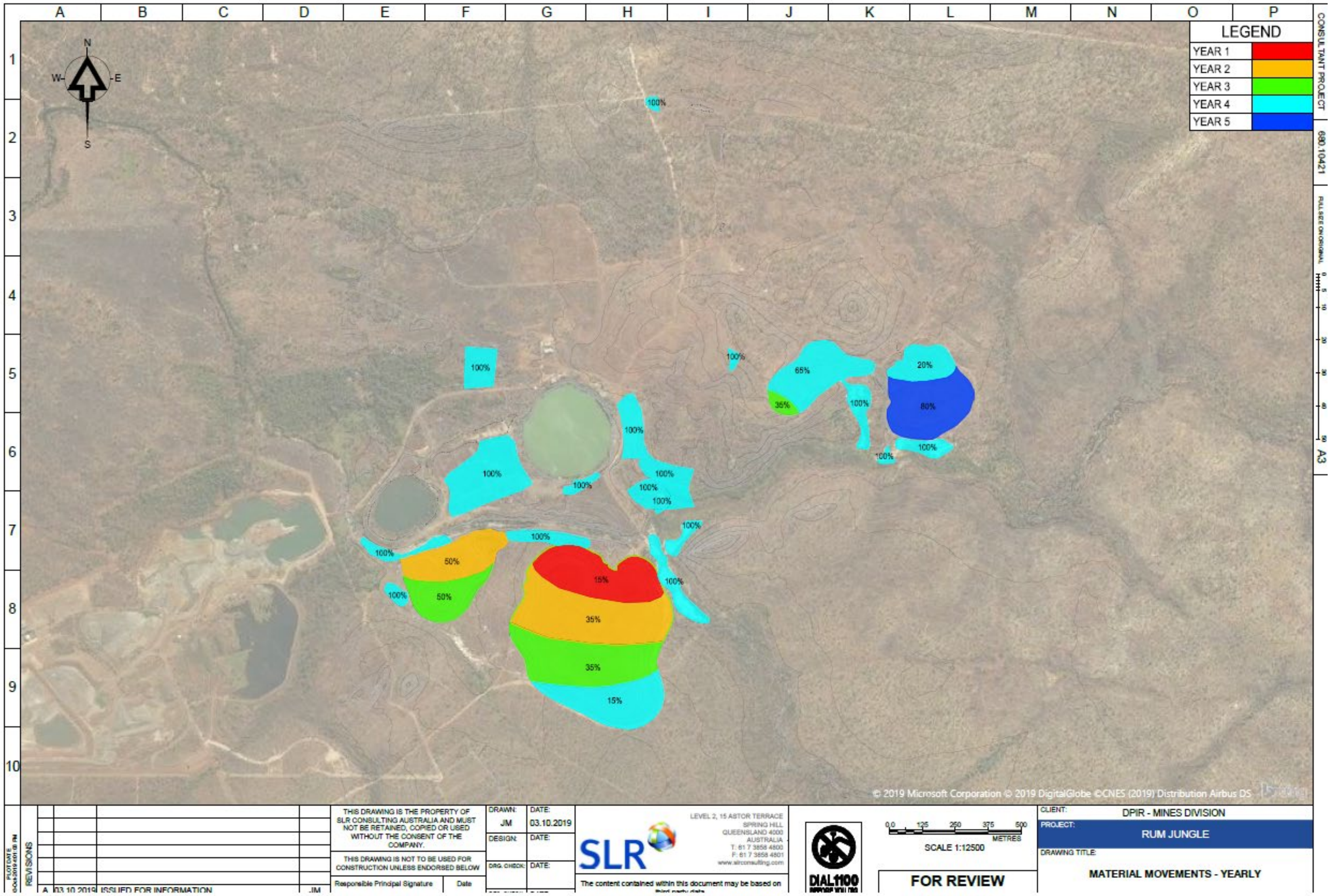

Figure 4-28. Residual Footprints Provided by SLR

4.8.3 Predicted Heads and Water Balance for Construction Phase

Figure 4-29 shows the predicted hydraulic heads in model layer 3 (shallow bedrock) for the dry season and wet season for Year 4 and 10, respectively. Figure 4-30 shows the predicted extent of drawdown for Year 4 and Year 10 dry seasons, respectively.

Figure 4-31 shows the predicted inflows and outflows for site features during the construction period (Year 1 to Year 10) compared to the calibration model period (2010-2018). In this figure, positive flow rates represent groundwater discharge (outflows) to the surface water system, while negative flow rates represent inflows from open pits to the groundwater system.

The model predicts the following significant changes to groundwater heads and flows for the construction phase vis-à-vis current conditions:

- Pumping from recovery bores is predicted to result in significant capture zones along their alignments in both wet and dry seasons.
- The hydraulic gradient between the Main Pit and the Intermediate Pit is predicted to increase by an order of magnitude from ~0.002 m/m for current conditions to ~0.02 m/m as a result of controlling the water level in the Main Pit at 59 m AHD while maintaining the pit water level in the Intermediate Pit at 49 m AHD (i.e. 10 m lower). .
- During backfilling of the Main Pit (Year 1 to Year 4), the predicted drawdown ranges from 0.5 m at the Main Pit to 9 m at the Intermediate Pit. The predicted drawdown extends north to the OTD area with an average magnitude of 2.5 m.
- At end of construction (Year 10) the predicted drawdown is largely limited to the capture zones developed as a result of pumping from the recovery bores.
- From Year 1 to Year 4, inflows to the Intermediate Pit are predicted to increase significantly (up to 3.5-fold) to range from 18 to 31 L/s.
- The recovery bores in the Copper Extraction Pad area are predicted to extract a combined total flow of 9 L/s during the dry season and 19 L/s during the wet season. These flows are the maximum rates able to be sustained by pumping based on the calibrated hydraulic properties for bedrock, i.e. Rum Jungle Complex near the Main WRD and Whites Formation near the Intermediate WRD. The predicted total pumping rates for the 13 SIS bores and the 4 pumping bores range from 7 L/s to 11 L/s and from 5 L/s to 8 L/s, respectively.
- Groundwater discharge to the EBFR Reach G is predicted to notably decrease (within Year 1 to Year 4) to a maximum of 0.5 L/s in wet seasons compared to about 7 L/s within Year 5 to Year 10, once the Main Pit is backfilled and dewatering operations in the Intermediate Pit have ceased.

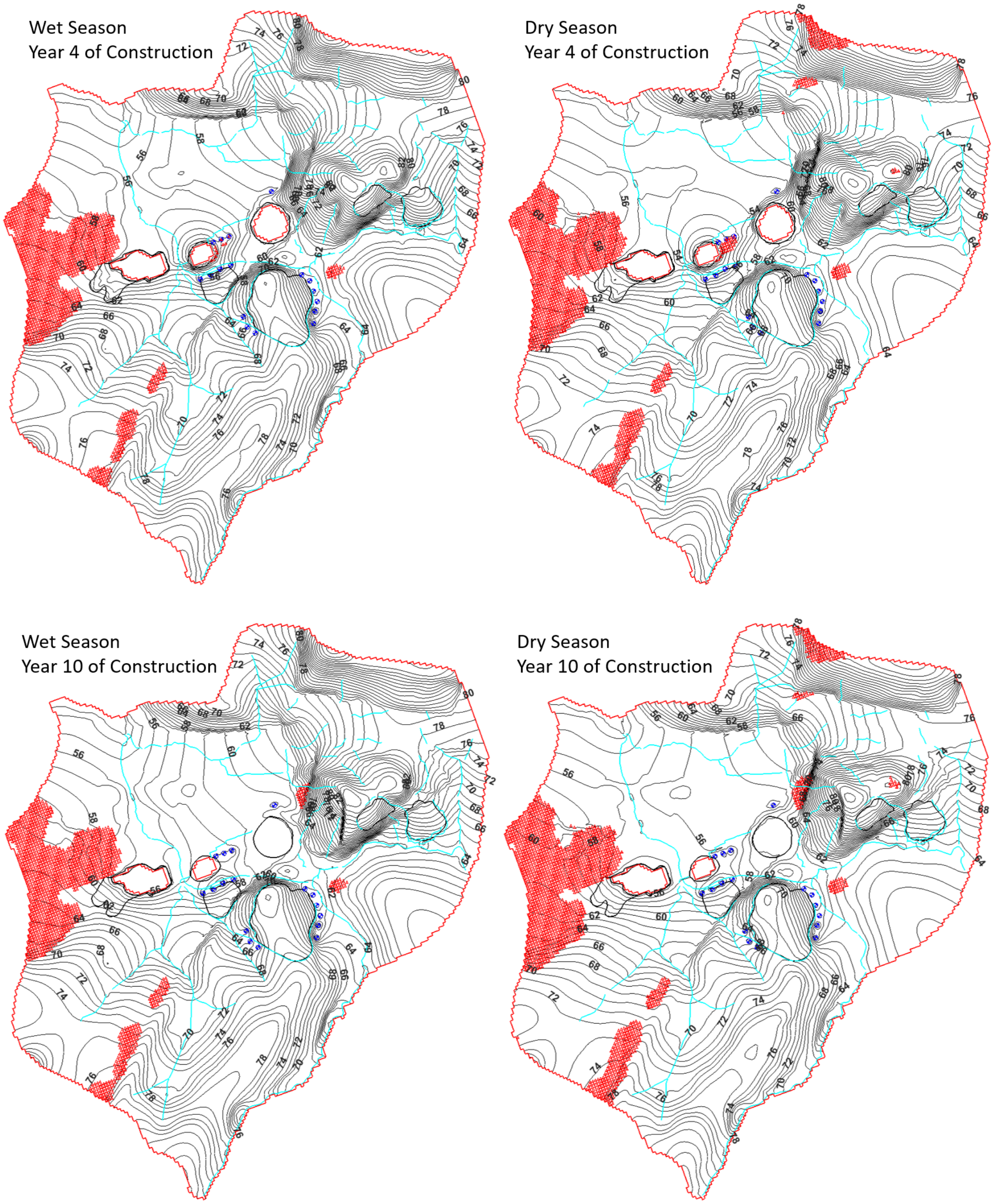

Figure 4-29. Predicted heads for Year 4 of Construction and Year 10 of Construction

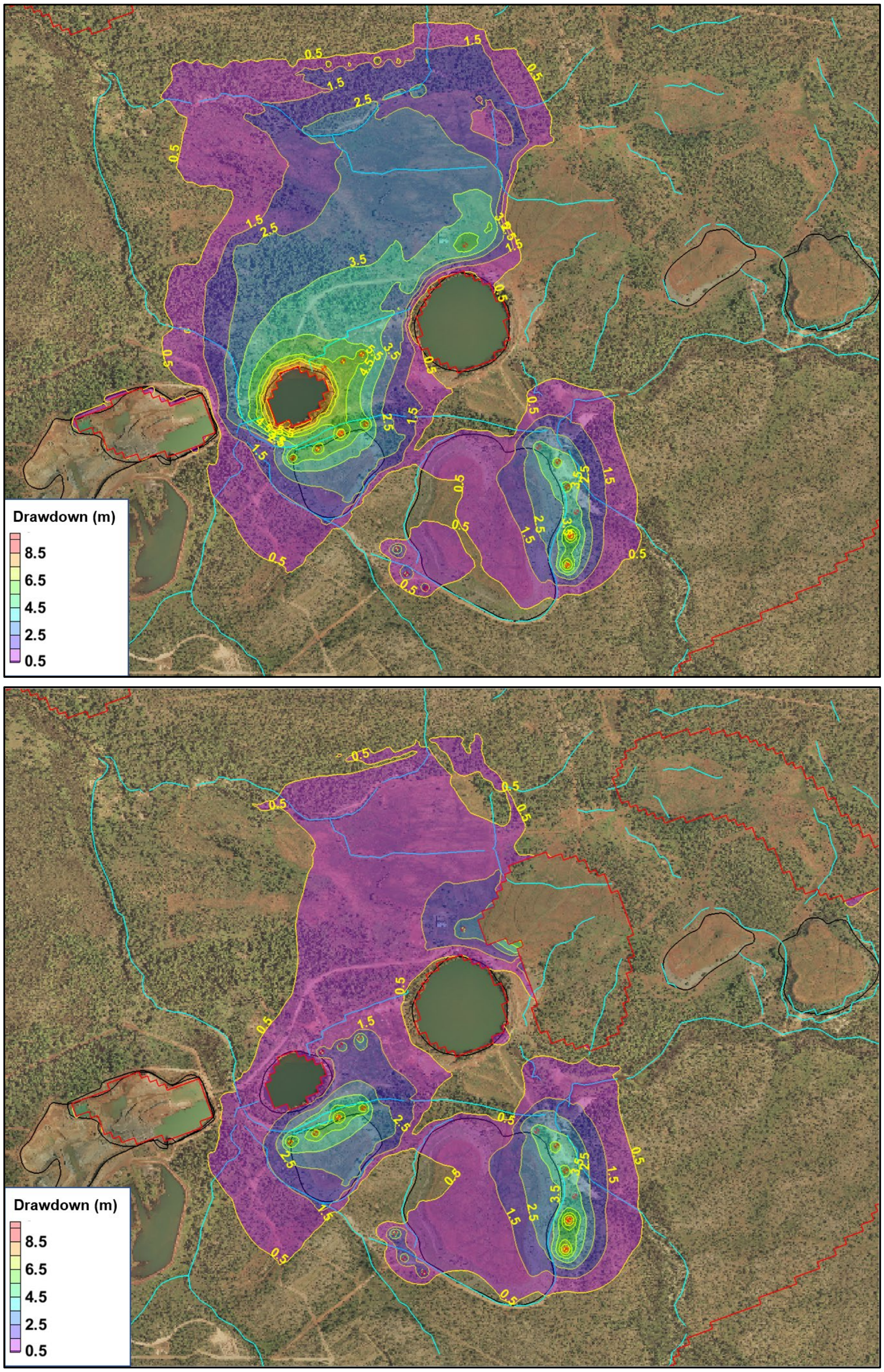

Figure 4-30. Predicted Drawdown Year 4 Dry Season of Construction (top) and Year 10 Dry Season of Construction (bottom)

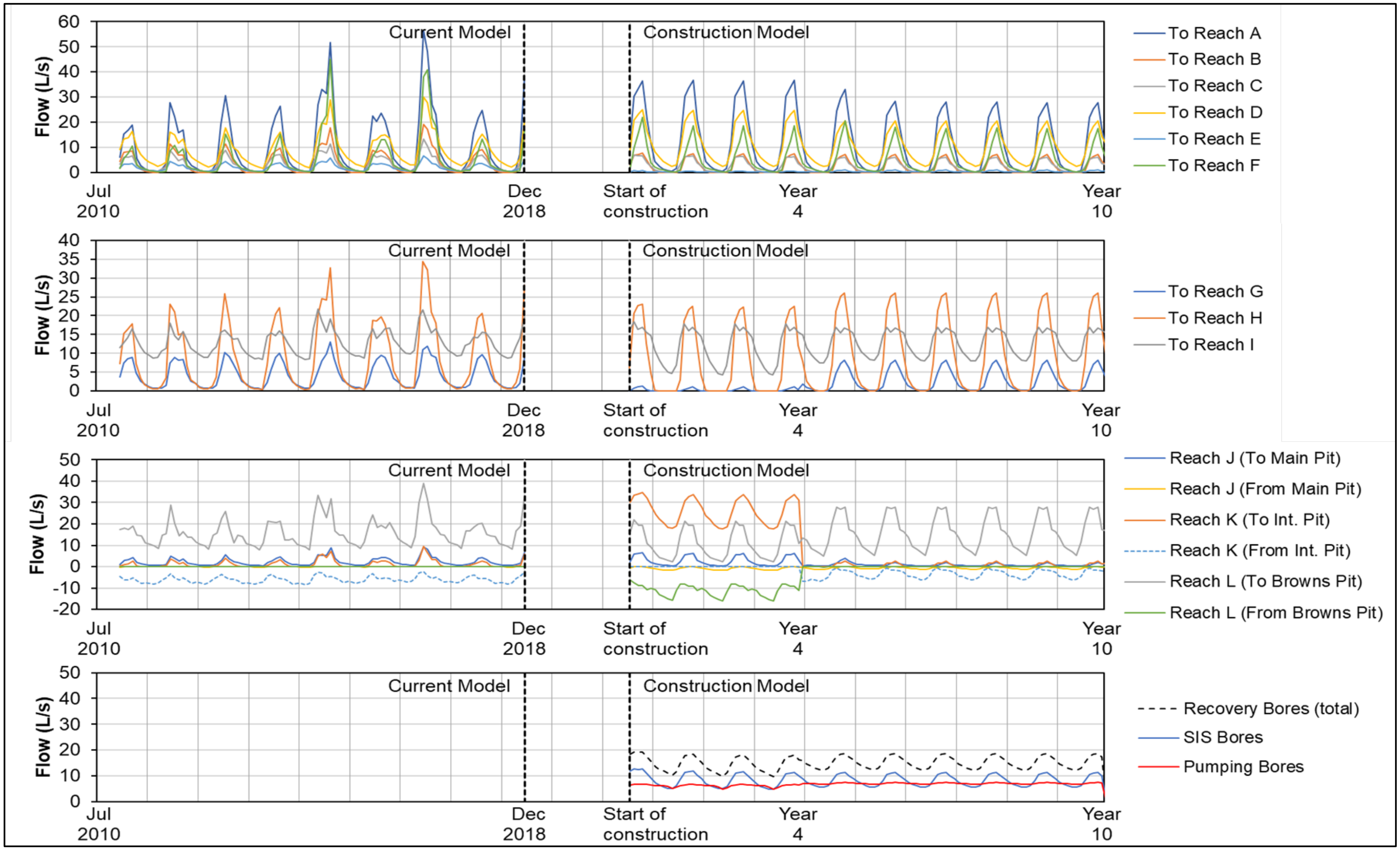

Figure 4-31. Predicted Inflows and Outflows for Site Features during Calibration Period (2010-2018) and Construction Period (Year 1 to Year 10)

4.8.4 Predicted Plumes and Loads for Construction Phase

Simulated SO_4 and Cu plumes for each year of the construction phase (Years 1 to 10) are shown in Figure 4-32 and Figure 4-33. Cross-sections showing predicted SO_4 and Cu concentrations in groundwater are provided in Figure 4-34, Figure 4-35, Figure 4-36, and Figure 4-37. See Figure 4-27 for the alignment of these sections. Simulated SO_4 and Cu concentrations in 1985 and for current conditions are also shown for comparison in these cross-sections. Monthly simulated and predicted SO_4 and Cu loads for current conditions, the construction period, and 30-years post-rehabilitation are shown in Figure 4-38 and Figure 4-39**.** Predicted SO_4 and Cu loads for Years 1 to 10 are summarized in Table 4-11 and Table 4-12**.**

Key observations from these figures and tables are summarized below:

- The extent of the simulated SO_4 and Cu plumes in groundwater is reduced to a greater extent after the currently active AMD sources on site (the WRDs and shallow backfill materials in Dyson's Pit) have been removed completely. This is particularly evident for SO_4 because it is assumed to be transported conservatively in groundwater. The rate of reduction of Cu loads in the system is much slower than for SO_4, since it is dependent on the rate of desorption/dissolution of Cu from the rock matrix (see Section 3.12 for details).
- The recovery bores are predicted to recover more than 1000 t/year SO_4 in Years 1, 2, and 3. Annual loads are then predicted to decrease as the extent of the SO_4 plumes is reduced by pumping, particularly after the Main and Intermediate WRDs have been re-located. The recovery bores in the CEPA recover 6 to 8 t/year Cu in Years 1 to 8 and slightly less in Years 9 and 10. The average annual Cu load recovered during the construction period is 6.6 t/year. This load is approximately twice the observed Cu load in the EBFR for current conditions, as the Cu load recovered in the Copper Extraction Pad area is predicted to be substantial.
- A substantial reduction during the construction period in the extent of the impacted groundwater is predicted by the model due to operating the SIS bores downgradient of the WRDs and recovery bores in the Copper Extraction Pad area and former ore stockpile area.
- Within Year 1 to Year 4, while the Intermediate Pit is being de-watered to maintain a minimum operating level of 49 m AHD, the load inflow to the Intermediate Pit is predicted to substantially increase to approximately three-fold for both SO_4 and Cu, compared to current conditions.
- Groundwater quality in Dyson's Area is not predicted to start to improve until waste rock from Dyson's WRD and shallow backfill materials from Dyson's pit are re-located and groundwater in this area begins to be flushed by rainfall without an AMD source present.
- In Year 5, a SO_4 plume is predicted to start emanating from the backfilled Main Pit and SO_4 plumes emanating from the WSF footprints are predicted to start developing in Year 6. This assumes seepage starts to occur almost immediately, as per O'Kane Consultants Inc. (2016).

The predicted SO_4 plume from the Northern WSF footprint migrates north and then west towards Old Tailings Creek. The SO_4 plume from the Western WSF is simulated to move west until it reaches the Main Pit. A Cu plume is also predicted to develop from the Main Pit backfill but is characterized by concentrations that are too small to differentiate from residual impacted groundwater in the Copper Extraction Pad area. A low-strength Cu plume from the WSF is restricted in extent and difficult to discern at the regional scale of the groundwater model.

- In Year 10, a substantial reduction in the extent of the impacted groundwater is predicted. The groundwater model predicts that SO_4 and Cu loads to the EBFR will be reduced to 66 t/year and 0.24 t/year, respectively. These loads are both an order-of-magnitude lower than the simulated SO_4 and Cu loads for current conditions.

Table 4-11. Predicted Sulphate Loads During Construction Period

Reach	Description	Current Conditions	Year 1	Year 2	Year 3	Year 4	Year 5	Year 6	Year 7	Year 8	Year 9	Year 10	Average (Years 5 to 10)	
		t/year	t/year	t/year	t/year	t/year	t/year	t/year	t/year	t/year	t/year	t/year	t/year	%
A	Dyson's Area	224	118	146	147	150	124	59	37	32	27	25	50	56%
B	Main WRD (east)	201	21	4	1	1	0	0	0	0	0	0	0	0%
C	Main WRD (west) and Int. WRD	154	22	13	9	6	3	3	2	2	1	1	2	2%
D	Middlebrook Creek	0	0	0	0	0	0	0	0	0	0	0	0	0%
E	EFDC near Main and Int. WRDs	484	9	10	8	6	5	5	4	4	3	3	4	5%
F	Former stockpile area	24	9	6	5	5	4	7	7	7	7	7	6	7%
G	EBFR downstream of GS8150200	58	2	0	0	0	5	13	13	13	13	13	12	13%
H	EBFR in Old Tailings Dam area	21	5	2	1	1	2	7	8	8	8	8	7	8%
I	EBFR near GS8150327	13	5	2	1	1	2	6	8	9	9	10	7	8%
	Simulated Load to EBFR:	**1,179**	**192**	**183**	**172**	**169**	**146**	**100**	**80**	**75**	**69**	**66**	**89**	**100%**
-	To Main Pit	61	42	47	46	48	37	37	26	25	25	25	29	86%
-	To Int. Pit	64	235	276	225	195	3	4	3	3	3	3	3	9%
-	To Browns Pit	9	0	0	0	0	1	2	2	2	2	2	2	5%
-	To Model Flooding Drains	8	1	1	1	0	0	0	0	0	0	0	0	0%
	Simulated Load to Pits:	**142**	**277**	**324**	**271**	**243**	**40**	**43**	**31**	**30**	**30**	**29**	**34**	**100%**
-	Load to SIS and recovery bores	-	1112	1398	1004	703	446	381	325	295	282	266	332	-

Table 4-12. Predicted Copper Loads During Construction Period

Reach	Description	Current Conditions	Year 1	Year 2	Year 3	Year 4	Year 5	Year 6	Year 7	Year 8	Year 9	Year 10	Average (Years 5 to 10)	
		t/year	t/year	t/year	t/year	t/year	t/year	t/year	t/year	t/year	t/year	t/year	t/year	%
A	Dyson's Area	0.40	0.24	0.29	0.29	0.31	0.28	0.25	0.22	0.21	0.20	0.19	0.23	84%
B	Main WRD (east)	0.36	0.04	0.02	0.01	0.01	0.01	0.01	0.01	0.01	0.01	0.01	0.01	3%
C	Main WRD (west) and Int. WRD	0.30	0.06	0.04	0.04	0.03	0.03	0.03	0.02	0.02	0.02	0.02	0.02	9%
D	Middlebrook Creek	0.00	0.0	0.0	0.0	0.0	0.0	0.0	0.0	0.0	0.0	0.0	0.0	0%
E	EFDC near Main and Int. WRDs	1.26	0.0	0.0	0.0	0.0	0.0	0.0	0.0	0.0	0.0	0.0	0.0	4%
F	Former stockpile area	0.01	0.0	0.0	0.0	0.0	0.0	0.0	0.0	0.0	0.0	0.0	0.0	1%
G	EBFR downstream of GS8150200	0.00	0.0	0.0	0.0	0.0	0.0	0.0	0.0	0.0	0.0	0.0	0.0	0%
H	EBFR in Old Tailings Dam area	0.00	0.0	0.0	0.0	0.0	0.0	0.0	0.0	0.0	0.0	0.0	0.0	0%
I	EBFR near GS8150327	0.00	0.0	0.0	0.0	0.0	0.0	0.0	0.0	0.0	0.0	0.0	0.0	0%
	Simulated Load to EBFR:	**2.33**	**0.35**	**0.36**	**0.35**	**0.36**	**0.33**	**0.30**	**0.26**	**0.25**	**0.24**	**0.23**	**0.27**	**100%**
-	To Main Pit	0.06	0.0	0.0	0.0	0.0	0.0	0.0	0.0	0.0	0.0	0.0	0.00	12%
-	To Int. Pit	0.38	0.7	1.2	1.2	1.3	0.0	0.0	0.0	0.0	0.0	0.0	0.02	86%
-	To Browns Pit	0.00	0.0	0.0	0.0	0.0	0.0	0.0	0.0	0.0	0.0	0.0	0.00	2%
-	To Model Flooding Drains	0.00	0.0	0.0	0.0	0.0	0.0	0.0	0.0	0.0	0.0	0.0	0.00	0%
	Simulated Load to Pits:	**0.45**	**0.7**	**1.3**	**1.3**	**1.3**	**0.0**	**0.0**	**0.0**	**0.0**	**0.0**	**0.0**	**0.02**	**100%**
-	Load to SIS and recovery bores	-	4.8	7.8	6.9	6.5	7.9	7.4	6.7	6.3	5.8	5.4	6.6	-

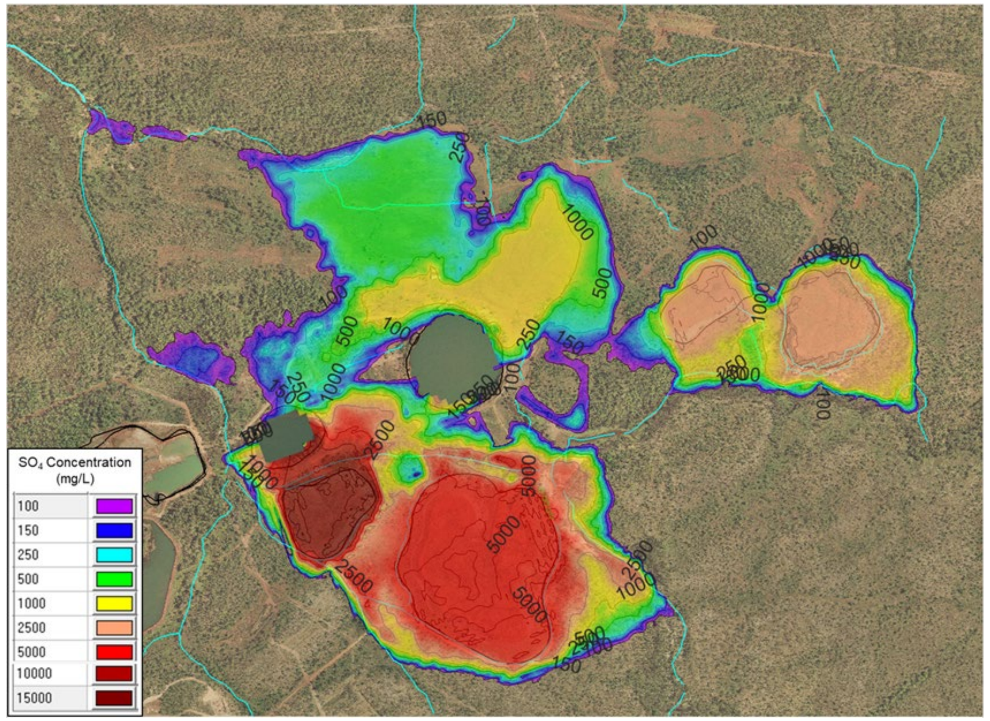

Year 1.

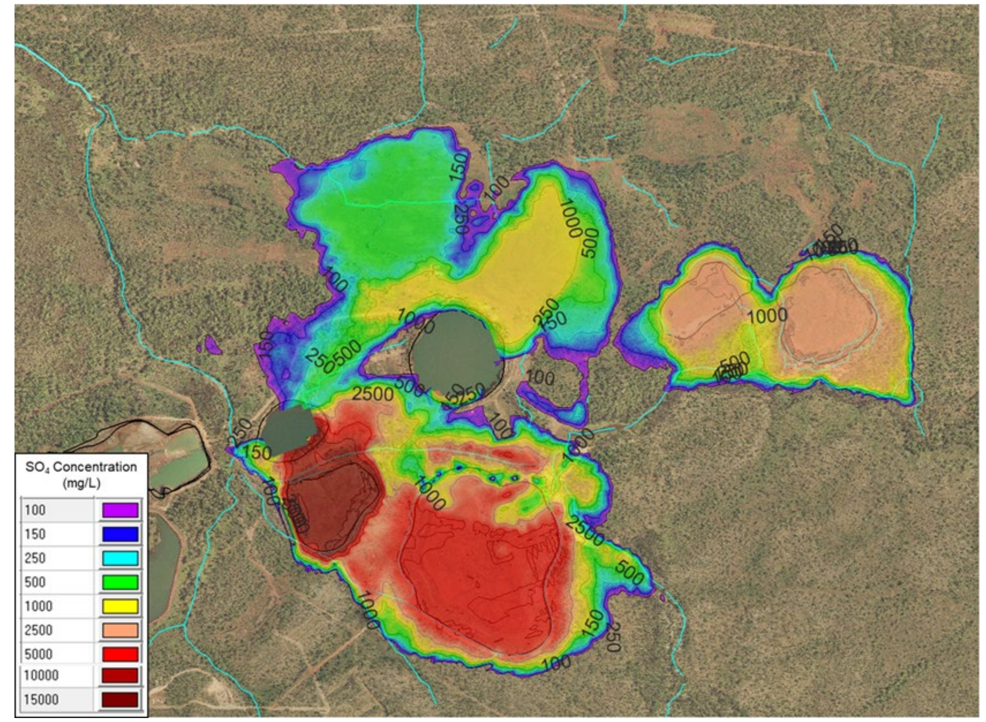

Year 2

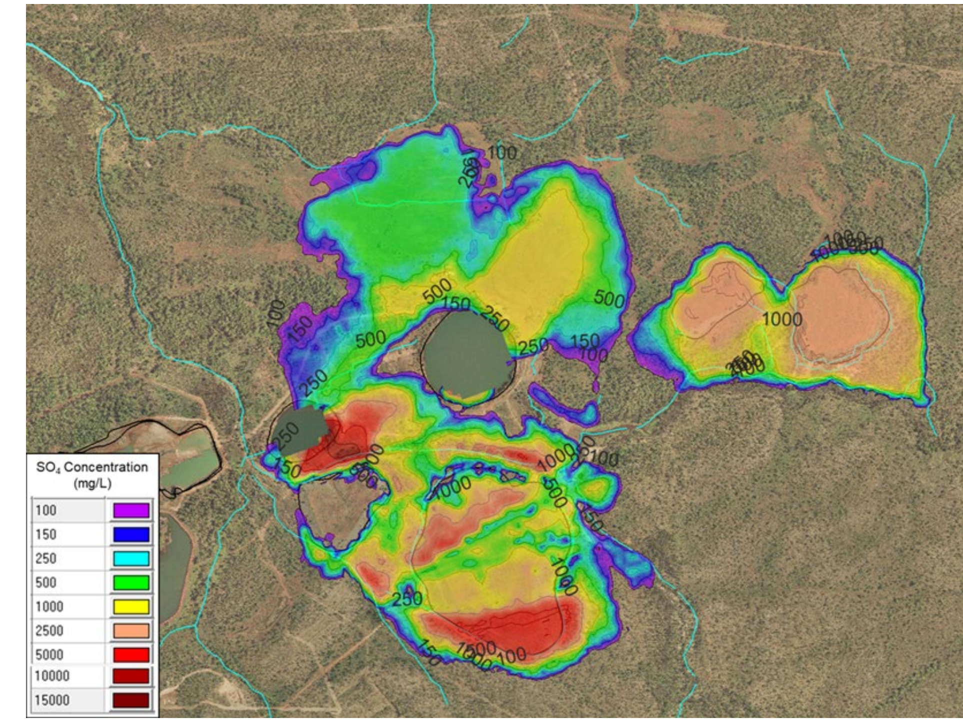

Year 4

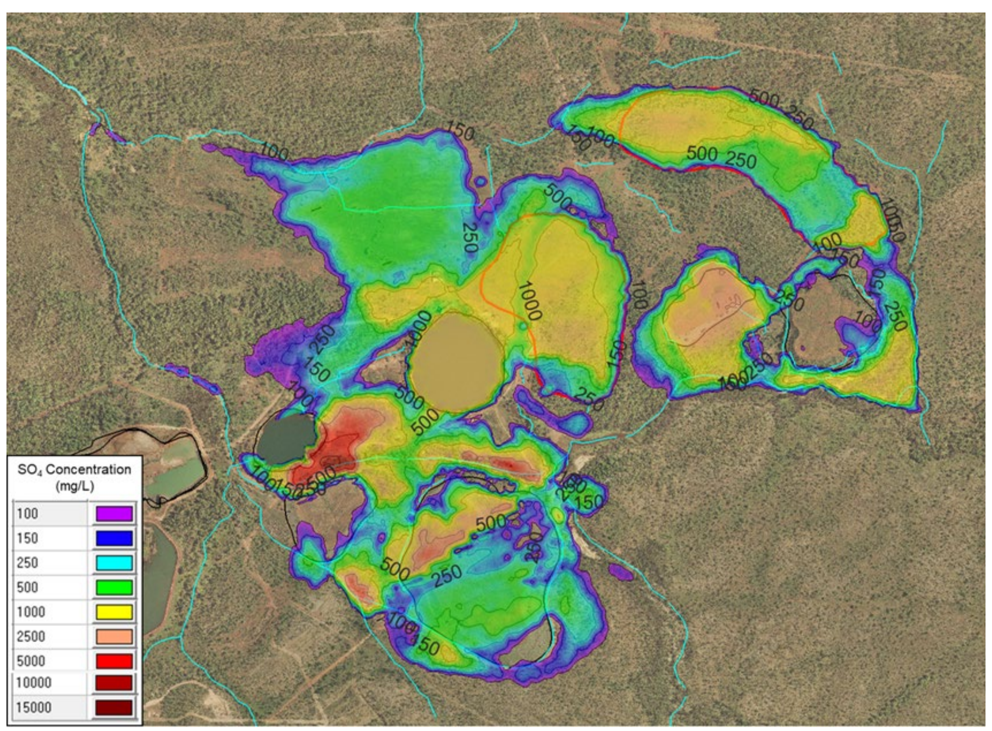

Year 6

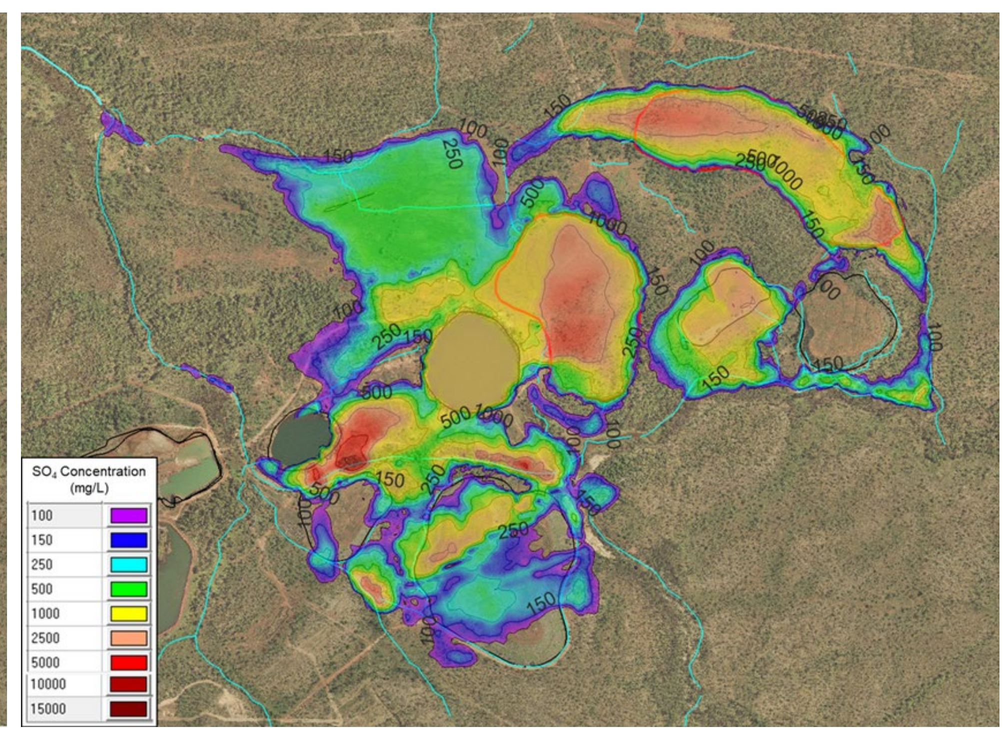

Year 8

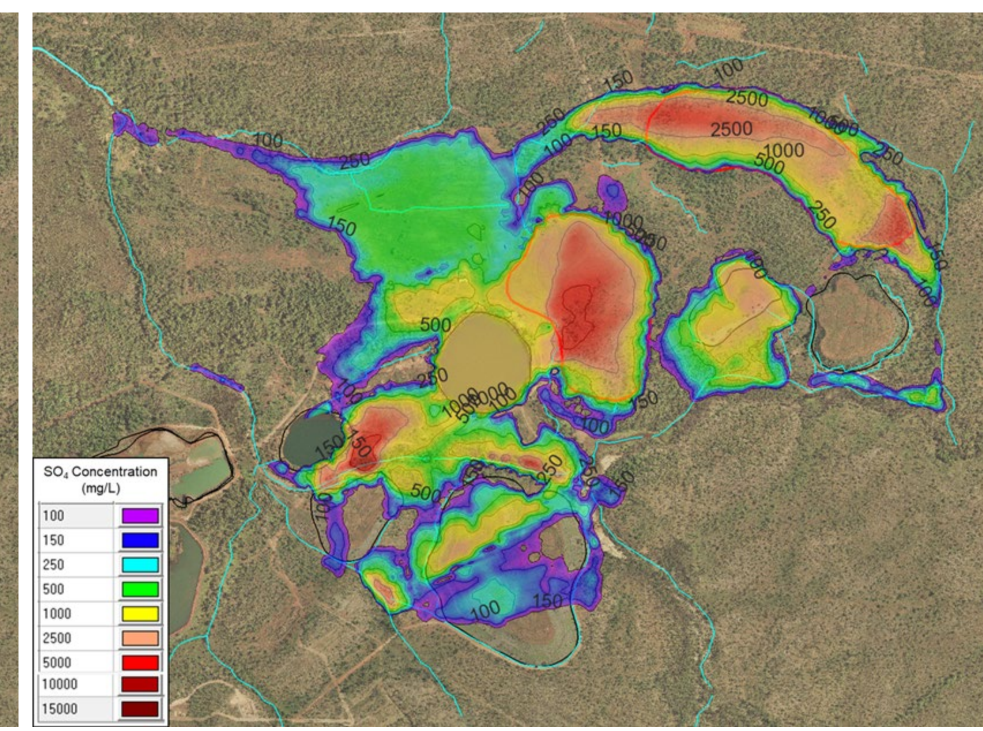

Year 10

Figure 4-32. Predicted Sulphate Plumes, Construction Period

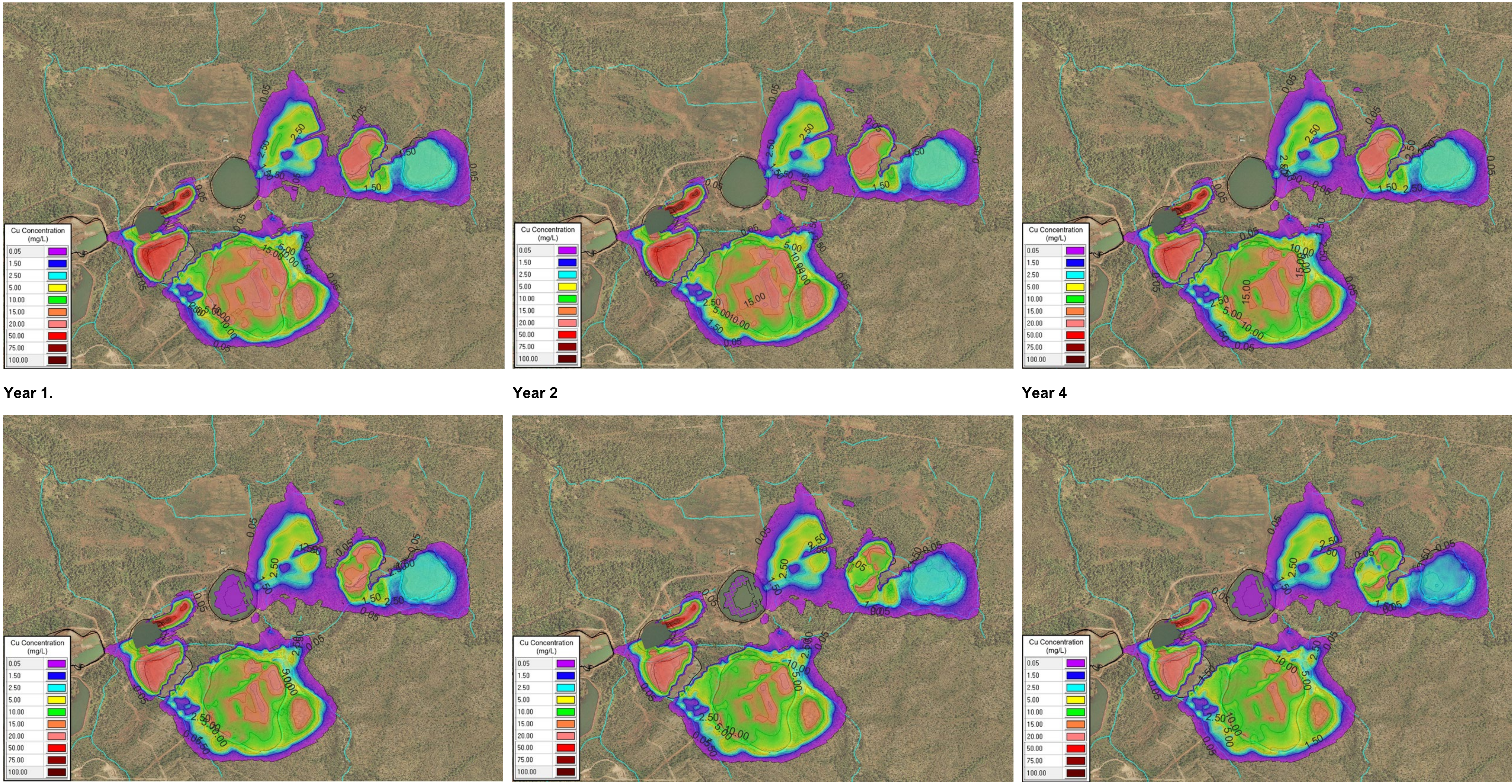

Year 1. **Year 2** **Year 4**

Year 6 **Year 8** **Year 10**

Figure 4-33. Predicted Copper Plumes, Construction Period

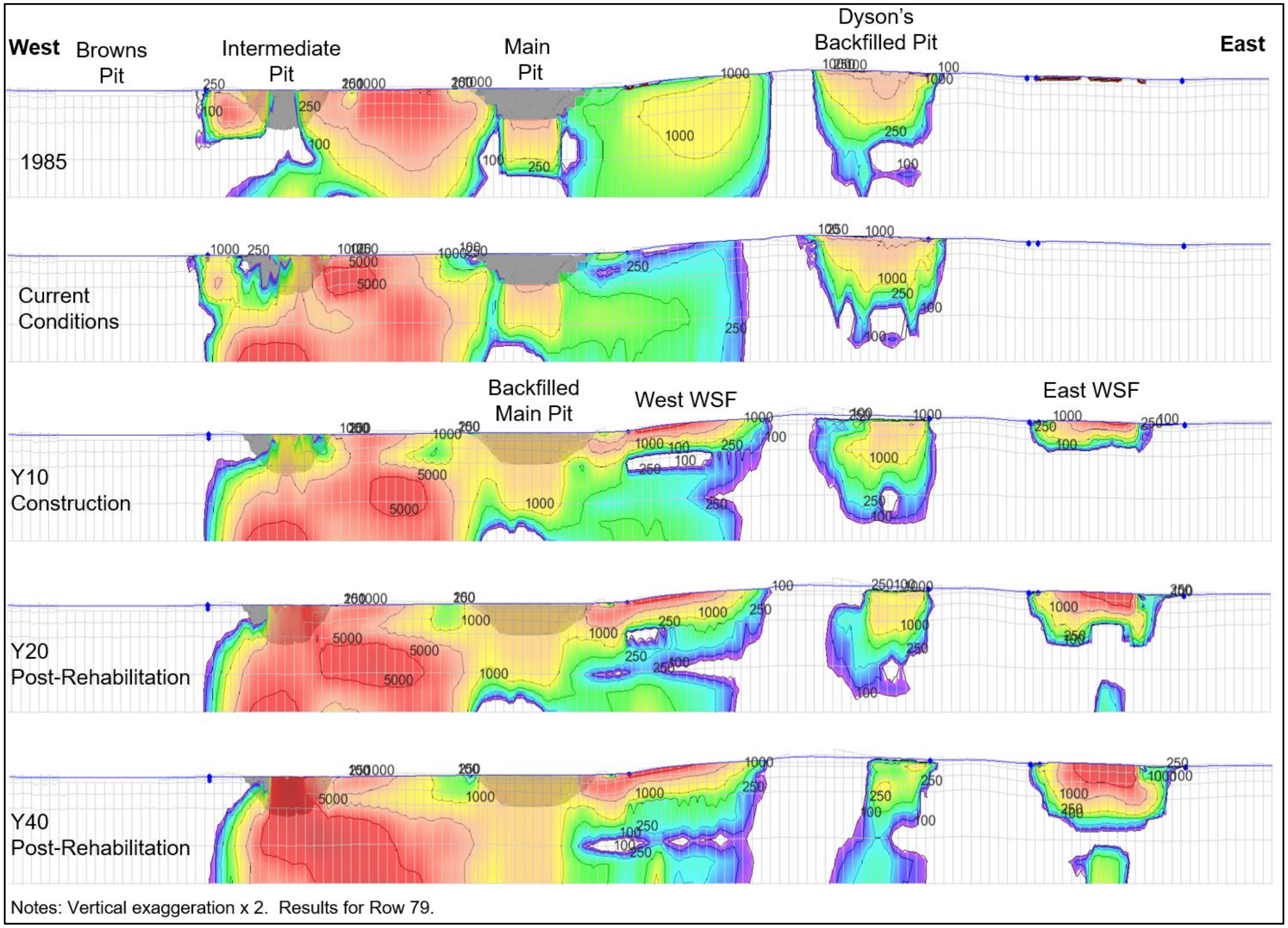

Figure 4-34. Cross-Section (Row 79) with Simulated Sulphate Plume

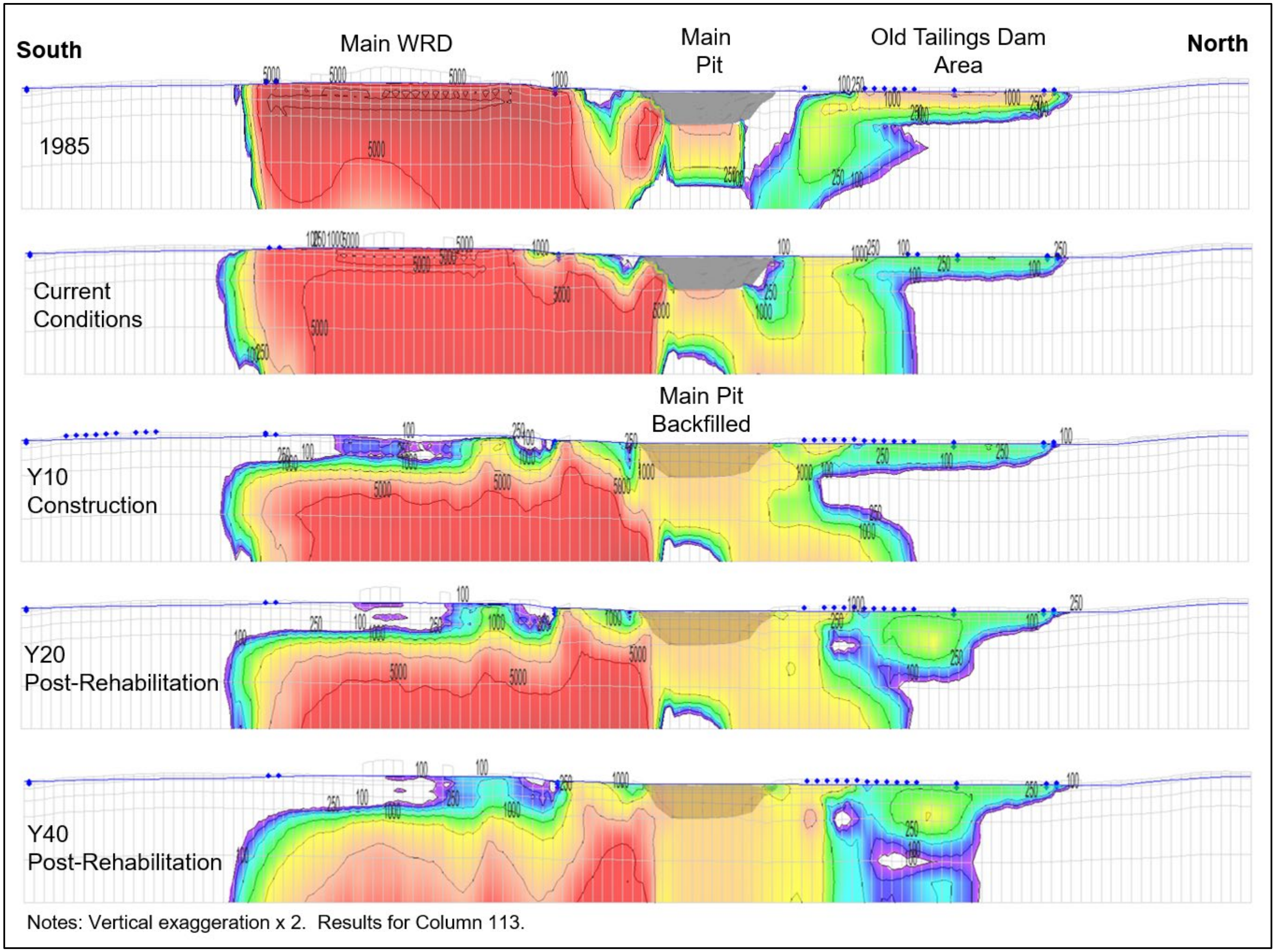

Figure 4-35. Cross-Section (Column 113) with Simulated Sulphate Plume

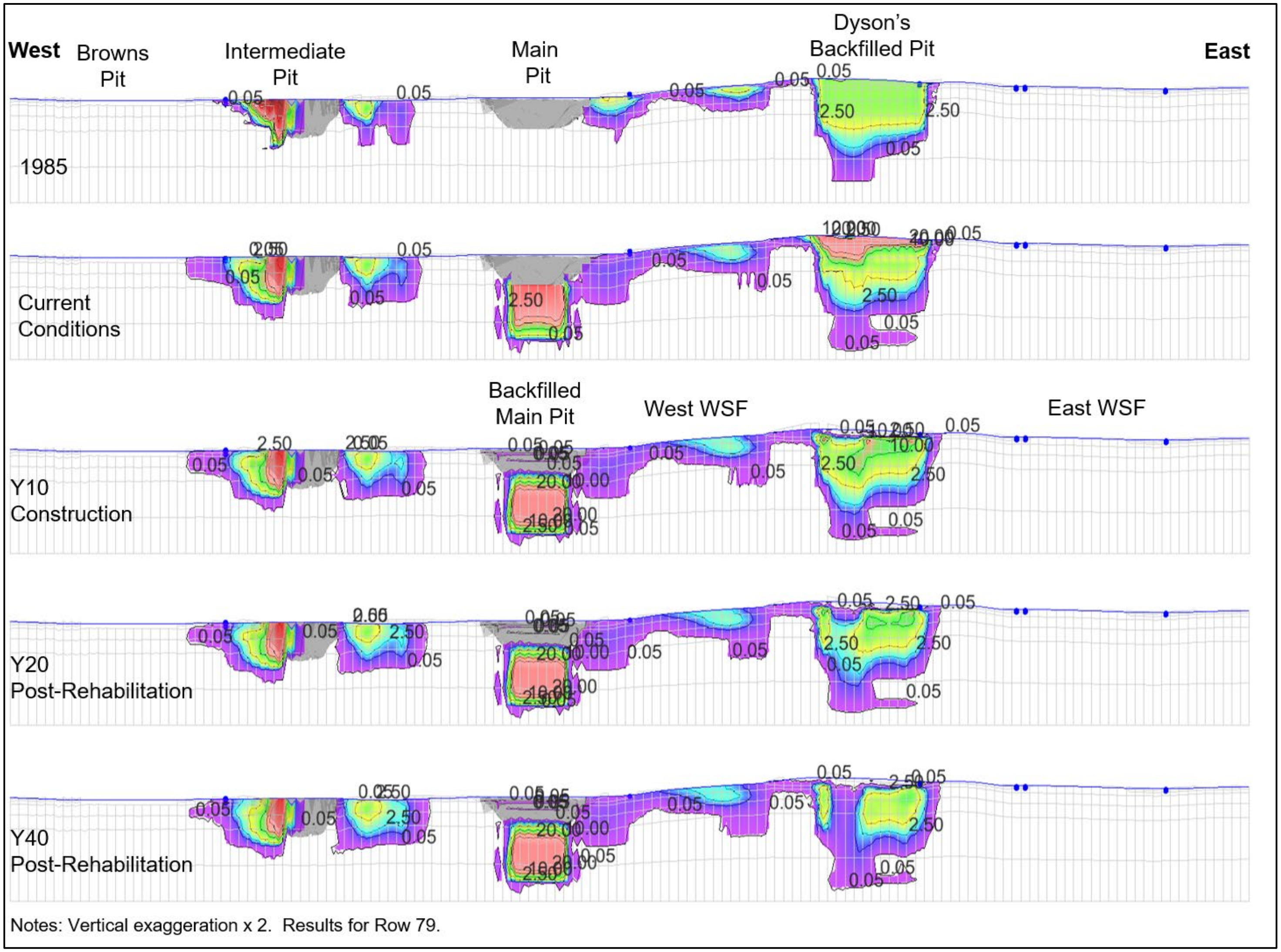

Figure 4-36. Cross-Section (Row 79) with Simulated Copper Plume

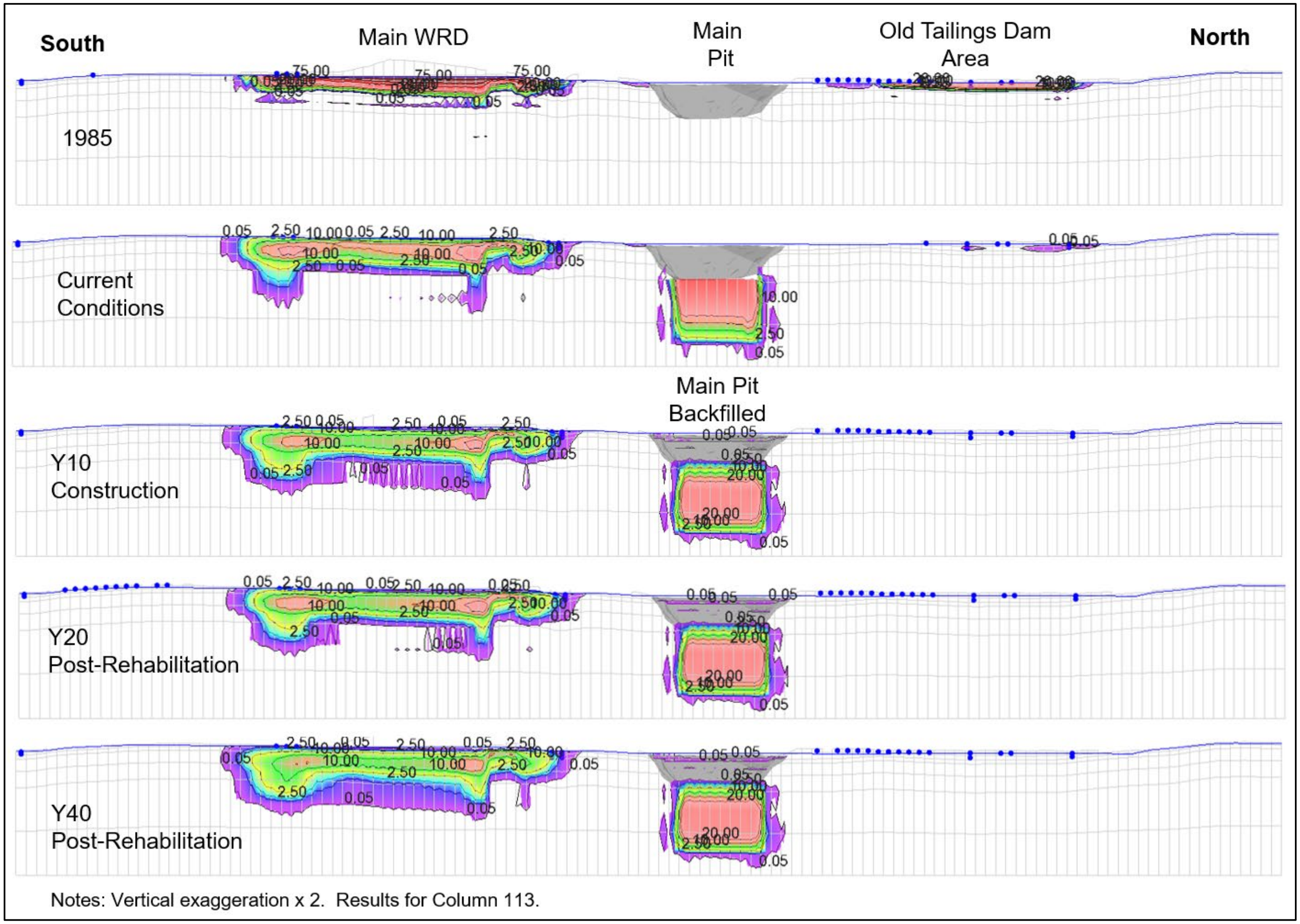

Figure 4-37. Cross-Section (Row 113) with Simulated Copper Plume

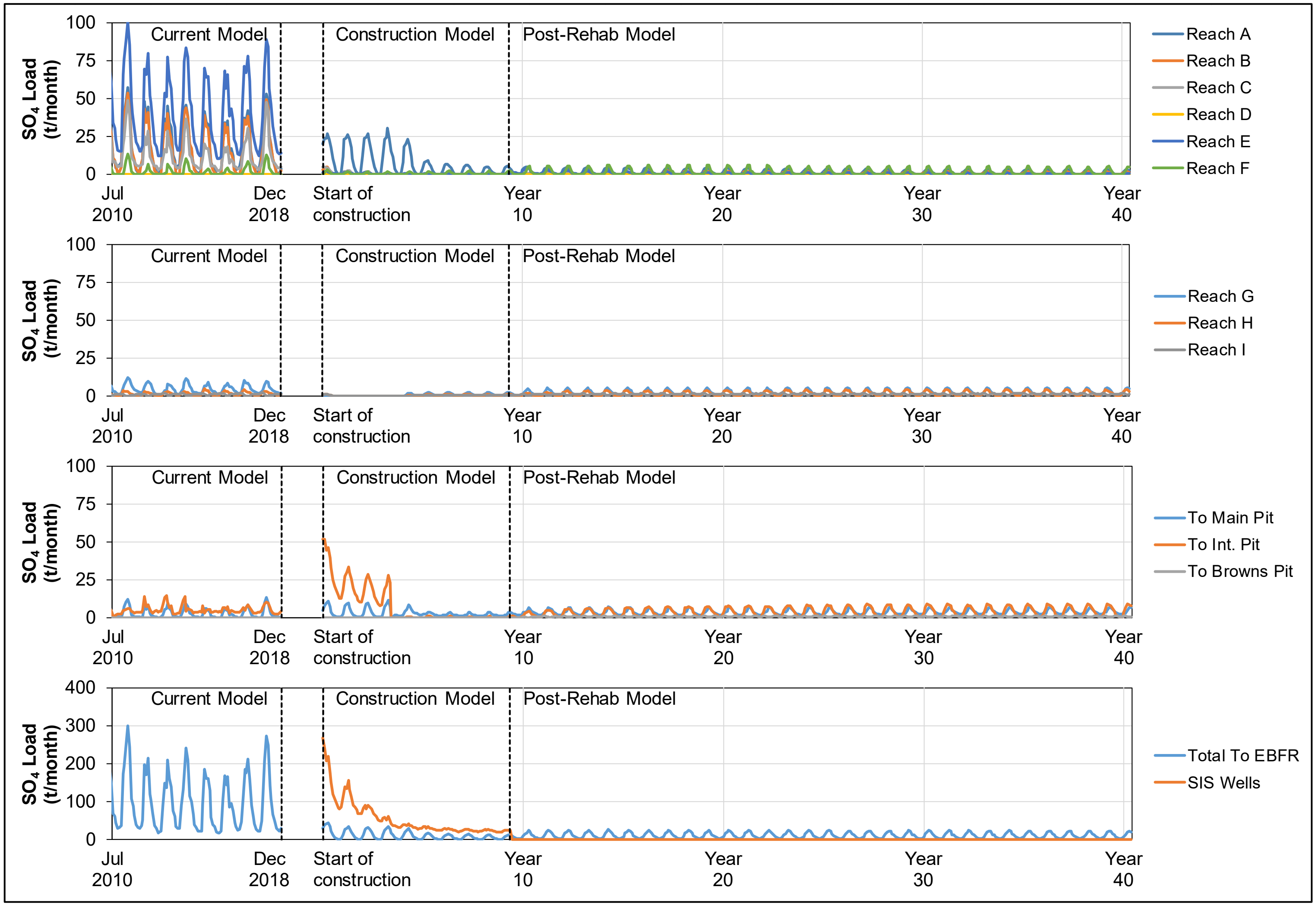

Figure 4-38. Predicted Groundwater Sulphate Loads to Site Features

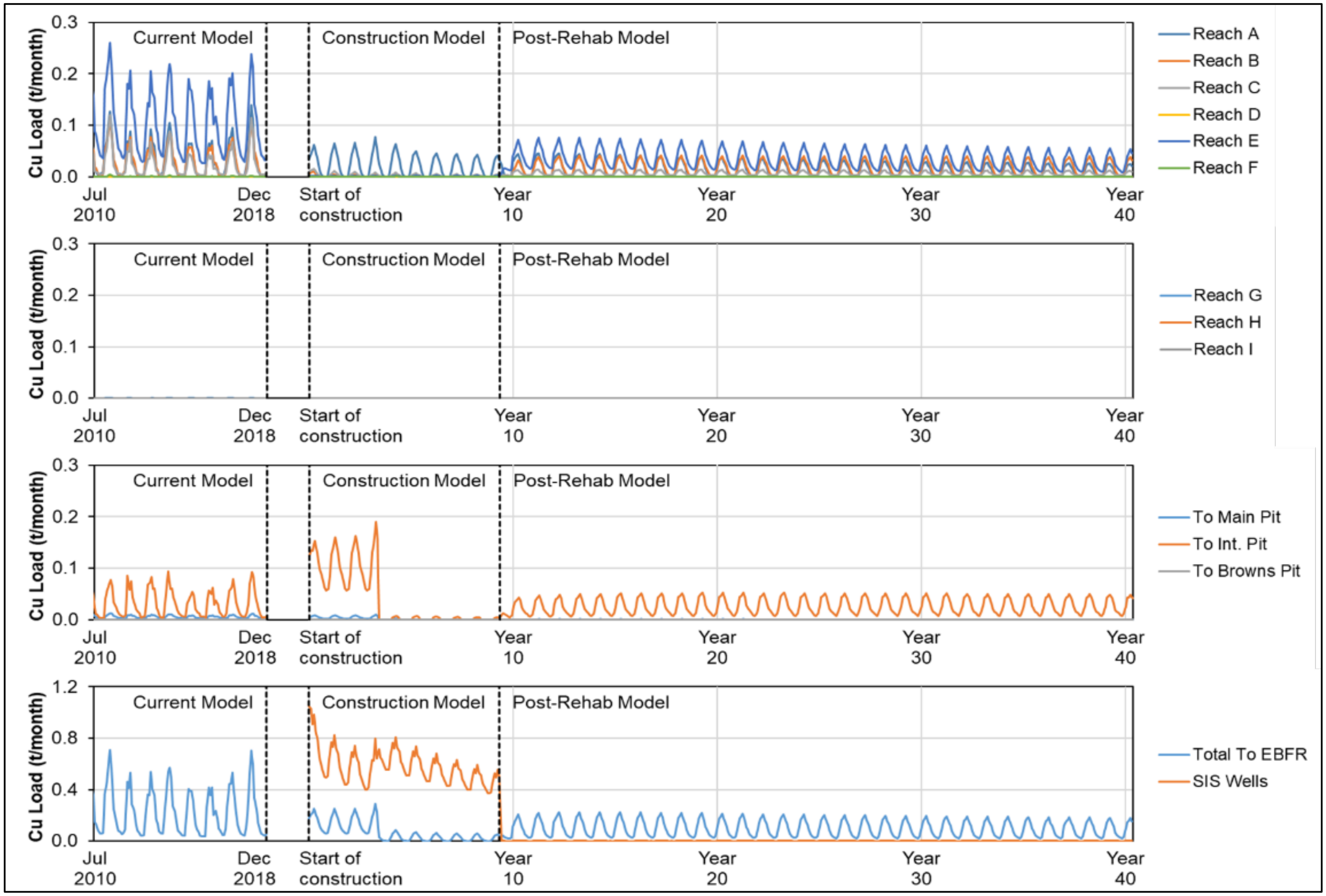

Figure 4-39. Predicted Groundwater Copper Loads to Site Features

4.9 PREDICTIVE MODELLING – POST-REHABILITATION

4.9.1 Model Setup for Post-Rehabilitation (Base Case)

The numerical model for the construction phase was modified to represent the future post-rehabilitation conditions for a 30-year period from Year 11 to Year 40. Changes to the construction model included the following modifications:

- The initial conditions used for the post-rehabilitation model runs are predicted groundwater conditions at the end of the construction model, i.e. after 10 years of operating the SIS and recovery bores.
- Seepage from the two new WSFs is assumed to continue to discharge to groundwater at the same rate and concentration for SO_4 and Cu.
- The saline drainage of SO_4 from the Main Pit backfill is assumed to continue for 19 years after the Main Pit is backfilled, i.e. from Year 5 to Year 24, at the same concentration (2,000 mg/L). This period represents the model predicted time to flush one pore volume of the Main Pit backfill materials assuming a conservative porosity value of 0.35.
- The saline drainage of Cu from the Main Pit backfill is assumed to continue for the full 30 years of post-rehabilitation, i.e. from Year 5 to Year 30, at the same concentration (0.2 mg/L).
- Residual impacted groundwater from the old WRD footprints and other sources continues to discharge to the EBFR.

4.9.2 Predicted Heads and Water Balance for Post-Rehabilitation (Base Case)

Figure 4-40 shows the simulated hydraulic heads in model layer 3 (shallow bedrock) for the dry season and wet season for Year 15, respectively. Figure 4-41 shows the predicted inflows and outflows for site features during the post-rehabilitation period. The water balance for the calibration model period (2010-2018) and the construction period (Year 1 to Year 10) are also shown for reference. In this figure, positive flow rates represent groundwater discharge (outflows) to the surface water system, while, negative flow rates represent inflows from open pits to the groundwater system.

The model predicts the following groundwater heads and flows for the post-rehabilitation period:

- The predicted groundwater flow fields for both wet and dry seasons are very similar to the typical flow field simulated for current conditions (see Figure 4-10), except for some slight differences within the CEPA and WSF areas.
- Groundwater discharge to the EBFR Reaches B, C, E, F and G is predicted to increase back to typical discharge conditions from Year 11, after pumping from recovery bores has ceased.

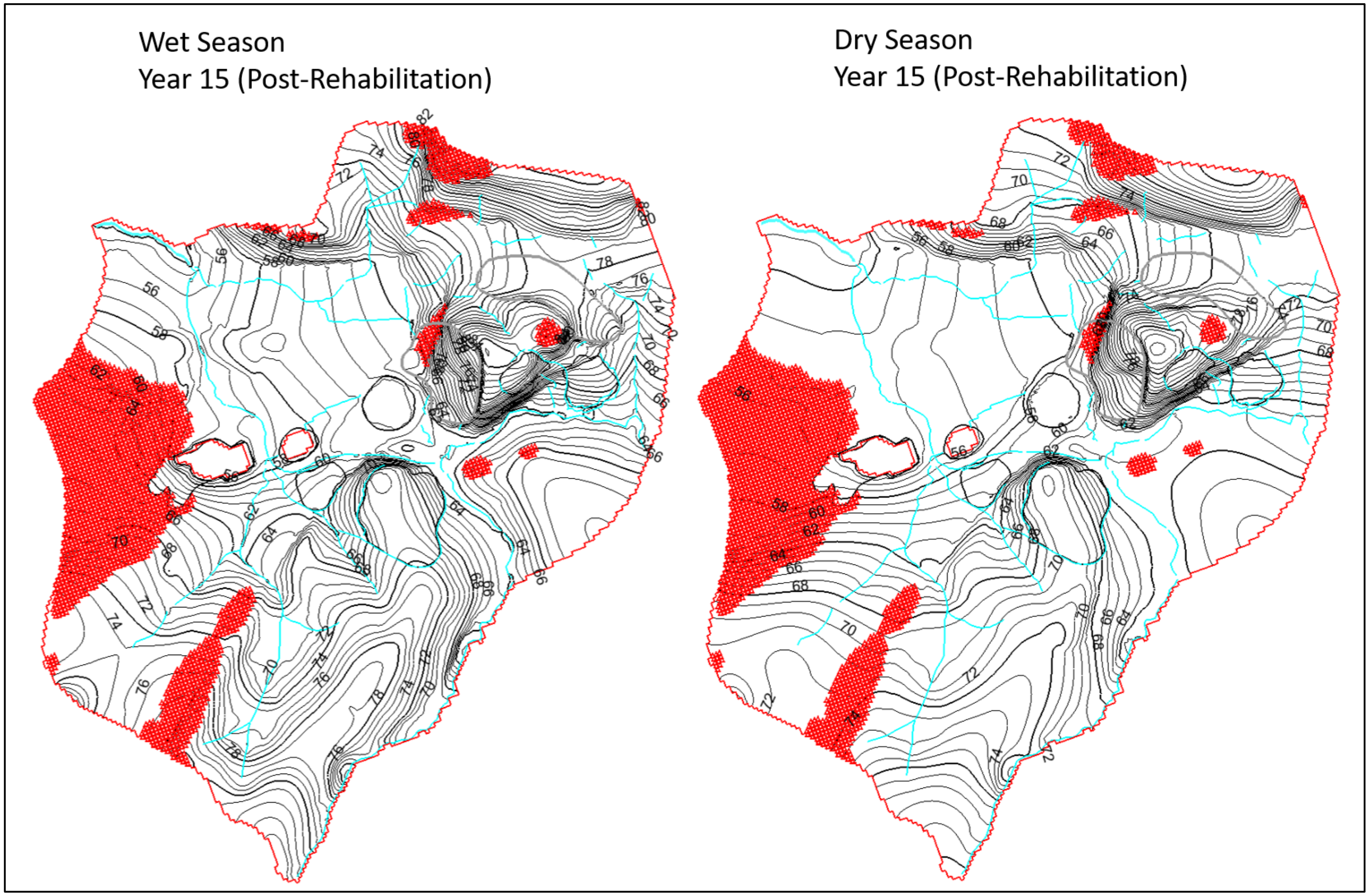

Figure 4-40. Simulated Heads for Year 15 Wet Season and Dry Season, Post-Rehabilitation

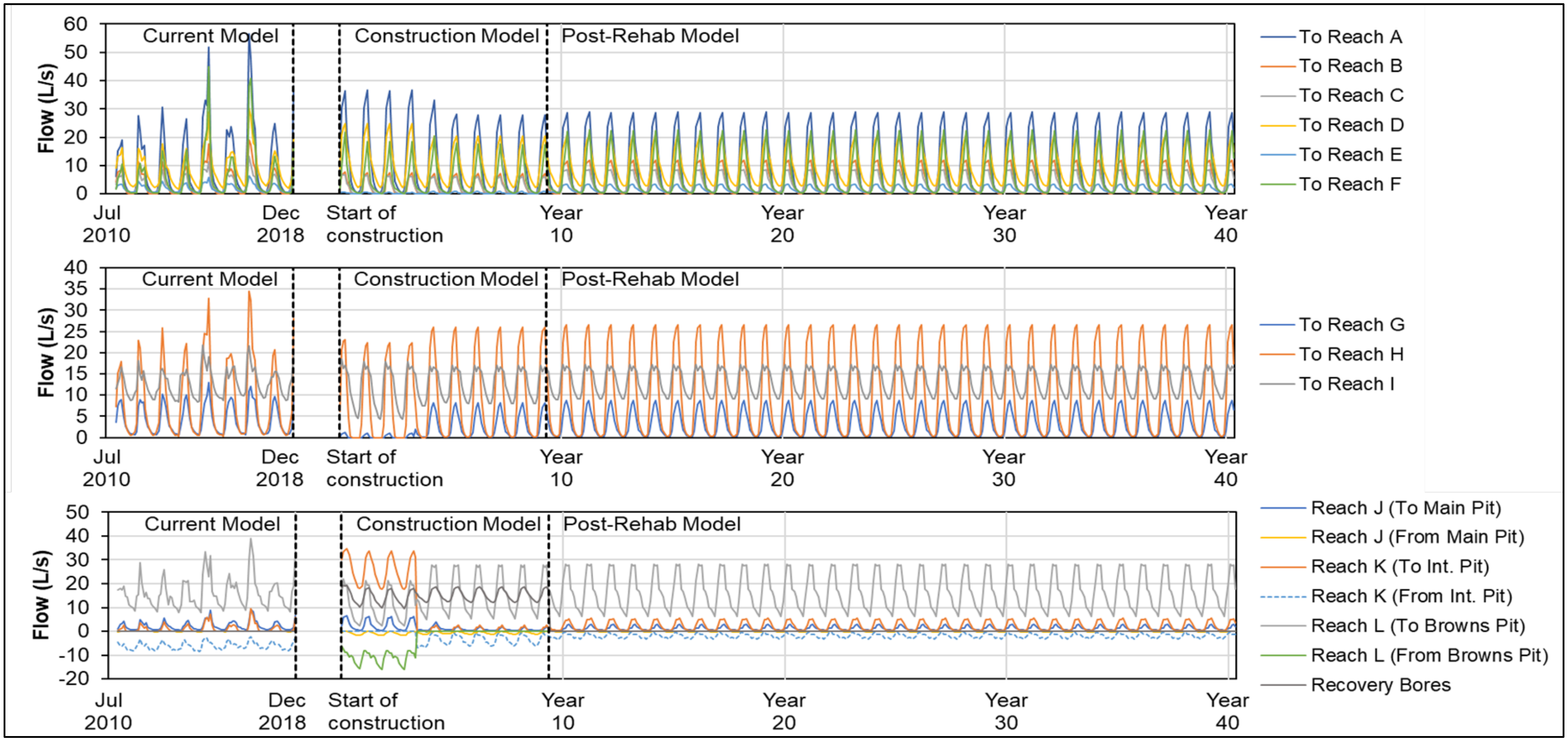

Figure 4-41. Model Water Balance for Site Features during Calibration Period (2010-2018), Construction Period (Year 1 to Year 10) and Post-Rehabilitation (Year 11 to Year 30)

4.9.3 Predicted Contaminant Plumes and Loads for Post-Rehabilitation (Base Case)

Predicted SO_4 and Cu plumes for Years 15, 20, 25 and 40 are shown in Figure 4-42 and Figure 4-43 respectively. Cross-sections showing predicted SO_4 and Cu concentrations in groundwater are provided in Figure 4-34, Figure 4-35, Figure 4-36, and Figure 4-37. See Figure 4-27for the locations of these sections. Simulated SO_4 and Cu concentrations in 1985 and for current conditions are also shown for comparison in these cross-sections. Monthly simulated and predicted SO_4 and Cu loads for current conditions, the construction period, and 30-years post-rehabilitation period are shown in Figure 4-38 and Figure 4-39**.** Predicted SO_4 and Cu loads for the post-rehabilitation period are summarized in Table 4-13 and Table 4-14**.**

Key observations from these figures and tables are summarized below:

- The groundwater model predicts the development of a sulphate plume with elevated SO_4 concentrations in groundwater within the footprints of the two new WSFs and immediately downgradient. The plume emanating from the Western WSF is predicted to report to the backfilled Main Pit, mainly from Layers 1 to 4 in the model, i.e. <50 m bgs. Most of the SO_4 load therefore reports to the portion of the pit that is backfilled. The SO_4 plume from the Northern WSF migrates along the northern lease boundary to Old Tailings Creek. A less concentrated SO_4 plume is also predicted to develop downgradient of the backfilled Main Pit.
- The groundwater model predicts no Cu plume to develop from the two WSFs due to the relatively low copper concentrations assumed for WSF seepage and assumed chemical precipitation of copper in bedrock units which have an adequate buffering capacity to neutralize AMD (e.g. in Coomalie Dolostone).
- Post-rehabilitation, the groundwater model predicts a total load of 235 t/year SO_4 in Year 15, i.e. 5 years after the SIS ceases to operate, including 134 t/year to the EBFR and about 100 t/year to pits. The predicted SO_4 load (126 t/year) to the EBFR in Year 40 is about 5% lower than the predicted load in Year 15 and 90% less than the simulated SO_4 load for current conditions (see Table 4-13).
- The groundwater model predicts a total load of 1.3 t/year Cu in Year 15 out of which 1.0 t/year Cu (75%) reports to the EBFR and 0.3 t/year Cu (25%) reports to the Intermediate Pit in Year 15. The predicted Cu load (0.6 t/year) to the EBFR in Year 40 is about 40% lower than the predicted load in Year 15 and 75% less than the simulated Cu load for current conditions (see Table 4-14).

Table 4-13. Predicted Post-Rehabilitation Sulphate Loads

Reach	Description	Current Conditions (2010 to 2018)		Year 15	Year 20	Year 30	Year 40	
		t/year	%	t/year	t/year	t/year	t/year	%
A	Dyson's Area	224	19%	23	22	18	18	14%
B	Main WRD (east)	201	17%	9	11	10	10	8%
C	Main WRD (west) and Int. WRD	154	13%	5	6	6	5	4%
D	Middlebrook Creek	0	0%	0	0	0	0	0%
E	EFDC near Main and Int. WRDs	484	41%	12	9	7	6	4%
F	Former stockpile area	24	2%	20	20	18	18	15%
G	EBFR downstream of GS8150200	58	5%	27	27	28	29	23%
H	EBFR in Old Tailings Dam area	21	2%	20	21	23	24	19%
I	EBFR near GS8150327	13	1%	16	17	18	17	14%
	Simulated Load to EBFR:	**1179**	**100%**	**134**	**132**	**126**	**126**	**100%**
-	To Main Pit	61	43%	46	46	47	50	43%
-	To Int. Pit	64	45%	44	48	53	54	46%
-	To Browns Pit	9	7%	10	11	12	13	11%
-	To Model Flooding Drains	8	6%	0	1	0	0	0%
	Simulated Load to Pits:	**142**	**100%**	**100**	**106**	**112**	**118**	**100%**
	TOTAL:	**1322**	**-**	**235**	**239**	**239**	**244**	**-**

Table 4-14. Predicted Post-Rehabilitation Copper Loads

Reach	Description	Current Conditions (2010 to 2018)		Year 15	Year 20	Year 30	Year 40	
		t/year	%	t/year	t/year	t/year	t/year	%
A	Dyson's Area	0.4	17%	0.2	0.2	0.1	0.1	17%
B	Main WRD (east)	0.4	15%	0.2	0.2	0.2	0.2	27%
C	Main WRD (west) and Int. WRD	0.3	13%	0.1	0.1	0.1	0.1	10%
D	Middlebrook Creek	0.0	0.0%	0.0	0.0	0.0	0.0	0%
E	EFDC near Main and Int. WRDs	1.3	54%	0.5	0.4	0.4	0.3	45%
F	Former stockpile area	0.0	0.2%	0.0	0.0	0.0	0.0	0%
G	EBFR downstream of GS8150200	0.0	0.1%	0.0	0.0	0.0	0.0	0%
H	EBFR in Old Tailings Dam area	0.0	0.0%	0.0	0.0	0.0	0.0	0%
I	EBFR near GS8150327	0.0	0.0%	0.0	0.0	0.0	0.0	0%
	Simulated Load to EBFR:	**2.3**	**100%**	**1.0**	**0.9**	**0.8**	**0.6**	**100%**
-	To Main Pit	0.1	14%	0.0	0.0	0.0	0.0	1%
-	To Int. Pit	0.4	85%	0.3	0.3	0.3	0.3	99%
-	To Browns Pit	0.0	0.2%	0.0	0.0	0.0	0.0	0%
-	To Model Flooding Drains	0.0	0.4%	0.0	0.0	0.0	0.0	0%
	Simulated Load to Pits:	**0.5**	**100%**	**0.3**	**0.3**	**0.3**	**0.3**	**100%**
	TOTAL:	**2.8**	**-**	**1.3**	**1.2**	**1.1**	**0.9**	**-**

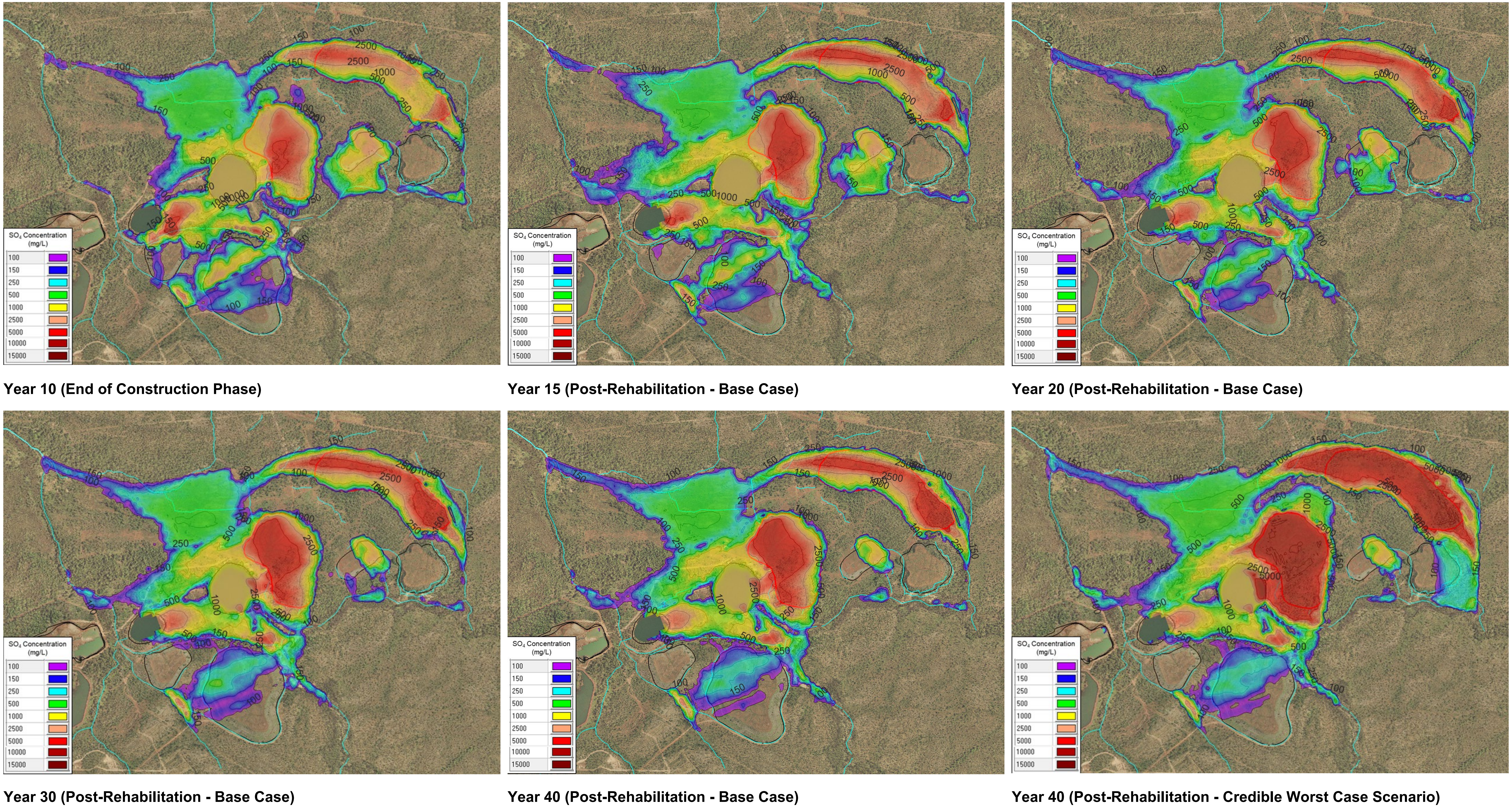

Figure 4-42. Predicted Sulphate Plumes, Post-Rehabilitation

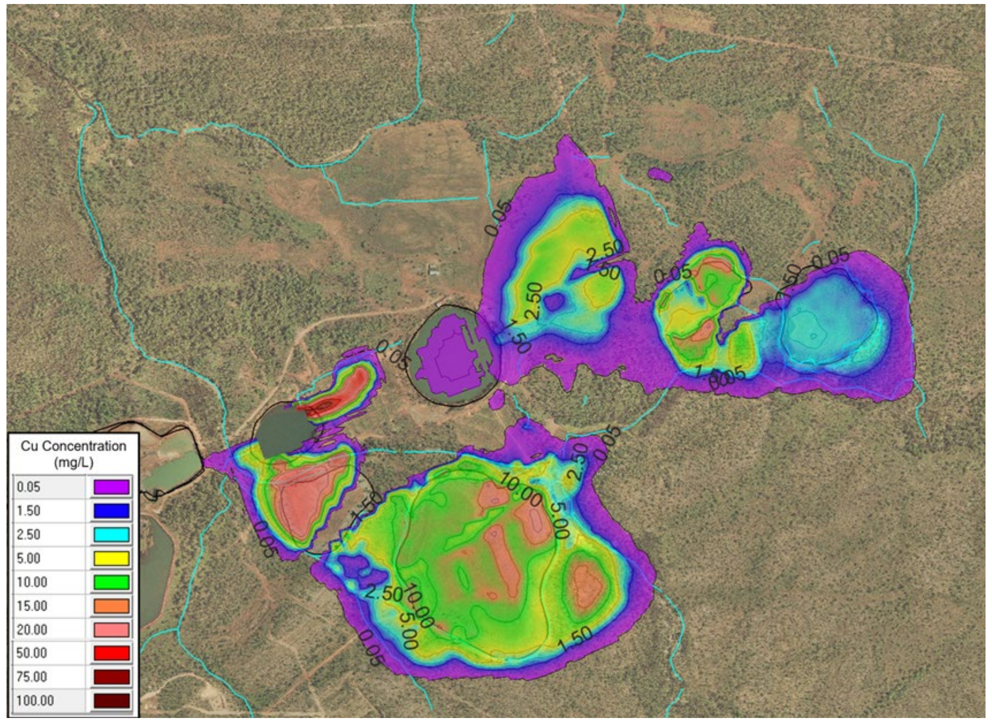

Year 10 (End of Construction Phase)

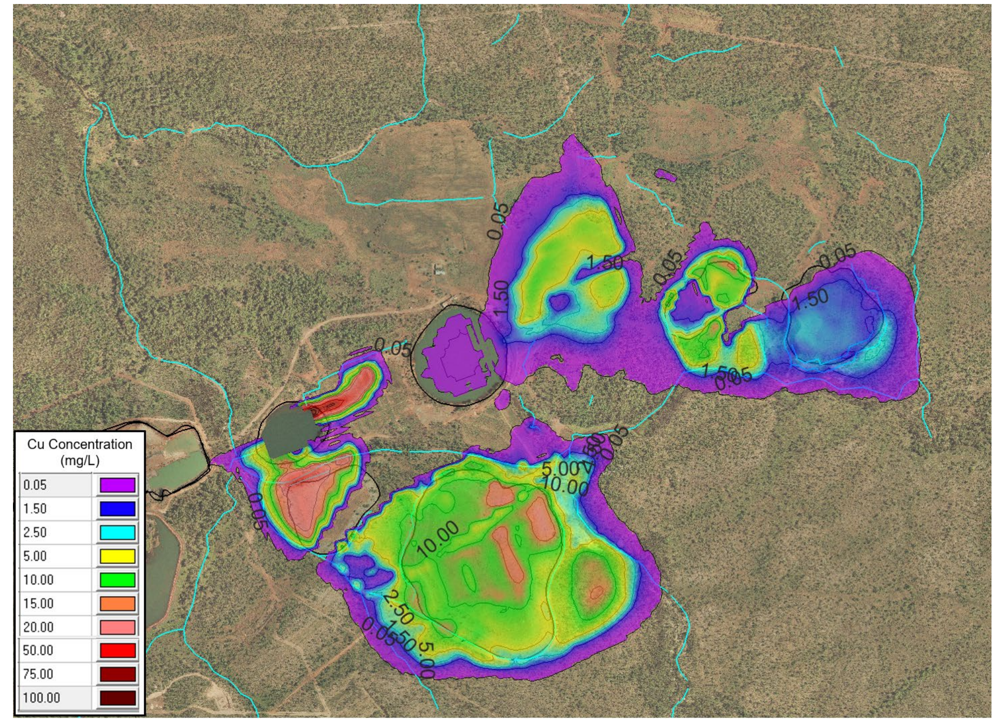

Year 15 (Post-Rehabilitation - Base Case)

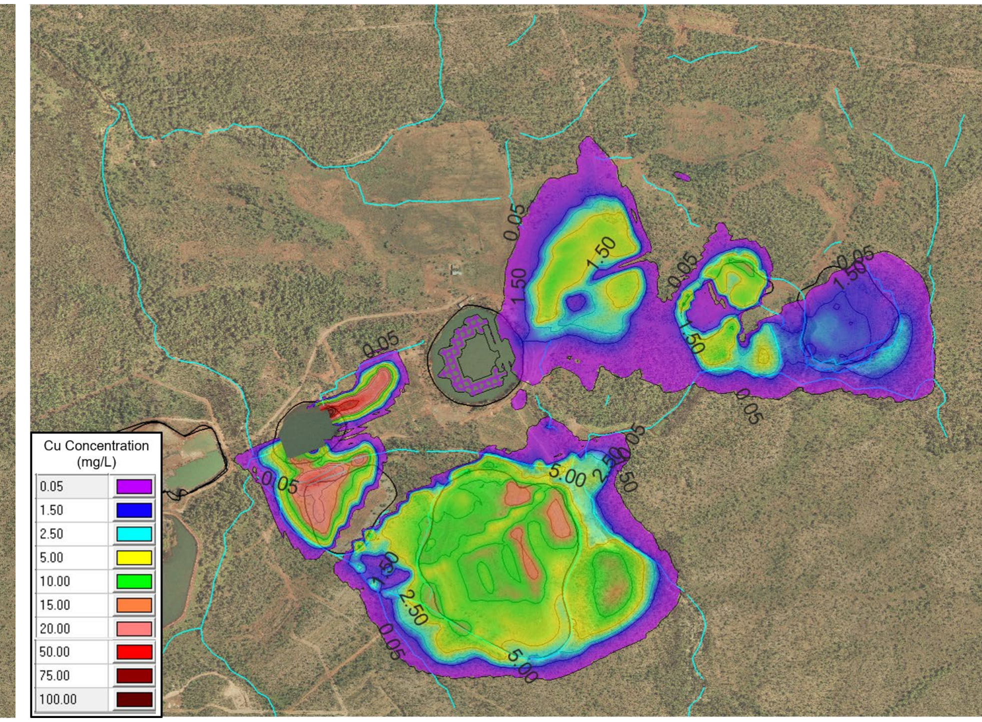

Year 20 (Post-Rehabilitation - Base Case)

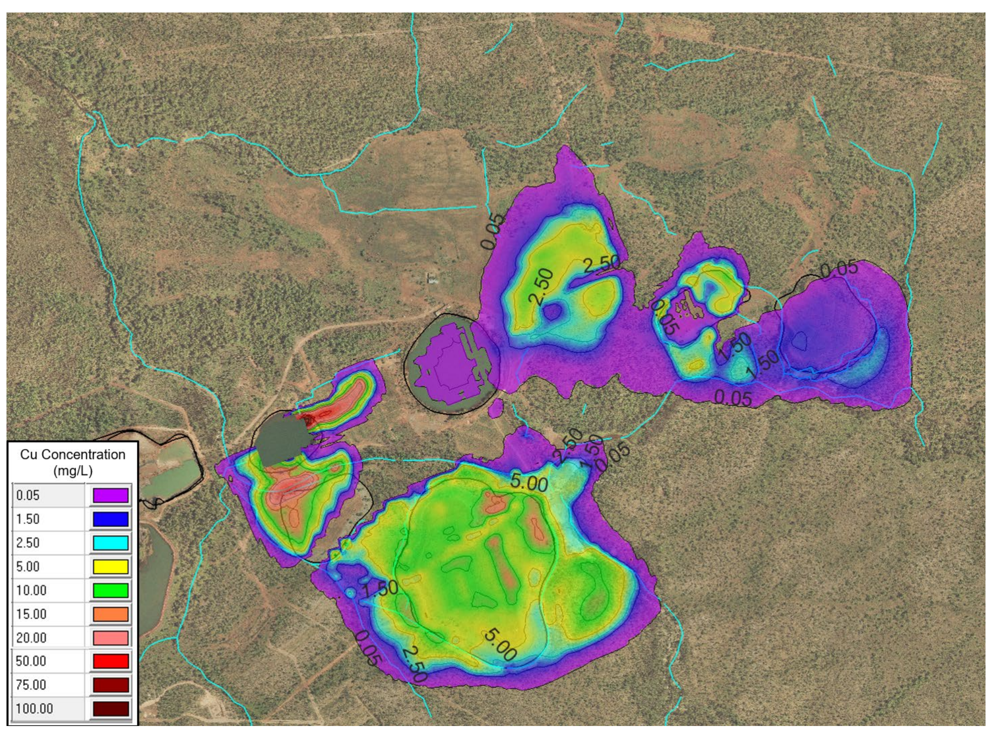

Year 30 (Post-Rehabilitation - Base Case)

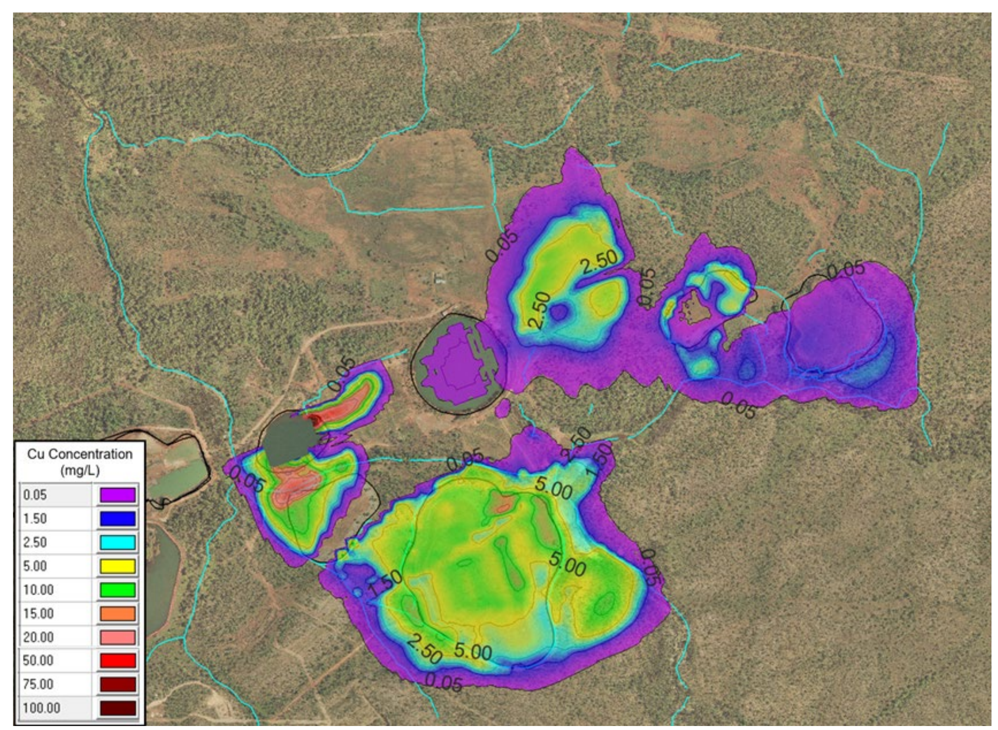

Year 40 (Post-Rehabilitation - Base Case)

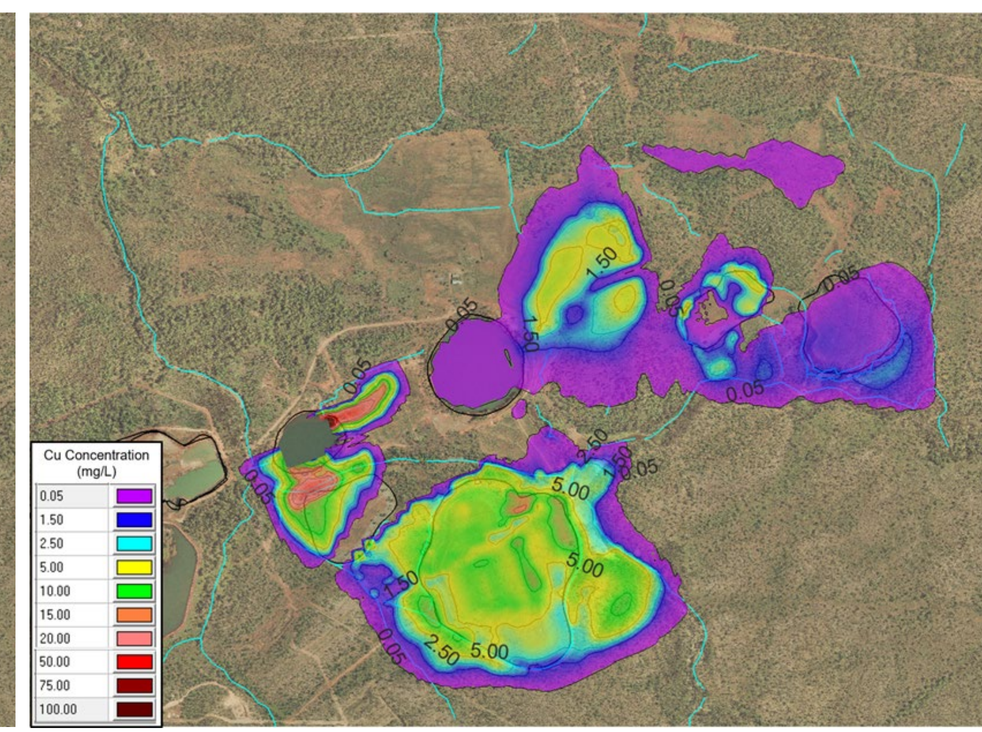

Year 40 (Post-Rehabilitation - Credible Worst Case Scenario)

Figure 4-43. Predicted Copper Plumes, Post-Rehabilitation

4.9.4 Model Setup for the Credible Worst-Case Scenario

A Credible Worst-Case scenario was run to characterize a less likely outcome in which the best management strategies implemented do not perform as intended. In the Credible Worst-Case scenario, changes to the base case post-rehabilitation model are as follows:

- Higher long-term infiltration rates from the new WSFs (Figure 4-27) are assumed with 100 mm/yr through the horizontal top and 87 mm/yr for the side-slopes.
- Seepage from the new WSF to groundwater is assigned an increased concentration for Cu of 0.5 mg/L for Cu (compared to 0.2 mg/L in base case) based on results from RGC and DJEE (2019). Note that the source concentration for SO_4 from these new WSFs remained unchanged (10,000 mg/L).
- Saline drainage from the Main Pit is assigned the same concentration for SO_4 (2000 mg/L) but an increased concentration for Cu of 0.1 mg/L (compared to 0.05 mg/L for base case) based on results from RGC and DJEE (2019).
- K for backfill materials in the Main Pit was increased by half an order of magnitude (5×10^{-6} m/s), compared to base case.

4.9.5 Predicted Plumes and Loads for the Credible Worst-Case Scenario

Monthly simulated and predicted SO_4 and Cu loads for current conditions, the construction period, and Credible Worst-Case scenario are shown in Figure 4-44 and Figure 4-45. Predicted SO_4 and Cu loads for the post-rehabilitation period are summarized in Table 4-15 and Table 4-16.

The model predicts the following changes to predicted concentrations and loads for the Credible Worst-Case scenario vis-à-vis post-rehabilitation base case conditions:

- The extent of the SO_4 plume emanating from the southwestern WSF footprint is predicted to grow notably towards the northeastern WSF footprint. Also, the extent of the SO_4 plume emanating from the northeastern WSF footprint is predicted to grow towards the south and reach the upper EBFR tributaries. The model predicts the SO_4 plume with elevated concentrations (10,000 mg/L) to expand largely within both footprints of the WSF, compared to the post-rehabilitation base case conditions (see Figure 4-42).
- A Cu plume emanating from the northeastern WSF footprint is predicted to develop albeit at low peak concentrations, ~0.05 mg/L by Year 40 (see, Figure 4-43).
- The groundwater model predicts a total load of 399 t/year SO_4 in Year 15, including 233 t/year to the EBFR and about 166 t/year to the pits. The predicted SO_4 load (273 t/year) to the EBFR in Year 40 is about 15% higher than the predicted load in Year 15 (233 t/year) and 75% less than the simulated SO_4 load for current conditions (see Table 4-15).

- The groundwater model predicts a total load of 1.3 t/year Cu in Year 15 out of which 1.0 t/year Cu (75%) reports to the EBFR and 0.3 t/year Cu (25%) reports to the pits. The predicted Cu load (0.7 t/year) to the EBFR in Year 40 is about 30% lower than the predicted load in Year 15 and 70% less than the simulated Cu load for current conditions (see Table 4-16**)**.

Table 4-15. Predicted Sulphate Loads for the Credible Worst-Case Scenario

Reach	Description	Current Conditions (2010 to 2018)		Year 15	Year 20	Year 30	Year 40	
		t/year	%	t/year	t/year	t/year	t/year	%
A	Dyson's Area	224	19%	58	60	63	66	24%
B	Main WRD (east)	201	17%	9	11	9	9	3%
C	Main WRD (west) and Int. WRD	154	13%	6	6	5	5	2%
D	Middlebrook Creek	0	0%	0	0	0	0	0%
E	EFDC near Main and Int. WRDs	484	41%	12	9	6	5	2%
F	Former stockpile area	24	2%	24	23	24	25	9%
G	EBFR downstream of GS8150200	58	5%	43	45	49	51	19%
H	EBFR in Old Tailings Dam area	21	2%	45	48	58	61	22%
I	EBFR near GS8150327	13	1%	36	40	52	50	18%
	Simulated Load to EBFR:	**1179**	**100%**	**233**	**241**	**266**	**273**	**100%**
-	To Main Pit	61	43%	66	70	131	138	50%
-	To Int. Pit	64	45%	81	93	102	105	38%
-	To Browns Pit	9	7%	17	22	27	32	12%
-	To Model Flooding Drains	8	6%	1	1	1	1	0%
	Simulated Load to Pits:	**142**	**100%**	**166**	**186**	**260**	**275**	**100%**
	TOTAL:	**1322**	**-**	**399**	**427**	**526**	**548**	**-**

Table 4-16. Predicted Copper Loads for the Credible Worst-Case Scenario

Reach	Description	Current Conditions (2010 to 2018)		Year 15	Year 20	Year 30	Year 40	
		t/year	%	t/year	t/year	t/year	t/year	%
A	Dyson's Area	0.4	17%	0.2	0.2	0.1	0.1	17%
B	Main WRD (east)	0.4	15%	0.2	0.2	0.2	0.2	27%
C	Main WRD (west) and Int. WRD	0.3	13%	0.1	0.1	0.1	0.1	10%
D	Middlebrook Creek	0.0	0.0%	0.0	0.0	0.0	0.0	0%
E	EFDC near Main and Int. WRDs	1.3	54%	0.5	0.4	0.4	0.3	46%
F	Former stockpile area	0.0	0.2%	0.0	0.0	0.0	0.0	0%
G	EBFR downstream of GS8150200	0.0	0.1%	0.0	0.0	0.0	0.0	0%
H	EBFR in Old Tailings Dam area	0.0	0.0%	0.0	0.0	0.0	0.0	0%
I	EBFR near GS8150327	0.0	0.0%	0.0	0.0	0.0	0.0	0%
	Simulated Load to EBFR:	**2.3**	**100%**	**1.0**	**0.9**	**0.8**	**0.7**	**100%**
-	To Main Pit	0.1	14%	0.0	0.0	0.0	0.0	2%
-	To Int. Pit	0.4	85%	0.3	0.3	0.3	0.3	98%
-	To Browns Pit	0.0	0.2%	0.0	0.0	0.0	0.0	0%
-	To Model Flooding Drains	0.0	0.4%	0.0	0.0	0.0	0.0	0%
	Simulated Load to Pits:	**0.5**	**100%**	**0.3**	**0.3**	**0.3**	**0.3**	**100%**
	TOTAL:	**2.8**	**-**	**1.3**	**1.3**	**1.2**	**1.1**	**-**

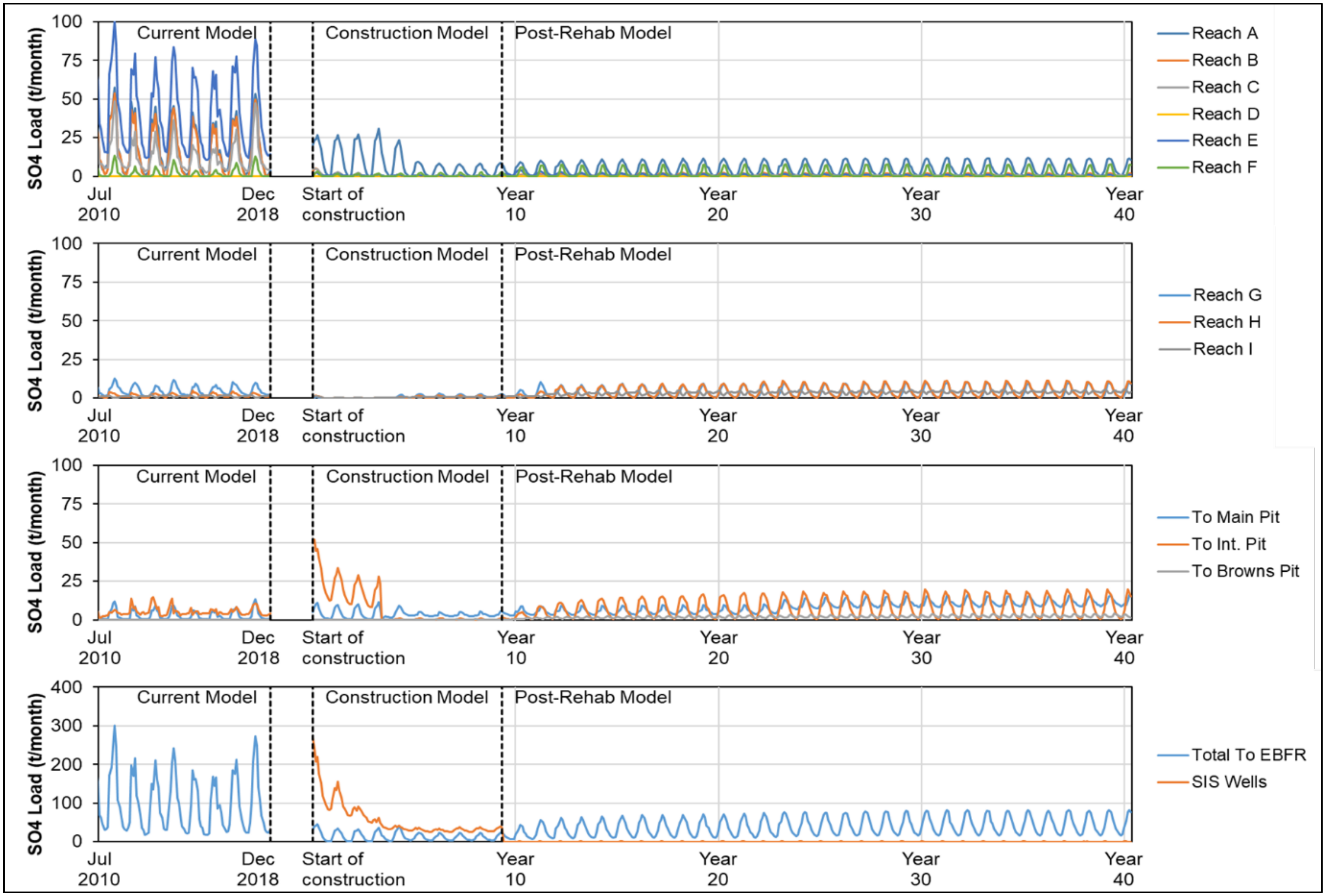

Figure 4-44. Simulated and Predicted Sulphate Loads, Credible Worst-Case Scenario

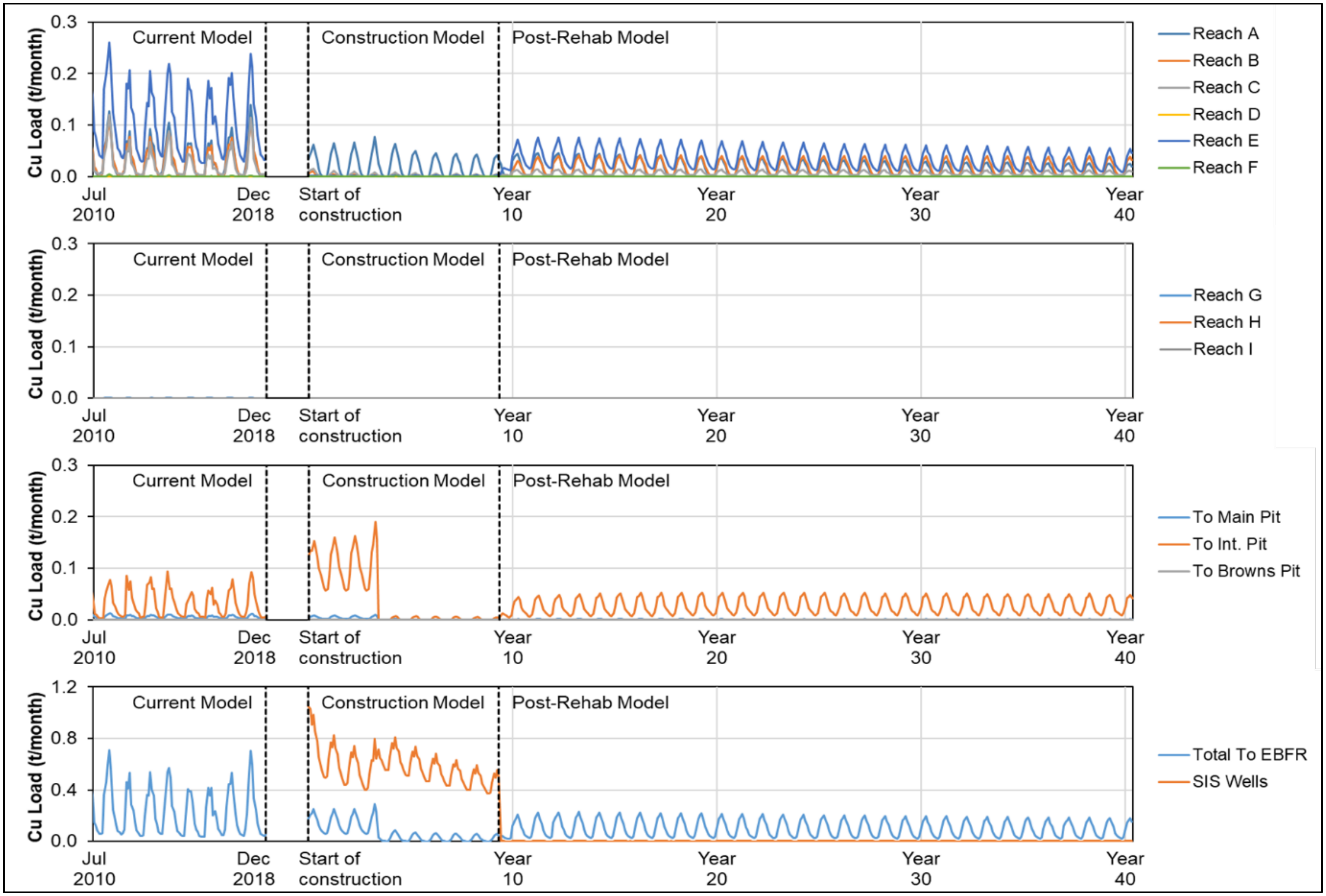

Figure 4-45. Simulated and Predicted Copper Loads, Credible Worst-Case Scenario

4.10 SENSITIVITY ANALYSIS FOR PREDICTIVE MODELS

Sensitivity analyses for future models including the construction phase model and the post-rehabilitation model were carried out to evaluate their sensitivity to variations in parameter values. The following flow and transport parameters were systematically adjusted following the same approach discussed above in Section 4.7:

- Hydraulic conductivity (± 25%)
- Natural recharge (± a factor of 1.5)
- Effective Porosity (± a factor of 2)
- Retardation factor for Cu simulations (± 50%)
- Dispersivity (± a factor of 2)

Results of sensitivity analyses for predictive model simulations are summarized below. Table 4-17 lists predicted sensitivity in flows to EFBR D/S (i.e. EBFR reach between gauge stations GS8150200 and GS8150327), combined with flows to the EFDC and recovery bores in Year 4, Year 10 and Year 40. Table 4-18 and Table 4-19 compare the predicted SO_4 and Cu loads, respectively, to those of the base case. Figure 4-46, Figure 4-47 and Figure 4-48 show predicted time trends of SO_4 loads for the various sensitivity runs during construction and post-rehabilitation. Figure 4 49, Figure 4 50 and Figure 4 51 show the predicted time trends of Cu loads for the various sensitivity runs.

Generally, model results for flows to the EBFR and recovery bores are predicted to be most sensitive to perturbations in recharge followed by hydraulic conductivity. Applied changes to recharge are predicted to cause the largest variations in predicted SO_4 loads to EBFR, Pits and recovery bores. This is followed by porosity, hydraulic conductivity and last is longitudinal dispersion. However, predicted Cu loads are mostly sensitive to recharge and retardation factor (Rf) compared to other parameters.

The key findings of the sensitivity analysis can be summarized as follows:

- Predicted flows:
    - Changing recharge by a factor of 1.5 up and down is predicted to cause a significant impact on flows to EFDC and EBFR D/S (see Table 4-17). For instance, these flows combined are predicted to vary in the range of 32% to 35% in Year 4. Flows extracted by recovery bores are predicted to be less sensitive to variability in recharge, with a difference range of 9% to 13% during construction.
    - Changing hydraulic conductivity (K) by ± 25% is predicted to cause less variability (compared to recharge) with 6% to 12% change on flows (to EBFR D/S and EFDC combined) during construction and post-rehabilitation and about 11% difference in extracted flows by recovery bores during construction.

- Predicted total SO_4 loads (to the entire EBFR, within the model domain including load discharge to the pits and collected in recovery bores):
  - Changing hydraulic conductivity K by ± 25% is predicted to result in limited impact on total SO_4 loads in the range of 5% to 10% during construction and post-rehabilitation.
  - Before relocating WRDs to the New WSFs, increasing recharge results in adding more mass to the aquifer system and therefore higher residual mass stored in the system and consequently higher loads discharging from the aquifer to the surface water system. The reverse is true for reduced recharge.
  - Changing recharge by a factor of 1.5 causes 12% to 19% variation in predicted total SO_4 loads during construction years, and 27% to 31% variation post-rehabilitation.
  - Increasing the effective porosity (n_e) results in longer travel time (slower transport velocity) and higher volume of stored residual plume in the aquifer system. Therefore, flushing of the residual plume is slower and the total mass discharging to surface water is higher. The reverse is true for reduced porosity. Changing n_e by two-fold is predicted to cause notable variation in predicted total SO_4 loads during construction years (18% to 38%), but less variation (8% to 12%) during post-rehabilitation.
  - It is predicted that changing the longitudinal dispersivity by two-fold up and down causes limited variations to total SO_4 loads (0.3% to 5%).
- Predicted total Cu loads (to the entire EBFR, within the model domain including load discharge to the pits and collected in recovery bores):
  - Changing the retardation factor by ± 50% is predicted to cause the most significant variation to predicted total Cu loads during construction years (18% to 50%), and post-rehabilitation (32% to 45%).
  - Changing hydraulic conductivity K by ± 25% is predicted to result in limited impact on total Cu loads in the range of 4% to 12% during construction and only marginal variation in the range of 0.5% to 2% during post-rehabilitation.
  - Changing recharge by a factor of 1.5 causes some small variation (1% to 7%) in predicted total Cu loads during construction years, increases to 8% to 15% during post-rehabilitation.
  - Changing n_e two-fold is predicted to cause marginal variation (0.5% to 2%) in predicted total Cu loads during construction years, and up to 4% during post-rehabilitation.
  - Changing longitudinal dispersivity two-fold is predicted to cause 6% to 15% variation in predicted total Cu loads during construction years, and 5% to 7% during post-rehabilitation.

4.10.1 Implications for Predictions

Predicted annual average flows to EBFR and to recovery bores during construction and post-rehabilitation vary by about 10% as inferred from sensitivity results on hydraulic conductivity. These flows to EBFR and to recovery bores are predicted to vary interannually in the range of 22% to 35% and 9% to 13%, respectively, as inferred from sensitivity on recharge.

Predicted total SO_4 loads are mostly sensitive to variations in recharge and effective porosity, however more sensitive to effective porosity during construction (18% to 38%) and to recharge (27% to 31%) during post-rehabilitation. Predicted total Cu loads are mostly sensitive to variation in retardation factor, with a wider range of variability in total Cu loads during construction years (18% to 50%) compared to post-rehabilitation (32% to 45%). Intercepted SO_4 and Cu loads by recovery bores are predicted to vary by up to 43% and 52%, respectively, considering uncertainty in effective porosity and retardation factor.

Table 4-17. Sensitivity Analyses Results for Predicted Flows to EBFR D/S, EFDC and Recovery Bores at Year 4, Year 10 and Year 40.

Parameter Change	Run ID	EBFR D/S + EFDC (L/s)	EBFR D/S + EFDC Diff. %	Recovery Bores SIS Bores (L/s)	Recovery Bores Pumping Bores (L/s)	Recovery Bores Total (L/s)	Recovery Bores Diff. %
Average Flows for Year 4							
Base Case	R421	18.5	-	*7.8*	*6.1*	*13.9*	-
Decrease K in all units by 25%	R426	17.1	-8%	6.5	5.8	12.3	-11%
Increase K in all units by 25%	R427	19.6	6%	9.0	6.4	15.4	11%
Increase Recharge (x1.5)	R428	25.1	35%	9.3	6.4	15.7	13%
Decrease Recharge (/1.5)	R429	12.6	-32%	6.6	5.6	12.2	-12%
Average Flows for Year 10							
Base Case		25.2	-	*8.1*	*7.1*	*15.2*	-
Decrease K in all units by 25%	R359a	22.3	-11%	6.8	6.6	13.4	-12%
Increase K in all units by 25%	R360a	27.6	10%	9.4	7.5	16.9	11%
Increase Recharge (x1.5)	R361a	32.0	27%	9.6	7.2	16.8	10%
Decrease Recharge (/1.5)	R362a	18.9	-25%	6.9	6.9	13.8	-9%
Average Flows for Year 40							
Base Case		28.1	-	-	-	-	-
Decrease K in all units by 25%	R359a	24.8	-12%	-	-	-	-
Increase K in all units by 25%	R360a	30.9	10%	-	-	-	-
Increase Recharge (x1.5)	R361a	34.9	24%	-	-	-	-
Decrease Recharge (/1.5)	R362a	22.0	-22%	-	-	-	-

EBFR D/S = East Branch of Finniss River between gauge stations GS8150200 and GS8150327
EFDC = East Finniss Diversion Channel
Diff. = Difference compared to base case

Table 4-18. Sensitivity Analyses Results for Predicted Total SO_4 Loads to EBFR, Pits and Recovery Bores at Year 4, Year 10 and Year 40.

Parameter Change	Run ID	Load to EBFR	Difference		Load to Pits	Difference		Load to Recovery Bores	Difference		Total Load	Difference	
		t/yr	t/yr	(%)	t/yr	t/yr	(%)	t/yr	t/yr	(%)	t/yr	t/yr	(%)
Year 4 Construction (before backfilling Main Pit)													
Base Case	R421	*188.3*	-	-	*246.6*	-	-	*732.5*	-	-	*1167.3*	-	-
Hk +25%	R427	193.4	5.1	2.7%	251.0	4.5	1.8%	785.1	52.7	7.2%	1229.6	62.3	5.3%
Hk -25%	R426	185.3	-2.9	-1.6%	225.9	-20.7	-8.4%	646.1	-86.3	-11.8%	1057.3	-110.0	-9.4%
Rech x1.5	R428	291.3	103.1	54.8%	307.4	60.8	24.7%	770.4	38.0	5.2%	1369.2	201.9	17.3%
Rech /1.5	R429	128.1	-60.2	-32.0%	177.4	-69.2	-28.1%	641.3	-91.2	-12.5%	946.7	-220.6	-18.9%
Porosity x2	R422	202.4	14.1	7.5%	283.5	36.9	15.0%	927.6	195.1	26.6%	1413.4	246.2	21.1%
Porosity /2	R423	181.6	-6.7	-3.5%	198.6	-47.9	-19.4%	563.5	-169.0	-23.1%	943.7	-223.6	-19.2%
Long. Disp. x2	R424	197.8	9.6	5.1%	241.9	-4.6	-1.9%	713.6	-18.9	-2.6%	1153.3	-13.9	-1.2%
Long. Disp. /2	R425	178.7	-9.6	-5.1%	245.8	-0.8	-0.3%	754.9	22.4	3.1%	1179.4	12.1	1.0%
Year 10 (End of Construction)													
Base Case	R354c	*65.0*	-	-	*30.0*	-	-	*268.2*	-	-	*363.2*	-	-
Hk -25%	R359a	61.5	-3.5	-5.4%	30.7	0.6	2.1%	237.1	-31.1	-11.6%	329.3	-34.0	-9.4%
Hk +25%	R360a	67.8	2.8	4.3%	28.6	-1.5	-4.9%	296.2	28.0	10.4%	392.6	29.3	8.1%
Rech x1.5	R361a	102.1	37.1	57.1%	62.9	32.9	109.6%	260.0	-8.3	-3.1%	425.0	61.7	17.0%
Rech /1.5	R362a	45.7	-19.3	-29.8%	15.7	-14.3	-47.7%	258.5	-9.8	-3.6%	319.8	-43.5	-12.0%
Porosity x2	R355a	89.1	24.1	37.1%	29.3	-0.7	-2.3%	382.6	114.4	42.6%	501.0	137.8	37.9%
Porosity /2	R356a	52.9	-12.1	-18.6%	32.0	2.0	6.7%	214.8	-53.4	-19.9%	299.7	-63.5	-17.5%
Long. Disp. x2	R357a	64.2	-0.8	-1.2%	30.5	0.5	1.7%	267.1	-1.1	-0.4%	361.9	-1.3	-0.4%
Long. Disp. /2	R358a	65.2	0.2	0.3%	30.4	0.3	1.1%	281.3	13.0	4.9%	376.8	13.6	3.7%
Year 40 (End of Post-Rehabilitation)													
Base Case	R354d	*133.9*	-	-	*123.3*	-	-	-	-	-	*257.2*	-	-
Hk -25%	R359b	120.7	-13.2	-9.8%	113.7	-9.6	-7.8%	-	-	-	234.5	-22.8	-8.8%
Hk +25%	R360b	147.4	13.5	10.1%	124.8	1.5	1.2%	-	-	-	272.2	15.0	5.8%
Rech x1.5	R361b	168.9	35.0	26.1%	167.6	44.3	35.9%	-	-	-	336.5	79.3	30.8%
Rech /1.5	R362b	120.1	-13.8	-10.3%	67.9	-55.4	-45.0%	-	-	-	187.9	-69.3	-26.9%
Porosity x2	R355b	152.2	18.2	13.6%	124.1	0.8	0.6%	-	-	-	276.2	19.0	7.4%
Porosity /2	R356b	113.0	-20.9	-15.6%	115.2	-8.1	-6.5%	-	-	-	228.2	-29.0	-11.3%
Long. Disp. x2	R357b	138.0	4.1	3.1%	123.2	-0.1	-0.1%	-	-	-	261.3	4.1	1.6%
Long. Disp. /2	R358b	133.1	-0.9	-0.6%	124.7	1.4	1.1%	-	-	-	257.8	0.5	0.2%

Table 4-19. Sensitivity Analyses Results for Predicted Total Cu Loads to EBFR, Pits and Recovery Bores at Year 4, Year 10 and Year 40.

Parameter Change	Run ID	Load to EBFR	Difference		Load to Pits	Difference		Load to SIS Wells	Difference		Total Load	Difference	
		t/yr	t/yr	(%)	t/yr	t/yr	(%)	t/yr	t/yr	(%)	t/yr	t/yr	(%)
Year 4 Construction (before backfilling Main Pit)													
Base Case	R407a	*0.36*	-	-	*1.32*	-	-	*6.50*	-	-	*8.18*	-	-
Hk +25%	R416	0.35	-0.01	-3.1%	1.43	0.12	8.8%	7.12	0.62	9.5%	8.90	0.73	8.9%
Hk -25%	R415	0.39	0.03	7.2%	1.16	-0.16	-12.1%	5.67	-0.83	-12.7%	7.22	-0.96	-11.7%
Rech x1.5	R417	0.63	0.27	73.2%	1.54	0.22	17.1%	6.55	0.05	0.8%	8.72	0.54	6.6%
Rech /1.5	R418	0.21	-0.16	-43.4%	1.06	-0.26	-19.4%	6.34	-0.16	-2.4%	7.60	-0.57	-7.0%
Porosity x2	R411	0.37	0.01	2.2%	1.33	0.01	0.7%	6.57	0.07	1.1%	8.27	0.09	1.1%
Porosity /2	R412	0.36	0.00	-1.2%	1.31	0.00	-0.3%	6.46	-0.04	-0.6%	8.13	-0.04	-0.5%
Long. Disp. x2	R413	0.37	0.01	2.0%	1.29	-0.03	-2.3%	5.74	-0.75	-11.6%	7.40	-0.78	-9.5%
Long. Disp. /2	R414	0.36	0.00	-0.7%	1.34	0.02	1.6%	6.99	0.50	7.6%	8.69	0.51	6.3%
Rf +50%	R409	0.37	0.01	1.8%	1.43	0.11	8.4%	7.84	1.34	20.7%	9.64	1.46	17.9%
Rf -50%	R410	0.36	0.00	-1.3%	1.06	-0.26	-19.9%	3.98	-2.52	-38.7%	5.39	-2.78	-34.0%
Year 10 (End of Construction)													
Base Case	R341	*0.23*	-	-	*0.02*	-	-	*5.44*	-	-	*5.69*	-	-
Hk -25%	R348	0.23	0.00	-0.3%	0.04	0.02	85.8%	5.03	-0.41	-7.5%	5.30	-0.39	-6.9%
Hk +25%	R349	0.23	0.00	0.4%	0.01	-0.01	-32.7%	5.65	0.20	3.8%	5.89	0.20	3.5%
Rech x1.5	R350	0.33	0.10	41.8%	0.08	0.06	309.7%	5.21	-0.24	-4.3%	5.61	-0.08	-1.4%
Rech /1.5	R351	0.14	-0.09	-38.0%	0.00	-0.02	-80.1%	5.66	0.22	4.1%	5.81	0.12	2.1%
Porosity x2	R344	0.24	0.01	4.3%	0.02	0.00	6.2%	5.53	0.09	1.6%	5.79	0.10	1.7%
Porosity /2	R345	0.23	0.00	-2.2%	0.02	0.00	-2.7%	5.40	-0.04	-0.7%	5.65	-0.05	-0.8%
Long. Disp. x2	R346	0.23	0.00	-0.3%	0.02	0.00	9.7%	4.61	-0.84	-15.4%	4.86	-0.84	-14.7%
Long. Disp. /2	R347	0.23	0.00	1.2%	0.02	0.00	-5.7%	6.02	0.58	10.6%	6.27	0.58	10.1%
Rf +50%	R342	0.25	0.02	8.4%	0.02	0.00	23.3%	7.44	1.99	36.6%	7.71	2.02	35.4%
Rf -50%	R343	0.19	-0.04	-15.7%	0.01	-0.01	-37.9%	2.63	-2.81	-51.6%	2.84	-2.85	-50.1%
Year 40 (End of Post-Rehabilitation)													
Base Case	R341	*0.76*	-	-	*0.31*	-	-	-	-	-	*1.07*	-	-
Hk -25%	R348	0.76	0.00	0.1%	0.31	0.00	-1.4%	-	-	-	1.07	0.00	-0.4%
Hk +25%	R349	0.74	-0.02	-2.7%	0.31	-0.01	-2.8%	-	-	-	1.05	-0.03	-2.7%
Rech x1.5	R350	0.80	0.04	5.4%	0.35	0.04	12.7%	-	-	-	1.16	0.08	7.6%
Rech /1.5	R351	0.70	-0.06	-8.5%	0.22	-0.09	-29.4%	-	-	-	0.92	-0.16	-14.6%
Porosity x2	R344	0.80	0.04	5.4%	0.32	0.01	1.7%	-	-	-	1.12	0.05	4.3%
Porosity /2	R345	0.74	-0.02	-2.8%	0.31	0.00	-0.8%	-	-	-	1.05	-0.02	-2.2%
Long. Disp. x2	R346	0.70	-0.06	-7.8%	0.30	-0.02	-5.6%	-	-	-	1.00	-0.08	-7.2%
Long. Disp. /2	R347	0.81	0.05	6.1%	0.32	0.01	3.5%	-	-	-	1.13	0.06	5.3%
Rf +50%	R342	1.04	0.28	36.9%	0.38	0.07	22.0%	-	-	-	1.42	0.35	32.5%
Rf -50%	R343	0.41	-0.35	-45.9%	0.18	-0.13	-42.6%	-	-	-	0.59	-0.48	-44.9%

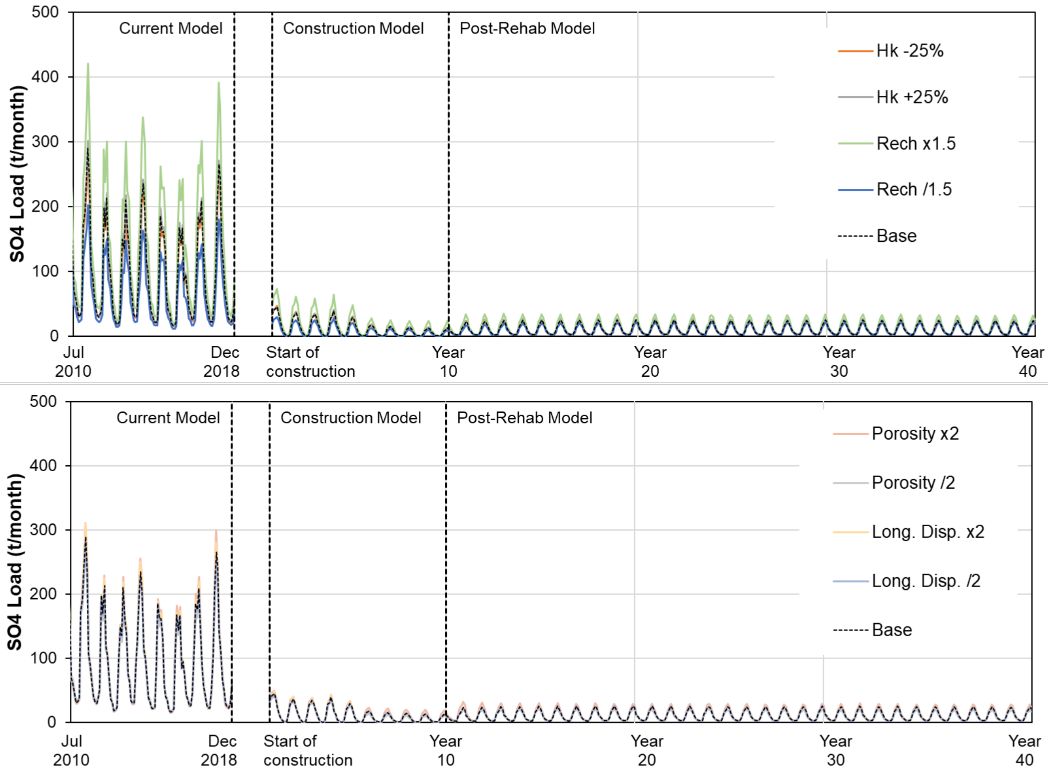

Figure 4-46. Sensitivity Analyses Results for Predicted Total SO_4 Loads to EBFR

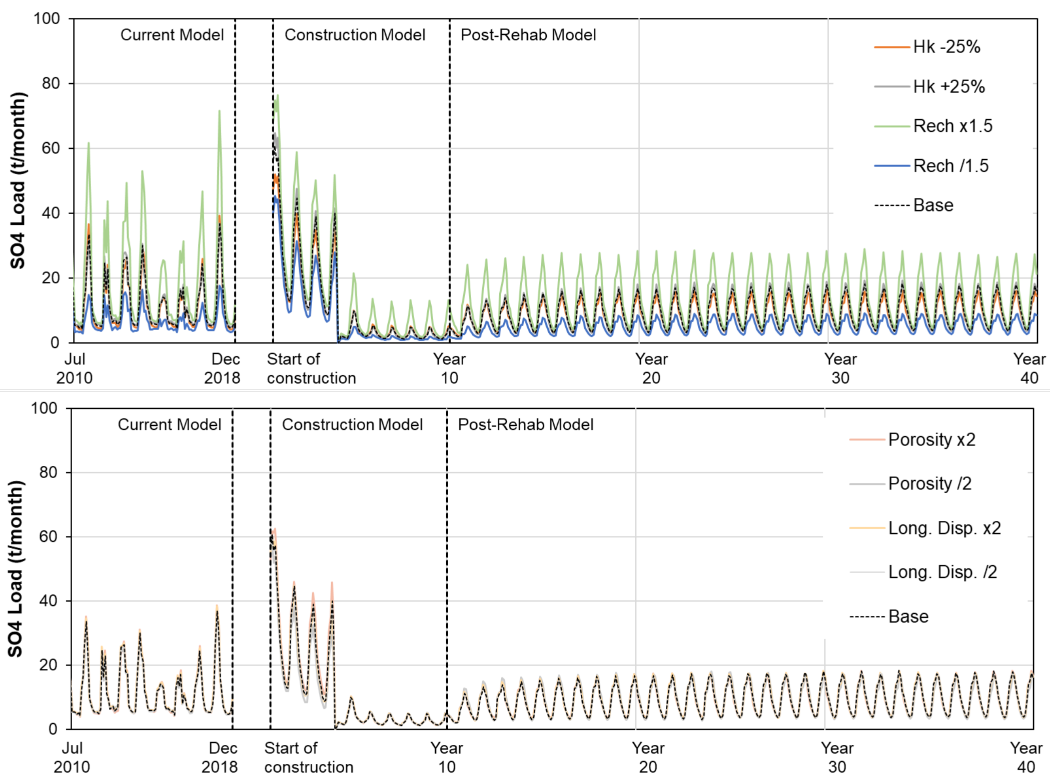

Figure 4-47. Sensitivity Analyses Results for Predicted Total SO_4 Loads to Pits

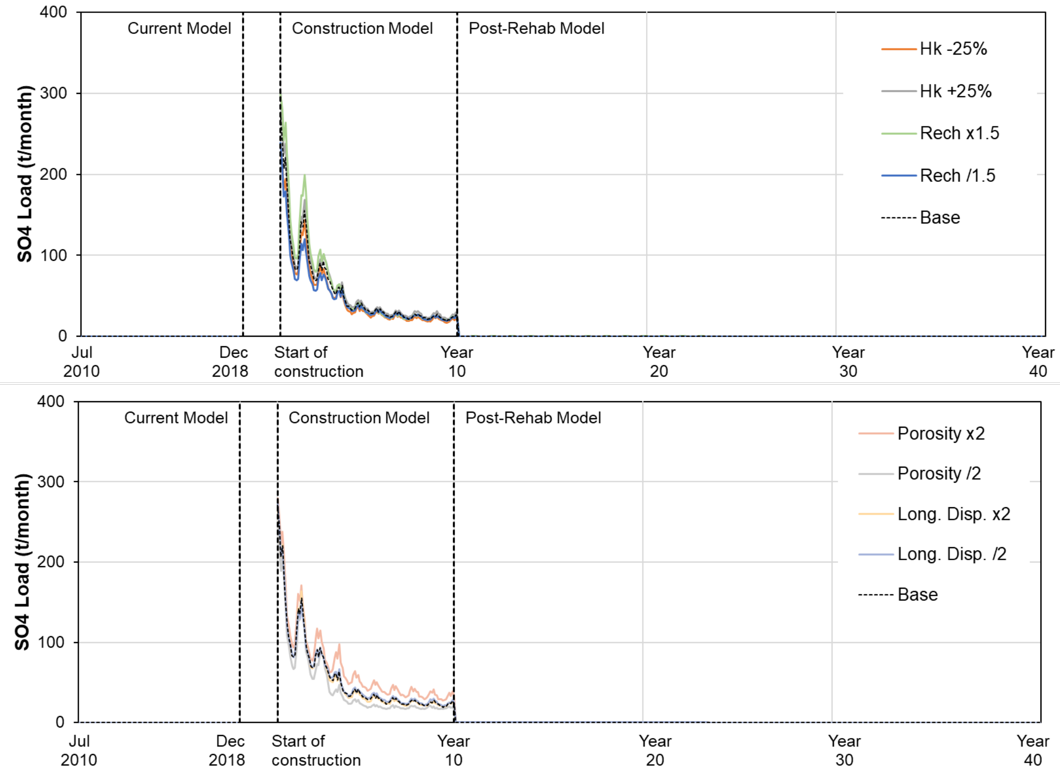

Figure 4-48. Sensitivity Analyses Results for Predicted Total SO_4 Loads to Recovery Bores

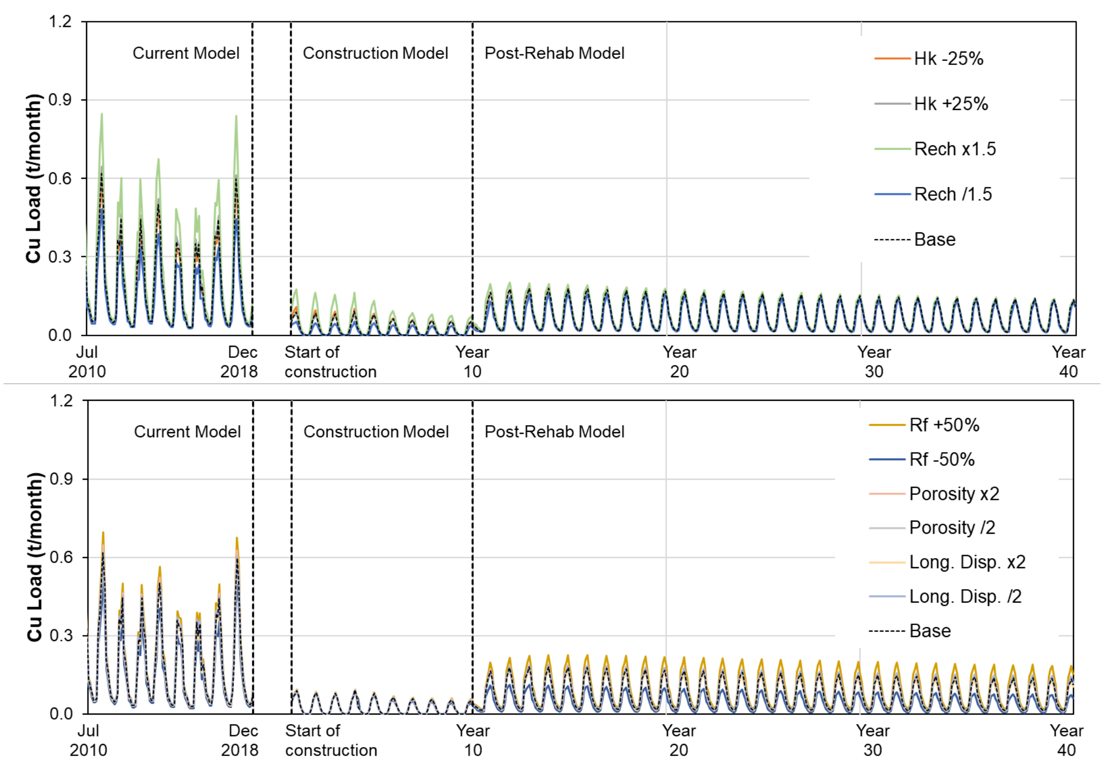

Figure 4-49. Sensitivity Analyses Results for Predicted Total Cu Loads to EBFR

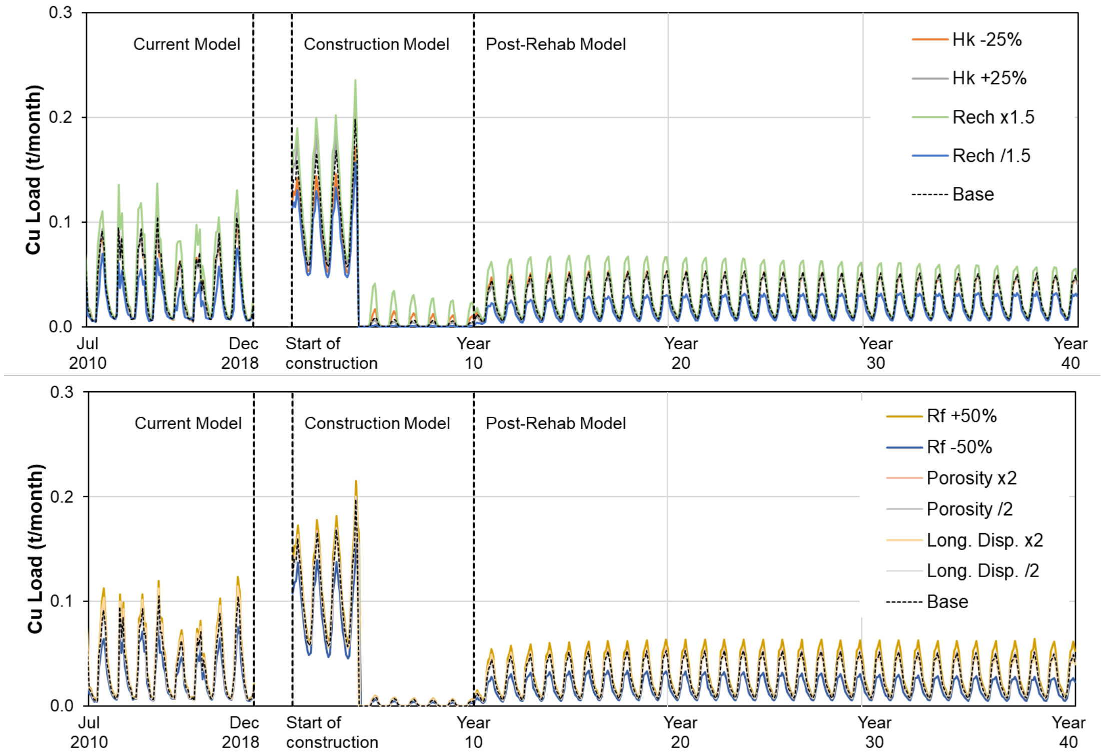

Figure 4-50. Sensitivity Analyses Results for Predicted Total Cu Loads to Pits

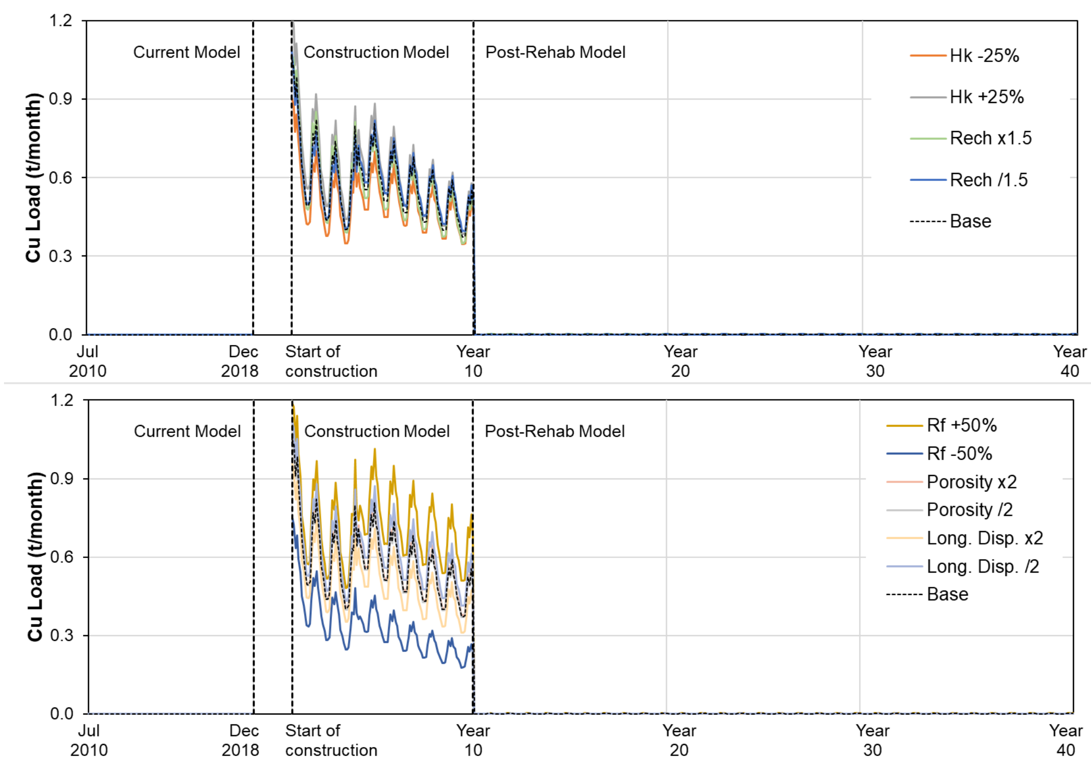

Figure 4-51. Sensitivity Analyses Results for Predicted Total Cu Loads to Recovery Bores

4.11 MODEL LIMITATIONS

4.11.1 Overview

The groundwater system at the Rum Jungle Mine Site exhibits a high degree of complexity, including a strong seasonality in recharge and ground water flow, highly heterogeneous subsurface conditions (typical for fractured bedrock), and a range of contaminant sources (waste rock, tailings) with variable contaminant loading in space and time.

As for any model, the complexity of the site features had to be reduced in our conceptual model such that it preserves the key features but is simple enough to allow representation by a numerical model of groundwater flow and solute transport. These model simplifications should be considered when interpreting model results.

Model limitations are briefly discussed in the next sections in terms of conceptual, numerical, and design limitations.

4.11.2 Conceptual Limitations

Conceptually, the model is affected by remaining data gaps (lack of hydrogeological information) and conceptual limitations (uncertainty in past and future conditions).

This includes:

- Lack of historical information on contaminant sources and groundwater monitoring data (groundwater levels and groundwater quality) prior to initial rehabilitation in the mid-1980s.
- Remaining gaps in hydrogeological site characterization of the local bedrock aquifer system to determine local variations in hydraulic parameters (K, S_y, S_s).
- Uncertainty in current and future recharge in undisturbed areas
- Uncertainty in current and future seepage rates and associated contaminant loading from waste storage facilities, and
- Uncertainty in transport parameters (n_e and α) and geochemical controls (primarily for copper).

The sensitivity analyses completed to date suggest that the lack of historical information and remaining uncertainty in hydrogeological data has only a relatively small effect on model predictions.

Considering the large foot print of the Rum Jungle mine site proper and the regional scale of the model domain, it is not practical to complete adequate hydrogeological characterization to justify an explicit representation of the heterogeneity of the bedrock aquifer (e.g. preferential flow channels and/or low-K faults representing barriers). It follows that while the model can be expected to describe the general trends in flow and transport, it may not be able to reproduce small-scale variations in flow and/or transport caused by aquifer heterogeneity. This limitation should be kept in mind when interpreting modeling results and designing mitigation and control measures.

A second important consideration is the uncertainty in transport parameters and their influence on transport predictions. Although the solute transport model was calibrated to overall loading targets there is remaining uncertainty on transport parameters, in particular, the effective porosity of the aquifer units and retardation factor for copper simulations. Sensitivity analyses have been completed to illustrate the potential impact of these uncertainties on predicted clean-up of the aquifer in response to rehabilitation. However, additional characterization work is recommended to further constrain this uncertainty in model predictions.

4.11.3 Numerical Limitations

From a numerical standpoint, the model is affected by the following limitations:

- Non-uniqueness
- Grid design & spatial discretization
- Model parameterization, and
- Monthly time stepping.

Although the model calibration is considered to be very good for flow, and satisfactory for transport, the flow and transport solutions obtained are not unique, i.e. alternative sets of solutions may exist and equally (or potentially better) match the temporal and spatial observations used for model calibration.

Numerical limitations such as a relatively coarse cell size (25m x 25m), layer thickness and choices or results in model parameterization (use of large, uniform zones), prevent the exact representation of discrete flow and/or transport processes, such as simulation of head losses nearby recovery bores or prediction of localized discharge and/or contaminant loading to specific reaches of the EBFR.

The current model uses monthly time steps to simulate groundwater flow. The model is therefore not able to predict short-term variations in groundwater flow and solute transport such as groundwater mounding and associated seepage and contaminant loading caused by a high precipitation event.

4.11.4 Implications for Design of Rehabilitation Plan

This latest RJ model provides a suitable tool to assist in design of the rehabilitation plan (at a conceptual engineering level) and assess the environmental impacts of the rehabilitation plan. This is supported by the good calibration statistics and the rigorous sensitivity analysis which was completed to evaluate the sensitivity of model results to variations in parameter values for current conditions and predictions.

However, the inherent difficulty of any regional model to represent the local heterogeneity (e.g. high permeability fractures/faults and/or low-permeability faults representing local flow barriers) restrict the ability of the model to predict pumping rates or contaminant concentrations at specific locations in the model. Therefore, for design purposes, the model should be considered only indicative of general ranges of pumping rates and contaminant concentrations.

Taking the above into consideration, RGC recommends that specific design details (e.g. number of recovery bores, screening intervals, pumping rates) be finalized based on field experience, review of the latest monitoring data collected (including data collected after model calibration) and testing during/after installation of mitigation measures. The model limitations discussed above should also be considered when interpreting and reviewing water quality data for performance monitoring purposes.